

UniversidadeVigo

**Escola Internacional de Doutoramento**

**Rubén Varela Rodríguez**

**TESE DE DOUTORAMENTO**

**Worldwide evolution of upwelling and its  
influence on SST trends**

Dirixida polos doutores:

Ramón Gómez Gesteira

María Inés Álvarez

2017

“Mención Internacional”

Universidade de Vigo, Campus de Ourense, Departamento de Física Aplicada, Environmental Physics Laboratory (Ephyslab).

**Rubén Varela Rodríguez** (ruvarela@uvigo.es).

Worldwide evolution of upwelling and its influence on SST trends.

Ourense, decembro de 2017.

# Universidade de Vigo

## Escola Internacional de Doutoramento

**Dr. Ramón Gómez Gesteira**, catedrático do Departamento de Física Aplicada da Universidade de Vigo e **Dra. María Inés Álvarez**, profesora titular do Departamento de Física Aplicada da Universidade de Vigo:

FAN CONSTAR que o presente traballo, titulado **“Worldwide evolution of upwelling and its influence on SST trends”**, que presenta Rubén Varela Rodríguez para a obtención do título de Doutor, foi elaborado baixo a súa dirección no programa de doutoramento “Ciencias Mariñas, Tecnoloxía e Xestión” baixo a modalidade de “Compendio de publicacións”.

Ourense, 12 de Decembro do ano 2017

Os directores da tesis doutoral

Dr. Ramón Gómez Gesteira

Dra. María Inés Álvarez





# Agradecimientos/Acknowledgments

No puedo comenzar estos agradecimientos sin nombrar a Moncho y Maite, los cuales, en representación del grupo Ephyslab, me dieron la oportunidad de continuar mis estudios hasta hoy, que presento el Doctorado. Sin su ayuda desde el primer día, su atención y todas las horas que pasaron a mi lado, con toda la paciencia del mundo, todo esto no sería posible.

También quiero nombrar a mi directora, Inés, la cual probablemente se haya ganado el cielo tras innumerables horas de correcciones a mis artículos, tesis...siempre con buena cara y presta a ayudar en lo que hiciera falta.

Pero como todo gran camino, éste tuvo un inicio, y fue hace ya más de 10 años, allá por 2006. Esto me hace recordar que muchos fuimos los que empezamos y sin embargo solo unos pocos continuamos nuestro camino juntos a lo largo de los años. En particular, quiero agradecer a dos personas que han estado ahí desde el principio, Diego y Deivid, los cuales me han acompañado en innumerables horas de estudio, de clases....y como no, de diversión, días y noches y muchas tardes de “subastado”, unos años que forman parte de lo mejor de mi vida y que nunca olvidaré.

Pero, especialmente a mi lado, ha estado uno de los pilares de mi vida, Laurita. La persona con la que he compartido los últimos 10 años de mi vida, siempre presente en mis mejores momentos y sosteniéndome en los malos. Nunca sabrá lo agradecido que estoy de haberla encontrado. Gracias.

Pero también he conocido a mucha gente desde que llegué al grupo Ephyslab, Fran, Alex, Ángel...todos han hecho que mi estancia aquí sea mejor. En particular, siempre tendrán un rincón en mi corazón los miembros de mi laboratorio, el grupo de los Pericos: “Marisela, Maestro, Susana, Miki, Santi, Lucía y Papito” ellos han hecho que cada mañana mereciera la pena venir a trabajar, ya que siempre había tiempo para unas risas y echarle una partidita de cartas, profundas charlas y amigos invisibles.

Por último, y no menos importante, tengo que hacer un agradecimiento a mi familia. Mis padres, que siempre han estado ahí, para todo lo que necesitase, en cualquier momento, bueno o malo, un apoyo, unos padres, unos amigos, lo que fuera. Si soy algo en la vida es gracias a ellos, sin más. También tengo que agradecer lo que soy a mi hermano, mi inspiración en la vida, él ha sido un ejemplo para todo lo bueno que siempre he intentado imitar, espero haberlo conseguido. También quiero recordar al resto de mi familia, abuelos, tías, primos...que siempre me han ayudado y han estado ahí para tenderme una mano cuando lo he necesitado. A los que están y a los que no, sé que, estéis donde estéis, os sentís orgullosos de mí como yo me he sentido y me siento de vosotros.

Este trabajo ha sido financiado por la Universidade de Vigo a través de las “Axudas predoutorais da convocatoria de axudas a investigación 2015”.

# Resumen

El océano es una gran fuente de recursos para el ser humano y, por tanto, es básico conocer en detalle aquellos mecanismos o variaciones que puedan ocurrir en él ya que pueden afectar de forma dramática tanto en términos socioeconómicos como de biodiversidad.

En este sentido, uno de los mecanismos más conocidos a nivel costero es el afloramiento. Este fenómeno ocurre cuando aparecen vientos paralelos a la costa, éstos provocan un movimiento de las masas de agua que son desviadas por el efecto Coriolis provocando lo que se conoce como Transporte de Ekman (Ekman, 1905), para que ocurra el afloramiento, es necesario que éste sea perpendicular a la costa. Debido a que el efecto Coriolis varía entre hemisferios, el Transporte de Ekman se produce a 90° en el sentido de las agujas del reloj respecto a la dirección del viento en el Hemisferio Norte. Sin embargo, en el Hemisferio Sur, se produce a 90° en el sentido contrario. Como consecuencia del movimiento de las aguas en sentido perpendicular a la costa, el agua desplazada es sustituida por agua más profunda la cual es usualmente más fría y rica en nutrientes, este hecho provoca un aumento de la productividad en la zona (Cushing, 1969; Ryther, 1969; Bakun, 1990; Carr and Kearns, 2003). Por lo tanto, es clave estudiar los cambios producidos en el afloramiento a lo largo de las últimas décadas ya que, éstos, pueden provocar variaciones en la productividad de las diferentes zonas e, incluso, migraciones de los peces o cambios en la tasa de captura de diferentes especies.

Algunas de las zonas más importantes de afloramiento son aquellas conocidas como EBUS (Eastern Boundary Upwelling Systems), estas son Benguela (Sur de África), Canarias (Norte de África), Humboldt (Sur de América) y California (Norte de América) (Patti et al., 2008; Patti et al., 2010; Narayan et al., 2010; Cheung et al., 2013). Sin embargo, estudios localizados en regiones más pequeñas gracias a los avances en bases de datos de alta resolución, han permitido sacar a la luz otras zonas de afloramiento entre las que destacan Somalia (Este de África), La Guajira (Sur del Mar Caribe), Java (Este del Océano Índico) o Yucatán (Sur del Golfo de México) entre otras (Susanto et al., 2001; Andrade and Barton, 2005; Santos et al., 2015; Ruiz-Castillo et al., 2016). La principal diferencia entre los EBUS y el resto de zonas de afloramiento es que las primeras suelen tener lo que se denomina como afloramiento permanente, esto significa que a lo largo de todo el año se presentan características favorables al afloramiento mientras que, en el resto, el afloramiento suele aparecer estacionalmente.

Numerosos estudios se han producido a lo largo de las últimas décadas para tratar de arrojar luz a la evolución del afloramiento. Quizá el avance más importante en ese sentido fue el realizado por Bakun, (1990) quien encontró un fortalecimiento de los sistemas de afloramiento más importantes del mundo. Además propuso que este fortalecimiento estaba siendo producido por el calentamiento global, esto se debía a que los continentes se estaban calentando más rápido que los océanos y, por tanto, se producía un aumento en el contraste termal entre tierra y océano. Esto, a su vez,

provocaría un incremento en los gradientes de presión entre tierra y océano y, finalmente, se reflejaría en un aumento de los vientos favorables al afloramiento. En consecuencia, el afloramiento aumenta, el aporte de agua más fría hacia la superficie se incrementa y, con ello, la productividad. Recientemente, diversos estudios han comprobado si la hipótesis de Bakun se está cumpliendo o no y, los resultados, difieren de forma significativa (Narayan et al., 2010; Sydeman et al., 2014). Si bien es cierto que algunos de los sistemas de afloramiento más importantes como California, Benguela o Humboldt presentan un reforzamiento en el afloramiento, también se observa que la tendencia difiere dependiendo de la zona estudiada, la duración del estudio, la época del año utilizada e, incluso, de la base de datos.

Otro foco importante de estudio ha sido y es la relación del afloramiento y la SST (temperatura superficial del océano). Como se mencionó anteriormente, como consecuencia de la aparición del afloramiento el agua costera presenta temperaturas inferiores a las oceánicas, efecto que puede observarse en la Figura 1 en las zonas más importantes de afloramiento. Esto supone que variaciones en el índice de afloramiento pueden provocar variaciones en la SST.

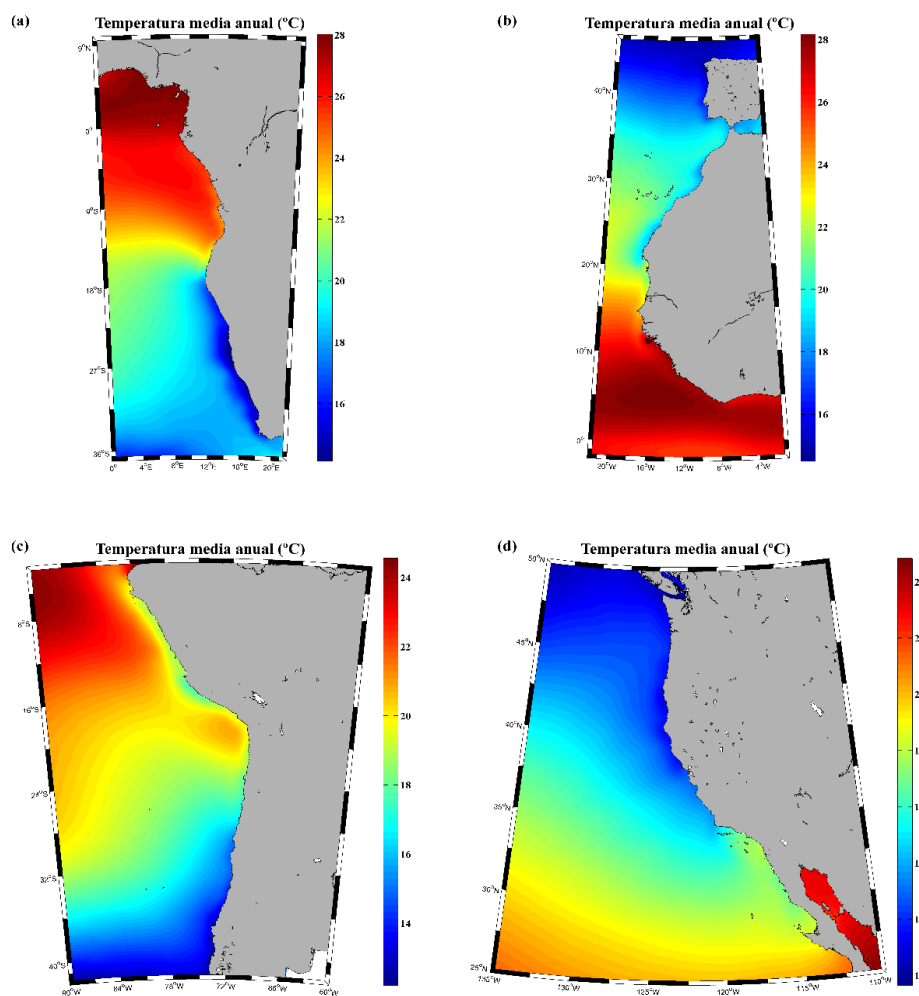


**Figura 1: Temperatura media anual (°C) en los cuatro sistemas de afloramiento más importantes. (a) Benguela, (b) Canarias, (c) Humboldt y (d) California**

Diferentes trabajos han sido realizados en los que se ha relacionado tendencias de afloramiento con cambios en la SST. En la Península Ibérica, Lemos and Sansó, (2006) y Santos et al., (2012a) encontraron diferencias de  $0.1^{\circ}\text{C dec}^{-1}$  entre océano y costa. En Benguela la diferencia aumentaba hasta los  $0.4^{\circ}\text{C dec}^{-1}$  y en Canarias alcanzaban los  $0.5^{\circ}\text{C dec}^{-1}$  (Santos et al., 2012b,c). Esto significa que aquellas zonas afectadas por el afloramiento parecen mantener tasas de calentamiento inferiores a las oceánicas e, incluso, algunas de las zonas más importantes de afloramiento muestran tasas de enfriamiento. Este hecho provoca que surja una importante pregunta: ¿está el afloramiento actuando como moderador del calentamiento global en las zonas afectadas por este mecanismo?

El calentamiento global a lo largo de las últimas décadas es un hecho probado por decenas de artículos (Cane et al., 1997; Harrison and Carson, 2007; Hansen et al., 2010; Lima and Wethey, 2012). Si bien este calentamiento no es homogéneo y depende de la zona de estudio (IPCC, 2014), una gran parte de los océanos mundiales presentan tasas de calentamiento, de hecho Lima and Wethey, (2012), encontraron que más del 71% de las costas mundiales se estaban calentando. Diferentes razones han sido expuestas para tratar de explicar la heterogeneidad de las tendencias de SST desde cambios en las corrientes oceánicas, el deshielo de los polos o variaciones en los patrones de vientos.

El objetivo principal de esta tesis es realizar un estudio de la evolución de las zonas de afloramiento a nivel mundial durante las últimas cuatro décadas para, posteriormente, comprobar cuál es el efecto de éstas sobre la SST. Además, se observará la influencia del afloramiento en zonas más particulares como son La Guajira, Java y Yucatán.

Para lograr estos objetivos es clave disponer de bases de datos de alta resolución tanto en tiempo como en espacio que puedan reproducir los efectos del afloramiento en las escalas necesarias para que se produzca este fenómeno. Anteriormente a la aparición de las medidas por satélite, las medidas eran mayoritariamente tomadas en campañas oceanográficas in-situ o por boyas. Esto provocaba que las medidas tuvieran diferentes problemas: no todas las áreas estaban igualmente estudiadas y eso provocaba falta de datos en muchas zonas del mundo, además el hecho de que las campañas se realizaran en momentos particulares suponía que los datos fueran discontinuos en el tiempo y, también, al ser datos tomados en zonas en particular éstos podían no representar con exactitud el comportamiento de la zona. Con la aparición de los satélites estos problemas fueron solucionados y, aunque como decíamos anteriormente los resultados siguen siendo dependientes de diferentes parámetros como la base de datos utilizada o la longitud de la misma, éstas suelen poderse utilizar para épocas largas y en zonas más grandes.

En particular, en esta tesis, se utilizarán diferentes bases de datos tanto de viento como de temperatura del océano, ya sea superficialmente como en profundidad. En cuanto al viento se utilizará la base de datos Climate Forecast System Reanalysis (CFSR) la cual ofrece datos de las últimas cuatro décadas con una resolución de aproximadamente  $0.3^{\circ} \times 0.3^{\circ}$ . Por otro lado, en cuanto a la temperatura se utilizarán diferentes bases de datos. La primera, conocida como Optimum Interpolation Sea Surface Temperature (OISST<sup>1/4</sup>), permite obtener datos de SST desde los años 80 con una resolución de  $0.25^{\circ} \times 0.25^{\circ}$ . En cuanto a las capas más profundas del océano se han utilizado dos bases diferentes. Por

un lado, Simple Ocean Data Assimilation (SODA) que dispone de datos desde la década de los 50 con 40 niveles de profundidad y una resolución horizontal de  $0.5 \times 0.5^\circ$ . Por el otro lado Hybrid Coordinate Ocean Model (HYCOM) permite una resolución de  $1/12^\circ \times 1/12^\circ$  horizontalmente con 40 niveles de profundidad desde los años 90 hasta hoy.

A continuación se detalla el contenido de los diferentes capítulos que conforman esta tesis:

En el Capítulo 1 se introducirán las motivaciones para la realización de la tesis. Para ello se definirá lo que es el afloramiento y se nombrarán algunos de los estudios que otros autores han realizado, de esta manera se pondrá de relieve la importancia del estudio de este fenómeno. Asimismo, se relacionará el afloramiento con el calentamiento global y se tratará de explicar los efectos y consecuencias de este calentamiento citando algunos de los trabajos más importantes, los cuales han mostrado como durante las últimas décadas la temperatura global ha ido aumentando.

En el Capítulo 2 se expondrán los objetivos principales de la tesis así como los medios utilizados para alcanzar dichos objetivos.

En el Capítulo 3 se realizará una breve introducción de los artículos que componen la tesis, se reflejarán sus autores, la revista en la que fueron publicados (así como sus características particulares) y el año de publicación. Posteriormente el capítulo 3 será subdividido en los diferentes artículos:

En el Capítulo 3.1 se realizará un estudio de la evolución del afloramiento en todas las costas mundiales en las últimas cuatro décadas. Para ello se utilizará como variable de estudio el wind stress, ya utilizada por Bakun, (1990) para mostrar un fortalecimiento del afloramiento en las regiones más importantes del mundo y definir la Hipótesis de Bakun anteriormente explicada. Cabe destacar que este estudio es el primero en el que todas las costas mundiales son estudiadas al mismo tiempo ya que, trabajos anteriores, se centraban solamente en las zonas más importantes de afloramiento o zonas muy particulares. Gracias al uso de una base de datos de alta resolución disponible para todo el mundo (CFSR), ha sido posible establecer una serie de condiciones iguales para todas las zonas que permitieron estudiar tanto las zonas más conocidas (EBUS) como otras menos conocidas. En particular, bajo los parámetros de estudio utilizados, se encontraron 10 sistemas de afloramiento: Benguela, Canarias, Sur del Mar Caribe, Chile, Perú, California, Oeste de Australia, Java, Norte de Kenia y Somalia-Oman. Los resultados de la evolución del afloramiento (a través del wind stress) en estas zonas mostraron una clara heterogeneidad entre los distintos sistemas de afloramiento. Mientras que para algunas zonas como Benguela, Canarias, Perú u Oeste de Australia la tendencia mostraba un reforzamiento en los vientos favorables al afloramiento, otras zonas como Chile, Java o Somalia mostraban una tendencia a disminuir el afloramiento. Otra zona importante como California no mostraba un comportamiento claro, teniendo tendencias negativas en el Sur y positivas en el Norte. Una comparación con trabajos de otros autores en todas las zonas consideradas sacó a la luz la dependencia de los resultados de diferentes parámetros. En primer lugar se observó que estudios en la misma zona diferían en resultado dependiendo de la base de datos utilizada. Asimismo, la longitud de la serie de datos o el período del año considerado como época de

afloramiento también eran claves en la comparación con otros estudios. Finalmente, la heterogeneidad de las tendencias de los vientos favorables al afloramiento deja dudas acerca de si se está cumpliendo la hipótesis de Bakun ya que si bien algunas de las zonas más importantes en cuanto a afloramiento mostraban un reforzamiento, muchas otras mostraban el comportamiento contrario.

El Capítulo 3.2 se centrará en mostrar cual es la influencia del afloramiento en el calentamiento global en las zonas costeras. Para ello se realizará un estudio de las diferencias entre costa y océano en todas las costas mundiales, de esta manera será posible estudiar el efecto del afloramiento comparando las diferencias de temperatura entre costa y océano en aquellas regiones afectadas por el afloramiento y aquellas que no lo están. Para llevar a cabo este proceso se dividirán las costas mundiales en 6 secciones: costa este y oeste del Océano Atlántico, Océano Pacífico y Océano Índico. Posteriormente se obtendrán las tendencias de temperatura para costa y océano para finalmente restarlas obteniendo las diferencias costa-océano. Para seleccionar las zonas de afloramiento que se tendrán en cuenta en la comparación se realizó un extenso estudio de trabajos previos a partir de los cuales se eligieron aquellas áreas más estudiadas y más importantes: en la costa Este del Océano Atlántico se encontraron Benguela, Canarias y la Península Ibérica; en la costa Oeste, Brasil, Sur del Mar Caribe y Yucatán; en la costa Este del Océano Pacífico se seleccionaron Chile, Perú y California mientras que en la costa oeste se encontró el Este de Australia; en la costa Este del Océano Índico se encontraron Sur de Australia, Oeste de Australia, Java-Sumatra y el Este de India; finalmente en la costa Oeste, Agulhas, Kenia, Somalia, Omán y Oeste de India. Los resultados a nivel global mostraron que el 92% de las localidades oceánicas presentaban calentamiento, mientras que se reducía sensiblemente en las zonas costeras a un 87%. Comparando las zonas oceánicas y costeras, se observó que un 66% de las localidades oceánicas tenían una tendencia mayor que las costeras adyacentes. Sin embargo, esta tendencia no es homogénea para todas las zonas del mundo observándose algunas diferencias entre las distintas cuencas. En particular, en la costa Este del Océano Índico se observó que el 74% del océano se calentaba más rápidamente que la costa mientras que, en la costa Este del Océano Pacífico, se reducía a un 47% siendo la única cuenca del mundo donde la costa muestra un mayor calentamiento que las localidades oceánicas adyacentes. Finalmente, se estableció la comparación entre lo que sucedía en las zonas afectadas por el afloramiento y las que no. Se observó que en las zonas de afloramiento el calentamiento era mayor en el océano que en la costa en más del 92% de las localizaciones. Este comportamiento se reducía drásticamente en las zonas sin afloramiento produciéndose prácticamente un balance entre costa y océano, ya que solamente el 58% de las localidades oceánicas mostraban un mayor calentamiento que las costeras. Por lo tanto, como conclusión, es evidente que aquellas zonas afectadas por el afloramiento muestran un calentamiento menor que aquellas que no están afectadas, actuando el afloramiento como un moderador del calentamiento global.

Entre el Capítulo 3.3 y el 3.5 los estudios se dirigirán a zonas particulares (La Guajira en Colombia, Java y Yucatán) para comprobar cuál es la influencia del afloramiento sobre las tendencias de la SST en esas zonas y cómo funciona este mecanismo.



En cuanto al Capítulo 3.3, estará centrado en la zona de La Guajira situada al Norte de Colombia. La Guajira está caracterizada por presentar un afloramiento estacional provocado por vientos asociados al Caribbean Low-Level Jet (CLLJ) principalmente durante los meses de Enero, Febrero y Marzo. Se comprobó que para estos meses se obtenía una tendencia al enfriamiento en la costa de La Guajira, lo cual contrastaba con una tendencia al calentamiento en la región del Caribe. Como se mencionó anteriormente, variaciones en el afloramiento podrían estar relacionadas con variaciones en la SST. Por ello, se llevó a cabo un estudio de la evolución del afloramiento en la zona. Los resultados mostraron una sección de la costa en la que el afloramiento había sufrido un reforzamiento a lo largo de las últimas cuatro décadas, sin embargo, esta zona no coincidía con el área en que la temperatura había mostrado un enfriamiento. Este hecho fue relacionado con la existencia de la conocida como Caribbean Coastal Undercurrent (CCU), la cual provoca un movimiento hacia el este de las masas de agua de la zona. Por tanto, aunque el afloramiento ocurre en una determinada área de la costa, el agua es desplazada verticalmente por el afloramiento y hacia el este por la corriente caribeña provocando que el enfriamiento no se produzca exactamente en la zona donde se produce el reforzamiento del afloramiento si no unos grados más hacia el este.

En el Capítulo 3.4 se evalúa la influencia del afloramiento sobre las tendencias de temperatura en la zona de Java. Esta zona presenta características similares a La Guajira, ya que se observa un afloramiento estacional en los meses de Julio a Octubre reflejado en una tendencia al enfriamiento en la costa. Sin embargo, al contrario que en el caso anterior esta tendencia no está relacionada con un fortalecimiento del afloramiento. Por lo tanto, se realizó un estudio más profundo de los diferentes forzamientos que provocan esa tendencia al enfriamiento. Una vez descartado el intercambio de calor entre el océano y la atmósfera como causa principal, se comprobó que las capas inferiores de agua, procedentes de la South Java Current (SJC) que afloraban en la costa, habían sufrido un enfriamiento durante las últimas tres décadas. Por lo tanto, aunque el afloramiento no se reforzó, el mecanismo seguía siendo suficiente para bombear el agua más fría de las capas inferiores.

Finalmente, el Capítulo 3.5, estará localizado en el sistema de afloramiento de Yucatán en el que se estudiarán los diferentes forzamientos que dan lugar a diferencias de tendencia de temperatura entre la costa y el océano. Al igual que en el caso de La Guajira y Java, Yucatán muestra un afloramiento estacional entre Mayo y Septiembre relacionado con vientos favorables al afloramiento. Como ocurría en Java, no se observa un fortalecimiento del afloramiento durante las últimas décadas y, por tanto, se estudiaron otros forzamientos que pudieran provocar el enfriamiento observado en la costa. Teniendo en cuenta trabajos de otros autores en la zona, se realizó un estudio de la Corriente de Yucatán, la cual, según estudios anteriores, podía ser un elemento clave en la zona ya que, dependiendo de la evolución de su trayectoria, producía cambios en el comportamiento del afloramiento en la costa de Yucatán. En este sentido, se observó que la Corriente de Yucatán mostraba un desplazamiento hacia el este a lo largo de las últimas décadas lo cual favorecía la aparición de un mayor transporte vertical en la zona este de la costa de Yucatán. Además, se encontró que la masa de agua que afloraba en Yucatán mostraba un enfriamiento desde la década de los 80 debido a una elevación de las isopícnas sin cambio en las propiedades intrínsecas de la masa de agua. Por lo tanto,

se concluyó que el enfriamiento en la costa norte de Yucatán era debido a una mezcla de diferentes forzamientos. En primer lugar, un desplazamiento hacia el este de la corriente de Yucatán favorecería mayores velocidades verticales en la zona este de Yucatán, provocando un ascenso de masas de agua que se habrían enfriado a lo largo de las últimas décadas. Finalmente, esa agua situada al este de Yucatán sufriría un desplazamiento hacia el oeste debido a la prevalencia de vientos de este a oeste, los cuales favorecen la aparición del afloramiento, para, finalmente, aflorar a lo largo de la costa norte de Yucatán.

En el Capítulo 4 se realizará una breve discusión sobre los artículos mostrados en el capítulo 3, dotando de coherencia y unidad a la tesis.

Por último, en el Capítulo 5, se expondrán las conclusiones finales y principales de la tesis como resumen de las cuestiones más importantes de la misma.





# Table of contents

Acknowledgments .....	i
Resume .....	ii
Table of contents .....	x
<b>Chapter 1: Introduction</b> .....	1
1.1. Motivation .....	1
1.2. Structure of this work .....	8
<b>Chapter 2: Objectives</b> .....	11
<b>Chapter 3: Set of publications</b> .....	13
3.1. “Has upwelling strengthened along worldwide coasts over 1982-2010?” .....	15
3.2. “Coastal warming and wind-driven upwelling: a global analysis” .....	31
3.3. “Influence of upwelling on SST Trends in La Guajira system” .....	62
3.4. “Influence of Coastal Upwelling on SST Trends along the South Coast of Java” .....	75
3.5. “Differences in coastal and oceanic SST trends north of Yucatan Peninsula” .....	90
<b>Chapter 4: Discussion</b> .....	121
<b>Chapter 5: Main conclusions</b> .....	126
Acronym and Abbreviation List .....	129
List of Figures .....	132

List of Tables .....	139
Bibliography .....	142
List of publications .....	162

# Chapter 1

## *Introduction*

### 1.1 Motivation

Coastal upwelling systems are among the most productive of the world's ecosystems being areas with high ecological and socio-economic impact. Thus, coastal upwelling is, possibly, one of the best-studied oceanographic processes all over the ocean. This phenomenon is generated by winds blowing parallel to the shoreline causing an Ekman Transport directed offshore. As a consequence, surface waters are displaced away from the coast and replaced by deeper water. This water, is normally colder than surface water and richer in nutrients, which enhances primary production. Figure 1 shows schematically how upwelling occurs in the eastern oceanic basins in the north Hemisphere.

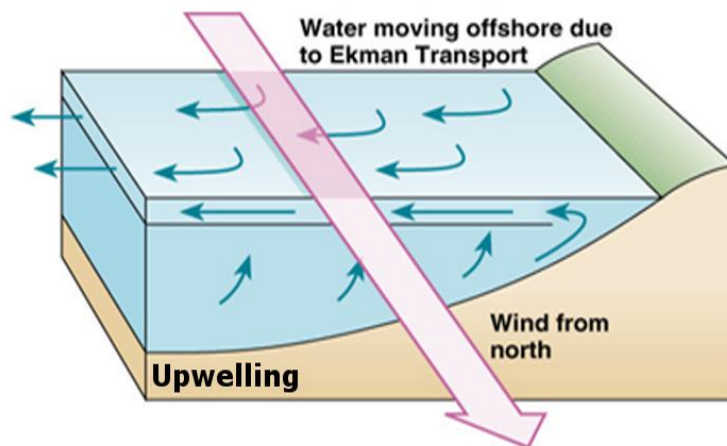


**Figure 1:** Scheme of the interaction between wind and oceanic water that causes upwelling. Source: NC State University Education

Upwelling systems are areas of great importance in economical and biological terms. In fact, they only cover 1% of the ocean areas worldwide but more than 20% of the fishing captures take place in these zones (Pauly and Christensen, 1995) (Figure 2). Knowing in depth how, when and where coastal upwelling occurs is therefore very useful, mainly for fishing activity.

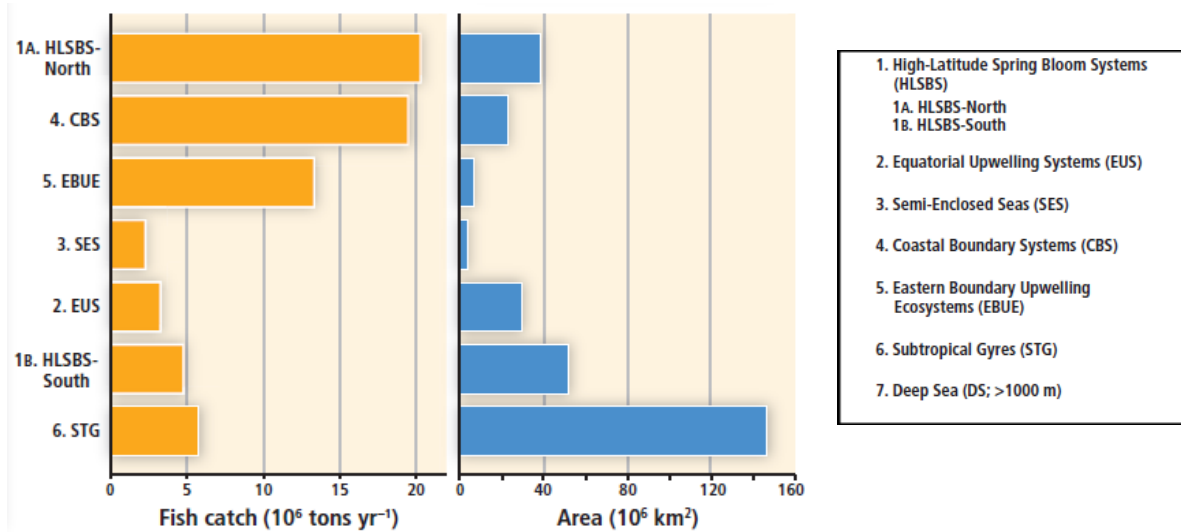


**Figure 2:** Relation between fish catches and the area of the ocean during the period 1970-2006. Source: Adaptation of the Figure 30-1 from IPCC, (2014)

Due to the importance of upwelling phenomena, these have been extensively studied over the world. The four most important upwelling systems are Benguela (South Africa), Canary (North Africa), Humboldt (South America) and California (North America), called the Eastern Boundary Upwelling Systems (EBUS) (Figure 3) (Carr and Kearns, 2003; Patti et al., 2008, Demarcq, 2009; Messie et al., 2009; Patti et al., 2010; Narayan et al., 2010; Pardo et al., 2011; Wang et al., 2015).

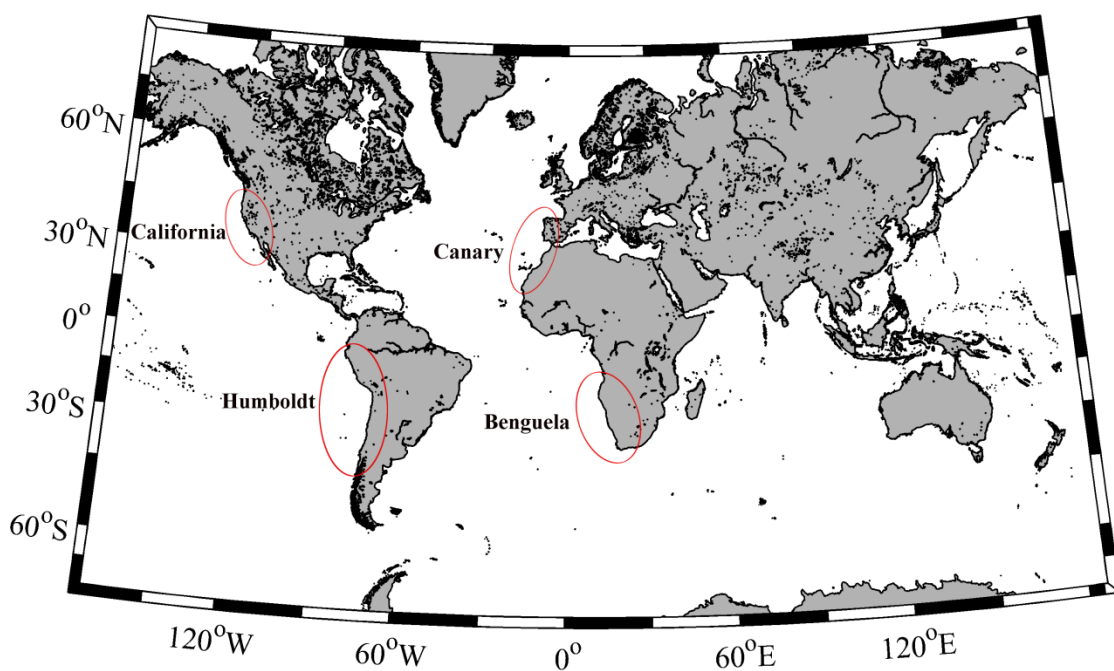


**Figure 3:** Situation of the Eastern Boundary Upwelling Systems (EBUS)

The Benguela upwelling system is considered one of the most important marine ecosystems in the world due to its biodiversity and productivity. The area supports large fish catches of many different species of commercial interest like lobster, sardines or haddock (Barange et al., 1991a,b; Timonin et al., 1992; Villanueva and Sánchez, 1993; Hewitson and Cruickshank, 1993). In fact, there is a marine protected area in the southern Namibian coast and in the adjacent islands due to the great importance of upwelling in the zone. This upwelling system is characterized by strong southeasterly trade winds (Nelson and Hutchings, 1983; Fennel, 1999) with latitudinal differences. Maximum alongshore winds are usually found around 25°S and decrease towards the frontiers of the upwelling system (Fennel, 1999).

The Canary upwelling system supports fishing activities in the area covering from North Africa to the Iberian Peninsula (until cape Finisterre) due to the abundance of small pelagic fish species (Belveze and Erzini, 1983; Kifani, 1998; ICES, 2002; Borges et al., 2003; Arístegui et al., 2004; Kämpf and Chapman, 2016). Previous studies considered that the Canary upwelling system is formed by two different areas separated by the Strait of Gibraltar, the first one in the area of the Canary Current in the northwest of Africa and the second one related to the Portugal Current in the western Iberian Peninsula (Kämpf and Chapman, 2016). Numerous studies focused on upwelling impact have been carried out over the last decade in the area (Gómez-Gesteira et al., 2008a; Patti et al., 2008; Arístegui et al., 2009; Pardo et al., 2011).

The particular characteristics of the Humboldt upwelling system turns the area into one of the most important spots in terms of fish catches (Sherman and Hempel, 2009). In particular, this area yields the higher catch rate for the anchovy in the world (Schwartzlose et al., 1999; Barange et al., 2010; Serra et al., 2012; Cahuin et al., 2013) and sustains the industrial economy of a larger number of areas in Chile and Peru. The Humboldt upwelling region occupies a wide area in the west of South America including the coasts of Chile to Peru where southerly winds sweep the coast inducing upwelling (Wooster and Reid, 1963; Brandhorst, 1971; Peterson et al., 1988; Ahumada, 1989; Cáceres and Arcos, 1991; Strub et al., 1998; Goubanova et al., 2011; Rahn and Garreaud, 2013). As for the previous EBUS, several studies focused on coastal upwelling have been carried out over the last decade (Yuras et al., 2005; Sobarzo et al., 2007; Renault et al., 2009; Falvey and Garreaud, 2009; Goubanova et al., 2011; Gutiérrez et al., 2011; Rahn, 2012; Rahn and Garreaud, 2013; Aravena et al., 2014).

The last EBUS is the California upwelling system. Although the occurrence of upwelling is highly variable depending on latitude, the entire area promotes the production of phytoplankton which feeds a wide range of marine fauna, for example, mesozooplankton (Roemmich and McGowan, 1995; Dorman et al., 2005; Hooff and Peterson, 2006), pelagic fish (Schirripa and Colbert, 2006) or seabirds (Miller and Sydeman, 2004; Schroeder et al., 2009). The economic value of the fisheries in the area is also very important with different species as dungeness crab, sablefish or salmon (Leet, 2001; Schroeder and Love, 2002). The occurrence of upwelling in the area is due

to northwesterly alongshore winds along the coast which cause a flow of cool water from the Gulf of Alaska (Snyder et al., 2003).

In addition to the major eastern boundary current systems, studies at regional scales have also shown other upwelling systems worldwide as La Guajira (Colombia), Yucatan (South Gulf of Mexico), Sumatra-Java (Eastern Indian Ocean) or Somalia (Western Indian Ocean) among others (Conan and Brummer, 2000; Susanto et al., 2001; Andrade and Barton, 2005; Qu et al., 2005; Zavala-Hidalgo et al., 2006; Rueda-Roa and Müller-Karger, 2013; Santos et al., 2015; Ruiz-Castillo et al., 2016).

Changes in upwelling strength and timing have attracted considerable scientific interest in recent decades due to the possible ecosystem and socio-economic effects caused by climatic modulations. In several studies, researchers have primarily focused on analyzing trends in wind strength due to climate variability and the resultant changes in the coastal upwelling process. In 1990, Bakun found a reinforcement of upwelling in some of the major upwelling systems (California, Peru and Canary) using wind data from 1945 to 1985 (Bakun, 1990). This fact was related to a mechanism which intensify the alongshore wind stress on the ocean surface, causing a strengthening of upwelling. This mechanism is based in the different rate of warming between the ocean and land due to the global warming. This difference is reflected in an increase of the pressure gradients between ocean and land which cause a raise in the upwelling favourable winds (Bakun, 1990).

Numerous studies on different upwelling regions have been conducted to investigate the Bakun hypothesis using historical wind data (Patti et al., 2010; Narayan et al., 2010; García-Reyes and Largier, 2010; Pardo et al., 2011; Seo et al., 2012; Barton et al., 2013; Cropper et al., 2014; Sydeman et al., 2014). Nevertheless, different results have been obtained, which indicate that wind estimates from different databases can differ in trends and variability (Hansen et al., 2006; Lemos and Sansó, 2006; McGregor et al., 2007; Álvarez et al., 2008; deCastro et al., 2009; Santos et al., 2012a,b,c; Barton et al., 2013; Cropper et al., 2014). In addition, numerous available time series present a spatial resolution that is too coarse to accurately resolve conditions at the scale of coastal upwelling in intense and localized upwelling zones.

Although most of the studies previously mentioned have been carried out in terms of upwelling favourable winds, the general warming of ocean temperatures is also an important process to analyze coastal upwelling. In fact, Di Lorenzo et al., (2005) found that upwelling favorable winds have intensified in average over the last decades (1949-2000) along the California current system. Nevertheless, a general warming in the upper 200 m was also reported producing a deepening of the thermocline and a stronger stratification which reduces the vertical transport associated with upwelling.

Several studies have been conducted in order to analyze the evolution of Sea Surface Temperature (SST) in the last decades of strong climate change due to the importance of the impacts of rapid climatic variations on the world that would entail major alterations in different biologic and socio-economic systems (Harley et al., 2006; Halpern et al.,

2008). Changes in the ocean are especially important due to its high thermal inertia. In this sense, several studies have reported an increase in the sea surface temperature and the heat gained by the ocean (Cane et al., 1997; Levitus et al., 2000, 2005; Mikaloff-Fletcher et al., 2006, Harrison and Carson, 2007; Belkin, 2009; Hansen et al., 2010, Levitus et al., 2012). Levitus et al., (2000) found an increase in the heat content of the world ocean around  $2 \times 10^{23}$  Joules between mid-1950 and mid-1990. This value represents a warming of  $0.06^{\circ}\text{C}$ . Belkin, (2009) using data from the U.K. Meteorological Office Hadley Centre SST climatology from 1957 to 2006 found a warming in most of the worldwide coasts, especially in the Subarctic Gyre, in the European Seas and in the East Asian Seas. However, the area of Humboldt and California upwelling systems showed a moderate cooling trend. Lima and Wetthey, (2012), found that more than 71% of the world's coastlines have warmed over the period 1982-2010. However, this warming is far from been homogenous. They observed that the regions with the highest warming were the Tropic of Cancer, Eastern China, Western Africa or Northeast South America among others, while for areas like West South America or West Australia SST tended to decrease (Figure 4).

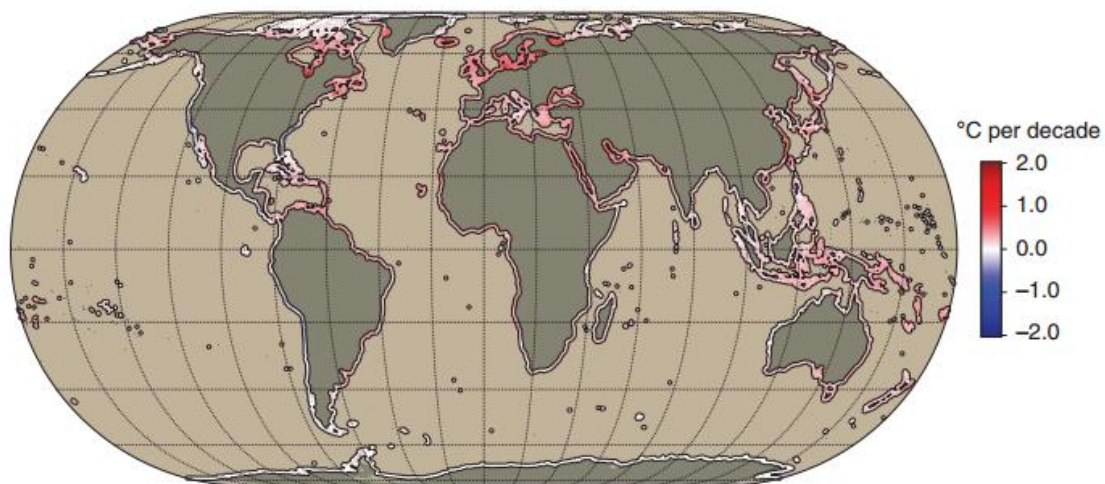


**Figure 4:** Warming rates for the period between 1982 and 2010, expressed in  $^{\circ}\text{C}$  per decade. Red indicates warming and blue indicates cooling. Source: Lima and Wetthey, (2012).

The heterogeneity of the warming trends has led to conduct numerous studies at regional scale. Over the last years, several authors have described differences between warming rates at coastal and adjacent ocean locations in different coastal upwelling systems (Lemos and Sansó, 2006; Santos et al., 2012a,b,c). Thus, Lemos and Sansó, (2006) found a difference of  $0.1^{\circ}\text{C dec}^{-1}$  between coast and ocean locations along the western Iberian Peninsula using data with a spatial resolution of  $0.25^{\circ} \times 0.25^{\circ}$  from 1901 to 2000. Similar results were obtained by Santos et al., (2012a) from 1958 to 2008 at a scale of  $0.5^{\circ}$ . In the Canary upwelling system, Santos et al., (2012b) detected an ocean warming rate higher than the coastal one (around  $0.5^{\circ}\text{C dec}^{-1}$ ) from 1982 to 2010 using high resolution SST data ( $4 \times 4$  km). Santos et al., (2012c) also observed weaker



warming trends at coastal locations along the Benguela upwelling system from 1970 to 2009 considering data on a  $1^\circ \times 1^\circ$  grid (difference ocean-coast  $\sim 0.4^\circ\text{C dec}^{-1}$ ). Most of these studies have linked the different warming rates between coast and ocean with the strengthening of coastal upwelling, suggesting the role of upwelling as a moderator of general SST increase in coasts affected by this mechanism.

These facts raise several questions about the role of coastal upwelling in the actual global warming scenario. Is coastal upwelling influencing coastal SST warming worldwide? Is coastal upwelling preventing warming in near-shore areas? Thus, the analysis of the effects of climate change on coastal upwelling systems is a very important task. Variations in the characteristics of the oceanic coastal areas can lead to dramatic consequences in terms of fishing, biodiversity or fish migration. Under a warming scenario and taking into account the Bakun hypothesis, upwelling intensity is expected to increase. However, an excessive increment of upwelling could lead to more hypoxic events, a rise in the acidity of the ocean and, in consequence, changes in the biological characteristics of the organisms of these areas (Lluch-Cota et al., 2014).

A resume of the potential impacts of changes in upwelling can be observed in Figure 5.

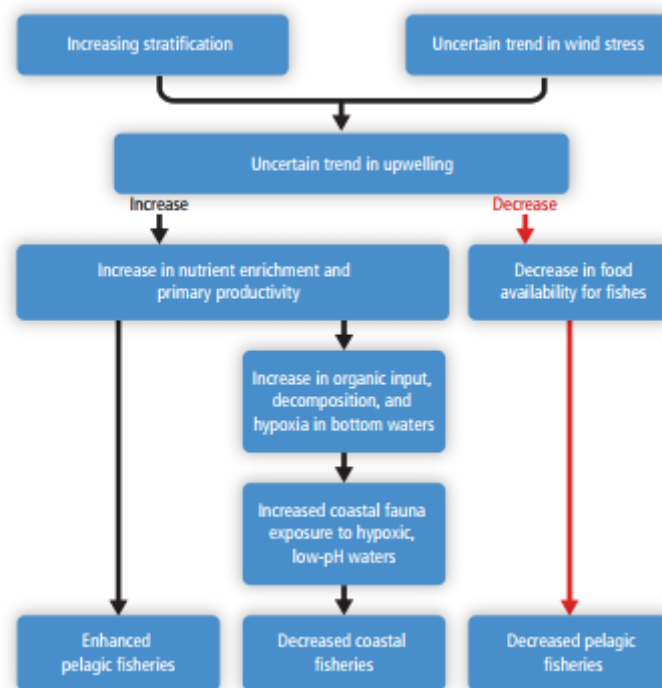


**Figure 5:** Potential impacts of changes in upwelling over the biodiversity. Source: Lluch-Cota et al., (2014).

As previously mentioned, several studies focused on different upwelling regions have been conducted over the last decades to investigate upwelling variations, both in terms of upwelling favorable winds and SST. Nevertheless, results obtained from different data products, even in the same area, may vary because they are highly dependent on the length of the time series. In addition, numerous available time series present a

spatial resolution that is too coarse to accurately resolve conditions at the scale of coastal upwelling in intense and localized upwelling zones. Thus, higher-resolution temporal scales and greater spatial-resolution studies are needed.

The use of satellite data provides global measurements about oceanographic patterns that can now be solved with high resolution. Taking advantage of this fact, all the coasts worldwide can be studied using the same database for the same period, allowing to investigate the evolution of upwelling along the last decades of strong climate change.

The present thesis has the motivation to objectively and decisively contribute to the progress in the research on upwelling variability. To achieve this purpose, this work aims to evaluate the worldwide evolution of upwelling and its influence in the SST trends using high resolution temporal and spatial data over the last decades.

Trends in coastal upwelling will be analyzed using the Climate Forecast System Reanalysis (CFSR) wind database, with high spatial resolution (approximately  $0.3^\circ$ ) from 1982 to 2010. This database facilitates the analysis of wind behavior at a small scale, which is a key factor when considering coastal mesoscale effects as upwelling. Recent studies have compared this database and different wind products with wind measured by several buoys along the Iberian Peninsula coast (Álvarez et al., 2014; Carvalho et al., 2014a,b) showing that datasets with finer spatial resolution, such as CFSR, gave better results, especially near the coast (Figure 6).

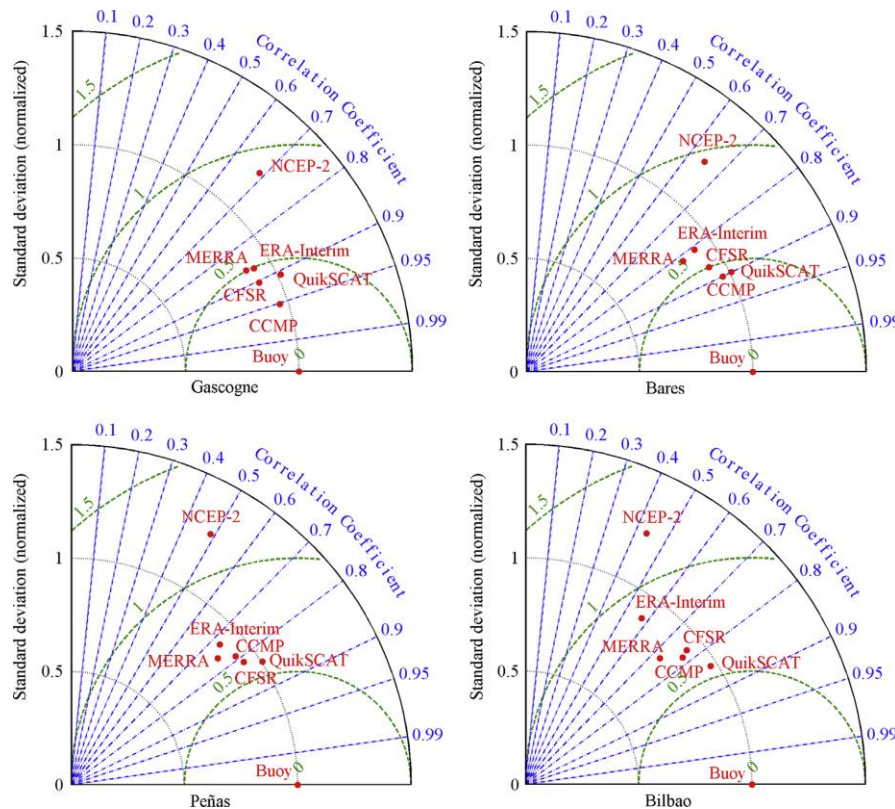


**Figure 6:** Taylor diagrams for wind speed for the comparison of buoy wind data and different wind products in four different locations. Source: Álvarez et al., (2014).

SST trends will be also analyzed worldwide using high resolution spatial data obtained from the Optimum Interpolation Sea Surface Temperature (OISST)  $\frac{1}{4}$  database. This database uses Advanced Very High Resolution radiometer (AVHRR) infrared satellite SST data as well as data from ships and buoys to build a regular global grid with a spatial resolution of  $0.25^\circ \times 0.25^\circ$ . Thus, SST trends will be related to upwelling during the last decades of strong climate change.

In addition to the worldwide study of upwelling and its influence in the SST, this work also investigates the influence of upwelling on SST trends in some localized areas where the relation between upwelling and SST trends shows particular conditions as La Guajira upwelling system, the South Coast of Java and north of Yucatan Peninsula. To accomplish this analysis, other variables as heat flux or ocean currents, will be additionally considered. A summary of the different variables and databases used in the present thesis is shown in Table 1.

Variable		Database	Spatial resolution	Temporal resolution
Wind		CFSR	$\sim 0.3^{\circ} \times 0.3^{\circ}$	1982-2015
SST	Surface	(OISST) $\frac{1}{4}$	$0.25^{\circ} \times 0.25^{\circ}$	1982-2015
	Deeper layers	SODA	$0.5^{\circ} \times 0.5^{\circ}$	1982-2010
		HYCOM	$1/12^{\circ} \times 1/12^{\circ}$	1993-2015
Heat flux		CFSR	$\sim 0.3^{\circ} \times 0.3^{\circ}$	1982-2015
Ocean currents		HYCOM	$1/12^{\circ} \times 1/12^{\circ}$	1993-2015

**Table 1:** Databases used in the present thesis. Temporal resolution is related to the periods used in the studies.

## 1.2 Structure of this work

Due to the fact that all the work developed in this thesis was already published (or is currently submitted for publication) in international peer-reviewed scientific journals, this thesis was structured in the following way:

*Chapter 1* presents the motivation of the work developed in the present thesis as well as literature surveys regarding the state of the art of the topic under investigation.

*Chapter 2* presents a description of the objectives to be achieved.

*Chapter 3* includes the published and submitted articles.

- *Article 1* details the research about the evolution of coastal upwelling worldwide in terms of wind stress data obtained from the CFSR database over 1982-2010. This work also intends to check if the Bakun hypothesis is being fulfilled during the last three decades of strong climate change.
- *Article 2* focuses in the analysis of coastal and oceanic worldwide SST trends to assess the role of upwelling in the heterogeneity of the SST trends from 1982 to 2015. Areas affected and unaffected by upwelling are compared to evaluate a possible influence of upwelling in SST trends using data from the OISST  $\frac{1}{4}$  database.
- *Article 3* details the influence of upwelling on the SST cooling observed in La Guajira upwelling system from 1982 to 2014.
- *Article 4* describes the origin of coastal cooling along the South Coast of Java evaluating variations in upwelling, heat fluxes and changes in the temperature of the water masses from the deeper layers that upwells along the coast.
- *Article 5* analyses differences in coastal and oceanic SST trends north of Yucatan Peninsula. Due to the complexity of the area, different forcings are investigated: upwelling evolution, heat fluxes, changes in the SST trends and changes in the direction of the Yucatan Current.

*Chapter 4* presents a general discussion about the results obtained in Chapter 3.

*Chapter 5* presents an integrated synthesis of the main conclusions derived from the research presented in Chapter 3.



# Chapter 2

## *Objectives*

The objectives of this thesis can be summarized as follows:

1. To analyze the evolution of coastal upwelling during the last three decades of intense climate change.
2. To investigate the influence of upwelling in the SST trends worldwide and in some localized areas.

To achieve these objectives, several analysis were carried out and divided in different articles. Thus, the first article presented in Chapter 3 aims, in a first step, to select the most important upwelling areas around the world in terms of wind stress taking advantage of a high resolution database (CFSR). Then, the evolution of these upwelling areas will be analyzed during the last decades of intense climate change (1982-2010). Results will be compared with those previously obtained by other authors along different areas and the Bakun hypothesis will be checked.

The second article intends to create a global map of SST differences between coast and ocean along the worldwide coasts using data from the OISST  $\frac{1}{4}$  database over the period 1982 to 2015. Results will be also compared with previous works to determine those upwelling areas which will be analyzed. Then, the influence of upwelling on SST trends will be studied by comparing the results obtained in areas considered as upwelling or non-upwelling regions.

The three last articles present some purposes in common. Thus, the main goal is to examine the influence of upwelling on SST trends along La Guajira upwelling system, the south coast of Java and north of Yucatan Peninsula. Firstly, SST trends between coast and ocean will be analyzed. Then, the cause of these trends will be investigated in terms of upwelling and other different forcings as heat fluxes or currents evolution.



## Chapter 3

### *Set of publications*

The first article presented in this thesis is titled: **"Has upwelling strengthened along worldwide coasts over 1982-2010?"** by R. Varela, I. Álvarez, F. Santos, M. deCastro and M. Gómez-Gesteira. Published in **2015** in the journal **"Scientific Reports"**.

The second article presented in this thesis is titled: **"Coastal warming and wind-driven upwelling: a global analysis"** by R. Varela, F. P. Lima, R. Seabra, C. Meneghesso and M. Gómez-Gesteira. The article is **under review** in the journal **"Science of the total environment"**.

The third article presented in this thesis is titled: **"Influence of upwelling on SST trends in La Guajira system"** by F. Santos, M. Gómez-Gesteira, R. Varela, M. Ruiz-Ochoa and J. M. Dias. Published in **2016** in the journal **"Journal of Geophysical Research: Oceans"**.

The fourth article presented in this thesis is titled: **"Influence of coastal upwelling on SST trends along the South coast of Java"** by R. Varela, F. Santos, M. Gómez-Gesteira, I. Álvarez, X. Costoya and J. M. Dias. Published in **2016** in the journal: **"Plos One"**.

The fifth article presented in this thesis is titled: **"Differences in coastal and oceanic SST trends north of Yucatan Peninsula"** by R. Varela, X. Costoya, M. Gómez-Gesteira and C. Enríquez. The article is **under review** in the journal **"Journal of marine systems"**.



In the Table 1 is showed a summary of the particular characteristics of each journal:

Journal	Category	Rank	Quartile	Impact Factor
Scientific Reports	Multidisciplinary Sciences	10/64	Q1	5.228
Science of the total environment	Environmental Sciences	22/229	Q1	4.900
Journal of Geophysical Research: Oceans	Oceanography	11/63	Q1	2.939
Plos One	Multidisciplinary Sciences	15/64	Q1	2.806
Journal of marine systems	Marine and freshwater biology	22/105	Q1	2.439

**Table 1:** Summary of the particular characteristics of the journals where were published the papers of this thesis.

# SCIENTIFIC REPORTS

OPEN

## Has upwelling strengthened along worldwide coasts over 1982-2010?

R. Varela<sup>1</sup>, I. Álvarez<sup>1,2</sup>, F. Santos<sup>1,2</sup>, M. deCastro<sup>1</sup> & M. Gómez-Gesteira<sup>1</sup>

Received: 30 October 2014

Accepted: 25 March 2015

Published: 08 May 2015

Changes in coastal upwelling strength have been widely studied since 1990 when Bakun proposed that global warming can induce the intensification of upwelling in coastal areas. Whether present wind trends support this hypothesis remains controversial, as results of previous studies seem to depend on the study area, the length of the time series, the season, and even the database used. In this study, temporal and spatial trends in the coastal upwelling regime worldwide were investigated during upwelling seasons from 1982 to 2010 using a single wind database (Climate Forecast System Reanalysis) with high spatial resolution (0.3°). Of the major upwelling systems, increasing trends were only observed in the coastal areas of Benguela, Peru, Canary, and northern California. A tendency for an increase in upwelling-favourable winds was also identified along several less studied regions, such as the western Australian and southern Caribbean coasts.

Wind-driven coastal upwelling results from the action of winds along a coast that generate an Ekman drift directed offshore. This causes pumping of cool and nutrient-rich water towards the sea surface along a narrow region close to the coast, which enhances primary production. Thus, coastal upwelling systems are among the most productive marine regions in the world's oceans.

Due to the ecological and economic importance of these regions, changes in upwelling strength and timing have attracted considerable scientific interest in recent decades. In several studies, researchers have primarily focussed on analysing trends in wind strength due to climate variability and the resultant changes in the coastal upwelling process. In 1990, Bakun<sup>1</sup> reported the strengthening of upwelling intensity along the major coastal upwelling systems of the world from 1945 to 1985. He proposed that this increase was due to global warming, which would create an intensification of the land-sea thermal contrast. This intensification would be reflected in increased land-sea pressure gradients, which in turn would cause the strengthening of upwelling-favourable winds that would result in cooling of the ocean surface.

Studies focused on different upwelling regions have been conducted to investigate the Bakun hypothesis through an analysis of available wind data. However, these studies reported contradictory results, which indicate that wind estimates from different databases can differ in trends and variability<sup>2</sup>. In addition, existing time-series data are limited in duration, quality, and spatial extent, and results obtained from different data products in the same area may vary because they are highly dependent on the length of the time series. Recently, Sydeman *et al.*<sup>3</sup> conducted an analysis of the literature on upwelling-favourable winds along the major eastern boundary current systems to test the Bakun hypothesis. They synthesized results from more than 20 studies published between 1990 and 2012 based on time series ranging in duration from 17 to 61 years. Most of published data support general wind intensification in the California, Benguela, and Humboldt upwelling systems and weakening in the Iberian system. This study highlighted the dependence of the results on the length of the time series and season, and it revealed contradictory results between observational data and model-data reanalysis. In addition, numerous available time series present a spatial resolution that is too coarse to accurately resolve conditions at the scale of coastal upwelling in intense and localized upwelling zones. Thus, higher-resolution temporal scales and greater spatial-resolution studies are needed.

<sup>1</sup>EPHysLab, Departamento de Física Aplicada, Facultade de Ciencias, Universidade de Vigo, Ourense, España.

<sup>2</sup>CESAM, Departamento de Física, Universidade de Aveiro, 3810-193, Aveiro, Portugal. Correspondence and requests for materials should be addressed to R.V. (email: ruvarela@uvigo.es)

The aim of this study was to identify the temporal and spatial trends in coastal upwelling regimes worldwide using wind stress data from the National Centers for Environmental Prediction (NCEP) Climate Forecast System Reanalysis (CFSR)<sup>4</sup> database. This database provides high spatial resolution (approximately 0.3°) with data available from 1982 to 2010. The length of this database allows detailed estimation of upwelling trends over the recent period of strong global warming, and the same database can be used for all areas of interest.

## Methods

Wind data were acquired from the NCEP CFSR database at <http://rda.ucar.edu/pub/cfsr.html> developed by the National Oceanic and Atmospheric Administration (NOAA). Data were retrieved from the NOAA National Operational Model Archive and Distribution System, which is maintained by the NOAA National Climatic Data Center. Detailed information about the CFSR database can be found in Saha *et al.*<sup>4</sup>. This worldwide database has a spatial resolution of approximately 0.3 × 0.3° and a temporal resolution of 6 hours from January 1982 to December 2010. The reference height of the wind data is 10 m. Coastal upwelling analysis requires the use of pixels as close to shore as possible to represent coastal processes. To avoid land contamination, only coastal pixels with less than 25% of land were used.

The process used to identify upwelling areas and to calculate trends is summarized below:

1. Wind data were initially averaged at a daily scale to smooth the effect of high frequency events such as breezes. In addition, upwelling events typically last 3–14 days<sup>5</sup>, so a daily scale seems accurate to describe them.
2. Alongshore wind stress  $\tau_l$  was calculated using the equation  $\tau_l = \rho_a C_D V_l (W_x^2 + W_y^2)^{1/2}$ , where  $\rho_a$  is the air density,  $C_D$  is the drag coefficient, and  $V_l$  is the upwelling-favourable wind.  $V_l$  can be calculated as  $V_l = -(\text{lat}/\text{abs}(\text{lat}))(W_x \cos(\theta - \pi/2) + W_y \sin(\theta - \pi/2))$ , where  $\text{lat}$  is the latitude,  $W_x$  is the zonal wind component,  $W_y$  is the meridional wind component,  $\theta$  is the angle defined by a unitary vector normal to the shoreline and pointing seaward and  $\text{abs}$  means absolute value. Alongshore wind stress has been previously used to estimate variations in upwelling intensity<sup>1,6,7</sup>. This variable provides information about upwelling intensity spreading both in time and in space without gaps, even in regions close to the Equator where other variables such as Ekman transport diverge.  $\tau_l$  and  $V_l$  were stored at the daily scale for each coastal pixel over the period 1982–2010.
3.  $\tau_l$  and  $V_l$  were averaged at a monthly scale to obtain  $\tau_l^m$  and  $V_l^m$  because the study was not focused on particular events but rather on identifying regions that show well-developed upwelling conditions lasting for long periods.
4.  $\tau_l$  and  $V_l$  climatology ( $\tau_l^{\text{clim}}$  and  $V_l^{\text{clim}}$ ) was calculated for the whole period. Different conditions were imposed on these variables to identify upwelling areas. First,  $V_l^{\text{clim}}$  must be higher than 5.4 ms<sup>-1</sup>, which corresponds to the transition from a gentle to a moderate breeze on the Beaufort scale. García-Reyes *et al.*<sup>5</sup> defined upwelling events as periods of time with alongshore winds stronger 5 ms<sup>-1</sup> following Cury and Roy<sup>8</sup>. Sensibility tests have shown that results are independent of the particular value of the threshold within the range 5 to 5.5 ms<sup>-1</sup>. This condition must be fulfilled for at least three consecutive months. Second, the area is considered to be an upwelling region only if at least 10 consecutive points (about three degrees) fulfil the previous condition. This second condition discards the appearance of small local areas.
5. Trends were calculated using only the months under strong upwelling conditions. Those months were selected from the climatology data considering  $\tau_l^{\text{clim}}$  values higher than the 50% percentile. As a consequence, the number of months per year to be used in the analysis differed from zone to zone. This number varied from five to seven months, dependent on the area, with six months being the most consistently found value.
6. Trends were calculated at each pixel as the slope of the linear regression of the alongshore monthly wind stress anomalies versus time. Monthly anomalies were calculated by subtracting from the alongshore wind stress of a certain month ( $\tau_l^m$ ) the mean alongshore wind stress of that month over the period 1982–2010<sup>9,10</sup>. All trends were calculated using raw data without any filter or running mean. The Spearman rank correlation coefficient was used to analyse the significance of trends due to its robustness to deviations from linearity and its resistance to the influence of outliers<sup>9,10</sup>. The significance level of each pixel is shown in the figures for those points that exceed 90% (circle) or 95% (square) of significance.
7. All figures herein were generated using Matlab.

## Results and discussion

The present study investigated trends in coastal upwelling for coastal regions of the world using the CFSR wind database with high spatial resolution (approximately 0.3°). This database facilitates the analysis of wind behaviour at a small scale, which is a key factor when considering coastal mesoscale effects as upwelling. Recent studies have compared this database and different wind products with wind measured

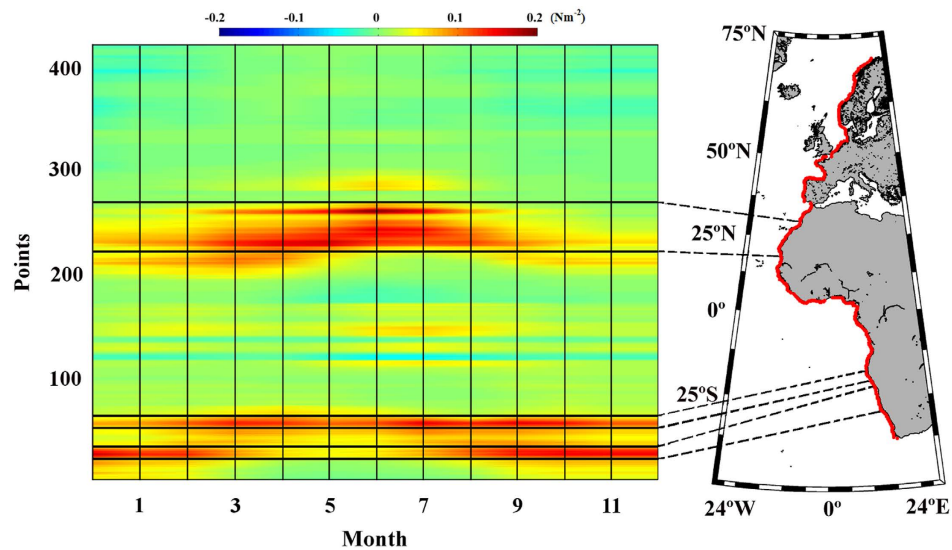


**Figure 1. Wind stress along the Eastern Atlantic Ocean.** Annual cycle of alongshore wind stress ( $\text{Nm}^{-2}$ ) for the period 1982–2010. Red points on the map show the coastal points studied. Black lines indicate those regions considered to be coastal upwelling areas. This figure has been performed using Matlab.

by several buoys along the Iberian Peninsula coast<sup>11–13</sup>. Statistical results confirmed that datasets with finer spatial resolution, such as CFSR, gave better results, especially near the coast.

In this study, 3025 coastal points worldwide were analysed to select the major upwelling regions and evaluate upwelling trends from 1982 to 2010. Under our terms of selection, ten upwelling systems were evaluated: Benguela, Canary, the southern Caribbean Sea, Chile, Peru, California (north and south), West Australia, Java, North Kenya, and Somalia–Oman. These systems were grouped together into several macroscopic zones, namely the eastern and western coasts of the Atlantic, Pacific, and Indian Oceans. No upwelling systems along the western Pacific Ocean were assessed. Alongshore wind stress was calculated over more than 600 points along this coast, and no region fulfilled the conditions required to be considered a coastal upwelling area.

**Eastern Atlantic Ocean.** Two upwelling systems were analysed along this coast from south to north: Benguela (South 30.13–23.26°S; North 20.76–16.39°S) and Canary (18.89–32.63°N) (Fig. 1). Along the Benguela upwelling system, which is one of the major upwelling regions of the world, two different areas (south and north) were assessed based on the results of the calculated alongshore wind stress (Fig. 1). Previous studies were focused mainly on the southern area from the southern tip of Africa to about 20°S. Nevertheless, several studies evaluated the entire area from south of 15°S. The results of the present study for the southern and northern areas will be described below, and then a comparison with results from previous studies will be presented.

**Benguela.** At the southern coast of the Benguela system, alongshore wind stress had positive values (upwelling-favourable conditions) throughout the year, but the highest values occurred during the austral spring and summer months (Fig. 1, points 16–38). The upwelling season was defined as September to March based on the annual cycle of alongshore wind stress meridionally averaged over these points.  $\tau_l$  trends were calculated during the upwelling season (Fig. 2a). Non-significant trends were identified south of 24°S, and only the three northernmost grid boxes (–23.3 to 24°S) displayed a significant positive trend. These significant positive trends continued throughout the Northern Benguela Zone (Fig. 3), although the defined upwelling season differed for this zone (from July to November). A significant positive trend was observed for the entire region, with values ranging from  $4 \times 10^{-3} \text{Nm}^{-2} \text{dec}^{-1}$  in the northern area to  $9.5 \times 10^{-3} \text{Nm}^{-2} \text{dec}^{-1}$  in the southern one.

Previous studies reported similar results. For example, Patti *et al.*<sup>14</sup> analysed data from the Comprehensive Ocean-Atmosphere Data Set (COADS) and found an increase in annual wind stress ( $\sim 10 \times 10^{-3} \text{Nm}^{-2} \text{dec}^{-1}$ ) for the area extending from 20 to 30°S, indicating upwelling reinforcement from 1958 to 2007. Narayan *et al.*<sup>15</sup> described a significant increase ( $\sim 5 \times 10^{-3} \text{Nm}^{-2} \text{dec}^{-1}$ ) in the COADS and National Center for Environmental Prediction/National Center for Atmospheric Research (NCEP/NCAR Reanalysis) meridional wind stress across 26–36°S from 1960 to 2001 using annual data. On the other hand, annual wind stress data from European Center for Medium range Weather Forecasting (ECMWF) Re-Analysis (ERA-40 Reanalysis) used in the same study<sup>15</sup> showed a non-significant trend for the same period. Analysis of upwelling trends along the Benguela Upwelling Ecosystem was also conducted using

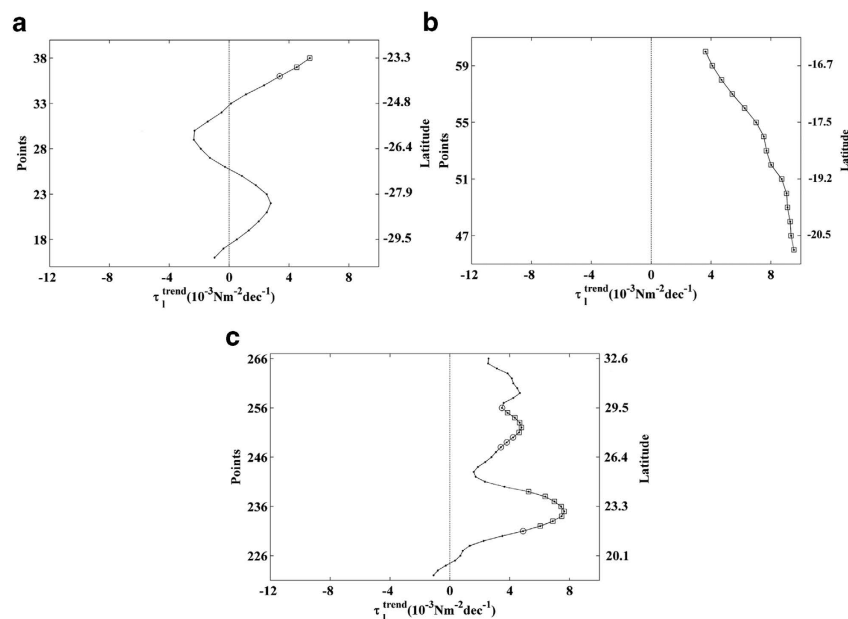


**Figure 2. Upwelling trends in the selected areas along the Eastern Atlantic Ocean.** (a) Alongshore wind stress trends along the southern Benguela coast calculated from September to March. (b) Alongshore wind stress trends along the northern Benguela coast calculated from July to November. (c) Alongshore wind stress trends along the Canary coast calculated from April to September. Those points with significance greater than 90% are marked with a circle, and those greater than 95% are marked with a square. A negative (positive) trend means a decrease (increase) in upwelling-favourable winds. This figure has been performed using Matlab.

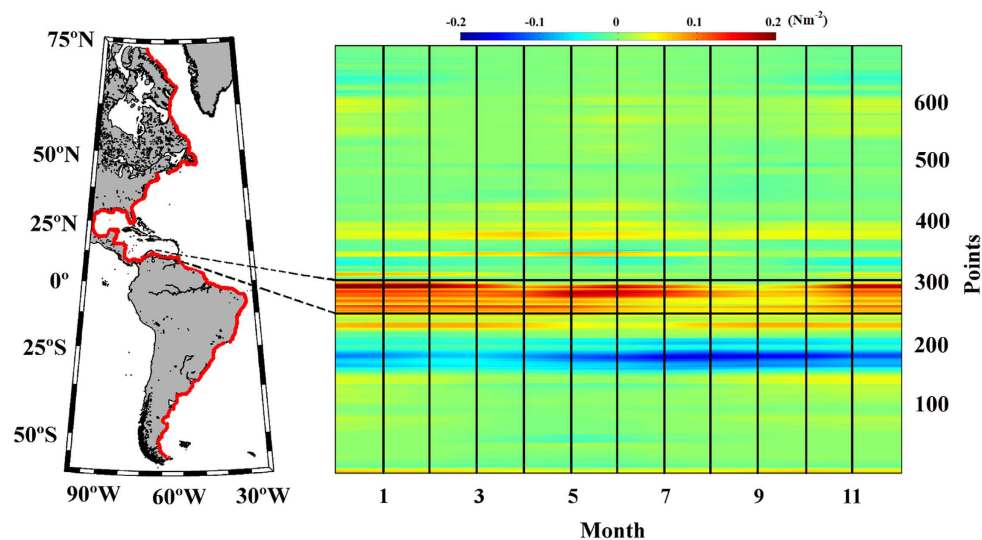


**Figure 3. Wind stress along the Western Atlantic Ocean.** Annual cycle of alongshore wind stress ( $\text{Nm}^{-2}$ ) for the period 1982–2010. Red points on the map show the coastal points analysed. Black lines indicate those regions considered to be coastal upwelling areas. This figure has been performed using Matlab.

a derived upwelling index in terms of Ekman transport to represent the estimated potential effects of wind stress on the ocean surface<sup>9,16</sup>. Pardo *et al.*<sup>16</sup> and Santos *et al.*<sup>9</sup> found a general increase in upwelling intensity over the last four decades for the areas 20–32°S and 16–30°S, respectively, using the NCEP/NCAR Reanalysis annual data.



**Canary.** Along the Canary coast, positive values of alongshore wind stress ( $\tau_l$ ) were observed throughout the year, with the highest values occurring in spring and summer months (Fig. 1, points 222–266). The upwelling season was considered to be April to September.  $\tau_l$  trends over this period were calculated (Fig. 2c), and positive trends were detected over almost the entire region. However, significant values were found only around 22–24°N ( $\sim 8 \times 10^{-3} \text{ Nm}^{-2} \text{ dec}^{-1}$ ) and 27–29°N ( $\sim 4 \times 10^{-3} \text{ Nm}^{-2} \text{ dec}^{-1}$ ). Published results regarding trends in upwelling along the Canary coast are controversial. Trends in upwelling can be highly dependent on the length of the time series, the selected area, and the season evaluated in the analysis. Results similar to those found in the present study were reported by Cropper *et al.*<sup>17</sup> using meridional wind speed from CFSR over the period 1981–2012 during summer (June–August). These authors found a non-significant increase in upwelling-favourable winds off Northwest Africa (11–35°N). On the other hand, different wind databases such as NCEP/Department Of Energy (NCEP/DOE II), ERA-Interim, 20 Century, and National Aeronautics and Space Administration-Modern Era Retrospective-Analysis for Research and Applications (NASA-MERRA) used in the same study for the same period showed a statistically significant increase north of 21°N and a generally significant decrease in upwelling-favourable winds south of 19°N. Results of previous studies are also in agreement with our finding of increasing trends in upwelling along the Canary coast. For example, McGregor *et al.*<sup>18</sup> described increasing trends in upwelling around 31°N using annual wind stress data from COADS for the period 1950–1992. Narayan *et al.*<sup>15</sup> and Patti *et al.*<sup>14</sup> also found significant increasing trends ( $\sim 4\text{--}5 \times 10^{-3} \text{ Nm}^{-2} \text{ dec}^{-1}$ ) using the same database across 24–32°N considering annual wind stress over the last four decades. Narayan *et al.*<sup>15</sup> reported a significant increase ( $\sim 2 \times 10^{-3} \text{ Nm}^{-2} \text{ dec}^{-1}$ ) in the ERA-40 Reanalysis meridional wind stress for the same period. In contrast, when they used the NCEP/NCAR reanalysis these authors<sup>15</sup> identified a reduction in meridional wind stress ( $\sim 4 \times 10^{-3} \text{ Nm}^{-2} \text{ dec}^{-1}$ ) over the last four decades (1960–2001) in the same region (24–32°N), indicating a reduction in coastal upwelling. More recently, Barton *et al.*<sup>2</sup> conducted an extensive study of wind-induced upwelling trends along the whole Canary current upwelling system. Using monthly meridional wind data from the Pacific Fisheries Environmental Laboratory (PFEL), NCEP/NCAR, ECMWF, ICOADS, and Wave and Anemometer-based Sea Surface Wind (WASWind) plus data from coastal meteorological stations over 40 years (1967–2007), these authors found that trends varied among different data products in the same area, as both negative and positive trends were evident. In addition, not statistically significant changes in meridional wind components were found. Contradictory results were also obtained using Ekman transport data in numerous upwelling trend studies conducted along the Canary Upwelling Ecosystem. Gomez-Gesteira *et al.*<sup>19</sup> detected a significant decreasing trend in upwelling strength for all seasons across 20–32°N from 1967 to 2006 using data from the PFEL. Pardo *et al.*<sup>16</sup> also found a general weakening of the upwelling intensity along the Iberian/Canary (26–43°N) and NW African (10–24°N) regions from 1970 to 2009 using the NCEP/NCAR Reanalysis. These trends were clearly observed in winter and autumn for both regions, and a weakening in the upwelling intensity was also detected in summer in the northwest African region. In contrast, Santos *et al.*<sup>10</sup> confirmed a spring-summer increasing trend across 22–33°N when they used the same database (NCEP/NCAR) from 1982 to 2010 in accordance with the present study. Opposite results observed in some of the studies described above using the same database (NCEP/NCAR) emphasize that linear trends are strongly dependent on the length of the time series and the season evaluated<sup>2,20</sup>.

**Western Atlantic Ocean.** Only one region along the coast of the western Atlantic Ocean fits the conditions required to be considered an coastal upwelling area: the southern Caribbean Sea (62.19–76.56°W) (Fig. 3). In the southern Caribbean upwelling region, alongshore wind stress had positive values throughout the year, with the highest values during the boreal winter months (Fig. 3, points 261–307). The upwelling season was considered to occur from December to April, and  $\tau_l$  trends were calculated for this period (Fig. 4). The eastern and western regions exhibited different behaviours. A negative trend was detected east of 71.25°W, with a significance level higher than 90% ( $\sim -4 \times 10^{-3}$  to  $-8 \times 10^{-3} \text{ Nm}^{-2} \text{ dec}^{-1}$ ) for almost all points. In the western region (71.25–76.56°W) a non-significant positive trend was observed in most of the area, with maximum values of around  $4 \times 10^{-3} \text{ Nm}^{-2} \text{ dec}^{-1}$ . This region was previously studied mainly in terms of upwelling occurrence using wind and sea surface temperature data<sup>21–25</sup>. As far as we know, no studies of upwelling trends in terms of wind have been conducted along the southern Caribbean upwelling system.

**Eastern Pacific Ocean.** Three upwelling systems were evaluated along this coast from south to north: Chile (37.62–28.88°S), Peru (16.39–10.15°S), and California (South 33.88–36.06°N; North 37.94–42.31°N) (Fig. 5).

**Chile.** Along the coast of Chile, positive values of alongshore wind stress were observed throughout the year, with the highest values during the austral spring and summer months (Fig. 5, points 78–106). The upwelling season was considered to last from October to April, and  $\tau_l$  trends were calculated for these months (Fig. 6a). Significant negative trends were observed south of 34°S and north of 31°S, with values between  $-4 \times 10^{-3}$  and  $-8 \times 10^{-3} \text{ Nm}^{-2} \text{ dec}^{-1}$ . Non-significant positive trends were detected at mid-latitudes. Previous studies along this coast have reported different results. For example, Garreaud and

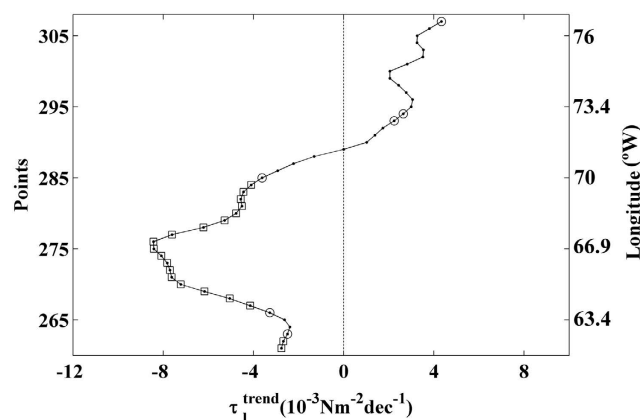


**Figure 4. Upwelling trends in the selected areas along the Western Atlantic Ocean.** Alongshore wind stress trends in the southern Caribbean Sea calculated from December to April. Those points with significance greater than 90% are marked with a circle, and those greater than 95% are marked with a square. A negative (positive) trend means a decrease (increase) in upwelling-favourable winds. This figure has been performed using Matlab.

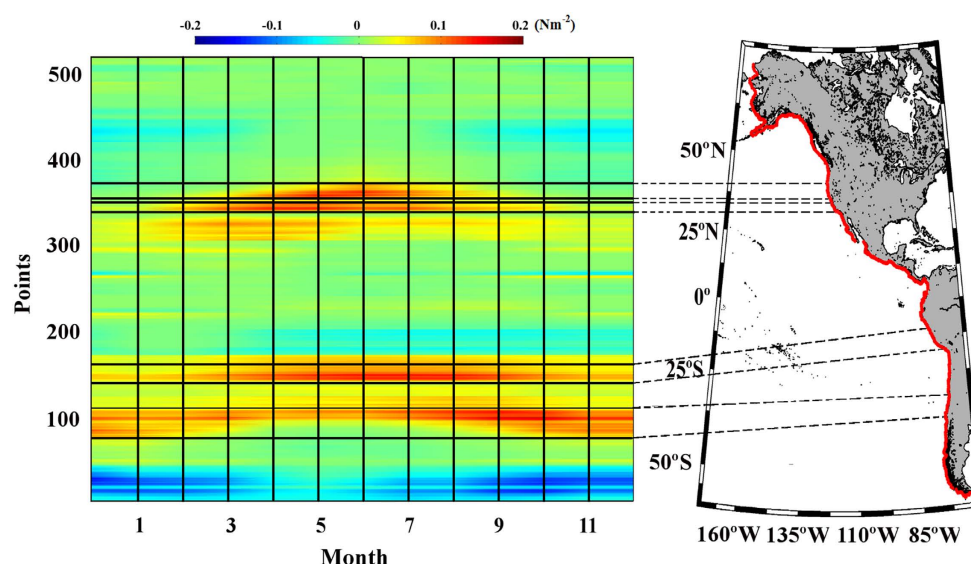


**Figure 5. Wind stress along the Eastern Pacific Ocean.** Annual cycle of alongshore wind stress ( $\text{Nm}^{-2}$ ) for the period 1982–2010. Red points on the map show the coastal points analysed. Black lines indicate those regions considered to be coastal upwelling areas. This figure has been performed using Matlab.

Falvey<sup>26</sup> analysed changes in the coastal winds along the west coast of subtropical South America (20–55°S; 70–85°W) using future climate scenarios. Different simulations were performed using the Providing REgional Climate for Impact Studies (PRECIS) regional climate model, and a significant trend in the coastal wind was absent during the late twentieth century (1961–1990). Similar results were observed by Goubanova *et al.*<sup>27</sup>, who used a statistical downscaling method to refine the representations of coastal winds for a global-coupled general circulation model (Institut Pierre Simon Laplace Climate Model (IPSL-CM4)) from 1970 to 1999. More recently, Rahn and Garreaud<sup>28</sup> used CFSR over the period 1979–2010 to present a synoptic climatology of the coastal wind along the Chile/Peru coast, paying special attention to prominent upwelling regions. Points located along the Chile coast (30 and 36.4°S) showed unclear trend over the last 30 years. Finally, Aravena *et al.*<sup>29</sup> used anomalies of Ekman transport data from 1980 to 2010 to assess the interannual evolution of upwelling along the northern-central coast of Chile (29–34°S). These Ekman transport anomalies obtained from PFEL showed a positive trend throughout the area. As previously mentioned, trends in upwelling can be highly dependent on factors such as the season evaluated in the analysis. This could explain the observed weakening in upwelling in most of the region in the present study, which we calculated using alongshore wind stress from October to April.

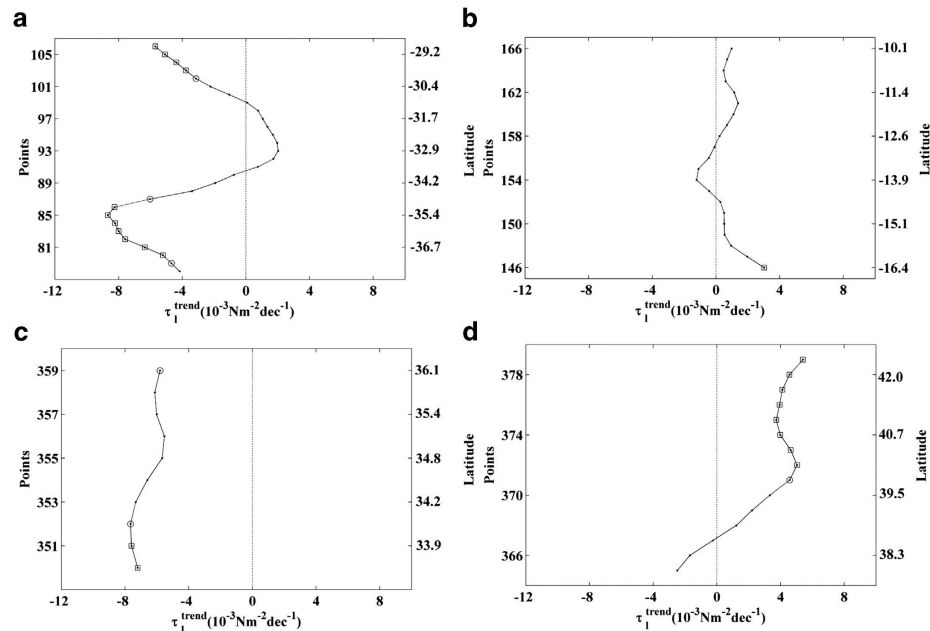


**Figure 6. Upwelling trends in the selected areas along the Eastern Pacific Ocean.** (a) Alongshore wind stress trends along the Chile coast calculated from October to April. (b) Alongshore wind stress trends along the Peru coast calculated from May to October. (c) Alongshore wind stress trends along the southern California coast calculated from April to September. (d) Alongshore wind stress trends along the northern California coast calculated from April to October. Those points with significance greater than 90% are marked with a circle, and those greater than 95% are marked with a square. A negative (positive) trend means a decrease (increase) in upwelling-favourable winds. This figure has been performed using Matlab.

When we recalculated  $\tau_l$  trends using annual data, the observed trend was unclear, which is in accordance with most of the studies previously conducted along this upwelling system. The dependence of trends on the season studied was also reported by Sydeman *et al.*<sup>3</sup>, who analysed more than 20 studies related to upwelling trends along the five major upwelling systems published over the last two decades. They found that some of the disagreement in previous studies could be resolved by considering winds during only the active upwelling seasons.

**Peru.** Along the Peru coast, alongshore winds had positive values throughout the year, with maxima from May to October (Fig. 5, points 146–166). The upwelling season was considered to occur during these months, and  $\tau_l$  trends were calculated for this time period (Fig. 6b). Small and non-significant positive trends were observed for almost the entire region except at the southernmost point (16.4°S), where a significance level higher than 95% was identified ( $-3.5 \times 10^{-3} \text{ Nm}^{-2} \text{ dec}^{-1}$ ). A non-significant negative trend with small values was observed at  $\sim 14^\circ\text{S}$ . Previous studies have shown that trends in upwelling along the Peru coast are contradictory. Results similar to those obtained in our study were reported by Rahn and Garreaud<sup>28</sup>, who analysed annual alongshore winds from CFSR from 1979 to 2010. These authors found a positive trend in alongshore wind from 1995 to 2010 ( $\sim 1 \text{ ms}^{-1}$ ) at  $15^\circ\text{S}$ , which is a prominent upwelling region along the Peru coast. Gutierrez *et al.*<sup>30</sup> used ERA-40 Reanalysis in a region around  $14^\circ\text{S}$  and also found an increase in upwelling-favourable winds from 1958 to 2001 for the spring season and using annual data. Bakun *et al.*<sup>31</sup> reported an increase in upwelling at  $\sim 10.5^\circ\text{S}$  using monthly wind stress data from COADS from 1948 to 2006. In contrast, Goubanova *et al.*<sup>27</sup> suggested the existence of a weakening of alongshore wind near  $15^\circ\text{S}$  from 1970 to 1999 based on statistical downscaling of the sea surface wind. Previous studies conducted over a wider region have also shown different results. Patti *et al.*<sup>14</sup> described an increase in annual wind stress using data from COADS for the area extending from 6 to  $16^\circ\text{S}$  and demonstrated the existence of upwelling reinforcement from 1958 to 2007. However, the trend they reported ( $\sim 7 \times 10^{-3} \text{ Nm}^{-2} \text{ dec}^{-1}$ ) was much higher than that found in the present study. Narayan *et al.*<sup>15</sup> also analysed the same region from 1960 to 2001 using different datasets. Annual wind stress data from COADS ( $\sim 5 \times 10^{-3} \text{ Nm}^{-2} \text{ dec}^{-1}$ ) and ERA-40 Reanalysis ( $\sim 0.9 \times 10^{-3} \text{ Nm}^{-2} \text{ dec}^{-1}$ ) revealed a significant increasing trend in upwelling, in agreement with the results reported by Patti *et al.*<sup>14</sup>, although in the latter case the trend value was much smaller. The general trend<sup>14,15,31</sup> is a similar to that observed in the present study. In contrast, Narayan *et al.*<sup>15</sup> identified a statistically non-significant decrease ( $\sim -0.7 \times 10^{-3} \text{ Nm}^{-2} \text{ dec}^{-1}$ ) at the Peruvian upwelling region ( $6\text{--}16^\circ\text{S}$ ) using meridional wind stress from the NCEP/



NCAR reanalysis. Pardo *et al.*<sup>16</sup> analysed annual Ekman transport using data from the NCEP/NCAR Reanalysis and found a general weakening of the upwelling intensity in the Peru region (6.7–16.2°S) from 1970 to 2009.

**California.** For the California upwelling region (Fig. 5), two different areas were assessed: South (33.88–36.06 °N) and North (37.94–42.31 °N). Almost all published reports about trends in upwelling along this system include the entire coast of California (32–42 °N). The results of the present study for the southern and northern areas will be described below, and then a comparison with results from previous studies will be presented.

Along the southern California coast, the highest values of alongshore wind stress were observed during the spring and summer months (Fig. 5, points 350–359). The upwelling season was considered to occur from April to September based on the annual cycle of wind stress meridionally averaged over these points, and  $\tau_l$  trends were calculated (Fig. 6c). Negative trends were observed for the entire region, but they were significant ( $\sim -8 \times 10^{-3} \text{ Nm}^{-2} \text{ dec}^{-1}$ ) only at the three southernmost points and at the northernmost one. Along the northern California coast, alongshore wind stress showed a similar behaviour, although the highest values were mainly observed in summer (Fig. 5, points 365–379). Thus,  $\tau_l$  trends were calculated between April and October (Fig. 6d). Non-significant negative trends were detected for the three southernmost points, with maximum values around  $-3 \times 10^{-3} \text{ Nm}^{-2} \text{ dec}^{-1}$ . Positive trends were observed north of 38.5 °N with a significance level higher than 90% for the northernmost region ( $4\text{--}6 \times 10^{-3} \text{ Nm}^{-2} \text{ dec}^{-1}$ ).

Controversial results in relation to the long-term variability in coastal upwelling were also found in the California upwelling system. In terms of wind speed, Mendelssohn and Schwing<sup>32</sup> reported trends of stronger upwelling-favourable winds along 32–40°N based on April–September COADS data from 1946 to 1990. Patti *et al.*<sup>14</sup> analysed a similar area between 34 and 40°N using annual wind stress data from the same database over the period 1958 to 2007. They described an increasing trend of around  $4 \times 10^{-3} \text{ Nm}^{-2} \text{ dec}^{-1}$ . Narayan *et al.*<sup>15</sup> also found a statistically significant increase in upwelling-favourable winds ( $\sim 3 \times 10^{-3} \text{ Nm}^{-2} \text{ dec}^{-1}$ ) using annual wind stress data from the same dataset from 1960 to 2001 for the same region. Although the southern area evaluated in the present study (33.88–36.06°N) is included in the region studied by Mendelssohn and Schwing<sup>32</sup>, Patti *et al.*<sup>14</sup>, and Narayan *et al.*<sup>15</sup>, the general trend observed in these three works and the present one is contradictory. In contrast, Narayan *et al.*<sup>15</sup> identified a significant decreasing trend in upwelling from the ERA-40 Reanalysis of annual wind stress data ( $\sim -0.6 \times 10^{-3} \text{ Nm}^{-2} \text{ dec}^{-1}$ ) from 34 to 40°N over the last four decades (1960–2001). This decrease is in good agreement with the results of the present study, although the trend value was much higher in our case ( $\sim -8 \times 10^{-3} \text{ Nm}^{-2} \text{ dec}^{-1}$ ). Different results were also reported in several studies that covered a wider region. For example, Garcia-Reyes and Largier<sup>33</sup> studied the California region from 33 to 42°N from 1982 to 2008 using wind speed data during the upwelling season (March–July) from the National Data Buoy Center (NDBC) buoys. They found significant increasing trends in upwelling winds north of 35°N and a decreasing trend in the southern region (33–35°N). Similar results were observed when data from the NDBC for June–August over the period 1980 to 2010<sup>34</sup> were used. The decreasing trend along the southern coast of California (33–35°N) reported in these two works is in agreement with the results of our study. On the other hand, positive trends were only observed north of 38.5°N in our case.

Ekman transport data also have been evaluated in different studies conducted along the California Upwelling Ecosystem. Rykaczewski and Checkley<sup>35</sup> found a positive summer trend around 34.5°N for the period 1948–2004 using Ekman transport data from the California Reanalysis Downscaling (CaRD10), which is a dynamically downscaled analysis of the NCEP/NCAR Reanalysis. Seo *et al.*<sup>34</sup> found similar results using the same database over the entire California coast (32–42°N) from 1980 to 2010. Garcia-Reyes and Largier<sup>33</sup> detected significant increasing trends in upwelling strength during March–July north of 34.5°N from 1982 to 2008 using data from the PFEL. Pardo *et al.*<sup>16</sup> also studied the California region from 33 to 45°N using NCEP/NCAR Reanalysis Ekman transport data from 1970 to 2009, and they reported an unclear annual trend. In contrast, Iles *et al.*<sup>36</sup> found an increasing trend in Ekman transport annual data from PFEL from 1967 to 2010 over the same region.

Considering that ENSO ([www.esrl.noaa.gov](http://www.esrl.noaa.gov)) can be an important source of variability along the Pacific upwelling systems, its influence on the estimated trends of  $\tau_l$  was analysed. No correlations were found between the variability of ENSO and  $\tau_l$ .

**Eastern Indian Ocean.** Two upwelling systems were assessed along this coast: West Australia (31.69–21.39 °S) and Java (105.62–116.87 °E) (Fig. 7).

**West Australia.** Along the western Australian coast, maximum values of alongshore wind stress were observed from October to March, which corresponds to the austral spring and summer months (Fig. 7, points 108–142). The upwelling season was considered to occur from October to March, and  $\tau_l$  trends were calculated over these months (Fig. 8a). Positive trends were detected for almost the whole region, with significant values between  $4\text{--}8 \times 10^{-3} \text{ Nm}^{-2} \text{ dec}^{-1}$  south of 25.5°S. Non-significant negative trends were found at the northernmost latitudes (21.4–22.9°S). As far as we know, no studies regarding upwelling trends in terms of wind have been conducted along the western coast of Australia. Previous studies have

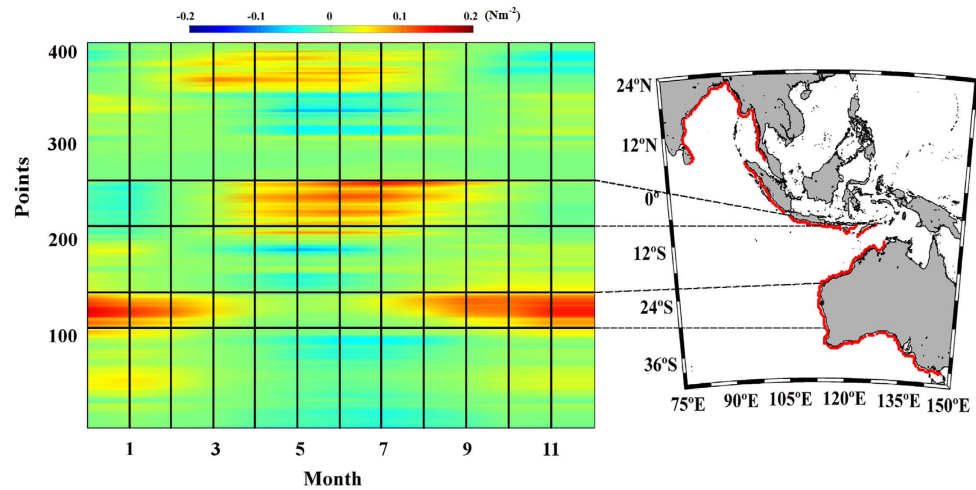


**Figure 7. Wind stress along the Eastern Indian Ocean.** Annual cycle of alongshore wind stress ( $\text{Nm}^{-2}$ ) for the period 1982–2010. Red points on the map show the coastal points analysed. Black lines indicate those regions considered to be coastal upwelling areas. This figure has been performed using Matlab.

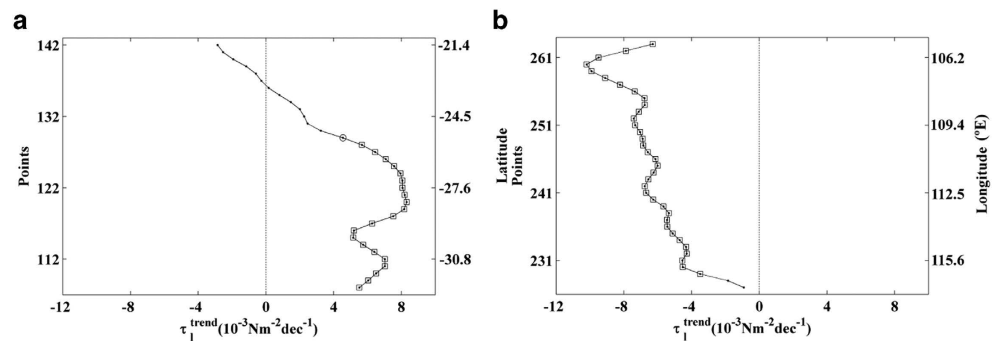


**Figure 8. Upwelling trends in the selected areas along the Eastern Indian Ocean.** (a) Alongshore wind stress trends along the Western Australia coast calculated from October to March. (b) Alongshore wind stress trends along the Java coast calculated from May to October. Those points with significance greater than 90% are marked with a circle, and those greater than 95% are marked with a square. A negative (positive) trend means a decrease (increase) in upwelling-favourable winds.

shown the absence of persistent upwelling off this coast despite a prevailing summer wind system favouring upwelling. This absence of upwelling has been attributed to the presence of the Leewin Current (LC), a warm poleward flow transporting nutrient-poor waters from the tropics<sup>37,38</sup>. Unlike other eastern boundary currents (e.g., the Benguela and Humboldt Currents at similar latitudes), the poleward flow of the LC suppresses the persistent upwelling of cool, nutrient-rich, subsurface water onto the western Australia continental shelf<sup>39,40</sup>. Thus, large-scale upwelling is incompatible with the poleward flowing LC. Nevertheless, localized seasonal upwelling associated with inner shelf wind-driven currents can appear along some regions, such as the Ningaloo (23–25°S) and Capes Currents (26–28°S), due to variations in the LC<sup>41–47</sup>.

**Java.** Along the Java coast, values of alongshore wind stress were higher during the austral winter (Fig. 8, points 227–263). The upwelling season was considered to last from May to October, and  $\tau_1$  trends were calculated for this time period (Fig. 8b). Significant negative trends were detected for almost the entire coast, with values between  $-4 \times 10^{-3} \text{ Nm}^{-2} \text{ dec}^{-1}$  at the easternmost region and  $-10 \times 10^{-3} \text{ Nm}^{-2} \text{ dec}^{-1}$  at the westernmost one. The existence of upwelling along the Java coast and its basic features have been documented in previous studies, mainly in terms of upwelling occurrence determined using wind and SST data, whereas upwelling trends have not been considered. Different researchers have found that upwelling occurs between June and November and is mostly forced both locally by the alongshore winds associated with the southeast monsoon and remotely by atmosphere-ocean circulation associated with ENSO<sup>48–53</sup>.

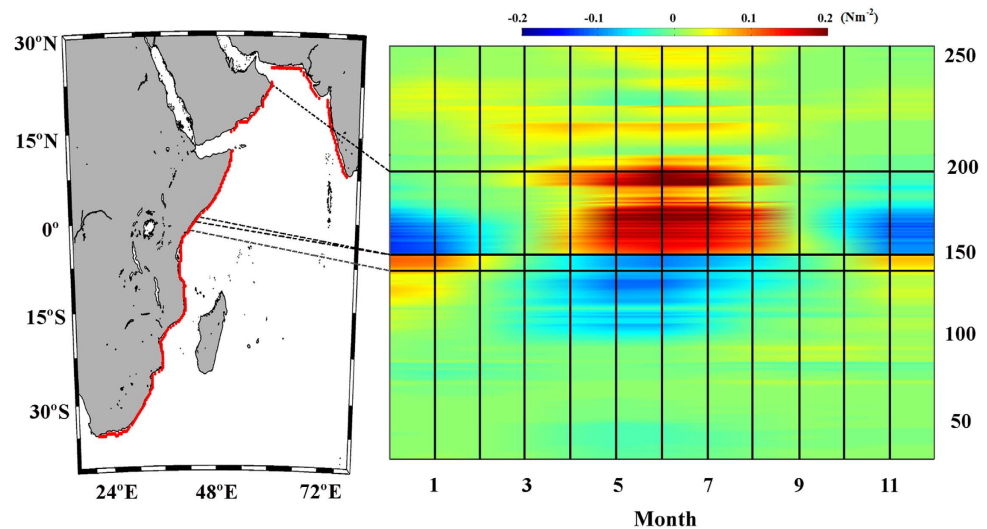


**Figure 9. Wind stress along the Western Indian Ocean.** Annual cycle of alongshore wind stress ( $\text{Nm}^{-2}$ ) for the period 1982–2010. Red points on the map show the coastal points analysed. Black lines indicate those regions considered to be coastal upwelling areas. This figure has been performed using Matlab.

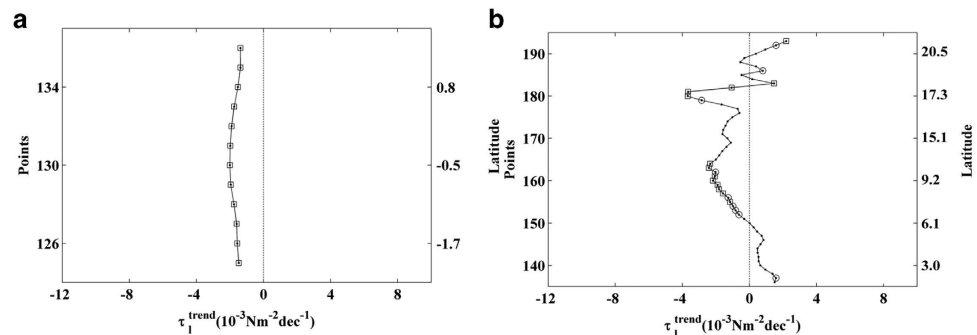


**Figure 10. Upwelling trends in the selected areas along the Western Indian Ocean.** (a) Alongshore wind stress trends along the Northern Kenya coast calculated from November to April. (b) Alongshore wind stress trends along the Somalia-Oman coast calculated from April to October. Those points with significance greater than 90% are marked with a circle, and those greater than 95% are marked with a square. A negative (positive) trend means a decrease (increase) in upwelling-favourable winds. This figure has been performed using Matlab.

**Western Indian Ocean.** Two upwelling systems were evaluated along this coast from south to north: North Kenya ( $2.03\text{--}1.40^\circ\text{N}$ ) and Somalia-Oman ( $1.72\text{--}22.01^\circ\text{N}$ ) (Fig. 9).

**North Kenya.** Along the northern Kenya coast, positive values of alongshore wind stress were observed from November to April (Fig. 9, points 125–136). The upwelling season was considered to occur from November to April, and  $\tau_1$  trends were calculated over this period (Fig. 10a). Significant negative trends were detected for the entire region, with values of around  $-2 \times 10^{-3} \text{ Nm}^{-2} \text{ dec}^{-1}$ . The coast of northern Kenya is characterized by the occurrence of an irregular upwelling linked to the northeast monsoon, which normally develops from November to March. Several researchers have related the occurrence of this upwelling to higher productivity in the area, although the fact that upwelling events are not regular has attracted relatively little scientific interest about upwelling trends in terms of wind. This region has been studied mainly in terms of changes in chemical and biological oceanographic parameters related to the occurrence of the northeast and southeast monsoons, which lead to important differences between the Kenya and Somalia coasts in terms of upwelling<sup>54–60</sup>.

**Somalia-Oman.** Along the Somalia-Oman coast, positive values of alongshore wind stress were found from April to October (Fig. 9, points 136–193). Using the annual cycle of the alongshore wind stress, the upwelling season was considered to last from April to October, and  $\tau_1$  trends were calculated

Zone	Author	Variable	Database (region)	Period (Upw. Season)	Trend
Benguela	Patti <i>et al.</i> (2010)	WSt	COADS (30-20°S)	1958-2007 (Annual)	+
	Narayan <i>et al.</i> (2010)	WSt	COADS (36-26°S)	1960-2001 (Annual)	+
	Narayan <i>et al.</i> (2010)	WSt	NCEP/NCAR (36-26°S)	1960-2001 (Annual)	+
	Narayan <i>et al.</i> (2010)	WSt	ERA-40 (36-26°S)	1960-2001 (Annual)	0
	Pardo <i>et al.</i> (2011)	ET	NCEP/NCAR (32-20°S)	1970-2009 (Annual)	+
	Santos <i>et al.</i> (2012)	ET	NCEP/NCAR (30-16°S)	1970-2009 (Annual)	+
	<b>This work</b>	<b>WSt</b>	<b>CFSR (30.1-23.3°S)</b>	<b>1982-2010 (SEP-MAR)</b>	+
	<b>This work</b>	<b>WSt</b>	<b>CFSR (20.8-16.4°S)</b>	<b>1982-2010 (JUL-NOV)</b>	+
Canary	Cropper <i>et al.</i> (2014)	WSp	CFSR (11-35°N)	1981-2012 (JUN-AUG)	+
	Cropper <i>et al.</i> (2014)	WSp	NCEP/DOE II (11-35°N)	1981-2012 (JUN-AUG)	+
	Cropper <i>et al.</i> (2014)	WSp	ERA-Interim (11-35°N)	1981-2012 (JUN-AUG)	+
	Cropper <i>et al.</i> (2014)	WSp	20 Century (11-35°N)	1981-2012 (JUN-AUG)	+
	Cropper <i>et al.</i> (2014)	WSp	NASA-MERRA (11-35°N)	1981-2012 (JUN-AUG)	+
	McGregor <i>et al.</i> (2007)	WSt	COADS (35°N)	1950-1992 (Annual)	+
	Patti <i>et al.</i> (2010)	WSt	COADS (24-32°N)	1958-2007 (Annual)	+
	Narayan <i>et al.</i> (2010)	WSt	COADS (24-32°N)	1960-2001 (Annual)	+
	Narayan <i>et al.</i> (2010)	WSt	NCEP/NCAR (24-32°N)	1960-2001 (Annual)	–
	Narayan <i>et al.</i> (2010)	WSt	ERA-40 (24-32°N)	1960-2001 (Annual)	+
	Barton <i>et al.</i> (2013)	WSp	PFEL (15.5-41.5°N)	1967-2007 (Annual)	–
	Barton <i>et al.</i> (2013)	WSp	NCEP/NCAR (15-42.5°N)	1967-2007 (Annual)	–
	Barton <i>et al.</i> (2013)	WSp	ECMWF (15-40°N)	1967-2007 (Annual)	+
	Barton <i>et al.</i> (2013)	WSp	ICOADS (15-41°N)	1967-2007 (Annual)	+
	Barton <i>et al.</i> (2013)	WSp	WASWind (16-44°N)	1967-2007 (Annual)	–
	Gomez-Gesteira <i>et al.</i> (2008)	ET	PFEL (20-32°N)	1967-2006 (Monthly)	–
	Pardo <i>et al.</i> (2011)	ET	NCEP/NCAR (10-43°N)	1970-2009 (Annual)	–
	Santos <i>et al.</i> (2012)	ET	NCEP/NCAR (22-33°N)	1982-2010 (MAY-SEP)	+
	<b>This work</b>	<b>WSt</b>	<b>CFSR (18.9-32.6°N)</b>	<b>1982-2010 (APR-SEP)</b>	+

**Table 1.** Studies in which upwelling trends were analysed in terms of wind along the Benguela and Canary coasts. Variable abbreviations: WSt (Wind Stress), Ekman Transport (ET), WSp (Wind Speed).

for these months (Fig. 10b). Negative trends were observed for almost the whole region except at the southernmost coast of Somalia (2–6°N) and the northernmost coast of Oman (18–22°N). Significant trends were observed mainly along the Somalia coast (6.5–10.5°N), with values between  $-1.5 \times 10^{-3} \text{ Nm}^{-2} \text{ dec}^{-1}$  and  $-3.5 \times 10^{-3} \text{ Nm}^{-2} \text{ dec}^{-1}$ . Upwelling is induced by an alongshore current driven by the southwest monsoon in summer. With the onset of the northeast monsoon the circulation pattern reverses, causing

Zone	Author	Variable	Database	Period (Upw. Season)	Trend
Chile	Garreaud and Falvey (2009)	WSp	PRECIS (55–20°S)	1961–1990 (Annual)	0
	Goubanova <i>et al.</i> (2011)	WSp	IPSL-CM4 (40–0°S)	1970–1999 (Annual)	0
	Rahn and Garreaud (2013)	WSp	CFSR (36.4–30°S)	1979–2010 (Annual)	0
	Aravena <i>et al.</i> (2014)	ET	PFEL (34–29°S)	1980–2010 (Annual)	+
	<b>This work</b>	<b>WSt</b>	<b>CFSR (37.6–28.9°S)</b>	<b>1982–2010 (OCT–APR)</b>	–
Peru	Rahn and Garreaud (2013)	WSp	CFSR (15°)	1979–2010 (Annual)	+
	Gutierrez <i>et al.</i> (2011)	WSp	ERA-40 (14°S)	1958–2001 (Annual)	+
	Bakun <i>et al.</i> (2010)	WSt	COADS (10.5°S)	1948–2006 (Monthly)	+
	Goubanova <i>et al.</i> (2011)	WSp	IPSL-CM4 (15°S)	1970–1999 (Annual)	–
	Patti <i>et al.</i> (2010)	WSt	COADS (16–6°S)	1958–2007 (Annual)	+
	Narayan <i>et al.</i> (2010)	WSt	COADS (16–6°S)	1960–2001 (Annual)	+
	Narayan <i>et al.</i> (2010)	WSt	NCEP/NCAR (16–6°S)	1960–2001 (Annual)	–
	Narayan <i>et al.</i> (2010)	WSt	ERA-40 (16–6°S)	1960–2001 (Annual)	+
	Pardo <i>et al.</i> (2011)	ET	NCEP/NCAR (16–6.7°S)	1970–2009 (Annual)	–
	<b>This work</b>	<b>WSt</b>	<b>CFSR (16.4–10.1°S)</b>	<b>1982–2010 (MAY–OCT)</b>	+
	Mendelsohn and Schwing (2002)	WSp	COADS (32–40°N)	1946–1990 (APR–SEP)	+
	Patti <i>et al.</i> (2010)	WSt	COADS (34–40°N)	1958–2007 (Annual)	+
	Narayan <i>et al.</i> (2010)	WSt	COADS (34–40°N)	1960–2001 (Annual)	+
California	Narayan <i>et al.</i> (2010)	WSt	ERA-40 (34–40°N)	1960–2001 (Annual)	–
	Garcia-Reyes and Largier (2010)	WSp	NDBC (33–35°N)	1982–2008 (MAR–JUL)	–
	Garcia-Reyes and Largier (2010)	WSp	NDBC (35–42°N)	1982–2008 (MAR–JUL)	+
	Garcia-Reyes and Largier (2010)	ET	PFEL (34.5–42°N)	1982–2008 (MAR–JUL)	+
	Seo <i>et al.</i> (2012)	WSp	NDBC (33–35°N)	1980–2010 (JUN–AUG)	–
	Seo <i>et al.</i> (2012)	WSp	NDBC (35–42°N)	1980–2010 (JUN–AUG)	+
	Seo <i>et al.</i> (2012)	ET	CaRD10 (32–42°N)	1980–2010 (JUN–AUG)	+
	Rykaczewski and Checkley (2008)	ET	CaRD10 (34.5°N)	1948–2004 (Summer)	+
	Pardo <i>et al.</i> (2011)	ET	NCEP/NCAR (33–45°N)	1970–2009 (Annual)	0
	Iles <i>et al.</i> (2012)	ET	PFEL (33–45°N)	1967–2010 (Annual)	+
	<b>This work</b>	<b>WSt</b>	<b>CFSR (33.9–36.1°N)</b>	<b>1982–2010 (APR–SEP)</b>	–
	<b>This work</b>	<b>WSt</b>	<b>CFSR (37.9–42.3°N)</b>	<b>1982–2010 (APR–OCT)</b>	+

**Table 2.** Studies in which upwelling trends were analysed in terms of wind along the Chile, Peru, and California coasts. Variable abbreviations: WSt (Wind Stress), Ekman Transport (ET), WSp (Wind Speed).

a cessation of the upwelling. This region has been widely studied in terms of SST and biodiversity related to the occurrence of these upwelling events<sup>61–65</sup>. Nevertheless, few studies have focused on upwelling trends in terms of wind. Goes *et al.*<sup>66</sup> reported an interannual escalation in the intensity of summer monsoonal winds accompanied by enhanced upwelling along the coast of Somalia (47–55°E, 5–10°N) using wind data from NCEP–NCAR reanalysis from 1997 to 2004. In contrast, using the same database and an advanced coupled atmosphere–ocean general circulation model, Izumo *et al.*<sup>67</sup> detected a decrease in upwelling from 1979 to 2006 caused by anomalously weak southwesterly winds in late spring over the Arabian Sea. More recently, Piontkovski *et al.*<sup>68</sup> described a declining trend in the zonal component of wind speed over the Sea of Oman (22–25°N) during summer monsoons from the late 1950s to 2010.

Results obtained for different upwelling systems around the world illustrate that it is not possible to describe a homogenous behaviour among them because trends change substantially, even in regions with similar oceanographic processes. Of the five major upwelling regions worldwide, increasing trends in upwelling were observed in the coastal areas of Benguela, Peru, Canary, and northern California, and



the increases were statistically significant only for the two last systems. A general decrease in upwelling intensity was observed along the Chile, southern and central California, and central Somalia coasts, with significant values in all regions. Thus, no evidence for a general intensification of upwelling along these systems was observed.

The general trends found in our study were similar to those reported in studies in which wind stress data were used (Tables 1 and 2). It is important to note that controversial results were also obtained by different authors using the same variable and even the same period of time<sup>2,15</sup>, which indicates a dependence of results on the database used.

Different trends were also detected along the less studied upwelling regions. For example, significant decreasing trends were observed along the coast of Java and northern Kenya, whereas a tendency to an increase in upwelling-favourable winds was detected in western Australia. In the southern Caribbean upwelling region, a significant negative (positive) trend was found east (west) of 71.25°W.

Our analysis covered the last three decades (1982–2010), which is the recent period of strongest global warming, thus it allowed detailed analysis of the influence of warming processes on upwelling trends. In another study, Lima and Wetthey<sup>69</sup> estimated changes in coastal SST by exploring monthly warming patterns along the world's coastline at a scale of 0.25° for the period 1982–2010. They found that even though most coastal areas worldwide have been warming, the magnitude of change has been highly heterogeneous in both space and season. They described a coastal SST decrease nearly year-round in the areas influenced by the California and Humboldt currents, which could be related to a tendency for intensification of upwelling following Bakun's hypothesis. Nevertheless, our results revealed an increasing trend in upwelling along the northern California (38–42°N) and Peru coasts and negative trends along the Chile and southern-central California coasts (Table 2). On the other hand, Lima and Wetthey<sup>69</sup> found a general SST increase in the areas of the Canary, Benguela, and Somali currents, which could indicate a decrease of upwelled, cooler waters linked to an upwelling reduction. Our results only revealed a decrease in upwelling-favourable winds along the Somalia coast.

Among the upwelling systems analysed in the present study, Lima and Wetthey<sup>69</sup> found that coastal temperatures have been warming almost homogeneously throughout the year along the southern Caribbean upwelling region and along the Java and northern Kenya coasts. The western Australia coast has become colder from January to September. These results can be linked to the upwelling trends found in the present work. We detected decreasing trends in upwelling along the southern Caribbean, Java, and northern Kenya coasts, whereas a general upward trend was found along the western Australia coast.

These results delve into a possible discussion about whether the Bakun hypothesis is being fulfilled or not taking into account the present study and those mentioned in Tables 1 and 2. Even in regions where previously not many studies regarding upwelling trends existed, like the Java coast or the southern Caribbean upwelling region, different behaviours can be observed contradicting the general upward trend predicted by Bakun due to global warming.

## References

1. Bakun, A. Global climate change and intensification of coastal upwelling. *Science* **247**, 198–201 (1990).
2. Barton, E. D., Field, D. B., Roy, C. Canary current upwelling: more or less? *Prog. Oceanogr.* **116**, 167–178 (2013).
3. Sydeman, W. J. *et al.* Climate change and wind intensification in coastal upwelling ecosystems. *Science* **345**, 77 (2014).
4. Saha S., *et al.* The NCEP Climate Forecast System Reanalysis. *Bull. Amer. Meteorol. Soc.* **91**, 1015–1057 (2010).
5. García-Reyes, M., Largier, J. L., Sydeman, W. J. Synoptic-scale upwelling indices and predictions of phyto- and zooplankton populations. *Prog. Oceanogr.* **120**, 177–188. (2014).
6. Bakun, A. Coastal upwelling indices, west coast of North America, 1946–71. NOAA-NMFS, Technical Memorandum, pp. 1–13 (1973).
7. Mason, J. E., Bakun, A. Upwelling index update, U.S. west coast 33N–48N latitude. NOAA-NMFS, Southwest Fisheries Center, Tech. Memo **67**, (8), 1 pp (1986).
8. Curry, P., Roy, C. Optimal environmental window and pelagic fish recruitment success in upwelling areas. *Can. J. Fish. Aquat. Sci.* **46**, 670–680 (1989).
9. Santos, F., Gómez-Gesteira, M., deCastro, M., Alvarez, I. Differences in coastal and oceanic SST trends due to the strengthening of coastal upwelling along the Benguela current system. *Contin. Shelf Res.* **34**, 79–86 (2012).
10. Santos, F., deCastro, M., Gómez-Gesteira, M., Alvarez, I. Differences in coastal and oceanic SST warming rates along the Canary upwelling ecosystem from 1982 to 2010. *Cont. Shelf Res.* **47**, 1–6. (2012).
11. Alvarez, I., Gómez-Gesteira, M., deCastro, M., Carvalho, D. Comparison of different wind products and buoy wind data with seasonality and interannual climate variability in the southern Bay of Biscay (2000–2009). *Deep-Sea Res. Pt II.* **106**, 38–48. (2014).
12. Carvalho, D., Rocha, A., Gómez-Gesteira, M., Silva Santos, C. Comparison of reanalyzed, analyzed, satellite-retrieved and NWP modelled winds with buoy data along the Iberian Peninsula coast. *Remote Sens. Environ.* **152**, 480–492. (2014).
13. Carvalho, D., Rocha, A., Gómez-Gesteira, M. Offshore wind energy resource simulation forced by different reanalyses: comparison with observed data in the Iberian Peninsula. *Appl. Energy.* **134**, 57–64. (2014).
14. Patti, B. *et al.* Effect of atmospheric CO<sub>2</sub> and solar activity on wind regime and water column stability in the major global upwelling areas. *Est. Coast. Shelf Sci.* **88**, 45–52 (2010).
15. Narayan, N., Paul, A., Multiza, S., Schulz, M. Trends in coastal upwelling intensity during the late 20th century. *Ocean Sci.* **6**, 815–823 (2010).
16. Pardo, P., Padín, X., Gilcoto, M., Farina-Busto, L., Pérez, F. Evolution of upwelling systems coupled to the long term variability in sea surface temperature and Ekman transport. *Clim. Res.* **48**, 231–246 (2011).
17. Cropper, T. E., Hanna, E., Bigg, G. R. Spatial and temporal seasonal trends in coastal upwelling off Northwest Africa, 1981–2012. *Deep-Sea Res.* **1**, 94–111 (2014).
18. McGregor, H. V., Dima, M., Fischer, H. W., Multiza, S. Rapid 20th-Century Increase in Coastal Upwelling off Northwest Africa. *Science* **315**, 637–639 (2007).

19. Gómez-Gesteira, M. *et al.* Spatio-temporal upwelling trends along the Canary Upwelling System (1967–2006). In: Trends and directions in climate research. *Ann. N. Y. Acad. Sci.* **1146**, 320–337 (2008).
20. Santos, F., Gomez-Gesteira, M., deCastro, M., Alvarez, I. Upwelling along the western coast of the Iberian Peninsula: dependence of trends on fitting strategy. *Clim. Res.* **48**, 213–218 (2011).
21. Black, D. E. *et al.* Eight centuries of North Atlantic Ocean atmosphere variability, *Science*, **286**, 1709–1713 (1999).
22. Muller-Karger, F. *et al.* Processes of coastal upwelling and carbon flux in Cariaco Basin, *Deep Sea Res., Part II*, **51**, 927–943 (2004).
23. Andrade, C. A., Barton, E. D. The Guajira upwelling system, *Cont. Shelf Res.*, **25**, 1003–1022 (2005).
24. Ruiz-Ochoa, M., Beier, E., Bernal, G., Barton, E. D. Sea surface temperature variability in the Colombian Basin, Caribbean Sea, *Deep Sea Res., Part I*, **64**, 43–53, (2012).
25. Rueda-Roa, D.T., Muller-Karger, F.E. The southern Caribbean upwelling system: sea surface temperature, wind forcing and chlorophyll concentration patterns. *Deep Sea Res. Part I Oceanogr Res. Pap* **78**, 102–114. (2013).
26. Garreaud, R. D., Falvey, M. The coastal winds off western subtropical South America in future climate scenarios. *Int. J. Climatol.*, **29**, 543–554 (2009).
27. Goubanova, K., *et al.* Statistical downscaling of sea-surface wind over the Peru-Chile upwelling region: Diagnosing the impact of climate change from the IPSL-CM4 model, *Clim. Dyn.* **36**, 1365–1378 (2011).
28. Rahn, D. A., Garreaud, R. D. A synoptic climatology of the near-surface wind along the west coast of South America. *Int. J. Climatol.* **34**, 780–792 (2013).
29. Aravena, G., Broitman, B., Stenseth, N. C. Twelve years of change in coastal upwelling along the central-northern coast of Chile: Spatially heterogeneous responses to climatic variability. *PLoS ONE* **9**, e90276, doi:10.1371/journal.pone.0090276 (2014).
30. Gutiérrez, D., *et al.* Coastal cooling and increased productivity in the main upwelling zone off Peru since the mid-twentieth century. *Geophys. Res. Lett.*, **38**, 6. (2011).
31. Bakun, A., Field, D., Redondo-Rodriguez, A., Weeks, S. Greenhouse gas, upwelling-favorable winds, and the future of coastal ocean upwelling ecosystems. *Glob. Change Biol.* **16**, 1213–28 (2010).
32. Mendelsohn, R., Schwing, F. B. Common and uncommon trends in SST and wind stress in the California and Peru-Chile current systems, *Prog. Oceanogr.*, **53**, 141–162, (2002).
33. Garcia-Reyes, M., Largier, J. Observations of increased wind-driven coastal upwelling off central California. *J. Geophys. Res., C*, **115**, C04010, doi:10.1029/2009JC005576 (2010).
34. Seo, H., Brink, K. H., Dorman, C. E., Koracin, D., Edwards, C. A. What determines the spatial pattern in summer upwelling trends on the U.S. West Coast? *J. Geophys. Res.* **117**, C08012, (2012).
35. Rykaczewski, R. R., Checkley, D. M. Influence of ocean winds on the pelagic ecosystem in upwelling regions, *Proc. Natl. Acad. Sci.*, **105**, 1965–1970, (2008).
36. Iles, A. C., *et al.* Climate-driven trends and ecological implications of event-scale upwelling in the California Current System. *Glob. Change Biol.* **18**, 783–796 (2012).
37. Church, J. A., Cresswell, G., Godfrey, J. S. The Leeuwin Current. In: Neshyba S.J., Mooers Ch. N. K., Smith R.L., Barber R.T., editors. Poleward flow along eastern ocean boundaries. *Coast. Estuar. Stud.* **34**. New York, : (Springer-Verlag. . p 230–54 (1989).
38. Smith, R. L., Huyer, A., Godfrey, J. S., Church, J. A. The Leeuwin current off western Australia, 1986–1987, *J. Phys. Oceanogr.*, **21**, 323–345, (1991).
39. Pearce, A. F. Eastern boundary currents of the southern hemisphere. *J. R. Soc. W. Aust.* **74**, 35–45 (1991).
40. Rousseaux, C. S. G., Lowe, R. J., Feng, M., Waite, A. M., Thompson, P. A. The role of the Leeuwin Current and mixed layer depth on the autumn phytoplankton bloom off Ningaloo Reef, Western Australia. *Cont. Shelf Res.* **32**, 22–35, (2012).
41. Gersbach, G. H., Pattiaratchi, C. B., Ivey, G. N., Cresswell, G. R. Upwelling on the south-west coast of Australia — source of the Capes Current? *Cont. Shelf Res.* **19**, 363–400 (1999).
42. Wilson, S. G., Carleton, J. H., Meekan, M. G. Spatial and temporal patterns in the distribution and abundance of macrozooplankton on the southern North West Shelf, Western Australia. *Est. Coast. Shelf Sci.* **56**, 897–908 (2003).
43. Hanson, C. E., Pattiaratchi, C. B., Waite, A. M. Sporadic upwelling on a downwelling coast: phytoplankton responses to spatially variable nutrient dynamics off the Gascoyne region of Western Australia. *Cont. Shelf Res.* **25**, 1561–1582 (2005).
44. Woo, M., Pattiaratchi, C. B., Schroeder, W. Summer surface circulation along the Gascoyne continental shelf, western Australia. *Cont. Shelf Res.* **26**, 132–152 (2006).
45. Furnas, M. Intra-seasonal and inter-annual variations in phytoplankton biomass, primary production and bacterial production at North West Cape, Western Australia: Links to the 1997–1998 El Niño event. *Cont. Shelf Res.* **27**, 958–980 (2007).
46. Thompson, P. A., *et al.* Contrasting oceanographic conditions and phytoplankton communities on the east and west coasts of Australia. *Deep-Sea Res.* **58**, 645–663 (2011).
47. Xu, J. *et al.* Dynamics of the summer shelf circulation and transient upwelling off Ningaloo Reef Western Australia, *J. Geophys. Res.*, **118**, 1099–1125, (2013).
48. Susanto, R. D., Gordon, A. L., Zheng, Q. Upwelling along the coasts of Java and Sumatra and its relation to ENSO. *Geophys. Res. Lett.*, **28**, 1599–1602 (2001).
49. Gordon, A. L. Oceanography of the Indonesian seas and their throughflow, *Oceanography*, **18**, 14–27 (2005).
50. Qu, T., Du, Y., Strachan, J., Meyers, G., Slingo, J. M. Sea surface temperature and its variability in the Indonesian region, *Oceanography Wash. D. C.*, **18**, 50–62 (2005).
51. Susanto, R. D., Marra, J. Effect of the 1997/98 El Niño on chlorophyll a variability along the coasts of Java and Sumatra. *Prog. Oceanogr.*, **18**, 124–127 (2005).
52. Andrúleit, H. Status of the Java upwelling area (Indian Ocean) during the oligotrophic northern hemisphere winter monsoon season as revealed by coccolithophores. *Mar. Micropaleontol.* **64**, 36–51. (2007).
53. Baumgart, A., Jennerjahn, T., Mohtadi, M., Hebbeln, D. Distribution and burial of organic carbon in sediments from the Indian Ocean upwelling region off Java and Sumatra, Indonesia. *Deep-Sea Res.* **57**, 458–467 (2010).
54. McClanahan, T. R. Seasonality in East Africa's coastal waters. *Mar. Ecol. Prog. Ser.* **44**, 191–199 (1988).
55. Semeneh, M. F., Dehairs, F., Goeyens, L. Uptake of nitrogenous nutrients by phytoplankton in the tropical Western Indian Ocean (Kenyan Coast): monsoonal and spatial variability. In: Heip C. M. A., Hemminga M. J. M. (Eds), Monsoons and Ecosystems in Kenya. *Kenya Mar. Fish. Res. Inst.*, Mombasa, Kenya, : 101–104 (1995).
56. Duineveld, G. C. A., *et al.* Benthic respiration and standing stock on two contrasting continental margins in the western Indian Ocean: The Yemen-Somali upwelling region and the margin off Kenya, *Deep Sea Res., Part II*, **44**, 1293–1317 (1997).
57. Kromkamp, J., *et al.* Primary production by phytoplankton along the Kenyan coast during the SE monsoon and November intermonsoon 1992, and the occurrence of Trichodesmium, *Deep Sea Res. Part II*, **44**, 1195–1212 (1997).
58. Mengesha, S., Dehairs, F., Elskens, M., Goeyens, L. Phytoplankton nitrogen nutrition in the western Indian Ocean: Ecophysiological adaptations of neritic and oceanic assemblages to ammonium supply, *Est. Coast. Shelf Sci.*, **48**, 589–598 (1999).
59. Mwaluma, J., Osore, M., Kamau, J., Wawiye, P. Composition, abundance and seasonality of zooplankton in Mida Creek, Kenya. Western Indian Ocean. *J. Mar. Sci.* **2**, 147–155 (2003).

60. Muthumbi, A. W., Vanreusel, A., Duineveld, G., Soetaert, K., Vincx, M. Nematode community structure along the continental slope off the Kenyan Coast, Western Indian Ocean. *Int. Rev. Gesamten Hydrobiol.*, **89**, 188–205 (2004).
61. Wyrski, K. Physical oceanography of the Indian Ocean. Pp. 18–36 in B. Zeitzschel, ed. *The biology of the Indian Ocean*. (Springer-Verlag, New York, (1973).
62. Prell, W. L. Variation of monsoonal upwelling: a response to changing solar radiation. In: Hansen, J., T. Takahashi, T. (Eds.), *Clim. Proc. and Clim. Sens.*, (AGU, , pp. 48–57 (1984).
63. Koning, E., *et al.* Selective preservation of upwelling-indicating diatoms in sediments off Somalia, NW Indian Ocean. *Deep-Sea Res. I* **48**, 2473–2495 (2001).
64. de Boyer Montegut, C., *et al.* Simulated seasonal and interannual variability of mixed layer heat budget in the northern Indian Ocean, *J. Clim.*, **20**, 3249 – 3268 (2007).
65. Valsala, K. V. Different spreading of Somali and Arabian coastal upwelled waters in the northern Indian Ocean: A case study, *J. Oceanogr.*, **65**, 803–816 (2009).
66. Goes, J. L., Thoppil, P. G., Gomes, H. do R., Fasullo, J. T. Warming of the Eurasian landmass is making the Arabian Sea more productive. *Science*, **308**, 545–547. (2005).
67. Izumo, T., *et al.* The role of the western Arabian Sea upwelling in Indian monsoon rainfall variability, *J. Clim.*, **21**, 5603–5623 (2008).
68. Piontkovski, S. A., AL-Gheilani, H. M. H., Jupp, B. P., Al-Azri, A. R., Al-Hashmi, K. A. Interannual changes in the Sea of Oman ecosystem. *Open Mar. Biol. J.* **6**, 38–52 (2012).
69. Lima, F. P., Wethey, D. S. Three decades of high-resolution coastal sea surface temperatures reveal more than warming. *Nature Commun.* **3**, 704 (2012).

## Acknowledgements

**Funding:** This work is partially supported by Xunta de Galicia under projects 10PXIB 383169PR and Programa de Consolidación e Estruturación de Unidades de Investigación (Grupos de Referencia Competitiva) funded by European Regional Development Fund (FEDER) and under the project EM2013/003. I. Alvarez is supported by the Ramón y Cajal Program. The funders had no role in study design, data collection and analysis, decision to publish, or preparation of the manuscript. F. Santos is supported by the Portuguese Science Foundation through a post-doctoral grant (SFRH/BPD/97320/2013).

## Author Contributions

Conceived and designed the experiments: R.V., I.A., F.S., M.dC. and M.G-G. Performed the experiments: R.V. Analyzed the data: R.V., I.A., F.S., M.dC. and M.G-G. Contributed reagents/materials/analysis tools: R.V., F.S. and M.G-G. Wrote the paper: R.V., I.A., M.dC. and M.G-G. All authors reviewed the manuscript.

## Additional Information

**Competing financial interests:** The authors declare no competing financial interests.

**How to cite this article:** Varela, R. *et al.* Has upwelling strengthened along worldwide coasts over 1982–2010? *Sci. Rep.* **5**, 10016; doi: 10.1038/srep10016 (2015).



This work is licensed under a Creative Commons Attribution 4.0 International License. The images or other third party material in this article are included in the article's Creative Commons license, unless indicated otherwise in the credit line; if the material is not included under the Creative Commons license, users will need to obtain permission from the license holder to reproduce the material. To view a copy of this license, visit <http://creativecommons.org/licenses/by/4.0/>





# Coastal warming and wind-driven upwelling: a global analysis

**\* Rubén Varela<sup>1</sup>, Fernando P. Lima<sup>2</sup>, Rui Seabra<sup>2</sup>, Claudia Meneghesso<sup>2</sup> and Moncho Gómez-Gesteira<sup>1</sup>**

*1 EPHYSLAB, Environmental PHYsics LABoratory, Facultad de Ciencias, Universidad de Vigo, Ourense, Spain, [ruvarela@uvigo.es](mailto:ruvarela@uvigo.es).*

*2 CIBIO, Centro de Investigação em Biodiversidade e Recursos Genéticos, Universidade do Porto, Campus Agrário de Vairão 4485-661 Vairão, Portugal.*

## **Abstract**

Near the coast, long-term sea surface temperature (SST) warming trends are not homogeneous. Even though recent reports suggested that some of this variability might result from the buffering effect of upwelling over the large-scale effects of global warming, no systematic analysis has been yet done at a global scale. Using data from NOAA's AVHRR OISST, we analyzed sea surface temperature trends over the period 1982-2015 at around 3500 worldwide coastal points and their oceanic counterparts with a spatial resolution of 0.25 arc-degrees. Significant warming was observed at most oceanic and coastal locations. Globally, higher temperatures were found offshore than inshore in upwelling-dominated regions, supporting the hypothesis that upwelling is associated with depressed warming rates near the coast. This result strongly suggests that upwelling regions have the potential to buffer the effects of global warming near the coast, with wide oceanographic, climatic, and biogeographic implications.

**Keywords:** Upwelling, sea surface temperature, wind, climate change, warming, cooling

## 1. Introduction

The communication of climate change on marine ecosystems is often expressed through simplified warming trends (Cane et al., 1997, Levitus et al., 2000, 2005, Harrison and Carson, 2007, Belkin, 2009, Hansen et al., 2010). However, in coastal areas, which harbor some of the most biodiverse but also variable environments of the ocean (Gray, 1997), warming is far from being homogenous. Understanding this variability is essential for explaining current patterns and predict changes not only in fisheries (Cheung et al., 2013), but also in biogeography and biodiversity in general (Hoegh-Guldberg and Bruno, 2010, Seabra et al., 2015). In 2012, Lima and Wetthey, (2012) reported that 71 % of the coast had been warming since the early 1980s, while 22% of the area had not been changing and 7% actually cooled significantly. The heterogeneity of warming has led to numerous regional studies (e.g., Mendelssohn and Schwing, 2002; Qu et al., 2005; Gómez-Gesteira et al., 2008a,b; Chollett et al., 2012; Barton et al., 2013; IPCC, 2014; García-Reyes et al., 2015), which raised several hypothesis to explain the observed variability in the geographical distribution of warming and its intensity.

Near the coast, global drivers are modified by topography and by local atmospheric and oceanographic circulation patterns, including upwelling. Upwelling is an oceanographic process whereby deep, cold water rises toward the surface near the coast (usually driven by wind stress). Loaded with nutrients, this water sustains hot spots of primary production and biological diversity, and is crucial for fisheries and for the economy (Constanza et al., 1997). In fact, despite covering only 1% of the coastal areas, upwelling systems yield more than 20% of worldwide catches (Pauly and Christensen, 1995). Apart from the nutrient load, upwelled water masses also have distinct thermal characteristics. It was recently shown that they are associated with depressed long-term warming rates, and thus may provide thermal refugia, stabilize changes in species distributions and enhance local biodiversity. Despite

some regional studies highlighting differences in warming rates between coastal and oceanic waters within some of the major upwelling systems (e.g., Santos et al., 2012a,b; Varela et al., 2016), no systematic analysis has been done and a global overview of this phenomenon is lacking.

The aims of this study were (i) to determine warming rates in nearshore and offshore waters around the world and (ii) to investigate whether differences between coastal and offshore locations were associated with upwelling regions.

## **2. Data and methods**

### *2.1 Temperature data*

Daily SST values were obtained from the Advanced Very High Resolution Radiometer Optimum Interpolation Sea Surface Temperature database at a resolution of  $0.25^\circ$  (AVHRR-Only OISST  $\frac{1}{4}$ ), accessed through NOAA's website (<https://www.ncdc.noaa.gov/oisst>).

Data was downloaded over the period 1982 to 2015 for 3410 nearshore points and 3410 corresponding oceanic points distributed worldwide. Offshore locations were selected at the distance of 1.5 arc-degrees perpendicular to the coast (close enough to feature the thermal characteristics of the water masses at regional scales but sufficiently distant to fall outside the area strongly influenced by upwelling). Daily SST were monthly averaged and the values obtained were subtracted from the monthly mean calculated over the entire period of study, thus resulting in monthly SST anomalies. For each pixel, annual SST trends were calculated as the slope of the linear regression of monthly SST anomalies versus time. A Spearman rank correlation coefficient was used to investigate the significance of SST trends.

## 2.2 Different warming rates at coastal and oceanic points

Differences between coastal and oceanic SST trends were calculated for each location to determine whether nearshore pixels presented differing warming trends than their respective offshore counterparts. Results from upwelling and non-upwelling locations (respectively, 681 and 2729 locations) were then compared to assess the influence of upwelling on the warming rates. Upwelling zones were selected according to previous studies (Oke and Middleton, 2000; Shi et al., 2000; Lutjeharms et al., 2000; Rao, 2002; Snyder et al., 2003; Kämpf et al., 2004; Yuras et al., 2005; Castelao and Barth, 2006; Susanto et al., 2006; Patti et al., 2008, 2010; Smitha et al., 2008; Arístegui et al., 2009; Falvey and Garreaud, 2009; Narayan et al., 2010; Gutiérrez et al., 2011; Pardo et al., 2011; Santos et al., 2012a,b; Santos et al., 2015; Varela et al., 2015; Ruiz-Castillo et al., 2016; Santos et al., 2016; Varela et al., 2016). A summary of the upwelling areas considered in this study and their geographical boundaries is reported in Table 1.

Although upwelling occurs seasonally in some of the areas considered in this study, calculations were carried out on an annual basis because (i) the duration and seasonality of upwelling is zone-dependent; (ii) there is a lag between the mechanism that induces upwelling (Ekman transport, Ekman pumping or the interaction of a coastal jet with the shelf) and the upwelled water SST signal, which makes the choosing of target months highly subjective; (iii) the imprint of upwelling on SST trends should be strong enough to be detected at an annual scale and not only during a few months; (iv) SST trends from upwelling locations will be compared to non-upwelling zones, for which there is no criterion for the selection of specific months for these analysis.

Results are reported according to seven large-scale coastal areas defined in this study: (i) Eastern Atlantic Ocean, (ii) Western Atlantic Ocean, (iii) Eastern Pacific Ocean, (iv) Western

Pacific Ocean, (v) Western Pacific Ocean (islands), (vi) Eastern Indian Ocean and (vii) Western Indian Ocean.

<b>Upwelling system</b>	<b>Latitude</b>	<b>Longitude</b>
South Benguela	35 - 24°S	14 - 19°E
North Benguela	21 - 17°S	11.5 - 13°E
Canary	21 - 33°N	343 - 351°E
Chile	40 - 18°S	286 - 290°E
Peru	17 - 13°S	283 - 287°E
South California	34 - 36°N	239 - 241°E
North California	38 - 42°N	235 - 237°E
Iberian Peninsula	37 - 43°N	350 - 351°E
Brazil	23 - 20°S	316 - 320°E
South Caribbean Sea	10 - 12°N	285 - 298°E
Yucatan	21 - 22°N	270 - 272°E
East Australia	31 - 27°S	153 - 154°E
South Australia	38 - 36°S	137 - 141°E
West Australia	33 - 25°S	113 - 116°E
Java - Sumatra	9°S - 5°N	95 - 116°E
East India	13 - 18°N	80 - 83°E
Agulhas	35 - 34°S	21 - 27°E
Kenia	0 - 4°N	43 - 47°E
Somalia	4 - 12°N	47 - 52°E
Oman	17 - 22°N	55 - 60°E
West India	8 - 15°N	74 - 77°E

**Table 1 | Geographical boundaries of the upwelling systems considered in this study.**

Upwelling systems were separated accordingly to the seasonality of upwelling: year-round (upper group) or monthly seasonality (lower group).

### 3. Results

Global analysis revealed that the great majority of coastal (87.1%) and offshore locations (92.0%) experienced warming over the last three decades (Fig. 1 and Table 2), with temperatures rising more intensely at oceanic locations than at their coastal counterparts in 65.8% of the cases. Coastal locations within upwelling areas, however, presented lower temperatures than their respective offshore waters (in 92% of the cases), against only 58% of non-upwelling locations.

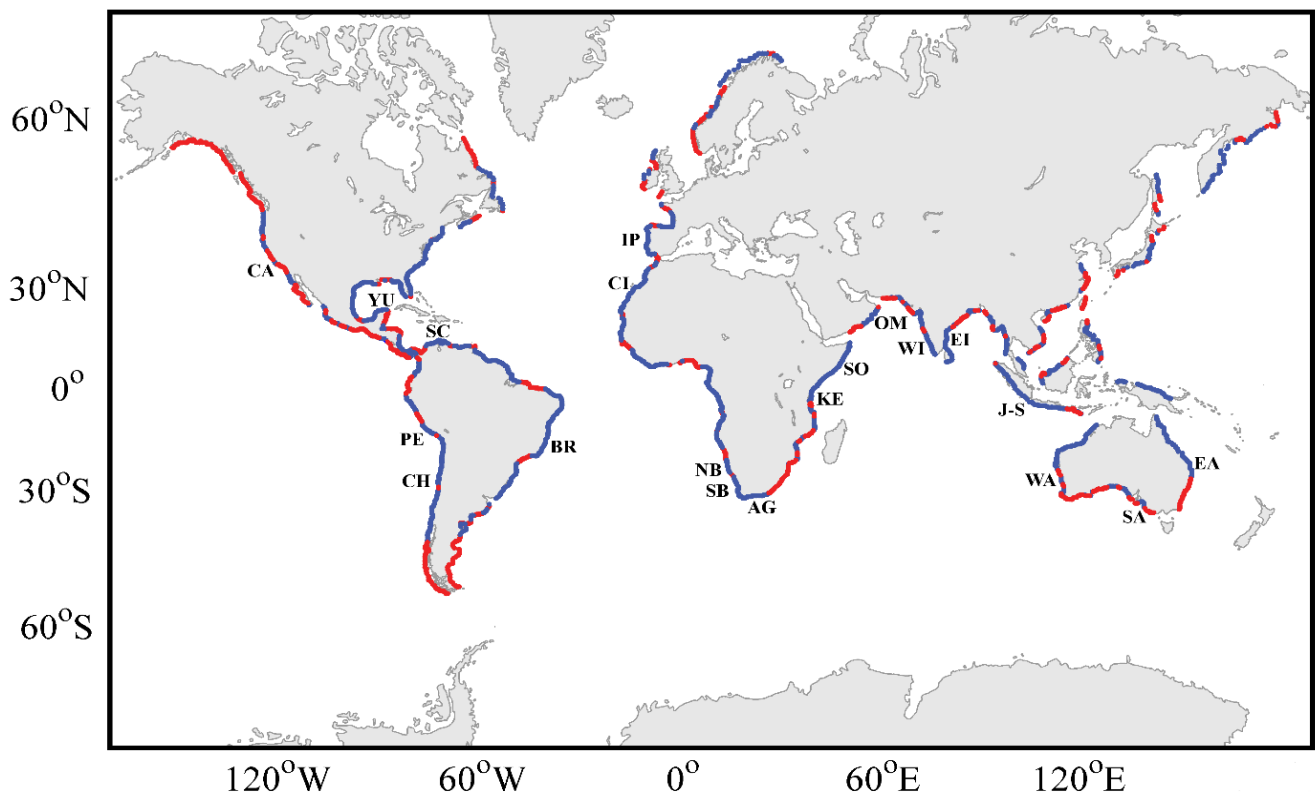


**Figure 1 | Worldwide coast-offshore differences in warming trends.** Red (blue) indicates that nearshore waters SSTs are warmer (colder) than their respective offshore waters. Twenty



upwelling areas were considered: SB (South Benguela), NB (North Benguela), CI (Canary Islands), IP (Iberian Peninsula), BR (Brazil), SC (South Caribbean), YU (Yucatan), CH (Chile), PE (Peru), CA (California), EA (East Australia), SA (South Australia), WA (West Australia), J-S (Java - Sumatra), EI (East India), AG (Agulhas), KE (Kenya), SO (Somalia), OM (Oman) and WI (West India).

Geographical area	Oceanic warming	Coastal warming	$Trend_{ocean} > Trend_{coast}$
<b>World</b>	92.0%	87.1%	65.8%
<b>Eastern Atlantic Ocean</b>	100%	95.1%	72.0%
<b>Western Atlantic Ocean</b>	96.9%	87.3%	67.4%
<b>Eastern Pacific Ocean</b>	45.8%	43.4%	46.9%
<b>Western Pacific Ocean (islands)</b>	100%	100%	73.7%
<b>Western Pacific Ocean</b>	100%	97.8%	63.5%
<b>Eastern Indian Ocean</b>	100%	98.1%	73.7%
<b>Western Indian Ocean</b>	100%	93.3%	70.8%
<b>Upwelling Systems</b>	80.3%	70.2%	92.36%
<b>Non-upwelling Systems</b>	93.2%	89.9%	58.56%

**Table 2 | Statistical analysis of the SST trends along the World's coastlines.** *Oceanic warming* indicates the percentage of oceanic points with positive (warming) SST trends. *Coastal warming* indicates the percentage of coastal points with positive (warming) SST trends.  $Trend_{ocean} > Trend_{coast}$  shows the percentage of points with SST trends higher in the ocean than in the coast (colder waters nearshore).

### 3.1 Eastern Atlantic Ocean (Figure 2).

Positive SST trends (warming) are found in all oceanic locations of the Eastern Atlantic Ocean area (Figure 2b) and for most of nearshore points (Figure 2c), resulting in a general positive warming trend. Only 5% of coastal locations showed a negative trend, coinciding with the areas where upwelling is prevalent. The southernmost cooling region is part of the Benguela Upwelling System, where coastal trends attained  $-0.25\text{ }^{\circ}\text{C dec}^{-1}$  in contrast with the  $0.15\text{ }^{\circ}\text{C dec}^{-1}$  found in offshore waters. These results are in agreement with Lima and Wethey, (2012) and also with Santos et al., (2012a), who associated such differences to an enhancement of upwelling. A reinforcement of upwelling winds was also supported by Varela et al., (2015) over a similar period (1982-2010) and region.

The northernmost cooling area coincides with the Canary Upwelling System, where a moderate cooling ( $\sim -0.1\text{ }^{\circ}\text{C dec}^{-1}$ ) was observed nearshore. Santos et al., (2012b) found the same patterns and associated them to a strengthening of upwelling, a hypothesis confirmed recently by other authors (Cropper et al., 2014; Varela et al., 2015). Similar results were obtained by Cheung et al., (2013). It is also worth mentioning the differences between coast and ocean ( $-0.2\text{ }^{\circ}\text{C dec}^{-1}$ ) found along the Iberian Peninsula, which is the northernmost limit of the Canary Upwelling System.

Despite the warming observed over the last three decades, global changes in temperature in the Eastern Atlantic appear to have less effect on coastal waters than offshore waters. Coastal SST trends were generally lower than offshore trends (negative differences in SST trends were found in 72% of the locations; Figure 2d, Table 2). Positive values were only found for Central Africa, West France and in the North Sea areas (warming rates were similar to those observed by Lima and Wethey, (2012) in Central Africa and in the North Sea and by deCastro et al., (2009) in the Bay of Biscay). The most negative differences were, not surprisingly, found along the Benguela and Canary upwelling zones.

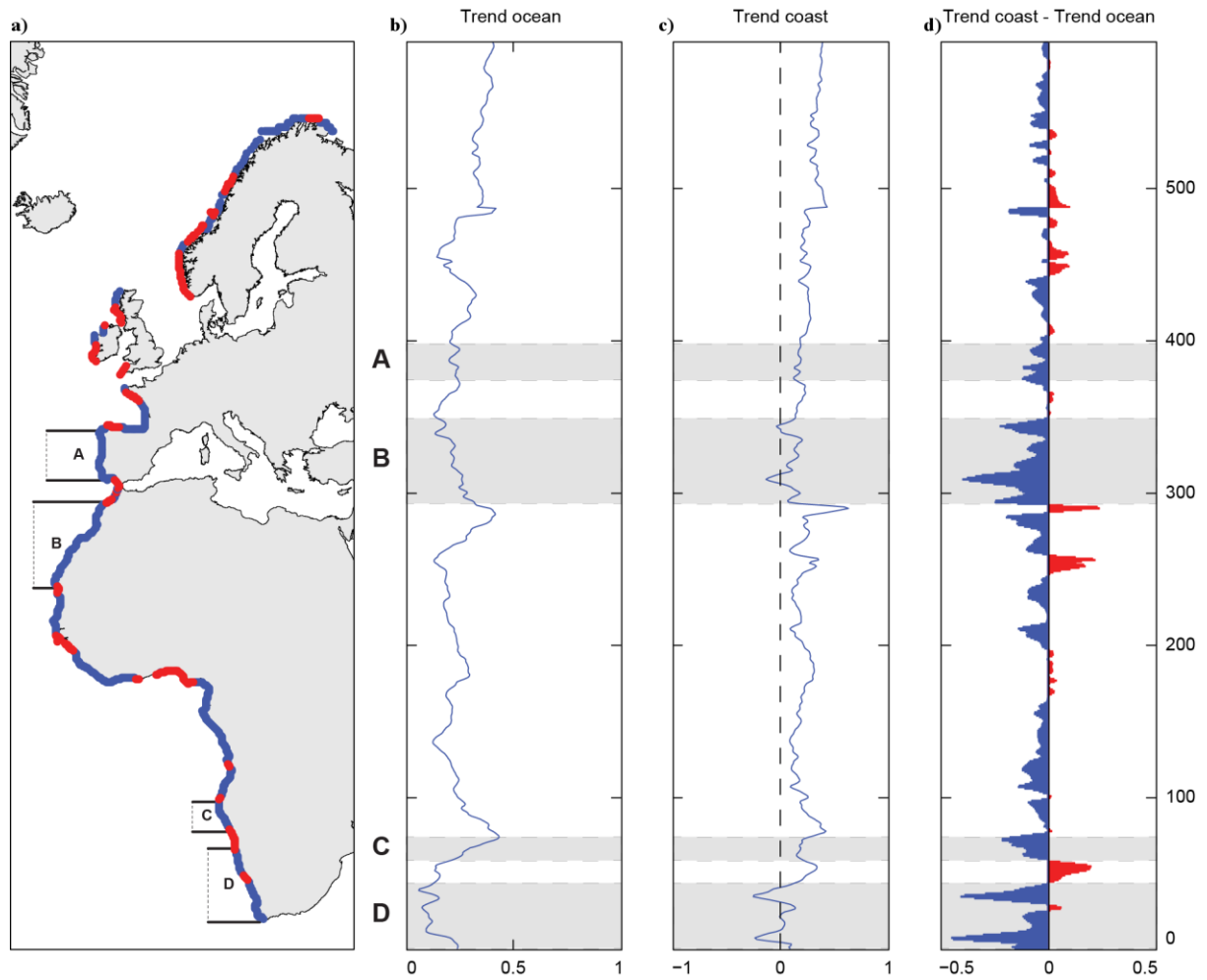


**Figure 2 | SST trends along the Eastern Atlantic Ocean.** From left to right: (a) coast-offshore differences in warming trends. Red (blue) indicates that nearshore waters SSTs are warmer (colder) than their respective offshore waters; dashed rectangles circumscribe the upwelling areas of Iberian Peninsula (A), Canary Islands (B), North Benguela (C) and South Benguela (D). (b) Oceanic and (c) coastal SST trends ( $^{\circ}\text{C dec}^{-1}$ ) and (d) their differences. Dashed grey areas identify points in upwelling zones.

### 3.2 Western Atlantic Ocean (Figure 3)

In the western side of the Atlantic, offshore and inshore waters were found to be warming over the last three decades (Figure 3b,c). Overall, 87% of the coastal points and 97% of the oceanic points have been warming (Table 2). The southern tip of America (Tierra del Fuego,

Argentina) was the only area that cooled both nearshore and offshore, as previously observed by Falvey and Garreaud, (2009). Coastal temperatures also decreased markedly along the east coast of Florida, where cooling trends reached  $-1\text{ }^{\circ}\text{C dec}^{-1}$ , the strongest worldwide. This pattern has been previously highlighted by other authors (Belkin, 2009; Lima and Wetthey, 2012; Cheung et al., 2013), and has been linked to changes in the path of the Gulf Stream. Other cooling trends were observed along the upwelling areas of Brazil (upwelling was described for Cabo Frio region by means of wind stress and SST by Lorenzzetti and Gaeta, (1996); Castelao and Barth, (2006)) and Yucatan ( $-0.3\text{ }^{\circ}\text{C dec}^{-1}$ ), and are likely associated with a reinforcement of upwelling favorable winds in the area (Varela et al., 2015). Similar trends in the Mexican coast were also observed by Castillo et al., (2016) and Carrillo et al., (2016), and were associated with the strengthening of the Yucatan Current. The remaining locations of the Gulf of Mexico also presented lower warming rates nearshore than offshore, with differences of around  $-0.4\text{ }^{\circ}\text{C dec}^{-1}$ . Contrary to previous research (Andrade and Barton, 2004; Santos et al., 2016), a cooling trend in the upwelling area of La Guajira was not observed in this study, probably because the seasonality of upwelling in this system was not reflected in the annual scale used for the calculations of SST trends.

Finally, the northern coast of the United States and Canada showed the highest warming trends both at coastal (Figure 3c) and oceanic (Figure 3b) locations (approximately  $0.5\text{ }^{\circ}\text{C dec}^{-1}$ ), in agreement with previous research (Lima and Wetthey, 2012; Cheung et al., 2013).

Similarly to the colder coastal waters observed in the Eastern Atlantic side, 67% of the Western Atlantic coast presented lower SST than their adjacent offshore waters (Figure 3d).

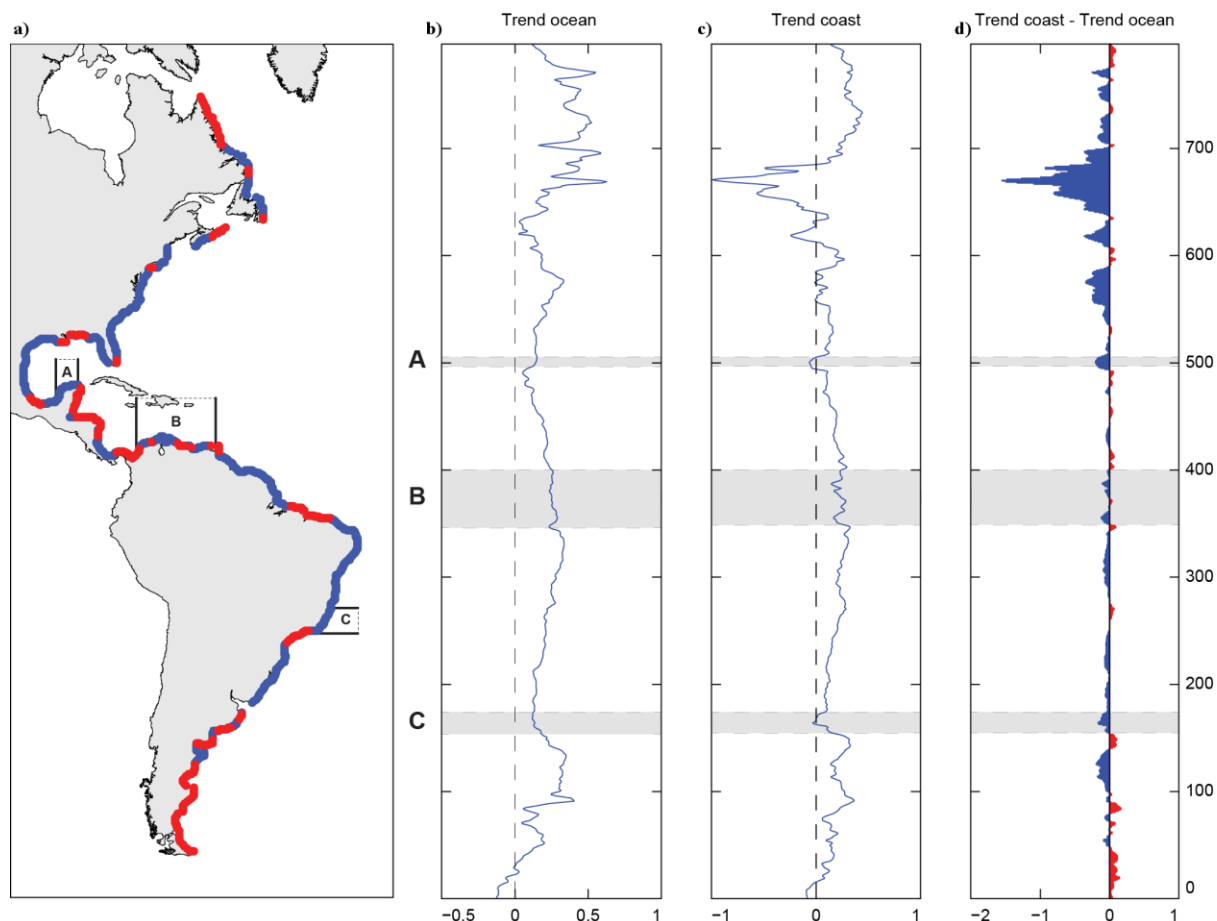


**Figure 3 | SST trends along the Western Atlantic Ocean.** From left to right: (a) coast-offshore differences in warming trends. Red (blue) indicates that nearshore waters SSTs are warmer (colder) than their respective offshore waters; dashed rectangles circumscribe the upwelling areas of Yucatan (A), South Caribbean (B), and Brazil (C). (b) Oceanic and (c) coastal SST trends ( $^{\circ}\text{C dec}^{-1}$ ) and (d) their differences. Dashed grey areas identify points in upwelling zones.

### 3.3 Eastern Pacific Ocean (Figure 4)

The Eastern Pacific Ocean basin is the only in which trends at oceanic and coastal locations were negative over extended latitudes (Figure 4b and c, Table 2). In fact, only 43% of nearshore and 46% of offshore waters warmed during the period of study, far less than observed in the other basins. In particular, trends were negative in zones located

approximately from -45°S to -10°S and from 20°N to 45°N (Figure 4a), with cooling more intense at coastal locations (Figure 4c). These areas coincide with the Humboldt and the California systems, two of the main Eastern Boundaries Upwelling Systems (EBUS) in the world. Similar trends were found for the South American area by Lima and Wethey, (2012) (-0.4 °C dec<sup>-1</sup> in the Humboldt Current), Demarcq, (2009) and Gutiérrez et al., (2011) (close to -0.3 °C dec<sup>-1</sup>, in both Chile and Peru). Even though these patterns might suggest that upwelling is getting stronger in the area, recent studies did not clearly support the intensification of upwelling along the coast of Chile (Falvey and Garreaud, 2009; Goubanova et al., 2011; Varela et al., 2015).

Coastal cooling trends in the California Upwelling System were found in the northern area, with values near -0.2 °C dec<sup>-1</sup>. Similar results were obtained by Macías et al., (2012) and by Lima and Wethey, (2012). Negative coastal trends were also observed in the southern California area, although less intense than in offshore waters. These latitudinal differences can be related to differences in the intensity of upwelling, a hypothesis supported by Varela et al., (2015), which showed that upwelling is increasing in northern California (in contrast with southern California, where upwelling seems to be weakening).

Comparative analysis between nearshore and offshore locations revealed that, contrasting with the patterns observed in other oceanic basins, in 53% of the points coastal warming was more intense than offshore warming (Figure 4d, Table 2). Differences between coastal and oceanic points were found to be up to 0.2 °C dec<sup>-1</sup> at the northernmost and southernmost areas of the Eastern Pacific Ocean basin. This is likely due to the influence of the Alaska Current and the Antarctic Subpolar Current in the area.

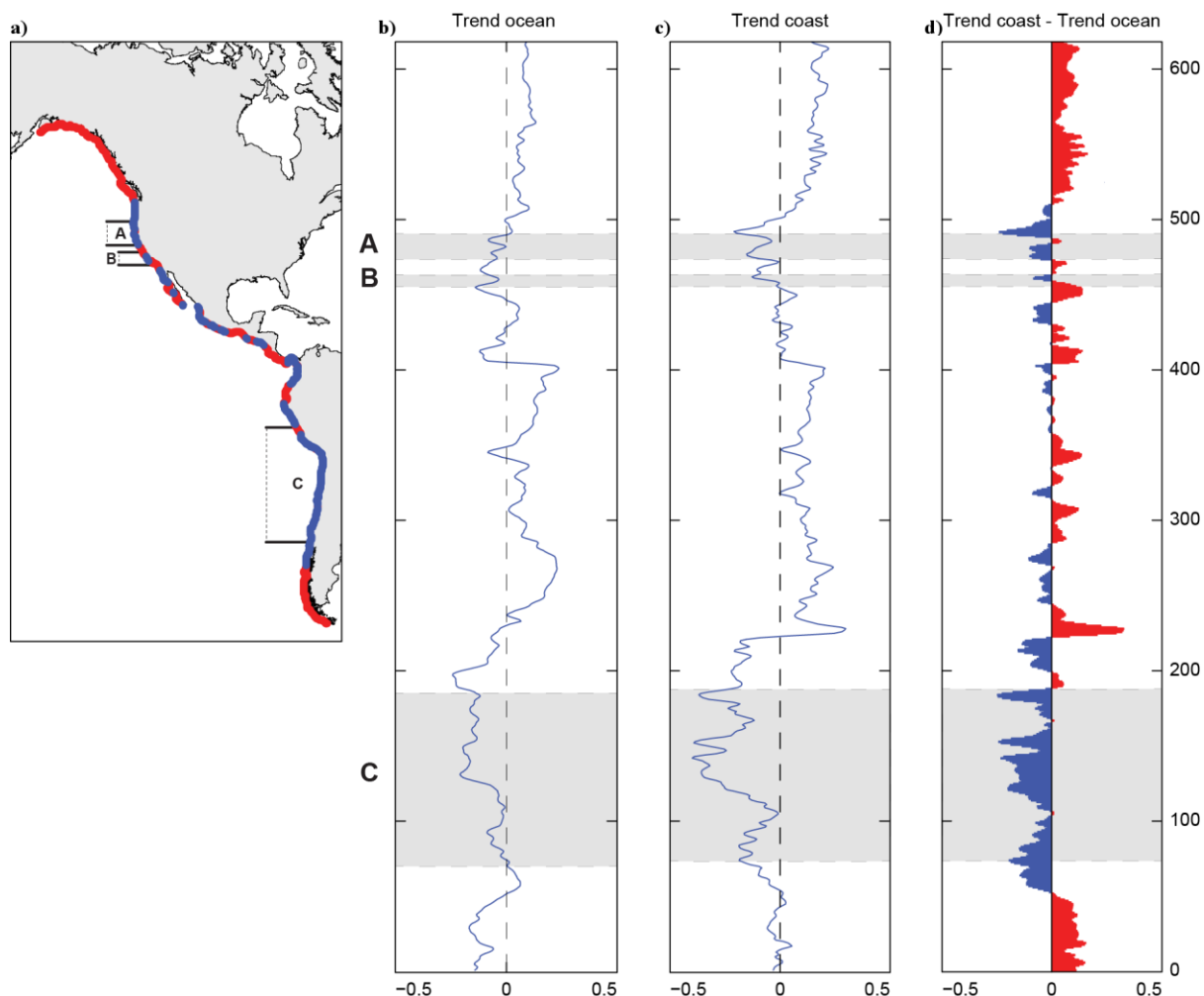


**Figure 4 | SST trends along the Eastern Pacific Ocean.** From left to right: (a) coast-offshore differences in warming trends. Red (blue) indicates that nearshore waters SSTs are warmer (colder) than their respective offshore waters; dashed rectangles circumscribe the upwelling areas of North (A) and South California (B) and the Chile-Peru system (C). (b) Oceanic and (c) coastal SST trends ( $^{\circ}\text{C dec}^{-1}$ ) and (d) their differences. Dashed grey areas identify points in upwelling zones.

### 3.4 Western Pacific Ocean (Islands) (Figure 5)

A general warming trend was observed along all the waters of the Western Pacific Ocean islands (Figure 5b,c). A temperature increase in the northernmost islands was also found by Shiu et al., (2009) near Taiwan over the period 1961 - 2005.

The highest coastal warming was found along eastern Australia ( $0.4\text{ }^{\circ}\text{C dec}^{-1}$ ), with values similar to those found by Lima and Wethey, (2012). Cheung et al., (2013) found that the southeast Australian waters had the highest warming rates within the Western Pacific islands, a trend that has been suggested to be related to changes in the East Australian Current (Ridgway, 2007). Despite local studies describing topographically induced upwelling originated in the East Australian Current and affecting the East coast of Australia (Oke and Middleton, 1999), this study failed to detect any cooling in the area, possibly because this seasonal phenomenon is not detected on an annual scale.

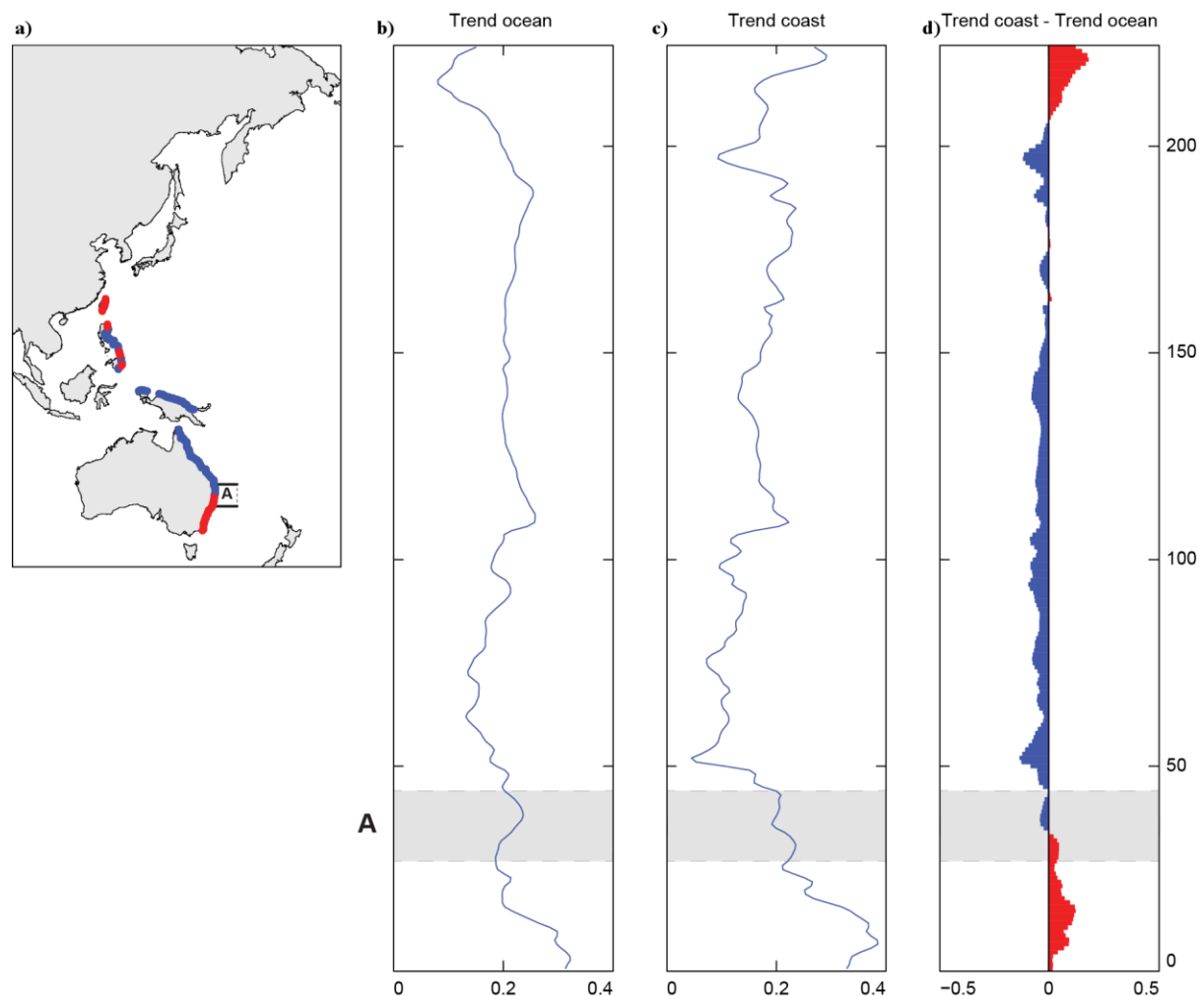


**Figure 5 | SST trends along the Western Pacific Ocean (islands).** From left to right: (a) coast-offshore differences in warming trends. Red (blue) indicates that nearshore waters SSTs are warmer (colder) than their respective offshore waters; dashed rectangles circumscribe the



upwelling areas of East Australia (A). (b) Oceanic and (c) coastal SST trends ( $^{\circ}\text{C dec}^{-1}$ ) and (d) their differences. Dashed grey areas identify points in upwelling zones.

Overall, in 74% of the locations, warming was lower nearshore (Figure 5d, Table 2). In particular, the areas of Papua New Guinea and the southern Philippines exhibited differences of up to  $-0.1\text{ }^{\circ}\text{C dec}^{-1}$  between coastal and oceanic points. The remaining 26% of the locations had warmer waters nearshore, ranging from 0.1 to  $0.2\text{ }^{\circ}\text{C dec}^{-1}$  in Taiwan, northern Philippines and eastern Australia.

### **3.5 Western Pacific Ocean (Figure 6)**

Positive (warming) trends were observed at all oceanic points (Figure 6b) and at almost all coastal points (98%, Figure 6c; Table 2). Maximum ocean SST trends were observed in southern Japan area, where temperatures increased up to  $0.5\text{ }^{\circ}\text{C dec}^{-1}$  (Figure 6b), a warming trend in agreement with the studies of Belkin, (2009), Lima and Wetthey, (2012) and Cheung et al., (2013). Similar to the general trends observed in the Western Pacific islands, 63% of offshore locations have been warming faster than nearshore locations (Table 2), being differences between  $-0.2$  and  $0.2\text{ }^{\circ}\text{C}$ . Maximum differences were found along the Japanese coast, with values around  $-0.6\text{ }^{\circ}\text{C dec}^{-1}$ . According to previous research (Yeh et al., 2010), this difference is associated with changes in the sensible heat flux caused by warm air advection in the area of the East Japan Sea.

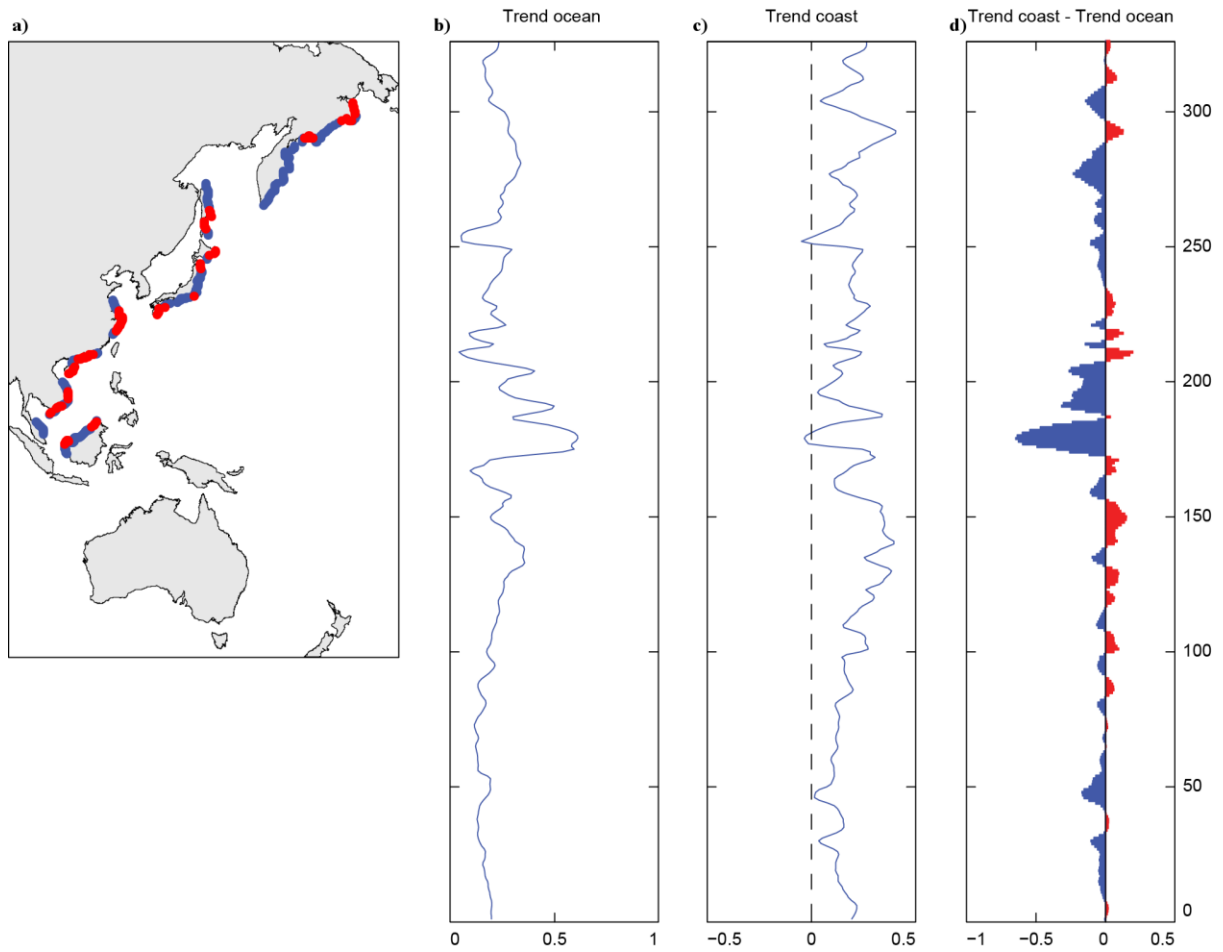


**Figure 6 | SST trends along the Western Pacific Ocean.** From left to right: (a) coast-offshore differences in warming trends. Red (blue) indicates that nearshore waters SSTs are warmer (colder) than their respective offshore waters. (b) Oceanic and (c) coastal SST trends ( $^{\circ}\text{C dec}^{-1}$ ) and (d) their differences. Dashed grey areas identify points in upwelling zones.

### 3.6 Eastern Indian Ocean (Figure 7)

Offshore waters along the Eastern Indian Ocean showed positive trends ranging from  $0.1^{\circ}\text{C dec}^{-1}$  to  $0.3^{\circ}\text{C dec}^{-1}$  (Figure 7b). Positive trends were also found at around 98% of the coastal locations (Figure 7c and Table 2), with the highest warming trends occurring in southern Australia ( $\sim 0.3^{\circ}\text{C dec}^{-1}$ ), in agreement with Lima and Wethey, (2012). In southeastern Australia, local studies described the existence of summer wind-driven upwelling (Kämpf et al., 2004, Kämpf, 2010; Gill et al., 2011), which explains the depressed warming trends at the

coast highlighted in Figure 7d (differences of around  $-0.1 \text{ }^{\circ}\text{C dec}^{-1}$ ). Lima and Wethey, (2012) obtained similar seasonal cooling trends for that area.

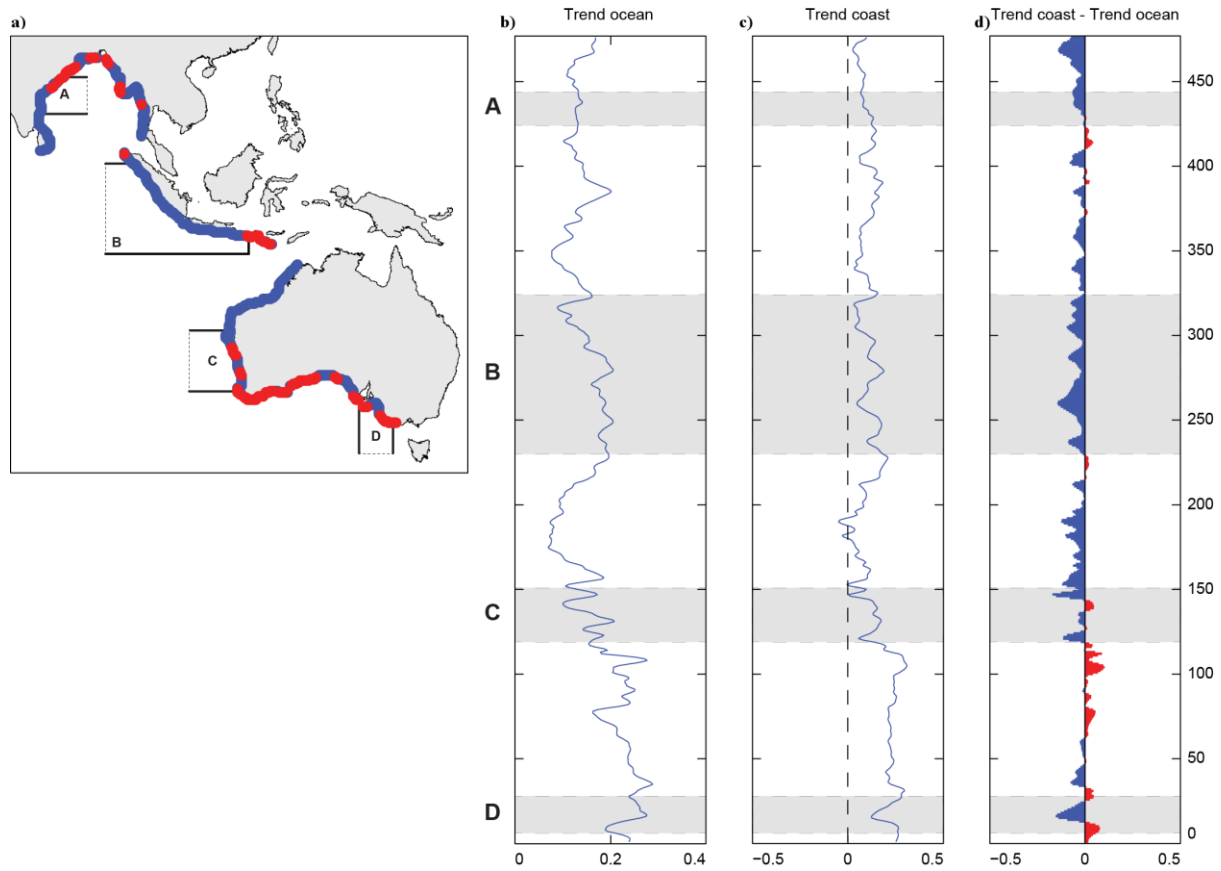


**Figure 7 | SST trends along the Eastern Indian Ocean.** From left to right: (a) coast-offshore differences in warming trends. Red (blue) indicates that nearshore waters SSTs are warmer (colder) than their respective offshore waters; dashed rectangles circumscribe the upwelling areas of East India (A), Java-Sumatra (B), West (C) and South Australia (D). (b) Oceanic and (c) coastal SST trends ( $^{\circ}\text{C dec}^{-1}$ ) and (d) their differences. Dashed grey areas identify points in upwelling zones.

The lowest warming trends were found for points located within the upwelling areas of West Australia (the lowest trends in the eastern Indian Ocean according to Lima and Wethey, (2012), likely associated to a reinforcement of upwelling (Varela et al., 2015) or changes in the Leewin Current (Furnas, 2007; Xu et al., 2013). No cooling trends were observed in the

area of Java-Sumatra, which contrasts with the previous work of Varela et al., (2016) and is most likely a consequence of the seasonality of upwelling, which is not reflected in the temporal scale used in this study. Differences of  $-0.2\text{ }^{\circ}\text{C dec}^{-1}$  between coastal and oceanic points were also found in eastern India and are possibly related to upwelling events induced by the southwest monsoon (Rao, 2002).

Differences in SST trends between coastal and oceanic locations range from  $-0.2\text{ }^{\circ}\text{C dec}^{-1}$  to  $0.1\text{ }^{\circ}\text{C dec}^{-1}$  (Figure 7d), being negative at around 74% of the points.

### **3.7 Western Indian Ocean. (Figure 8)**

Warming was observed at all oceanic locations (Figure 8b), with the southern tip of Africa being the area with the highest increase in temperature (up to  $0.5\text{ }^{\circ}\text{C dec}^{-1}$ ). Positive trends were also found in 93% of the nearshore locations (Table 2, Figure 8c). Coastal points with negative trends coincide with two areas where upwelling is prevalent, the Agulhas Bank and Somalia Upwelling Systems. In the Agulhas Bank, a mechanism of enhancement of upwelling due to the transition of a coastal jet from a narrow shelf to a wider shelf was proposed (Gill and Schumann, 1979). More recently, Lutjeharms et al., (2000) associated the lower SST values found in the coast of South Africa to both the action of the wind in the area and to Ekman drift.

Off Somalia, cooling trends were in the order of  $-0.1\text{ }^{\circ}\text{C dec}^{-1}$  near the northern tip of the country, in agreement with the findings from Lima and Wetthey, (2012). Santos et al., (2015) showed that this nearshore cooling over the last three decades is a result of the displacement of the Great Whirl, which may have induced a change in the local geostrophic currents. This likely also affected the upwelling area of Oman (Shi et al., 2000), where upwelling is driven by the southwest monsoon.

Summer monsoons were also suggested to induce upwelling along southwest India (Krishna, 2008; Smitha et al., 2008), however no cooling trends were observed in this study, most likely because of the annual scale of our analysis. A difference of  $-0.1\text{ }^{\circ}\text{C dec}^{-1}$  was, however, observed between coastal and oceanic points in this area.

The highest negative differences between oceanic and coastal trends (Figure 8d) were observed at the upwelling areas mentioned above, being particularly marked ( $\sim -0.5\text{ }^{\circ}\text{C dec}^{-1}$ ) off southern Africa.

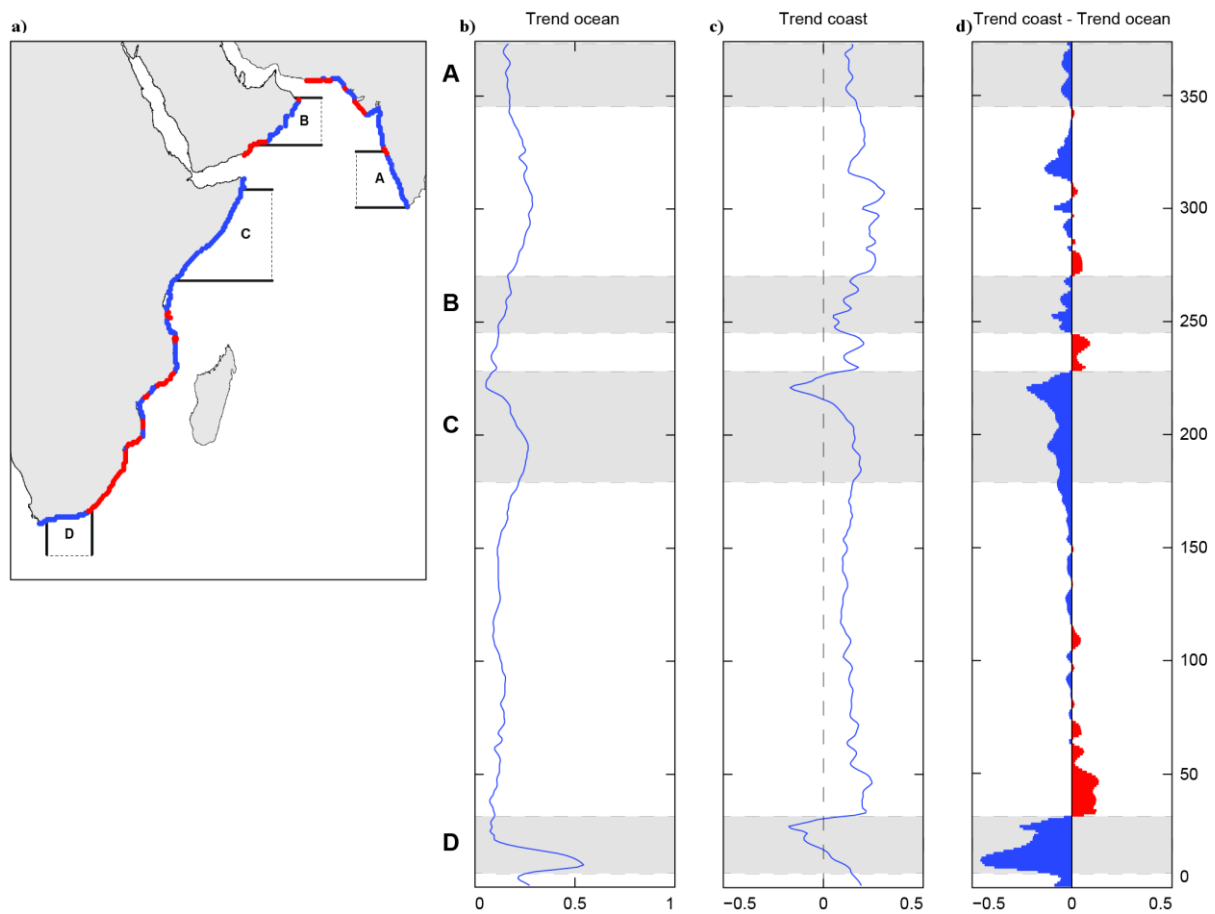


**Figure 8 | SST trends along the Western Indian Ocean.** From left to right: (a) coast-offshore differences in warming trends. Red (blue) indicates that nearshore waters SSTs are warmer (colder) than their respective offshore waters; dashed rectangles circumscribe the upwelling areas of West India (A), Oman (B), Kenya and Somalia (C) and Agulhas (D). (b) Oceanic and (c) coastal SST trends ( $^{\circ}\text{C dec}^{-1}$ ) and (d) their differences. Dashed grey areas identify points in upwelling zones.

#### 4. Discussion

Our results indicate that, in the last three decades, the great majority of both offshore (~ 92%) and coastal locations (~ 87%) have been significantly warming. Although our values are higher than those previously obtained by Lima and Wethey, (2012) (~ 71%), a higher percentage of locations significantly warming was expected, due to two reasons. First, multiple high temperature records have been broken worldwide in the last years and second, our analysis excluded the Arctic and Antarctic regions, which are known to have particularly low rates of change (Lima and Wethey, 2012).

Importantly, warming has been less intense nearshore than offshore in 66% of the locations, although with rates of warming variable between oceanic basins (in agreement with Belkin, 2009; Lima and Wethey, 2012; Cheung et al., 2013). Thus, although coastal temperatures are increasing, in 2/3 of the area considered in this study warming was less intense nearshore than offshore. This pattern is even more pronounced within upwelling regions, where more than 92% of the coastal locations have been warming less than their respective offshore locations. This contrasts with non-upwelling areas, where the percentage of coastal locations that have been warming less than their offshore equivalents is 58%. Although these results are already impressive, real differences are expected to be even more pronounced, given recent studies demonstrating that most remotely-sensed SST products largely overestimate coastal temperatures in areas dominated by upwelling.

Other studies recently evidenced that warming rates are generally depressed near the coast, within upwelling regions. Within the Benguela upwelling system, Santos et al., (2012a) found differences of approximately  $-0.2\text{ }^{\circ}\text{C dec}^{-1}$  between coastal and oceanic locations from 1970 to 2009. In a different study, Santos et al., (2012b) analyzed the Canary system from 1982 to 2010 and found differences of up to  $-0.1\text{ }^{\circ}\text{C dec}^{-1}$  between coastal and offshore locations. In the Caribbean region, Santos et al., (2016) observed a moderate cooling (around  $-0.05\text{ }^{\circ}\text{C dec}^{-1}$

<sup>1</sup>) for the months with strong upwelling in La Guajira upwelling system, contrasting with the SST increase in the Caribbean region (up to  $0.25\text{ }^{\circ}\text{C dec}^{-1}$ ) from 1982 to 2014. Focusing on the Java upwelling system (1982-2015), Varela et al., (2016) found that warming rates between coastal and oceanic locations differed in approximately  $-0.3\text{ }^{\circ}\text{C dec}^{-1}$ , with cooling trends occurring near the coast. These studies also advanced the hypothesis that the uplift of deep and cold water has been buffering the increase in temperature observed at the surface.

Despite the above-mentioned regional studies, a global analysis was necessary to validate the hypothesis that upwelling phenomena, independently of their extension or intensity, could be shielding the coast from the effects of global warming. Thus, in this study, we analyzed not only the most important and intensively studied upwelling systems (Benguela, Canary, South Caribbean, Humboldt, California, West Australia, Java-Sumatra, Kenya, Somalia and Oman) (Varela et al., 2015), but also other systems where upwelling is less intense and highly seasonal [Agulhas Bank (Lutjeharms et al., 2000), Yucatan Shelf (Castillo et al., 2016, Carrillo et al., 2016), West Iberian Peninsula (Lemos and Pires, 2004, Santos et al., 2011), Brazil (Lorenzzetti and Gaeta, 1996; Castelao and Barth, 2006), East and South Australia (Oke and Middleton, 1999; Kämpf et al., 2004, 2010; Gill et al., 2011) and East and West India (Rao, 2002; Krishna, 2008; Smitha et al., 2008)]. The area of Eastern Florida was not considered as the long-term cooling near the coast has other causes than upwelling (Belkin, 2009; Lima and Wethey, 2012).

This study illustrates the ubiquity of the association between upwelling and depressed warming rates along the World's coastlines. It also suggests that, depending on the intensity and prevalence, coastal upwelling has the potential to buffer global changes (e.g., changes in the thermal environment, changes in circulation, or changes in the distribution of single species or communities) at varying spatial and temporal scales. Finally, the fact that upwelling is highly variable in extension and intensity around the globe may (at least

partially) explain the heterogeneity in coastal warming rates previously reported in various studies (Belkin, 2009; Lima and Wetthey, 2012; Cheung et al., 2013). Upwelling is probably a key factor buffering ocean warming.

### **Acknowledgements**

FPL and CM were supported by Fundação para a Ciência e a Tecnologia (IF/00043/2012 and PD/BD/114038/2015, respectively). RS was supported by MARINFO - NORTE- 01-0145-FEDER-000031, funded by Norte Portugal Regional Operational Program (NORTE2020), under the PORTUGAL 2020 Partnership Agreement, through the European Regional Development Fund (ERDF). This research was partially supported by Xunta de Galicia under project GRC-2013-001 Programa de Consolidación e Estructuración de Unidades de Investigación Competitivas (Grupos de Referencia Competitiva) co-funded by European Regional Development Fund (FEDER). R. Varela is supported by the University of Vigo through the Axudas predoutorais da convocatoria de axudas a investigación 2015.

### **References**

1. Cane, M. A., Clement, A. C., Kaplan, A., Kushnir, Y., Pozdnyakov, D., Seager, R; Zebiak, S. E. and Murtugudde, R., 1997. Twentieth-century sea surface temperature trends. *Science*, 275(5302), 957-960.
2. Levitus, S., Antonov, J. I., Boyer, T. P. and Stephens, C., 2000. Warming of the world ocean. *Science*, 287(5461), 2225-2229.
3. Levitus, S., Antonov, J. and Boyer, T., 2005. Warming of the world ocean, 1955–2003. *Geophysical Research Letters*, 32(2).
4. Harrison, D. E. and Carson, M., 2007. Is the world ocean warming? Upper-ocean temperature trends: 1950–2000. *Journal of Physical Oceanography*, 37(2), 174-187.



5. Belkin, I. M., 2009. Rapid warming of large marine ecosystems. *Progress in Oceanography*, 81(1), 207-213.
6. Hansen, J., Ruedy, R., Sato, M. and Lo, K., 2010. Global surface temperature change. *Reviews of Geophysics*, 48, RG4004.
7. Gray, J. S., 1997. Marine biodiversity: patterns, threats and conservation needs. *Biodiversity & Conservation*, 6(1), 153-175.
8. Cheung, W. W. L., Watson, R. and Pauly, D., 2013, Signature of ocean warming in global fisheries catch, *Nature*, 497, 365- 369.
9. Hoegh-Guldberg, O. and Bruno, J. F., 2010. The impact of climate change on the world's marine ecosystems. *Science*, 328(5985), 1523-1528.
10. Seabra, R., Wethey, D. S., Santos, A. M. and Lima, F. P., 2015. Understanding complex biogeographic responses to climate change. *Scientific reports*, 5.
11. Lima F. P. and Wethey, D. S., 2012. Three decades of high-resolution coastal sea surface temperatures reveal more than warming. *Nature Communications*.; 3: 704
12. Mendelssohn, R. and Schwing, F. B., 2002. Common and uncommon trends in SST and wind stress in the California and Peru–Chile current systems. *Progress in Oceanography*, 53(2), 141-162.
13. Qu, T., Du, Y., Strachan, J., Meyers, G. and Slingo, J. M., 2005. Sea surface temperature and its variability in the Indonesian region, *Oceanography Wash. D. C.*, 18, 50–62.
14. Gómez-Gesteira, M., deCastro, M., Álvarez, I., Lorenzo, M. N., Gesteira, J. L. G. and Crespo, A. J. C., 2008a. Spatio-temporal Upwelling Trends along the Canary Upwelling System (1967–2006). *Annals of the New York Academy of Sciences*, 1146(1), 320-337.
15. Gómez-Gesteira, M., deCastro, M., Alvarez, I. and Gómez-Gesteira, J. L., 2008b. Coastal sea surface temperature warming trend along the continental part of the Atlantic Arc (1985–2005). *Journal of Geophysical Research: Oceans*, 113(C4).

16. Chollett, I., Müller-Karger, F. E., Heron, S. F., Skirving, W. and Mumby, P. J., 2012.  
Seasonal and spatial heterogeneity of recent sea surface temperature trends in the Caribbean Sea and southeast Gulf of Mexico. *Marine Pollution Bulletin*, 64(5), 956-965.
17. Barton, E. D., Field, D. B. and Roy, C., 2013. Canary current upwelling: More or less?.  
*Progress in Oceanography*, 116, 167-178.
18. Intergovernmental Panel on Climate Change, 2014. *Climate Change 2014–Impacts, Adaptation and Vulnerability: Regional Aspects*. Cambridge University Press.
19. García-Reyes, M., Sydeman, W. J., Schoeman, D. S., Rykaczewski, R. R., Black, B. A., Smit, A. J. and Bograd, S. J., 2015. Under pressure: climate change, upwelling, and eastern boundary upwelling ecosystems. *Frontiers in Marine Science*, 2, 109.
20. Costanza, R., d'Arge, R., De Groot, R., Farber, S., Grasso, M., Hannon, B., Limburg, K., Naeem, S., O'Neill, R. V., Paruelo, J., Raskin, R. G., Sutton, P. and van den Belt, M., 1997.  
The value of the world's ecosystem services and natural capital. *Nature*, 387(6630), 253-260.
21. Pauly, D. and Christensen, V., 1995. Primary production required to sustain global fisheries.  
*Nature* 374, 255.
22. Santos, F., Gómez-Gesteira, M., deCastro, M. and Álvarez, I., 2012a. Differences in coastal and oceanic SST trends due to the strengthening of coastal upwelling along the Benguela current system. *Continental Shelf Research*; 34: 79–86
23. Santos, F., Gómez-Gesteira, M., deCastro, M. and Álvarez I., 2012b. Differences in coastal and oceanic SST warming rates along the Canary Upwelling Ecosystem from 1982 to 2010. *Continental Shelf Research*; 47: 1–6
24. Varela, R., Santos, F., Gómez-Gesteira, M., Álvarez, I., Costoya, X. and Días, J. M., 2016.  
Influence of Coastal Upwelling on SST Trends along the South Coast of Java. *PloS one*, 11(9), e0162122.

25. Oke, P. R. and Middleton, J. H., 2000. Topographically induced upwelling off eastern Australia. *Journal of Physical Oceanography*, 30(3), 512-531.
26. Shi, W., Morrison, J. M., Böhm, E. and Manghnani, V., 2000. The Oman upwelling zone during 1993, 1994 and 1995. *Deep Sea Research Part II: Topical Studies in Oceanography*, 47(7), 1227-1247.
27. Lutjeharms, J. R. E., Cooper, J. and Roberts, M., 2000. Upwelling at the inshore edge of the Agulhas Current. *Continental Shelf Research*, 20(7), 737-761.
28. Rao, T. N., 2002. Spatial distribution of upwelling off the central east coast of India. *Estuarine, Coastal and Shelf Science*, 54(2), 141-156.
29. Snyder, M. A., Sloan, L. C., Diffenbaugh, N. S. and Bell, J. L., 2003. Future climate change and upwelling in the California Current. *Geophysical Research Letters*, 30(15).
30. Kämpf, J., Doubell, M., Griffin, D., Matthews, R. L. and Ward, T. M., 2004. Evidence of a large seasonal coastal upwelling system along the southern shelf of Australia. *Geophysical Research Letters*, 31(9).
31. Yuras, G., Ulloa, O. and Hormazábal, S., 2005. On the annual cycle of coastal and open ocean satellite chlorophyll off Chile (18–40 S). *Geophysical Research Letters*, 32(23).
32. Castelao, R. M. and Barth, J. A., 2006. Upwelling around Cabo Frio, Brazil: The importance of wind stress curl. *Geophysical Research Letters*, 33(3).
33. Susanto, R. D., Moore, T. S. and Marra, J., 2006. Ocean color variability in the Indonesian Seas during the SeaWiFS era. *Geochemistry, Geophysics, Geosystems*, 7(5).
34. Patti, B., Guisande, C., Vergara, A.R., Riveiro, I., Maneiro, I., Barreiro, A., Bonanno, A., Buscaino, G., Cuttitta, A., Basilone, G. and Mazzola, S., 2008. Factors responsible for the differences in satellite-based chlorophyll a concentration between the major global upwelling areas. *Estuarine, Coastal and Shelf Science* 76, 775e786.

35. Patti, B., Guisande, C., Riveiro, I., Thejll, P., Cuttitta, A., Bonanno, A., Basilone, G., Buscaino, G. and Mazzola, S., 2010. Effect of atmospheric CO<sub>2</sub> and solar activity on wind regime and water column stability in the major global upwelling areas. *Estuarine, Coastal and Shelf Science*, 88(1), 45-52.
36. Smitha, B. R., Sanjeevan, V. N., Vimalkumar, K. G. and Revichandran, C., 2008. On the upwelling off the southern tip and along the west coast of India. *Journal of Coastal Research*, 24(sp3), 95-102.
37. Arístegui, J., Barton, E. D., Álvarez-Salgado, X. A., Santos, A. M. P., Figueiras, F. G., Kifani, S., Hernández-León, S., Mason, E., Machu, E. and Demarq, H., 2009. Subregional ecosystem variability in the Canary current upwelling. *Progress in Oceanography* 83,33–48.
38. Falvey, M., and Garreaud, R. D., 2009. Regional cooling in a warming world: Recent temperature trends in the southeast Pacific and along the west coast of subtropical South America (1979–2006). *Journal of Geophysical Research: Atmospheres*, 114(D4).
39. Narayan, N., Paul, A., Mulitza, S. and Schulz, M., 2010. Trends in coastal upwelling intensity during the late 20th century. *Ocean Science*, 6, 815–823.
40. Gutiérrez, D., Bouloubassi, I., Sifeddine, A., Purca, S., Goubanova, K., Graco, M., Field, D., Méjanelle, L., Velazco, F., Lorre, A., Salvattecí, R., Quispe, D., Vargas, G., Dewitte, B. and Ortlieb L., 2011. Coastal cooling and increased productivity in the main upwelling zone off Peru since the mid-twentieth century. *Geophysical Research Letters*, 38(7).
41. Pardo, P. C., Padín, X. A., Gilcoto, M., Farina-Busto, L. and Pérez, F. F., 2011. Evolution of upwelling systems coupled to the long-term variability in sea surface temperature and Ekman transport. *Climate Research*, 48(2-3), 231-246.
42. Santos, F., Gómez-Gesteira, M., deCastro, M. and Días, J. M., 2015. A dipole-like SST trend in the Somalia region during the monsoon season. *Journal of Geophysical Research: Oceans*, 120(2), 597-607.

43. Varela, R., Álvarez, I., Santos, F. and Gómez-Gesteira, M., 2015. Has upwelling strengthened along worldwide coasts over 1982-2010?. *Scientific reports*, 5.
44. Ruiz-Castillo, E., Gomez-Valdes, J., Sheinbaum, J. and Rioja-Nieto, R., 2016. Wind-driven coastal upwelling and westward circulation in the Yucatan shelf. *Continental Shelf Research*, 118, 63-76.
45. Santos, F., Gómez-Gesteira, M., Varela, R., Ruiz-Ochoa, M. and Días, J. M., 2016. Influence of upwelling on SST trends in La Guajira system. *Journal of Geophysical Research: Oceans*, 121(4), 2469-2480.
46. Cropper, T. E., Hanna, E. and Bigg, G. R., 2014. Spatial and temporal seasonal trends in 518 coastal upwelling off Northwest Africa, 1981–2012. *Deep-Sea Research*, 1, 94–111.
47. deCastro, M., Gómez-Gesteira, M., Álvarez, I. and Gesteira, J. L. G., 2009. Present warming within the context of cooling–warming cycles observed since 1854 in the Bay of Biscay. *Continental Shelf Research*, 29(8), 1053-1059.
48. Lorenzzetti, J. A. and Gaeta, S. A., 1996. The Cape Frio upwelling effect over the South Brazil Bight northern sector shelf waters: a study using AVHRR images. *International Archives of Photogrammetry and Remote Sensing*, 21(part B7).
49. Carrillo, L., Johns, E. M., Smith, R. H., Lamkin, J. T. and Largier, J. L., 2016. Pathways and hydrography in the Mesoamerican Barrier Reef System Part 2: Water masses and thermohaline structure. *Continental Shelf Research*, 120, 41-58.
50. Andrade, C. A. and Barton, E. D., 2004. The Guajira upwelling system. *Continental Shelf Research*, 25(9), 1003-1022.
51. Demarcq, H., 2009. Trends in primary production, sea surface temperature and wind in upwelling systems (1998–2007). *Progress in Oceanography*, 83(1), 376-385.
52. Goubanova, K., Echevin, V., Dewitte, B., Codron, F., Takahashi, K., Terray, P. and Vrac, M., 2011. Statistical downscaling of sea-surface wind over the Peru–Chile upwelling region:

- diagnosing the impact of climate change from the IPSL-CM4 model. *Climate Dynamics*, 36(7-8), 1365-1378.
53. Macías, D., Landry, M. R., Gershunov, A., Miller, A. J. and Franks, P. J., 2012. Climatic control of upwelling variability along the western North-American coast. *Plos One*, 7(1), e30436.
  54. Shiu, C. J., Liu, S. C. and Chen, J. P., 2009. Diurnally asymmetric trends of temperature, humidity, and precipitation in Taiwan. *Journal of climate*, 22(21), 5635-5649.
  55. Ridgway, K.R., 2007. Long-term trend and decadal variability of the southward penetration of the East Australian Current. *Geophysical Research Letters*, 34.
  56. Yeh, S. W., Park, Y. G., Min, H., Kim, C. H. and Lee, J. H., 2010. Analysis of characteristics in the sea surface temperature variability in the East/Japan Sea. *Progress in Oceanography*, 85(3), 213-223.
  57. Kämpf, J., 2010. On preconditioning of coastal upwelling in the eastern Great Australian Bight. *Journal of Geophysical Research: Oceans*, 115(C12).
  58. Gill, P. C., Morrice, M. G., Page, B., Pirzl, R., Levings, A. H. and Coyne, M., 2011. Blue whale habitat selection and within-season distribution in a regional upwelling system off southern Australia. *Marine Ecology Progress Series*, 421, 243-263.
  59. Furnas, M., 2007. Intra-seasonal and inter-annual variations in phytoplankton biomass, primary production and bacterial production at North West Cape, Western Australia: Links to the 1997–1998 El Niño event. *Cont. Shelf Res.* 27, 958–980.
  60. Xu, J., Lowe, R. J., Ivey, G. N., Pattiaratchi, C., Jones, N. L. and Brinkman, R., 2013. Dynamics of the summer shelf circulation and transient upwelling off Ningaloo Reef, Western Australia. *Journal of Geophysical Research: Oceans*, 118(3), 1099-1125.

61. Gill, A.E. and Schumann, E.H., 1979. Topographically induced changes in the structure of an inertial coastal jet: application to the Agulhas Current. *Journal of Physical Oceanography* 9, 975-991.
62. Krishna, K. M., 2008. Coastal upwelling along the southwest coast of India? ENSO modulation. *Ocean Science Discussions*, 5(1), 123-134.
63. Lemos, R.T. and Pires, H.O., 2004. The upwelling regime off the west Portuguese coast, 1941–2000. *International Journal of Climatology* 24, 511–524.





## RESEARCH ARTICLE

10.1002/2015JC011420

## Special Section:

Physical Processes Responsible for Material Transport in the Gulf of Mexico for Oil Spill Applications

## Key Points:

- All Caribbean region ( $0.25^{\circ}\text{C dec}^{-1}$ ), while in the La Guajira upwelling system ( $-0.05^{\circ}\text{C dec}^{-1}$ )
- This cooling is in good agreement with the upwelling increase  $0.04\text{ m}^2\text{ s}^{-1}\text{ dec}^{-1}$  during winter months
- The trends shown here had not been documented in previous research

## Correspondence to:

F. Santos,  
fsantos@uvigo.es

## Citation:

Santos, F., M. Gómez-Gesteira, R. Varela, M. Ruiz-Ochoa, and J. M. Díaz (2016), Influence of upwelling on SST trends in La Guajira system, *J. Geophys. Res. Oceans*, 121, 2469–2480, doi:10.1002/2015JC011420.

Received 4 NOV 2015

Accepted 2 MAR 2016

Accepted article online 7 MAR 2016

Published online 13 APR 2016

## Influence of upwelling on SST trends in La Guajira system

F. Santos<sup>1,2</sup>, M. Gómez-Gesteira<sup>1</sup>, R. Varela<sup>1</sup>, M. Ruiz-Ochoa<sup>3</sup>, and J. M. Díaz<sup>2</sup>
<sup>1</sup>Ephyslab, Environmental Physics Laboratory, Facultad de Ciencias, Universidad de Vigo, Ourense, Spain, <sup>2</sup>CESAM, Departamento de Física, Universidade de Aveiro, Aveiro, Portugal, <sup>3</sup>Coordinación de Ingeniería Ambiental, Facultad de Ciencias Naturales e Ingenierías, Unidades Tecnológicas de Santander, Bucaramanga, Colombia

**Abstract** La Guajira upwelling system has shown a moderate cooling ( $\sim -0.05^{\circ}\text{C dec}^{-1}$ ) over the period 1982–2014 for the months with strong upwelling (JFM). This contrasts with the general warming observed for most of the Caribbean region ( $\sim 0.25^{\circ}\text{C dec}^{-1}$ ) over the same period. Cooling is in good agreement with the upwelling increase ( $\sim 0.04\text{ m}^2\text{ s}^{-1}\text{ dec}^{-1}$ ) observed in the region during winter months, although the position of the peaks in upwelling and SST trends does not coincide exactly due to the presence of the Caribbean Coastal Undercurrent.

## 1. Introduction

Ocean heat content and temperature have increased worldwide since the mid-20th century [Levitus *et al.*, 2000, 2005, 2012], which can strongly affect global fisheries [Cheung *et al.*, 2013]. SST increase is especially important at nearshore areas due to its impact on coastal ecosystems. For an overview on coastal SST changes, the reader is referred to Lima and Wethey [2012], who analyzed the period 1982–2010 and concluded that around 70% of the world coastal locations have experienced a warming trend of  $0.25 \pm 0.13^{\circ}\text{C dec}^{-1}$ .

Previous works have highlighted the importance of regional analysis to properly understand SST patterns at certain regions whose behavior cannot be extrapolated from global patterns. Thus, some authors have shown that SST trends at coastal areas can be modulated by the presence of coastal upwelling [Relvas *et al.*, 2009; Santos *et al.*, 2011, 2012a, 2012b, 2012c].

La Guajira upwelling system (located in Colombian Caribbean, see Figure 1) presents some features that are uncommon at other ocean areas. Thus, for example, the semiannual and annual harmonics are approximately on the same order of magnitude [Ruiz-Ochoa *et al.*, 2012]. In most of the basins, the annual component is usually much bigger than the semiannual component since solar warming is the main forcing. In addition, although wind stress and wind stress curl can affect SST variability in the Colombian Basin, only the wind stress plays a key role in La Guajira [Ruiz-Ochoa, 2011].

La Guajira is characterized by the presence of seasonal upwelling which is disrupted during the winter-to-spring transition [Lonin *et al.*, 2010]. Thus, during the upwelling season the direction of the prevalent winds associated to the Caribbean Low-Level Jet (CLLJ) is almost parallel the coast and wind stress due to Northern Trade winds becomes the main forcing for surface currents. The main physical features of La Guajira upwelling system have been previously described by Andrade [2000], Andrade and Barton [2005], and Rueda-Roa and Muller-Karger [2013]. For additional information about upwelling implications on the biology and the fisheries of the zone, the reader is referred to Corredor [1979], Ciales-Hernandez *et al.* [2006], García *et al.* [2007], and Paramo *et al.* [2011].

Upwelling in La Guajira mainly occurs during the northern Hemisphere winter in contrast with the major upwelling systems located in the northern Hemisphere [Patti *et al.*, 2008] (Canary and California). See Varela *et al.* [2014], for a complete description of the timing and evolution of the main upwelling systems all over the world.

In this paper, we analyze the changes in SST observed in La Guajira upwelling system over the period 1982–2014. Differences between warming rates at open ocean and coastal locations will be discussed in terms of changes in upwelling intensity.

## 2. Material and Methods

The area under study corresponds to La Guajira coastal zone from  $8^{\circ}\text{N}$  to  $15^{\circ}\text{N}$  and  $76.5^{\circ}\text{W}$  to  $71^{\circ}\text{W}$ , which belongs to the Colombian Basin of the Caribbean Sea (Figure 1). This coast presents two orientations one

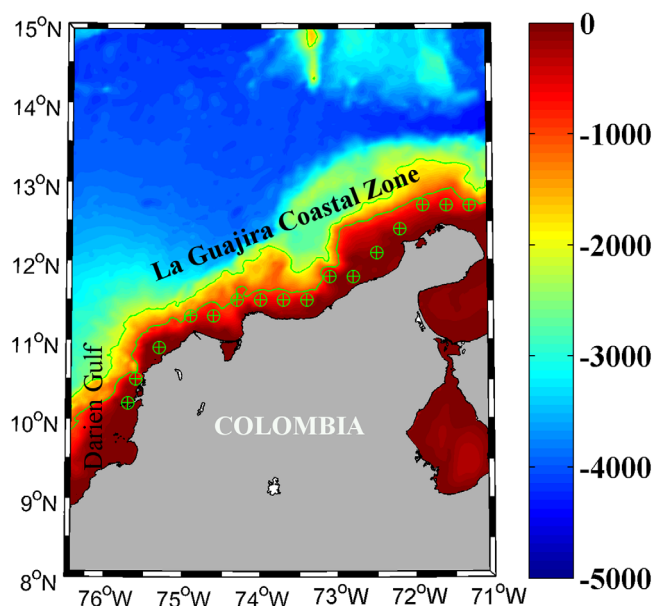


**Figure 1.** Bathymetry of the Area under study. Circles mark points where wind and SST data from CFSR and OI1/4 were sampled.

S-N and another SW-NE, being the latter under the effect of seasonal upwelling [Andrade and Barton, 2005; Ruiz-Ochoa et al., 2012].

SST values were retrieved from NOAA OI1/4 Degree Daily SST data provided by NOAA's National Climatic data Center. Daily data extend back to 1982 with a spatial resolution of  $0.25^\circ \times 0.25^\circ$ . A full description of OI algorithm and its bias treatment can be found in Reynolds [2009] and Reynolds and Chelton [2010]. The period under study spans from 1982 to 2014.

Wind data were obtained from NCEP Climate Forecast System Reanalysis (CFSR) [Saha et al., 2010]. This database was developed by NOAA's National Centers for Environmental Prediction (NCEP). Data were retrieved from NOAA's National Operational Model Archive and Distribution Sys-

tem (NOMADS), which is maintained at NOAA's National Climatic Data Center (NCDC). Although the database exists since 1979, only data from 1982 are corrected and without gaps. Wind is calculated at a reference height of 10 m with 6 hourly time resolution. The spatial resolution is  $0.3^\circ \times 0.3^\circ$  from January 1982 to April 2011 and  $0.2^\circ \times 0.2^\circ$  from then on. Data from the latter period were interpolated on a  $0.3^\circ \times 0.3^\circ$  grid to use a common resolution over the whole period.

Wind data were used to calculate the Ekman transport (ET) [Ekman, 1905] following:

$$Q_x = \frac{\rho_a C_d}{\rho f} (W_x^2 + W_y^2)^{1/2} W_y$$

$$Q_y = -\frac{\rho_a C_d}{\rho f} (W_x^2 + W_y^2)^{1/2} W_x$$
(1)

where  $W_x$  and  $W_y$  are the components of wind speed at a reference height of 10 m ( $x$  subscript corresponds to the zonal component and  $y$  to the meridional one),  $\rho$  is the density of sea water ( $1025 \text{ kg m}^{-3}$ ),  $C_d$  is a dimensionless drag coefficient ( $1.4 \times 10^{-3}$ ),  $\rho_a$  is the air density ( $1.22 \text{ kg m}^{-3}$ ), and  $f$  is the Coriolis parameter defined as twice the vertical component of the Earth's angular velocity,  $\Omega$ , about the local vertical given by  $f = 2\Omega \sin(\varphi)$  at latitude  $\varphi$ . The upwelling Index (UI) can be defined as the component of Ekman transport in the direction perpendicular to the shoreline [Nykjaer and Van Camp, 1994] following:

$$UI = -\sin(\theta - \pi/2) Q_x + \cos(\theta - \pi/2) Q_y$$
(2)

where  $\theta$  is the angle of the unitary vector perpendicular to the coastline pointing oceanward. In the present study, angles ranged from  $80^\circ$  to  $180^\circ$  depending on coastal orientation. Positive (negative) upwelling indices correspond to upwelling-favorable (unfavorable) conditions. Six hourly UI data were then averaged at monthly scale. Both UI and SST were calculated at the set of points marked in Figure 1. Points were located as close as possible to the shore line but avoiding land contamination [Lima and Wetthey, 2012; deCastro et al., 2014].

### 3. Results and Discussion

Mean SST and ET fields were calculated for comparison with previous literature [Andrade and Barton, 2005; Ruiz-Ochoa et al., 2012; Rueda-Roa and Muller-Karger, 2013]. Monthly SST mean fields (Figure 2) can be

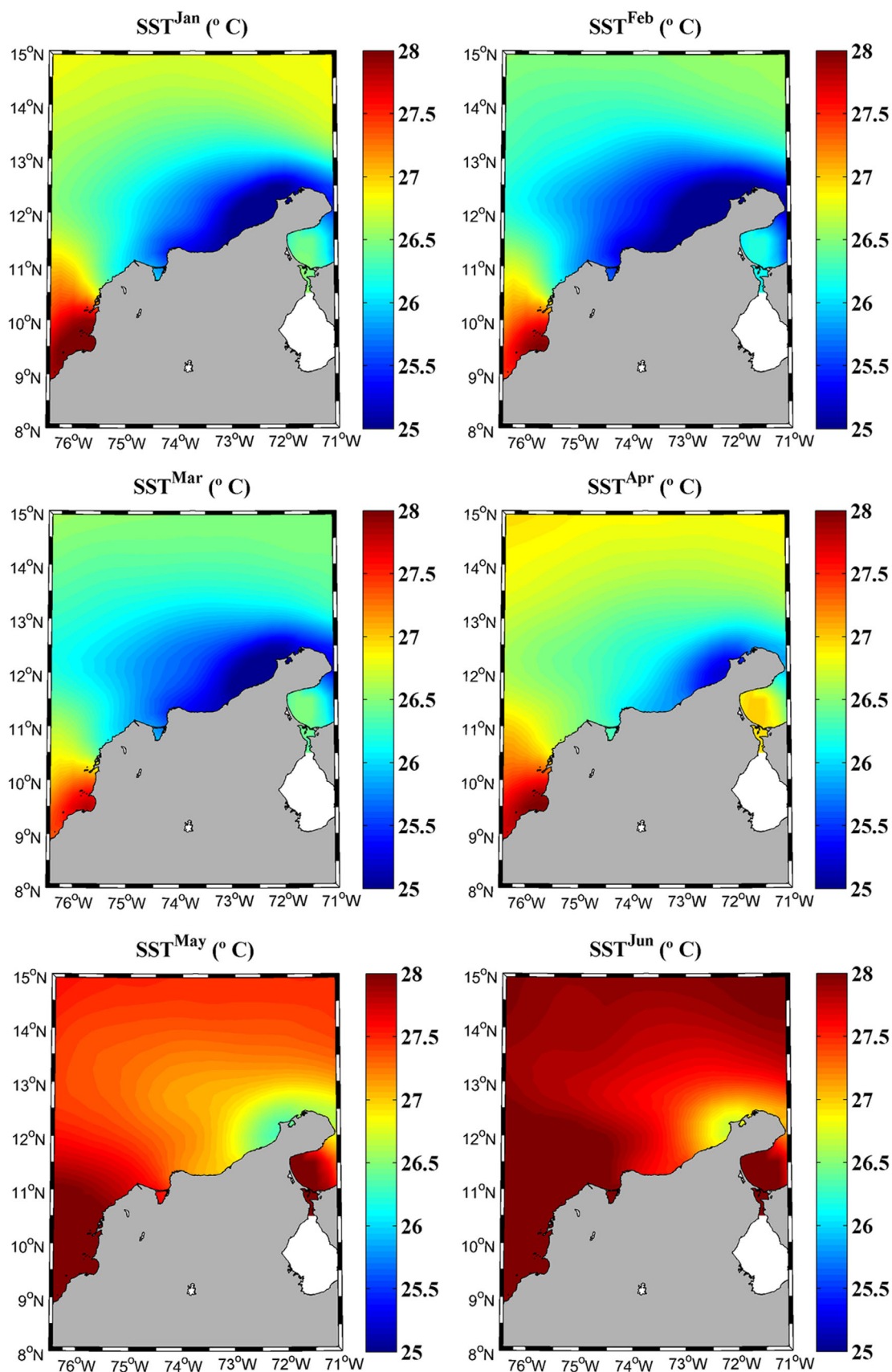


**Figure 2.** Mean monthly SST (°C) calculated over the period 1982–2014 using OI1/4 database.

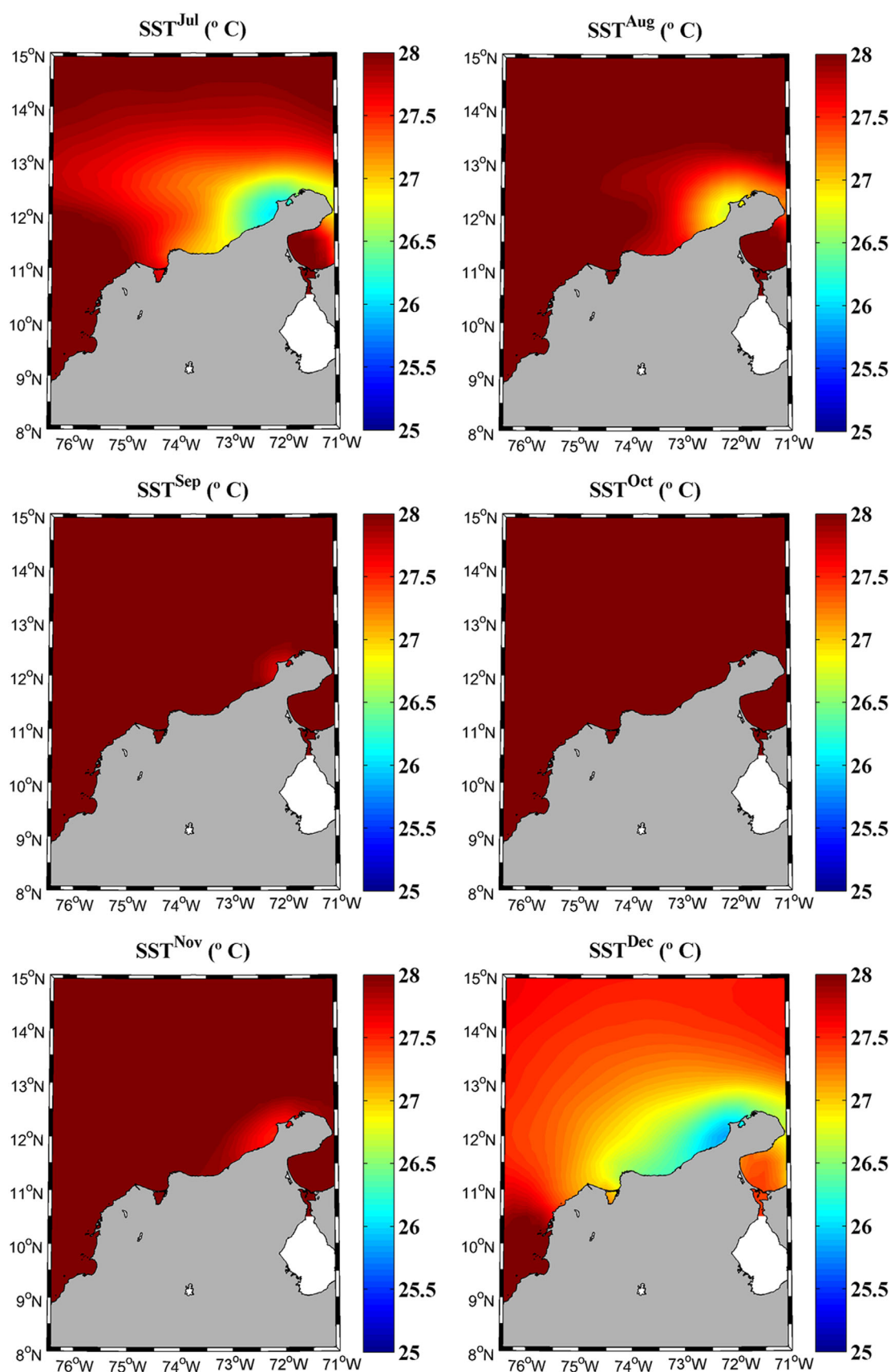
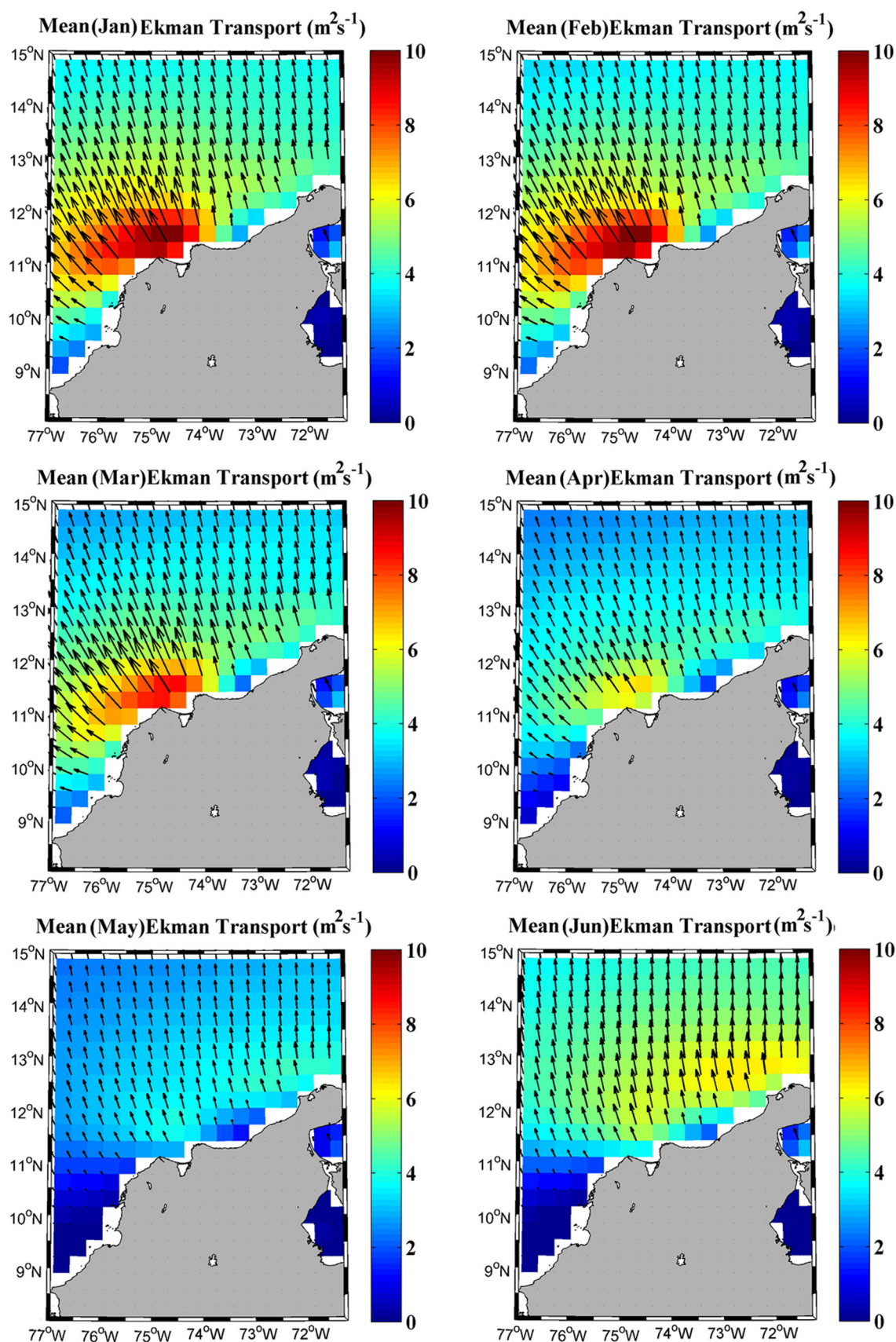


Figure 2. (continued)





**Figure 3.** Mean monthly Ekman Transport ( $\text{m}^2 \text{s}^{-1}$ ) calculated over the period 1982–2014 using CFSR database.

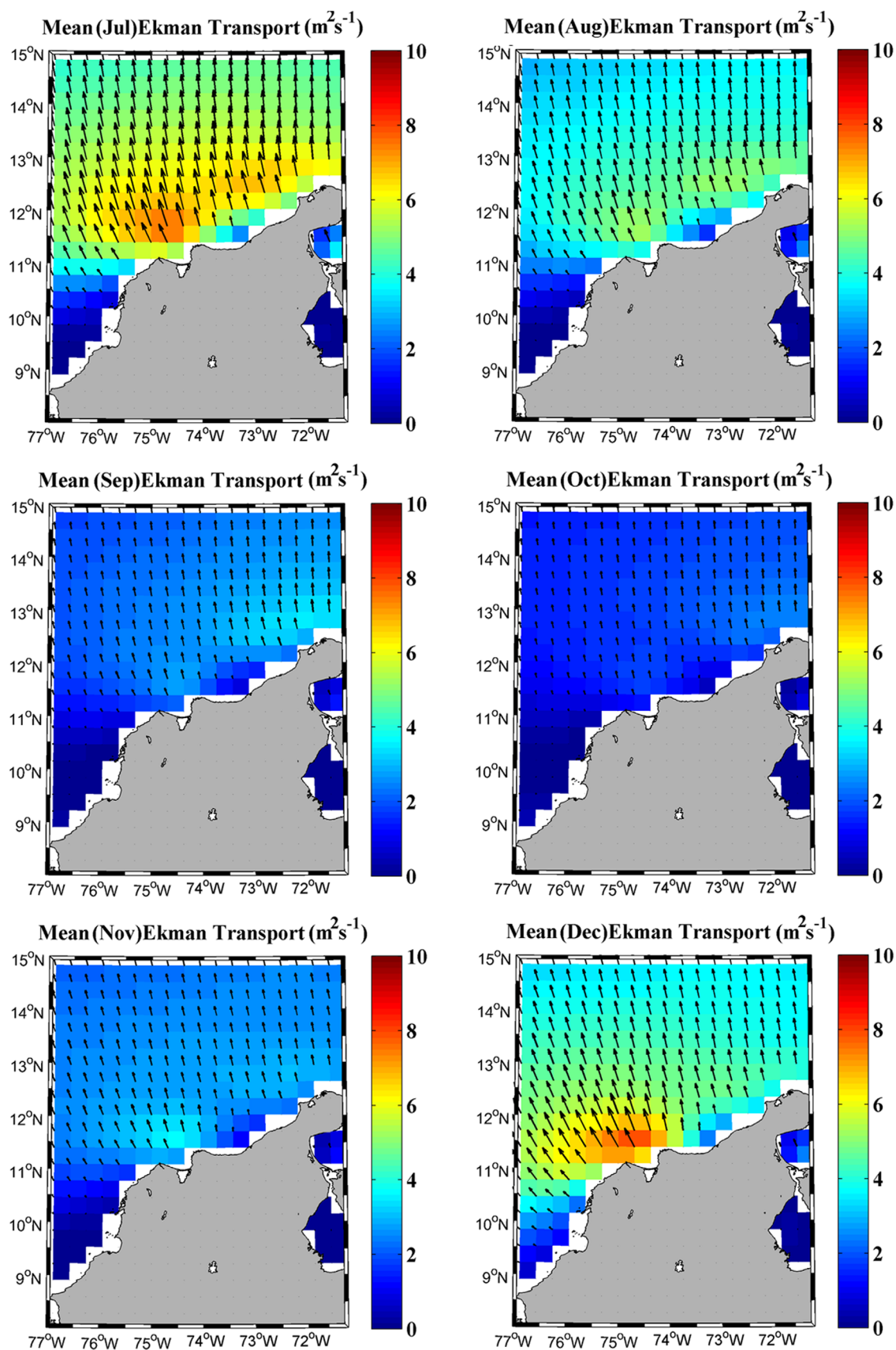
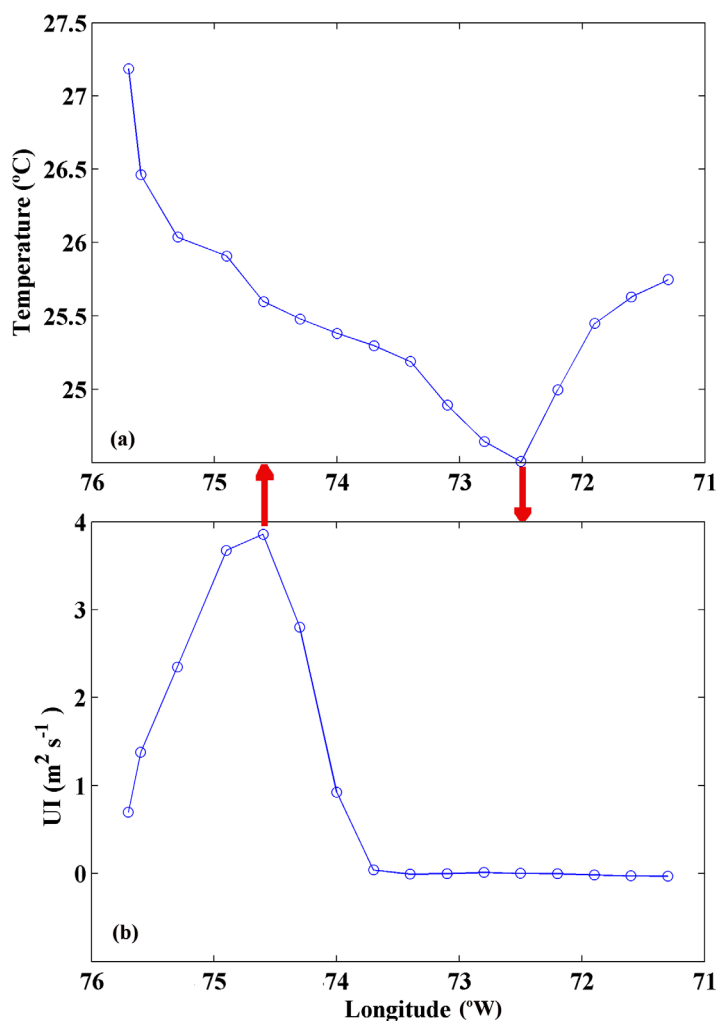


Figure 3. (continued)



**Figure 4.** Mean (a) SST and (b) UI calculated along the coast, for the months of highest upwelling (JFM).

grouped together according to the prevalent patterns. A marked dipole is observed over the period January–March (JFM). Temperatures at the northern part of the coast (75–72°W) are on the order of 25°C with higher values (~28°C) at the southern part (76.5–75°W) which, in fact, is part of the Darien Gulf. April is a transition month with a behavior similar to the one observed in JFM but with the cool part of the dipole markedly smaller and warmer. Most of the zone shows SST values higher than 27.5°C from May to August. Only in a small area located at the northern part of the coast (73–71.5°W) the SST is on the order of 26.5°C. Finally, from September to November (SON), SST attains values higher than 28°C for the whole area. December is also a transition month with a behavior that resembles the one described for JFM. These seasonal patterns are consistent with previous research conducted by Ruiz-Ochoa *et al.* [2012] and Rueda-Roa and Muller-Karger [2013].

Previous studies [Santos *et al.*, 2012a, 2012b, 2012c, 2015] have shown that coastal upwelling can modulate warming trends at nearshore areas. Thus, mean ET patterns were calculated for the area under study (Figure 3). The highest ET was observed in JFM with values around  $9 \text{ m}^2 \text{ s}^{-1}$  near coast between 75.5 and 74°W. Coastal ET values were more moderate ( $6\text{--}7 \text{ m}^2 \text{ s}^{-1}$ ) in June–July between 75 and 71.5°W. ET is negligible during the rest of the year, except in December, when the pattern described for JFM starts developing. Rueda-Roa and Muller-Karger [2013] described similar wind stress patterns being the highest values attained over the period December–February (DJF). Andrade and Barton [2005] also mentioned the existence of seasonal wind patterns, with the highest values during the northern Hemisphere winter (December–March) and the lowest ones during the rainy season (October–November).

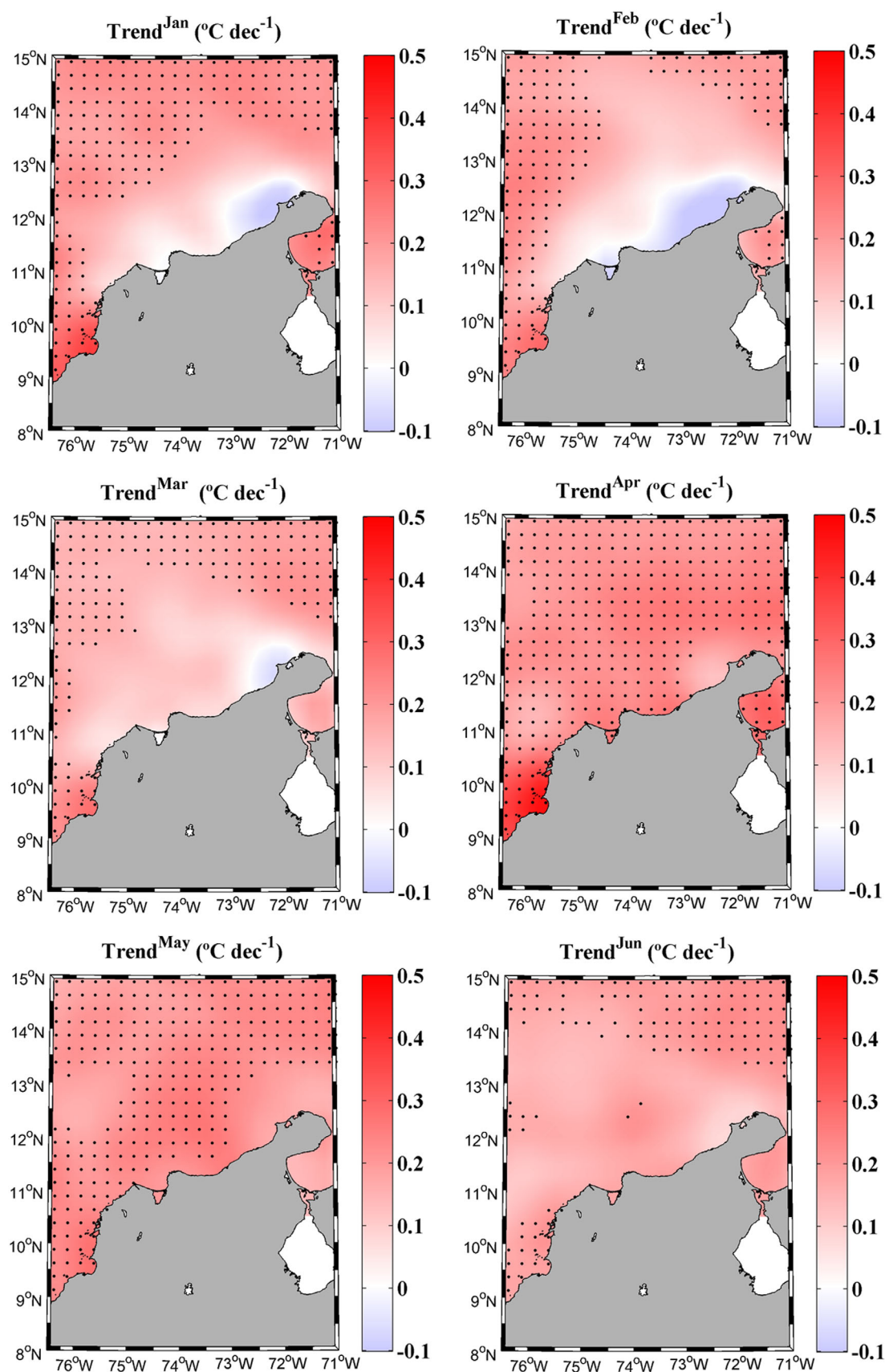


**Figure 5.** Monthly SST trend ( $^{\circ}\text{C dec}^{-1}$ ) calculate over the period 1982–2014 using OI1/4 database. Black dots correspond to trends with significance  $p$ -value  $< 0.05$ .



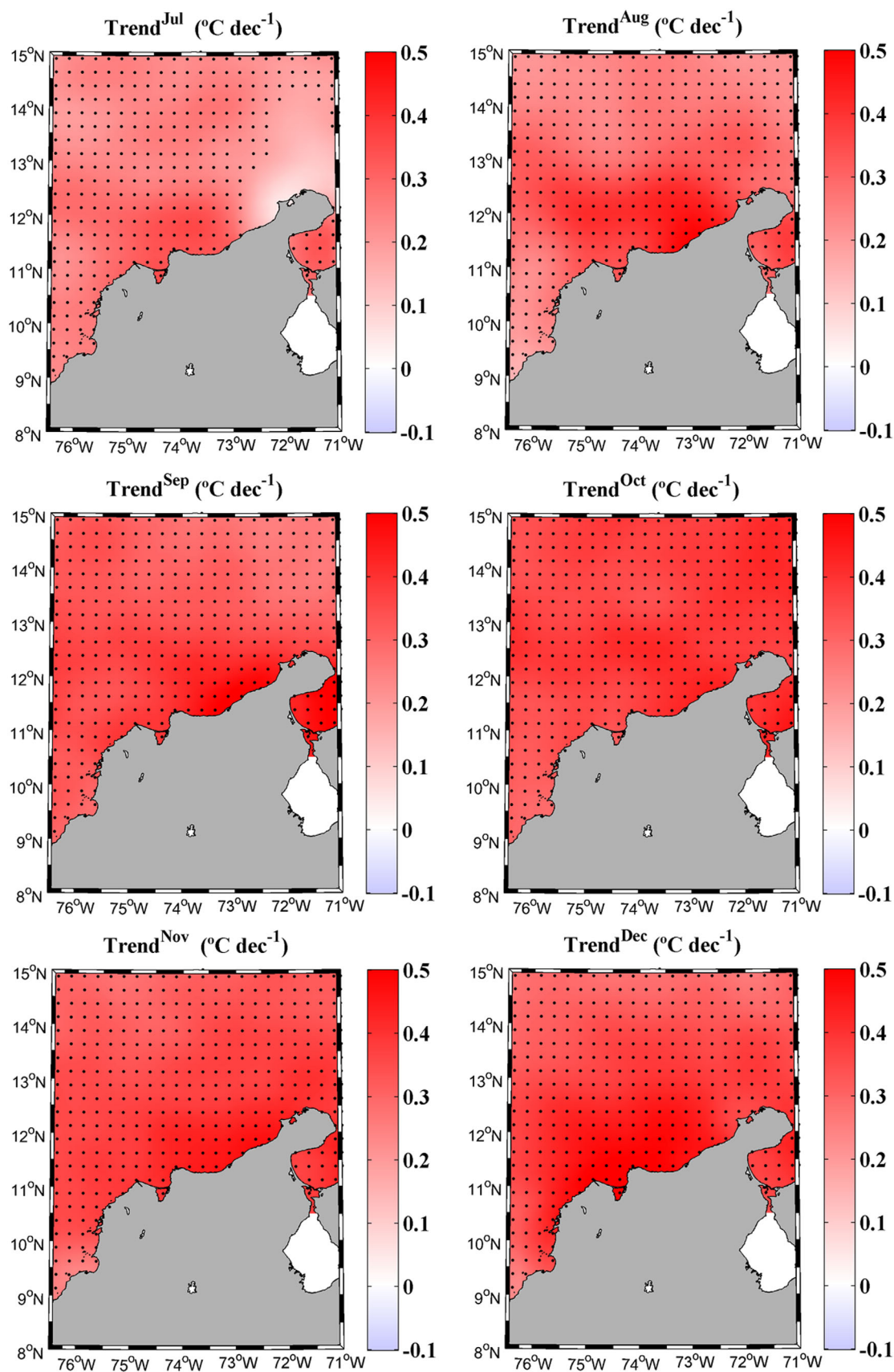
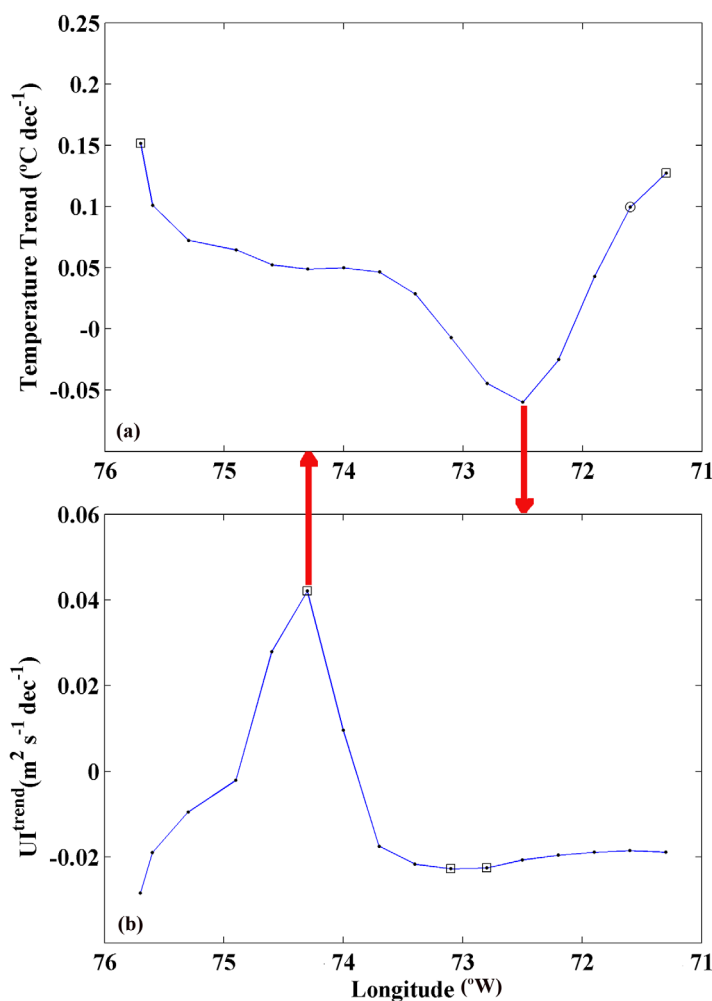


Figure 5. (continued)



**Figure 6.** Trends in (a) SST in  $^{\circ}\text{C dec}^{-1}$  and in (b) UI in  $\text{m}^2 \text{s}^{-1} \text{dec}^{-1}$  along the coast of La Guajira upwelling system over the months JFM. Black squares (circles) mark trends with significance higher than 95% (90%).

JFM mean UI and SST values were calculated (Figure 4) at the coastal points marked with circles in Figure 1. These are the months with the highest ET intensity. The minimum SST peak (Figure 4a) with values around  $24.5^{\circ}$  is observed between  $73$  and  $72^{\circ}\text{W}$  while the maximum UI peak (Figure 4b) with values around  $4 \text{ m}^2 \text{s}^{-1}$  is observed between  $75.5$  and  $74.5^{\circ}\text{W}$ . Note that the position of both peaks does not match exactly since the SST peak is displaced eastward around  $2^{\circ}$  when compared with UI peak. This is in good agreement with previous research conducted by *Rueda-Roa and Muller-Karger* [2013] (see Figures 2a and 7b in their manuscript) and possibly linked to the eastward advection of cold upwelled water due to the Caribbean Coastal Undercurrent (CCU) [*Andrade et al.*, 2003; *Jouanno et al.*, 2008]. According to *Bernal et al.* [2010] and *Ruiz-Ochoa* [2011], this current is more intense over the period December–May when the westward Caribbean Current weakens. Note that according to the same authors the CCU is a surface current West of  $73.5^{\circ}\text{W}$  that becomes a subsurface current from them on. Thus, the point where SST attains its minimum practically coincides with the point where the CCU sinks.

The evolution of the SST over the period of 1982–2014 is shown in Figure 5. Overall, water tends to warm within a context of global warming. Ocean trends are higher than  $0.2^{\circ}\text{C dec}^{-1}$  during most of the year and can even reach values on the order of  $0.52^{\circ}\text{C dec}^{-1}$  from September to December. The mean trend at annual scale is  $0.25^{\circ}\text{C dec}^{-1}$  which is considerably higher than provided by *Hartmann et al.* [2013] for the global ocean over the period 1979–2012 using HAdSST3 data ( $0.124 \pm 0.03^{\circ}\text{C dec}^{-1}$ ). *Chollet et al.* [2012] calculated the mean SST trend over the southeastern Gulf and the Caribbean Sea from 1985 to 2009 using raw Pathfinder data, obtaining a value of  $0.29^{\circ}\text{C dec}^{-1}$ , which is similar that the value shows in this study.

A negative trend  $\sim 0.05^{\circ}\text{C dec}^{-1}$  (no significant) was observed near coast for months under strong and well-developed upwelling conditions (JFM) (Figure 5). This contrasts with the significant positive trend observed at adjacent ocean locations. Despite their lack of significance, near shore trends prove that that region is affected by drivers different from the ones observed at open sea locations (e.g., coastal upwelling). Coastal trends less intense than the oceanic one were also found by *Chollet et al.* [2012] during winter although these authors carried their study in a more macroscopic way, considering the whole Caribbean Sea and southeast Gulf of Mexico and paying less attention to small areas like La Guajira upwelling system. This proves the interest of regional assessment at small scales (typically a few degrees). We should note that, according to *Andrade and Barton* [2005], the baroclinic Rossby radius of the area is approximately 30 km and mesoscale features range from tens to several hundred kilometers.

JFM UI and SST trends were calculated at the costal points where mean values were previously analyzed (Figure 6). Temperature tends to increase in most of the area following the global pattern. Only in a small area centered around  $72\text{--}73^{\circ}\text{W}$ , the trend is slightly negative. A similar behavior was observed for UI, with small negative trends in most of the area and a significant positive trend around  $74.5^{\circ}\text{W}$ . The same area was recently analyzed by *Varela et al.* [2014], who found a more marked upwelling strengthening although they considered an extended period including April, when upwelling is still present although at a lesser extent. Once again, the point of maximum SST decrease ( $\sim -0.06^{\circ}\text{C dec}^{-1}$ ) is displaced eastward from the point of maximum UI increase ( $0.04 \text{ m}^2 \text{ s}^{-1} \text{ dec}^{-1}$ ) located between  $75$  and  $74^{\circ}\text{W}$ , which can also be explained in terms of changes in CCU as mentioned above. Previous research suggests that upwelling can be responsible of ocean warming modulation at coastal areas [*Relvas et al.*, 2009; *Gómez-Gesteira et al.*, 2008a, 2008b, 2011; *Santos et al.*, 2012a, 2012c]. In particular, *Santos et al.* [2012a, 2012c], showed that warming is less intense near shore than at ocean locations along the Canary system. This modulation also affects the number of extreme hot days [*deCastro et al.*, 2014]. Finally, *Santos et al.* [2012b], also showed nearshore water cooling along the Benguella Upwelling Ecosystem in contrast with warming at adjacent ocean locations. This coastal cooling showed to be in good agreement with upwelling strengthening in the area.

## 4. Conclusions

Within the context of SST increase for the Caribbean region ( $\sim 0.25^{\circ}\text{C dec}^{-1}$ ), La Guajira upwelling system showed a moderate cooling ( $\sim -0.05^{\circ}\text{C dec}^{-1}$ , no significant) for the months with strong upwelling (JFM).

This cooling is in good agreement with the upwelling increase observed in the region at a rate of  $0.04 \text{ m}^2 \text{ s}^{-1} \text{ dec}^{-1}$  during winter months, although the position of the peaks in upwelling and SST trends do not coincide exactly, which is probably due to the presence of the Caribbean Coastal Undercurrent.

The trends shown here had not been documented in previous research where the focus was on higher spatial scales. This highlights the interest of regional assessments at scales of just a few degrees, which are especially important in the vicinity of coastal areas affected by upwelling.

## References

- Andrade, C. A. (2000), The circulation and variability of the Colombian basin in the Caribbean Sea, doctorate thesis, 229 pp. Univ. of Wales, Cardiff.
- Andrade, C. A., and E. D. Barton (2005), The Guajira upwelling system, *Cont. Shelf Res.*, *25*, 1003–1022.
- Andrade, C. A., E. D. Barton, and C. N. K. Mooers (2003), Evidence for an eastward flow along the Central and South American Caribbean coast, *J. Geophys. Res.*, *108*(C6), 3185, doi:10.1029/2002JC001549.
- Bernal, G., M. Ruiz-Ochoa, and E. Beier (2010), *Variabilidad Estacional e Interanual Océano-Atmósfera en la Cuenca Colombia in Cuadernos del Caribe*, La Invest. en Cienc. del mar de la Univ. Nac. de Colombia, Medellín Colombia.
- Cheung, W. W. L., R. Watson, and D. Pauly (2013), Signature of ocean warming in global fisheries catch, *Nature*, *497*, 365–369.
- Chollet I., F. E. Müller-Kargerc, S. F. Herond, W. Skirvingd, and P. J. Mumbyb (2012), Seasonal and spatial heterogeneity of recent sea surface temperature trends in the Caribbean Sea and southeast Gulf of Mexico, *Mar. Pollut. Bull.*, *64*, 956–965.
- Corredor, J. E. (1979), Phytoplankton response to low level nutrient enrichment through upwelling in the Columbian Caribbean Basin. *Deep Sea Res.*, *26A*, 731–741.
- Criales-Hernández, M. I., C. B. García, and M. Wolff (2006), Flujos de biomasa y estructura de un ecosistema de surgencia tropical en La Guajira, Caribe colombiano, *Rev. Biol. Trop.*, *54*(4), 1257–1282.
- deCastro, M., M. Gómez-Gesteira, X. Costoya, and F. Santos (2014), Upwelling influence on the number of extreme hot SST days along the Canary Upwelling ecosystem, *J. Geophys. Res. Oceans*, *119*, 3029–3040, doi:10.1002/2013JC009745.
- Ekman, W. K. (1905), On the influence of earth's rotation on ocean currents, *Ark. Mat. Astronomi och Fys.*, *2*, 8–19.

## Acknowledgments

The Portuguese Science Foundation (FCT) partially supported this research through a Postdoctoral grant (SFRH/BPD/97320/2013) of the first author and through the project Pest (C/MAR/LA0017/2013). This research was also partially supported by Xunta de Galicia under project GRC-2013-001 "Programa de Consolidación e Estructuración de Unidades de Investigación Competitivas (Grupos de Referencia Competitiva)" cofunded by European Regional Development Fund (FEDER). CFSR data were obtained from Environmental Modeling Center/ National Centers for Environmental Prediction/National Weather Service/ NOAA/U.S. NCEP Climate Forecast System Reanalysis (CFSR) Monthly Products. Research Data Archive at the National Center for Atmospheric Research, Computational, and Information Systems Laboratory. <http://rda.ucar.edu/datasets/ds093.2/>.

- García, C. B., L. O. Duarte, J. Altamar, and L. M. Manjarres (2007), Demersal fish density in the upwelling ecosystem off Colombia, Caribbean Sea: Historic outlook, *Fish. Res.*, **85**, 68–73.
- Gómez-Gesteira, M., M. deCastro, I. Álvarez, and J. L. Gómez-Gesteira (2008a), Coastal Sea surface temperature warming trend along the continental part of the Atlantic Arc (1985–2005), *J. Geophys. Res.*, **113**, C04010, doi:10.1029/2007JC004315.
- Gómez-Gesteira, M., M. deCastro, I. Álvarez, M. N. Lorenzo, J. L. G. Gómez-Gesteira, and A. J. C. Crespo (2008b), Spatio-temporal upwelling trends along the canary upwelling system (1967–2006), *Ann. N. Y. Acad. Sci.*, **1146**, 320–337.
- Gómez-Gesteira, M., et al. (2011), The state of climate in North-West Iberia, *Clim. Res.*, **48**, 109–144.
- Hartmann, D. L., et al. (2013), Observations: Atmosphere and surface, in *Climate Change 2013: The Physical Science Basis. Contribution of Working Group I to the Fifth Assessment Report of the Intergovernmental Panel on Climate Change*, edited by T. F. Stocker et al., Cambridge Univ. Press, Cambridge, U. K.
- Jouanno, J., J. Sheinbaum, B. Barnier, J. M. Molines, L. Debreuc, and F. Lemarié (2008), The mesoscale variability in the Caribbean Sea. Part I: Simulations and characteristics with and embedded model, *Ocean Modell.*, **23**, 82–101.
- Levitus, S., J. I. Antonov, T. P. Boyer, and C. Stephens (2000), Warming of the world ocean, *Science*, **287**, 2225–2229.
- Levitus, S., J. I. Antonov, and T. P. Boyer (2005), Warming of the world ocean, 1955–2003, *Geophys. Res. Lett.*, **32**, L02604, doi:10.1029/2004GL021592.
- Levitus, S., et al. (2012), World ocean heat content and thermosteric sea level change (0–2000 m), 1955–2010, *Geophys. Res. Lett.*, **39**, L10603, doi:10.1029/2012GL051106.
- Lima, F. P., and D. S. Wetzel (2012), Three decades of high-resolution coastal sea surface temperatures reveal more than warming, *Nat. Commun.*, **3**, 1–13.
- Lonin, S. A., J. L. Hernández, and D. M. Palacios (2010), Atmospheric events disrupting coastal upwelling in the southwestern Caribbean, *J. Geophys. Res.*, **115**, C06030, doi:10.1029/2008JC005100.
- Nykjaer, L., and L. Van Camp (1994), Seasonal and interannual variability of coastal upwelling along northwest Africa and Portugal from 1981 to 1991, *J. Geophys. Res.*, **99**, 14,197–14,207.
- Paramo, J., M. Correa, and S. Núñez (2011), Evidencias de desacople físico-biológico en el sistema de surgencia en La Guajira, Caribe colombiano, *Rev. Biol. Mari. Oceanogr.*, **46**(3), 421–430.
- Patti, B., et al. (2008), Factors responsible for the differences in satellite-based chlorophyll a concentration between the major global upwelling areas, *Estuarine Coastal Shelf Sci.*, **76**, 775–786.
- Relvas, P., J. Luís, and A. M. P. Santos (2009), Importance of the mesoscale in the decadal changes observed in the northern Canary upwelling system, *Geophys. Res. Lett.*, **36**, L22601, doi:10.1029/2009GL040504.
- Reynolds, R. W. (2009), *What's New in Version 2*. [Available at [http://www.ncdc.noaa.gov/oa/climate/research/sst/papers/whats\\_new\\_v2.pdf](http://www.ncdc.noaa.gov/oa/climate/research/sst/papers/whats_new_v2.pdf).]
- Reynolds, R. W., and D. W. Chelton (2010), Comparisons of daily sea surface temperature analysis for 2007–08, *J. Clim.*, **23**, 3545–3562, doi:10.1175/2010JCLI3294.
- Rueda-Roa, D. T., and F. E. Muller-Karger (2013), The southern Caribbean upwelling system: Sea surface temperature, wind forcing and chlorophyll concentration patterns, *Deep Sea Res., Part I*, **78**, 102–114.
- Ruiz-Ochoa, M. (2011), Variabilidad de la Cuenca Colombia (mar Caribe) asociada con El Niño-Oscilación del Sur, vientos Alisios y procesos locales, thesis. Universidad Nacional de Colombia, Facultad de Minas, Escuela de Geociencias y Medio Ambiente, Medellín, Colombia.
- Ruiz-Ochoa, M., et al. (2012), Sea Surface temperature variability in the Colombian Basin, Caribbean Sea, *Deep Sea Res., Part I*, **64**, 43–53.
- Saha, S., et al. (2010), The NCEP climate forecast system reanalysis, *Bull. Am. Meteorol. Soc.*, **91**, 1015–1057.
- Santos, F., M. Gómez-Gesteira, and M. deCastro (2011), Coastal and oceanic SST variability along the western Iberian Peninsula, *Cont. Shelf Res.*, **31**, 2012–2017.
- Santos, F., M. Gómez-Gesteira, M. deCastro, and I. Álvarez (2012a), Variability of coastal and ocean water temperature in the upper 700 m along the Western Iberian Peninsula from 1975 to 2006, *PLoS One*, **7**(12), 1–7.
- Santos, F., M. Gómez-Gesteira, M. deCastro, and I. Álvarez (2012b), Differences in coastal and oceanic SST trends due to the strengthening of coastal upwelling along the Benguela current system, *Cont. Shelf Res.*, **34**, 79–86.
- Santos, F., M. Gómez-Gesteira, M. deCastro, and I. Álvarez (2012c), Differences in coastal and oceanic SST warming rates along the Canary Upwelling Ecosystem from 1982 to 2010, *Cont. Shelf Res.*, **47**, 1–6.
- Santos, F., M. Gómez-Gesteira, M. deCastro, and J. M. Dias (2015), A dipole-like SST trend in the Somalia region during the monsoon season, *J. Geophys. Res. Oceans*, **120**, 597–607, doi:10.1002/2014JC010319.
- Varela, R., I. Álvarez, F. Santos, M. deCastro, and M. Gómez-Gesteira (2014), Has upwelling strengthened along worldwide coasts over 1982–2010?, *Sci. Rep.*, **5**, 10016, doi:10.1038/srep10016.



RESEARCH ARTICLE

# Influence of Coastal Upwelling on SST Trends along the South Coast of Java

R. Varela<sup>1\*</sup>, F. Santos<sup>1,2</sup>, M. Gómez-Gesteira<sup>1</sup>, I. Álvarez<sup>1,2</sup>, X. Costoya<sup>1</sup>, J. M. Díaz<sup>2</sup>

**1** Ephyslab, Environmental Physics Laboratory, Facultad de Ciencias, Universidad de Vigo, 32004 Ourense, Spain, **2** CESAM, Departamento de Física, Universidade de Aveiro, 3810–193 Aveiro, Portugal

\* [ruvarela@uvigo.es](mailto:ruvarela@uvigo.es)



## OPEN ACCESS

**Citation:** Varela R, Santos F, Gómez-Gesteira M, Álvarez I, Costoya X, Díaz JM (2016) Influence of Coastal Upwelling on SST Trends along the South Coast of Java. PLoS ONE 11(9): e0162122. doi:10.1371/journal.pone.0162122

**Editor:** Shang-Ping Xie, University of California San Diego, UNITED STATES

**Received:** March 22, 2016

**Accepted:** August 17, 2016

**Published:** September 8, 2016

**Copyright:** © 2016 Varela et al. This is an open access article distributed under the terms of the [Creative Commons Attribution License](https://creativecommons.org/licenses/by/4.0/), which permits unrestricted use, distribution, and reproduction in any medium, provided the original author and source are credited.

**Data Availability Statement:** Wind and heat flux data were acquired from the NCEP CFSR database at <http://rda.ucar.edu/pub/cfsr.html> developed by the National Oceanic and Atmospheric Administration (NOAA). Daily files with a spatial resolution of 0.25°×0.25° were obtained from the NOAA website (<http://www.ndbc.noaa.gov/sst/>). Sea Temperature data beneath the sea surface were also obtained from the Simple Ocean Data Assimilation (SODA). This project has reanalyzed data from different sources (oceanographic cruises, satellite, model simulations). Reanalysis data are available at monthly scale with a horizontal resolution of

## Abstract

The south coast of Java has warmed at a much lower rate than adjacent ocean locations over the last three decades (1982–2015). This behavior can be observed during the upwelling season (July–October) and it is especially patent in August and September when upwelling attains the highest values. Although different warming rates (ocean–coast) had been previously observed in other areas around the world, this behavior was always linked to situations where upwelling increased or remained unchanged. South Java warming is observed at ocean locations and cooling near shore but under a scenario of decreasing upwelling (~30% in some cases). The origin of coastal cooling is due to changes in the vertical structure of the water column. A vein of subsurface water, which has cooled at a rate higher than 0.3°C per decade, is observed to enter from the northwestern part of the study area following the South Java Current. This water only manifests at surface near coast, where it is pumped up by coastal upwelling.

## Introduction

Climate change is affecting a wide range of systems. In particular are important the impacts over the oceans which have been subject to global rising temperatures in the last decades [1–3]. Recently, Lima and Wethey [3] analyzed changes in coastal Sea Surface Temperature (SST) worldwide at a scale of 0.25° over the last three decades (1982–2010). They found that 71% of the world's coastlines have been significantly warming and that rates of change have been highly heterogeneous in both space and season. Since upwelling systems are one of the most important spots of productivity it is also necessary to analyze in detail the evolution of SST patterns over these areas. Over the last years, several authors have described differences between warming rates at coastal and ocean locations in different coastal upwelling systems [4–8]. Thus, Lemos and Sanso [4] found a difference of 0.1°C dec<sup>-1</sup> between coast and ocean locations along the western Iberian Peninsula using data with a spatial resolution of 0.25°×0.25° from 1901 to 2000. Similar results were obtained by Santos et al. [5] from 1958 to 2008 at a scale of 0.5°. In the Canary upwelling system, Santos et al. [6] detected an ocean warming rate higher than the coastal one (around 0.5°C dec<sup>-1</sup>) from 1982 to 2010 using high resolution SST data (4 x 4 km). Santos et al. [7] also observed weaker warming trends at coastal locations along the Benguela upwelling system from 1970 to 2009 considering data on a 1°x1° grid (difference



0.5°×0.5° and a vertical resolution of 40 levels (<http://apdrc.soest.hawaii.edu/las/v6/dataset?catitem=3273>) from 1958 to 2010.

**Funding:** This research was also partially supported by Xunta de Galicia under projects GRC-2013-001 "Programa de Consolidación e Estructuración de Unidades de Investigación Competitivas (Grupos de Referencia Competitiva)" co-funded by European Regional Development Fund (FEDER). The Portuguese Science Foundation (FCT) partially supported this research through a Post-doctoral grant (SFRH/BPD/97320/2013) of the second author and through the project Pest (C/MAR/LA0017/2013). CFSR data was obtained from Environmental Modeling Center/National Centers for Environmental Prediction/National Weather Service/NOAA/U.S. NCEP Climate Forecast System Reanalysis (CFSR) Monthly Products. Research Data Archive at the National Center for Atmospheric Research, Computational and Information Systems Laboratory (<http://rda.ucar.edu/datasets/ds093.2/>). The funders had no role in study design, data collection and analysis, decision to publish, or preparation of the manuscript.

**Competing Interests:** The authors have declared that no competing interests exist.

ocean-coast  $\sim 0.4^{\circ}\text{C dec}^{-1}$ ). More recently, Santos et al. [8] described the existence of a difference around  $0.15\text{--}0.2^{\circ}\text{C dec}^{-1}$  between coast and ocean locations along La Guajira upwelling system from 1982–2014 at a scale of  $0.25^{\circ}$ . These differences between coast and ocean along the different upwelling systems can be linked to the strengthening of coastal upwelling also detected by some of the previous authors. Recently, Varela et al [9] analyzed trends in the coastal upwelling regime worldwide using wind data over the last three decades. They also found increasing trends in upwelling in the coastal areas of Benguela and Canary. These results suggest the role of upwelling as a moderator of general SST increase in coasts affected by this mechanism. This fact shows the interest to direct the spotlight towards other local areas of the world where upwelling is also an important forcing as, for example, the south coast of Java.

Java is located in the Eastern Indian Ocean where the southeast (SE) monsoon dominates during the austral winter [10–15]. This SE monsoon generates seasonal upwelling which produces cold water in the surface, creating a difference on SST and biological productivity between coastal and ocean-ward locations [13, 16–20]. During the rest of the year, westerly winds linked to the west monsoon arise generating periods of weak and variable winds without upwelling productivity.

Upwelling along the south coast of Java has been mainly characterized in terms of upwelling occurrence. This coast presents a constant E-W orientation, showing a different behavior between the eastern and western coast. The western zone usually presents more intense zonal winds while coastal upwelling is stronger in the eastern area [15, 21]. Different researchers have found that upwelling starts in the eastern area and move towards the equator [10, 11, 16, 22–24]. Lower temperature values were also observed along the eastern area associated with strong upwelling [19, 21].

Upwelling trends along this coast have only been recently analyzed by Varela et al. [9] in terms of wind stress at a scale of  $0.3^{\circ}$ . They described a significant negative trend for the entire coast during the considered upwelling season (May–October) from 1982 to 2010. On the other hand, Lima and Wetthey [3] estimated changes in coastal SST along this coast over the same period of time (1982–2010) at a scale of  $0.25^{\circ}$ . These authors found a general coastal warming almost throughout the year except from June to September mainly at the western area where negligible and even small negative trends were detected. Considering the results of these two studies, a decrease in upwelling favorable winds and a small coastal cooling was detected along the south coast of Java over the last three decades. To investigate these observed patterns, coastal upwelling and SST trends along this coast will be analyzed in detail during the upwelling season.

The aim of this paper was to analyze SST trends along the south Java coast and its relation with upwelling during the last 34 years of strong climate change using high spatial resolution data. Differences in the warming rates between coastal and oceanic locations were also characterized to examine the role played by coastal upwelling. For this purpose, daily SST and wind data at a scale of  $0.25^{\circ}$  and  $0.3^{\circ}$ , respectively, were evaluated during the upwelling season defined from July to October. Information about the vertical structure of temperature was also provided considering data from the Simple Ocean Data Assimilation (SODA) project with a horizontal resolution of  $0.5^{\circ}$  and a vertical resolution of 40 levels.

## Material and Methods

The area under study is the south coast of Java. Fig 1 shows the SST mean for the entire region over the period 1982–2015 from July to October (upwelling season). SST differences can be observed between the western and eastern coastal areas with the lowest temperature values at the easternmost zone. Differences between coast and ocean are also observed with SST

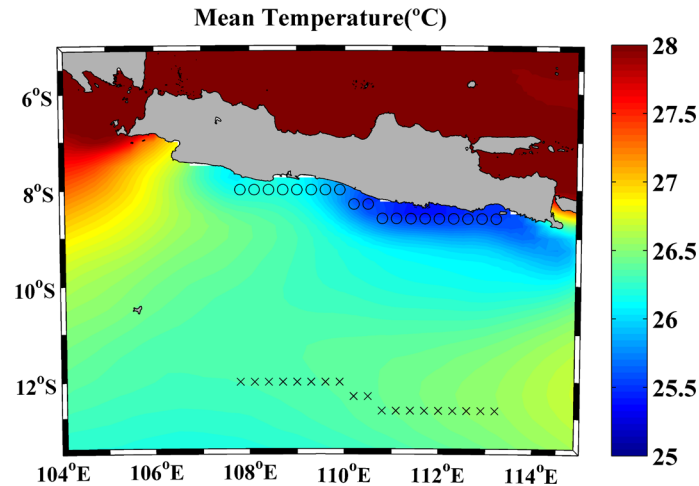


**Fig 1. Mean temperature (°C) calculated from 1982 to 2015 for the upwelling season (July to October) using OISST 1/4 database.** Circles and crosses mark points where wind and SST data from CFSR and OISST 1/4 were considered.

doi:10.1371/journal.pone.0162122.g001

increasing seaward. The presence of cooler surface water along the coast reveals the existence of coastal upwelling. Thus, to analyze in detail SST trends and its relation with upwelling, the area under study was focused on the central region of the southern Java coast from 107° to 113°E. Circles and crosses in Fig 1 represent the points under study in terms of Upwelling Index (UI) and SST data.

## Wind and Heat Fluxes Data

Wind and heat fluxes data were acquired from the NCEP CFSR database at <http://rda.ucar.edu/pub/cfsr.html> developed by the National Oceanic and Atmospheric Administration (NOAA). Data were obtained from the NOAA National Operational Model Archive and Distribution System, which is supported by the NOAA National Climatic Data Center. Additional information about the CFSR database can be found in Saha et al. [25]. The spatial resolution is 0.3°×0.3° from January 1982 to April 2011 and 0.2°×0.2° from then on. Data from the latter period were interpolated on a 0.3°×0.3° grid to use a common resolution over the whole period. Wind is calculated at a reference height of 10 m with 6-hourly time resolution.

Coastal upwelling analysis needs the use of pixels as close to shore as possible to represent coastal processes. To avoid problems with land contamination, only coastal pixels with less than 25% of land were used.

Daily wind data were averaged at monthly scale in order to calculate wind module using the equation:  $|W| = (W_x^2 + W_y^2)^{1/2}$  where  $W_x$  is the zonal wind component and  $W_y$  is the meridional wind component.

Ekman Transport components were calculated as follows:

$$Q_x = \frac{\rho_a C_d}{\rho_w f} (W_x^2 + W_y^2)^{1/2} W_y \quad (1)$$

$$Q_y = -\frac{\rho_a C_d}{\rho_w f} (W_x^2 + W_y^2)^{1/2} W_x \quad (2)$$

where  $\rho_w = 1025 \text{ Kg m}^{-3}$  is the sea water density,  $C_d = 1.4 \times 10^{-3}$  the drag coefficient,  $\rho_a =$



$1.22\text{Kg m}^{-3}$  the air density and  $f$  is the Coriolis parameter defined as  $f = 2\Omega\sin(\theta)$  where  $\Omega$  is the angular velocity and  $\theta$  is the latitude.

UI is defined as the Ekman transport component in the direction perpendicular to the shoreline as follows [26]:

$$UI = -\sin\left(\theta - \frac{\pi}{2}\right)Q_x + \cos\left(\theta - \frac{\pi}{2}\right)Q_y \quad (3)$$

where  $\theta$  is the angle of the unitary vector perpendicular to the coastline pointing oceanward. In this study, angles ranged from  $250^\circ$  to  $270^\circ$ . Positive (negative) upwelling indices correspond to upwelling-favorable (unfavorable) conditions.

Heat fluxes (shortwave, longwave, latent and sensible) were also obtained from the CFSR database at monthly scales. The net heat flux ( $Q_T$ ) through the ocean surface was calculated following Eq (4):

$$Q_T = Q_{SW} + Q_{LW} + Q_S + Q_L \quad (4)$$

where  $Q_{SW}$  is the shortwave flux,  $Q_{LW}$  is the longwave flux,  $Q_S$  is the sensible heat flux and  $Q_L$  is the latent heat flux. A negative (positive) heat flux implies that ocean is losing (gaining) heat.

## Temperature data

Daily SST values were obtained from the Optimum Interpolation Sea Surface Temperature (OISST)  $\frac{1}{4}$  database. This database uses Advanced Very High Resolution radiometer (AVHRR) infrared satellite SST data and data from ships and buoys to build a regular global grid (more information can be found in Reynolds [27] and Reynolds and Chelton [28]). Daily files with a spatial resolution of  $0.25^\circ \times 0.25^\circ$  were obtained from the NOAA website (<http://www.ndbc.noaa.gov/sst/>). Daily SST values were averaged at monthly scale in order to calculate SST assuming linear regression.

Sea Temperature data beneath the sea surface were also obtained from the Simple Ocean Data Assimilation (SODA). This project has reanalyzed data from different sources (oceanographic cruises, satellite, model simulations). Reanalysis data are available at monthly scale with a horizontal resolution of  $0.5^\circ \times 0.5^\circ$  and a vertical resolution of 40 levels (<http://apdrc.soest.hawaii.edu/las/v6/dataset?catitem=3273>) from 1958 to 2010. Detailed information about the methodology can be found in Carton et al. [29–30].

## Upwelling index, heat flux and Temperature trends

Trends were calculated at each pixel as the slope of the linear regression of UI, heat flux and temperature anomalies versus time. Monthly anomalies were calculated by subtracting from the UI, heat flux and temperature of a certain month the mean UI, heat flux and temperature of that month over the period 1982–2015. All trends were calculated using raw data without any filter or running mean. The Spearman rank correlation coefficient was used to analyse the significance of trends due to its robustness to deviations from linearity and its resistance to the influence of outliers. The significance level of each pixel is shown in the figures for those points that exceed 90% (circle) or 95% (square) of significance.

## Results and Discussion

Fig 2 shows the annual cycle of SST (Fig 2A) and UI (Fig 2B) calculated along the coastal points marked in Fig 1 (circles). The lowest SST values ( $24.5\text{--}26.5^\circ\text{C}$ ) are detected from July to October (Fig 2A) for almost the entire region. Minimum values are obtained between  $110^\circ\text{E}$  and  $113^\circ\text{E}$  in accordance with previous works [21]. For the rest of the year SST values are around

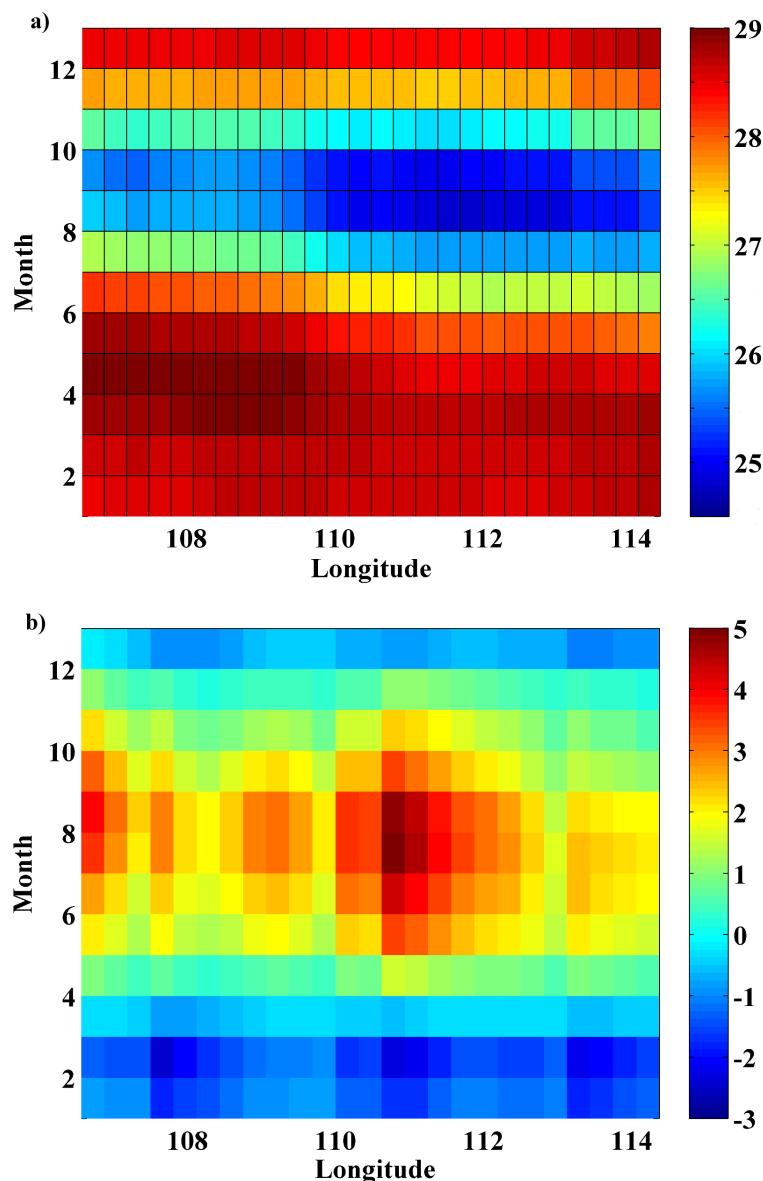


**Fig 2. (a) Annual cycle of SST ( $^{\circ}\text{C}$ )** along the coast of Java ([Fig 1](#) circles) calculated for the period 1982 to 2015 using OISS ¼ database; **(b) Annual cycle of UI ( $\text{m}^2\text{s}^{-1}$ )** along the coast of Java ([Fig 1](#) circles) calculated for the period 1982 to 2015 using CFSR database.

doi:10.1371/journal.pone.0162122.g002

27–29°C. The annual cycle of UI ([Fig 2B](#)), shows positive values from April to November all along the coast as pointed out in previous studies [16, 31]. The highest values are observed from July to September when southeast monsoon prevails. Considering the UI pattern along the coast, maxima are found from 110°E to 112°E with values up to  $4.5 \text{ m}^2\text{s}^{-1}$ . In contrast, from December to March westerly winds dominate and negative values of UI (around  $-2.5 \text{ m}^2\text{s}^{-1}$ ) are obtained.

To analyze the differences in SST at coastal and oceanic locations, the annual cycle of SST meridionally averaged over the points shown in [Fig 1](#), both coastal (circles) and ocean (crosses), was calculated ([Fig 3A](#)). From November to June coastal and oceanic SST values remain very similar, while from July to October differences between coastal and oceanic points

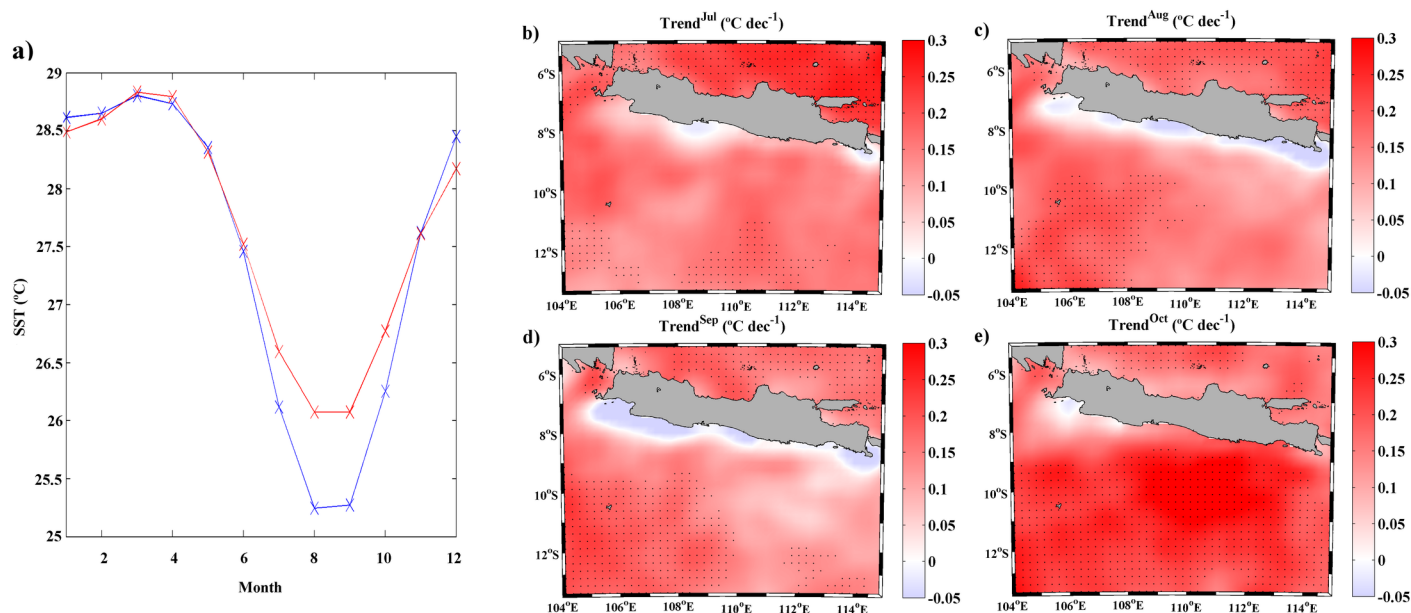


**Fig 3. (a) Annual cycle of SST (°C) meridionally averaged** along the coastal (blue line) and ocean locations (red line) for the period 1982 to 2015 using OISST 1/4 database. **(b-d) Monthly SST trends (°C dec<sup>-1</sup>)** calculated for the period 1982 to 2015 from July to October using OISST 1/4 database.

doi:10.1371/journal.pone.0162122.g003

are clearly detected. The highest differences ( $\sim 1^{\circ}\text{C}$ ) occur between August and September when UI presents higher values (Fig 2B). This different behavior between coastal and oceanic locations indicates a clear influence of upwelling on SST pattern along the coast. Upwelling forcing on SST is an important oceanographic feature in coastal upwelling regions due to the intense pumping of cooler and deeper water to the surface. The importance of this mechanism as a moderator of SST increase has been analyzed by several researchers along different coastal upwelling systems. Thus, Gomez-Gesteira et al. [32] studied the Canary Upwelling System from 1986 to 2006 finding SST differences between coast and ocean on the order of  $3^{\circ}\text{C}$  from August to October linked with the existence of upwelling favorable conditions. Similar results were obtained by Barton et al. [33] for the period 1981–1991 and by Santos et al. [6] from 1982 to 2010. Along the western Iberian Peninsula, Santos et al. [34] found  $\sim 1^{\circ}\text{C}$  of difference between coastal and oceanic locations from 1900 to 2008. Moreover, Santos et al. [7] observed differences between coast and ocean SST values up to  $2^{\circ}\text{C}$  for the period 1900–2009 along the Benguela upwelling system.

The differences in SST evolution at coastal and oceanic locations along the south coast of Java over the last decades of climate change were also evaluated in terms of warming rates. Considering the seasonal differences shown above, the analysis was carried out from July to October. Fig 3B–3E shows the monthly SST trends for the entire region over the period 1982–2015 during these months. A general warming trend is observed for all months especially in the open ocean. The coastal area presents a different behavior with warming rates lower than the oceanic one. In fact, during July and October no tendency is observed along the coast. Only a spot of small negative trends is detected between  $107^{\circ}\text{E}$  and  $109^{\circ}\text{E}$  in July. Focusing on August and September, when UI presents higher values (Fig 2B), a negative trend can be observed all along the coast with values up to  $-0.05^{\circ}\text{C dec}^{-1}$ . As previously mentioned, Lima and Wethey [3] analyzed changes in coastal SST along this coast using the same database than the present study during 1982–2010. They also reported small negative trends around June and July. It is necessary to take into account that these authors analyzed trends of SST along the

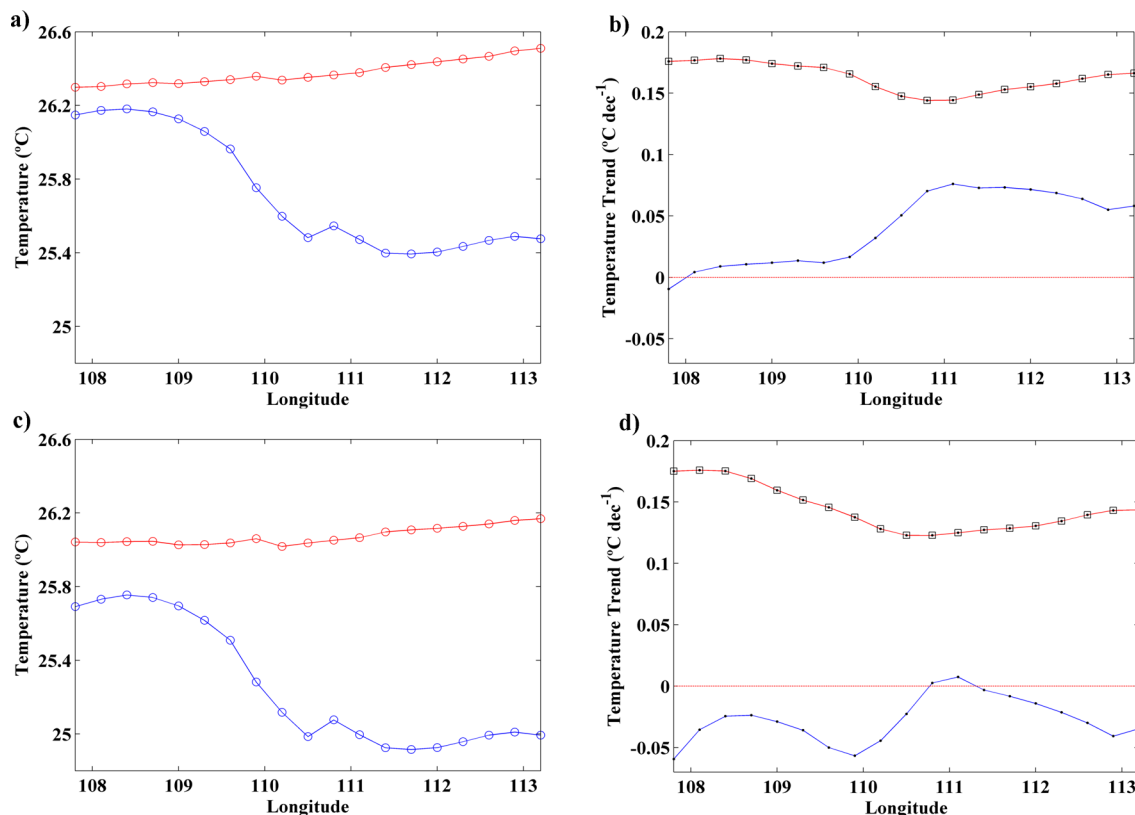


**Fig 4.** (a) SST mean ( $^{\circ}\text{C}$ ) along the coastal (blue line) and ocean locations (red line) from July to October for the period 1982 to 2015 using OISST  $\frac{1}{4}$  database. (b) SST trends ( $^{\circ}\text{C dec}^{-1}$ ) along the coastal (blue line) and ocean locations (red line) from July to October for the period 1982 to 2015 using OISST  $\frac{1}{4}$  database. (c) SST mean ( $^{\circ}\text{C}$ ) along the coastal (blue line) and ocean locations (red line) from August to September for the period 1982 to 2015 using OISST  $\frac{1}{4}$  database. (d) SST trends ( $^{\circ}\text{C dec}^{-1}$ ) along the coastal (blue line) and ocean locations (red line) from August to September for the period 1982 to 2015 using OISST  $\frac{1}{4}$  database. Those points with significance greater than 90% are marked with a circle and those with significance greater than 95% are marked with a square.

doi:10.1371/journal.pone.0162122.g004

south coast of Java as part of the whole Eastern Indian Ocean. Thus, it is difficult to clearly identify the months and coastal zones where negative trends were detected.

A more complete analysis of the differences between the coast and open ocean along the south coast of Java can be observed in Fig 4 in terms of SST means and trends. Fig 4A and 4B (c,d) shows the SST mean and trend from July to October (August-September) for the points located along the coast (blue line) and in the ocean (red line). SST means and trends present higher values at the ocean locations than near the coast for both cases. From July to October (Fig 4A), SST at ocean points presents a similar value all over the region while at coastal locations SST decreases from west to east. The lowest difference ( $\sim 0.2^{\circ}\text{C}$ ) between coast and ocean locations is observed at the western region. This difference increases eastward reaching a maximum of  $1^{\circ}\text{C}$  around  $111^{\circ}\text{E}$ , which corresponds to the area with stronger UI values (Fig 2B). Analyzing SST trends (Fig 4B), positive values are obtained in both cases (coast and ocean), although the ocean warming rate is higher than the coastal one at all longitudes. The lowest differences between coast and ocean are detected from  $111^{\circ}\text{E}$  to  $113^{\circ}\text{E}$  where ocean and coastal trends are closer. The same analysis was also carried out from August to September (Fig 4C and 4D), the months with the highest difference between coastal and ocean points (Fig 3A). Considering SST means, a pattern similar to the one shown for July-October can be observed with higher values in the ocean locations. Nevertheless, in this case, differences between coast

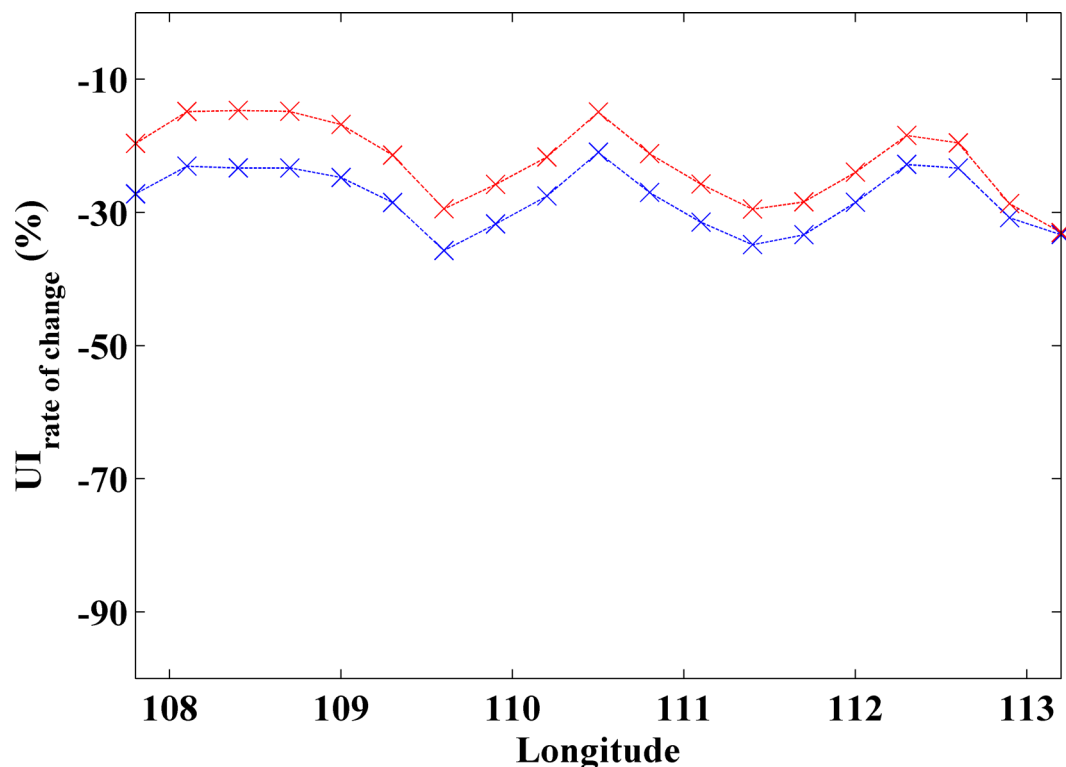


**Fig 5. Rate of change of UI (%) along the coastal locations (Fig 1 circles) calculated for the period 1982 to 2015 using CFSR database. Blue line corresponds to July-October and red line to August-September.**

doi:10.1371/journal.pone.0162122.g005

and ocean increase, reaching values around  $0.4^{\circ}\text{C}$  at the western region and  $1.2^{\circ}\text{C}$  at the easternmost longitudes. In terms of SST trends (Fig 4D), the pattern is different from the previous case (Fig 4B). Thus, trend values along the coastal points are mostly negative for the entire region with a difference around  $0.25^{\circ}\text{C dec}^{-1}$  in relation to the ocean.

Previous results have shown that SST trends along the coast can change substantially depending on the different months considered to the analysis. Earlier studies on different upwelling areas showed a high dependence of trends on the length of the time series and even on the season evaluated in the analysis [9, 35–36].

As previously mentioned, differences between coastal and ocean warming rates have been previously reported along different upwelling regions as the Western coast of the Iberian Peninsula, the Canary Upwelling system and the Benguela Upwelling System [4–7]. These differences were linked to the strengthening of coastal upwelling acting as a moderator of SST increase. The variation of UI along the last three decades of intense climate change along the south coast of Java is shown in Fig 5. Results are shown from July to October (blue line) and from August to September (red line). The rate of change of UI decreases for both periods, being more negative from July to October with values around 30%. From August to September the rate of change is around 15–20%. These results are in good agreement with upwelling trends recently obtained by Varela et al. [9] in terms of wind stress from 1982 to 2010. They detected a significant decreasing trend for the entire coast considering the upwelling season from May to October.

Results obtained in the present study show that ocean warming is significant and coastal warming negligible during the upwelling season (July to October). In addition, cooling is observed near shore and warming at the ocean during the central months of the upwelling season (August-September). Nevertheless, UI was observed to decrease in both cases. This

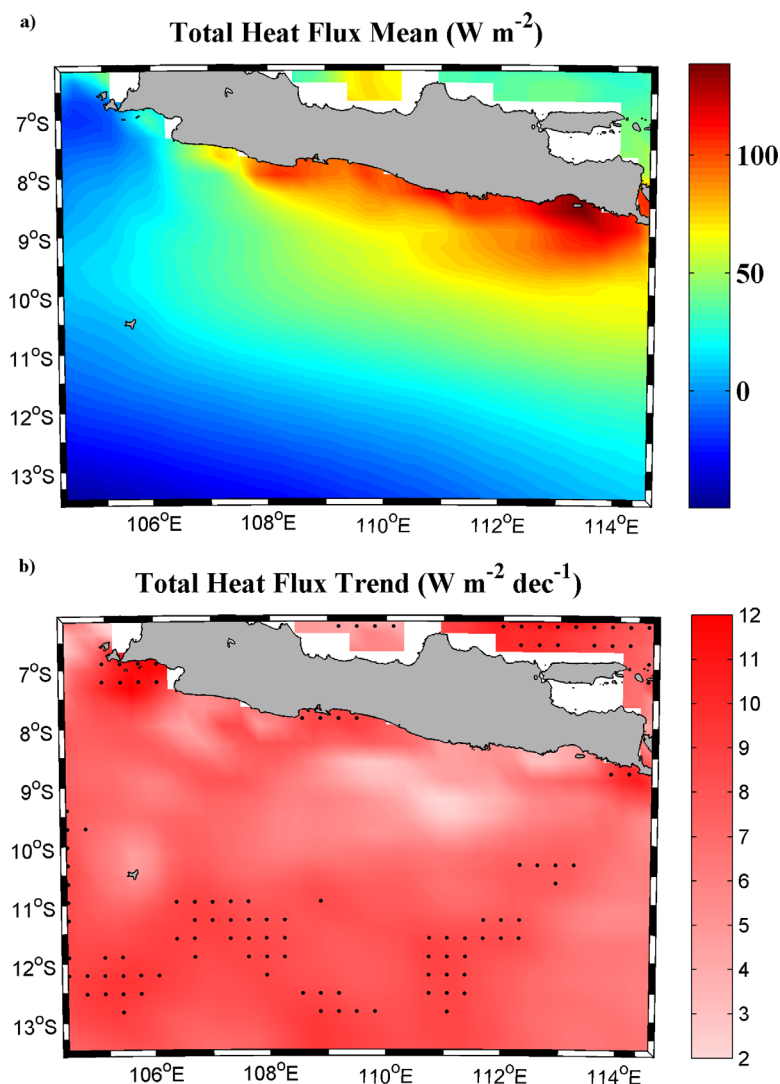


**Fig 6. (a) Heat flux mean ( $\text{W m}^{-2}$ ) and (b) trend ( $\text{W m}^{-2} \text{dec}^{-1}$ )** calculated over the period 1982–2015 (July–October). Black dots represent grid points with significance higher than 95%. A negative (positive) value implies that ocean is losing (gaining) heat.

doi:10.1371/journal.pone.0162122.g006

behavior is different from the one observed at other upwelling regions worldwide [6–9, 35, 37–40], where the different warming rates (sometimes cooling near shore) were due to unchanged or enhanced upwelling scenarios. Upwelling was considered as the main driver in such a way that its mere presence, which pumped cold water up, was enough to hinder surface water warming at the same rate as adjacent ocean water. In those cases where upwelling strengthened, the mechanism became even more efficient and limited warming could turn into cooling as observed in Benguela and La Guajira Upwelling Systems [7, 8].

To better understand the apparent contradiction along the south coast of Java, the role of heat exchange between ocean and atmosphere (Fig 6) and the influence of advection processes (Fig 7) were analyzed. Fig 6 shows the mean heat flux and its trend calculated over the upwelling season (July–October). Ocean gains heat (positive values) over a large part of the area under scope (Fig 6A). The highest values are observed nearshore, especially in the central and eastern parts, which coincide with the area where the lowest mean SST values are detected (Fig 1).



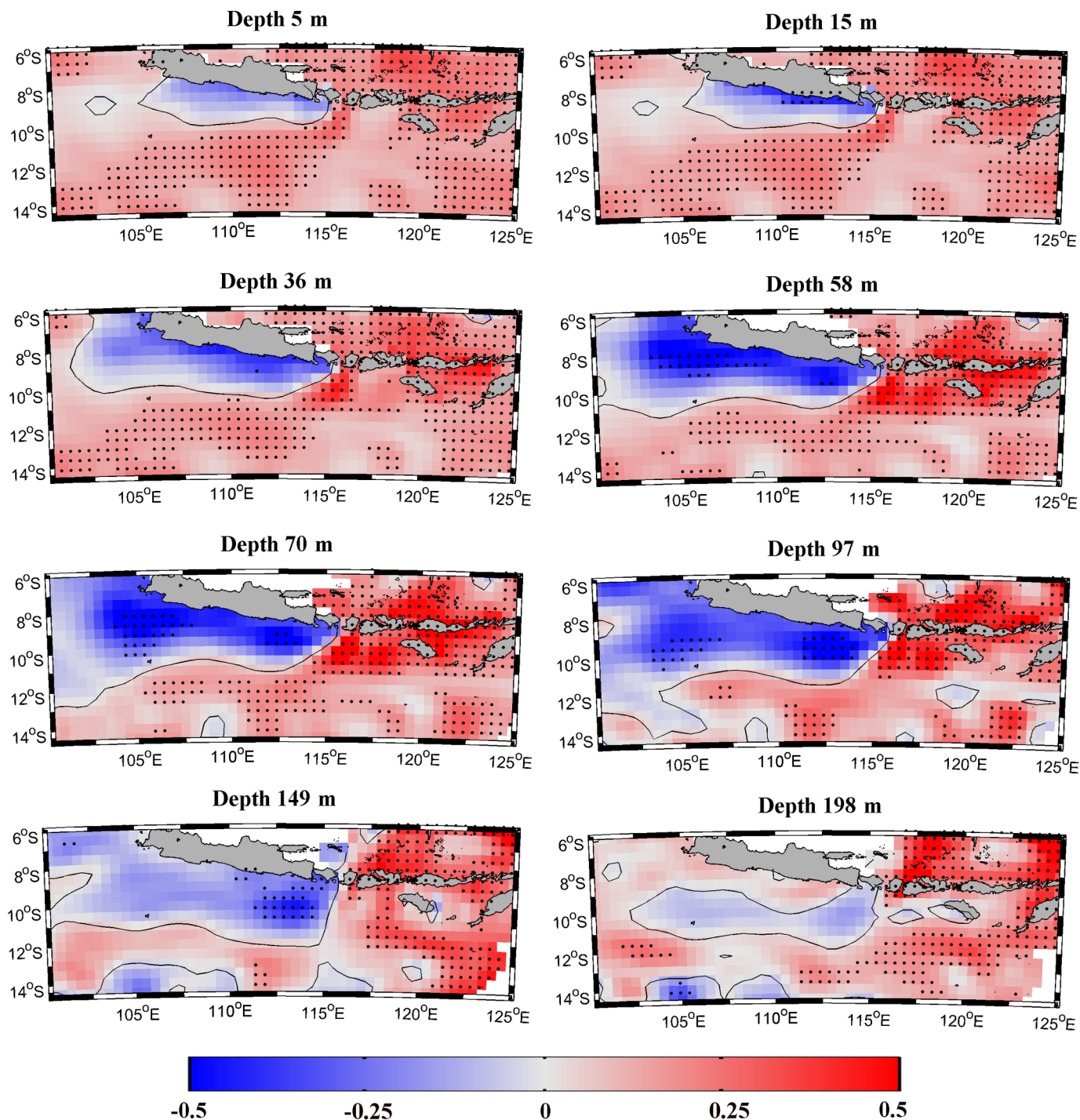


**Fig 7. Temperature trend (°C dec<sup>-1</sup>) calculated for the period 1982 to 2010 from July to October at different layers around the south coast of Java using SODA database.**

doi:10.1371/journal.pone.0162122.g007

Total heat flux trends (Fig 6B) show an increase for the whole area with values between 3–12 W m<sup>-2</sup> dec<sup>-1</sup>. These results suggest that heat exchange between ocean and atmosphere is not the forcing that drives the cooling pattern found in the upwelling area since no differences in heat exchange were detected between coastal and ocean locations.

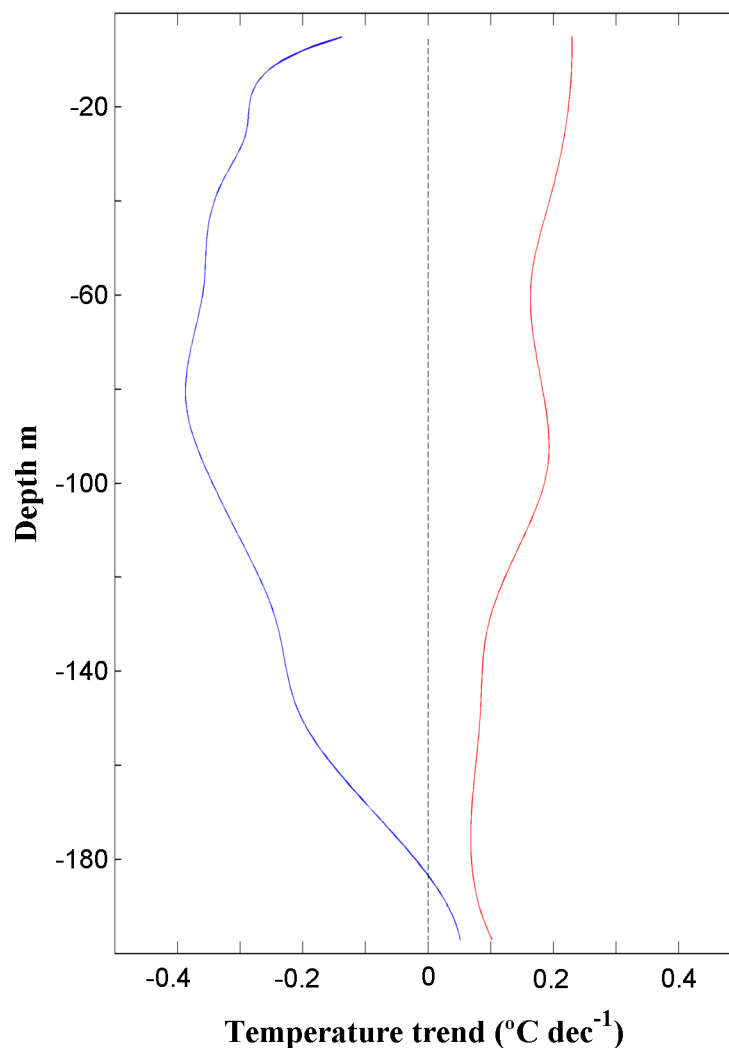


**Fig 8. Temperature trend ( $^{\circ}\text{C dec}^{-1}$ )** calculated for the period 1982 to 2010 from July to October near coast (blue line) and at the ocean (red line) along the longitude  $110^{\circ}\text{E}$  using SODA database.

doi:10.1371/journal.pone.0162122.g008

Changes in the temperature of the water column (obtained from SODA) were also analyzed as a possible cooling mechanism along the south coast of Java. Fig 7 shows the temperature trends calculated in a wide region around the south coast of Java for eight different layers (from 5 to 200 m) over the upwelling season (July–October). The upper layer (5 m) shows a general warming trend all over the region except along the south coast of Java where a negative temperature trend around  $-0.1^{\circ}\text{C dec}^{-1}$  and  $-0.2^{\circ}\text{C dec}^{-1}$  is observed. This cooling trend spreads to the south and west of the region reaching its maximum extension around 100 m with minimum values around  $-0.5^{\circ}\text{C dec}^{-1}$ . From then on, the area where the temperature trend is negative becomes smaller with depth and beneath 200 m the negative trend disappears. Note that white regions along the northern coast of Java and at the southeast corner of the map represent no data due to the shallowness. This figure clearly indicates that the water from subsurface layers along the south coast of Java shows a cooling trend over the last three decades. Two vertical sections along the longitude  $110^{\circ}\text{E}$  (Fig 8) were also analyzed using SODA to better analyze the vertical structure of temperature trend from July to October near coast and at ocean locations. Blue (red) line shows the vertical profile calculated near the coast averaging data from  $8^{\circ}$  to



9.5°S (11.5° to 13°S). Trends are positive at the ocean (red line) decreasing from the upper to deeper layers. As shown in the previous figure, trends are negative near shore (blue line), being the highest value (around  $-0.4^{\circ}\text{C dec}^{-1}$ ) observed between 40–100 m.

In summary, previous results indicate that the role of heat exchange between ocean and atmosphere is negligible to explain the different warming patterns observed at coastal and oceanic areas when compared with ocean processes. Thus, horizontal advection (cool water advected by the South Java Current [41, 42]) and vertical entrainment due to upwelling are the main forcings that drive cooling off Java. In spite of the moderate decrease in UI, the combination of both processes is still efficient to bring cooled water to the surface.

## Conclusions

Within a context of climate change with a general upward trend in terms of SST, the south coast of Java has shown a different behavior over the last three decades (1982–2015). A small coastal warming was detected over the upwelling season (July–October) along with a moderate decrease in UI. This behavior contrasts with that observed in other upwelling regions as Benguela, Canary or La Guajira upwelling Systems where a moderate coastal warming, or even cooling, was linked to the strengthening in coastal upwelling.

The analysis of the heat exchange between ocean and atmosphere showed that this forcing was not the responsible of the cooling trend found in the upwelling area. In fact, the vertical structure of water temperature along the south coast of Java showed that subsurface layers have experienced a cooling trend over the last three decades. Thus, although UI presented a negative trend, it can still pump cooled water to the surface.

Trends shown in this work confirm the interest of studying local areas where upwelling is an important forcing, taking advantage of the high spatial resolution of databases to resolve conditions at the scale of coastal upwelling. The obtained results also showed the interest of analyzing the properties of subsurface water masses, especially in areas where they can be brought to surface by upwelling.

## Acknowledgments

This research was also partially supported by Xunta de Galicia under projects GRC-2013-001 “Programa de Consolidación e Estructuración de Unidades de Investigación Competitivas (Grupos de Referencia Competitiva)” co-funded by European Regional Development Fund (FEDER). The Portuguese Science Foundation (FCT) partially supported this research through a Post-doctoral grant (SFRH/BPD/97320/2013) of the second author and through the project Pest (C/MAR/LA0017/2013). CFSR data was obtained from Environmental Modeling Center/ National Centers for Environmental Prediction/ National Weather Service/ NOAA/ U.S. NCEP Climate Forecast System Reanalysis (CFSR) Monthly Products. Research Data Archive at the National Center for Atmospheric Research, Computational and Information Systems Laboratory. <http://rda.ucar.edu/datasets/ds093.2/>.

## Author Contributions

**Conceptualization:** RV FS MG-G.

**Data curation:** RV MG-G.

**Formal analysis:** RV MG-G XC.

**Funding acquisition:** MG-G IA.

**Investigation:** RV IA.

**Methodology:** RV FS MG-G.

**Project administration:** MG-G IA.

**Resources:** FS MG-G IA.

**Software:** RV FS MG-G IA XC JMD.

**Supervision:** RV MG-G IA XC JMD.

**Validation:** RV FS MG-G IA XC.

**Visualization:** RV MG-G IA XC.

**Writing – original draft:** RV MG-G IA XC.

**Writing – review & editing:** RV MG-G IA XC.

## References

1. Levitus S, Antonov J, and Boyer T. Warming of the world ocean, 1955–2003. *Geophys Res Lett*. 2005; 32: L02604
2. Harrison DE, and Carson M. Is the world ocean warming? Upper ocean trends, 1950–2000. *J Phys Oceanogr*. 2007; 37: 174–187
3. Lima FP, and Wetthey DS. Three decades of high-resolution coastal sea surface temperatures reveal more than warming. *Nature Commun*. 2012; 3: 704
4. Lemos RT, and Sansó B. Spatio-temporal variability of ocean temperature in the Portugal Current System. *J Geophys Res*. 2006; 111: C04010
5. Santos F, Gómez-Gesteira M, deCastro M, and Álvarez I. Variability of coastal and ocean water temperature in the upper 700 m along the Western Iberian Peninsula from 1975 to 2006. *PLoS One*. 2012a; 7(12): 1–7
6. Santos F, Gómez-Gesteira M, deCastro M, and Álvarez I. Differences in coastal and oceanic SST warming rates along the Canary Upwelling Ecosystem from 1982 to 2010. *Cont Shelf Res*. 2012b; 47: 1–6
7. Santos F, Gómez-Gesteira M, deCastro M, and Álvarez I. Differences in coastal and oceanic SST trends due to the strengthening of coastal upwelling along the Benguela current system. *Cont Shelf Res*. 2012c; 34: 79–86
8. Santos F, Gómez-Gesteira M, Varela R, Ruiz-Ochoa M, Días JM. Influence of upwelling on SST trends in La Guajira system. In press
9. Varela R, Álvarez I, Santos F, deCastro M, and Gómez-Gesteira M. Has upwelling strengthened along worldwide coasts over 1982–2010? *Sci Rep*. 2015; 5: 1–15
10. Saji NH, Goswami BN, Vinayachandran PN, and Yamagata T. A dipole mode in the tropical Indian Ocean. *Nature*. 1999; 401: 360–363 PMID: [16862108](#)
11. Webster PJ, Moore AM, Loschnigg JP, and Leben RR. Coupled ocean temperature dynamics in the Indian Ocean during 1997–98. *Nature*. 1999; 401: 356–360 PMID: [16862107](#)
12. Rao AS, Behera SK, Masumoto Y, Yamagata T. Interannual variability in the subsurface tropical Indian Ocean. *Deep-Sea Res II*. 2002; 49: 1549–1572
13. Susanto RD, and Marra J. Effect of the 1997/98 El Niño on chlorophyll a variability along the coasts of Java and Sumatra. *Prog Oceanogr*. 2005; 18: 124–127
14. Du Y, Qu T, and Meyers G. Interannual variability of the sea surface temperature off Java and Sumatra in a global GCM. *J Climate*. 2007; 21: 2451–2465
15. Purba M. Dynamics of south off Java—Sumbawa Island in Southeast Monsoon. *Torani Jurnal Ilmu Kelautan dan Perikanan*. 2007; 2: 140–150 (in Indonesian)
16. Susanto RD, Moore TS, and Marra J. Ocean color variability in the Indonesian Seas during the SeaWiFS era. *Geochemistry, Geophysics, Geosystem*. 2006; 7: Q05021
17. Iskandar I, Sasaki H, Sasai Y, Masumoto Y, Mizuno K. A numerical investigation of eddy-induced chlorophyll bloom in the southeastern tropical Indian Ocean during Indian Ocean Dipole—2006. *Ocean Dyn*. 2009; 60: 731–742

18. Currie JC, Lengaigne M, Vialard J, Kaplan DM, Aumont O, Naqvi SWA, et al. Indian Ocean Dipole and El Niño/Southern Oscillation impacts on regional chlorophyll anomalies in the Indian Ocean. *Biogeosciences*. 2013; 10: 5841–5888
19. Xue L, Wang H, Jiang LQ, Cai WJ, Wei Q, Song H, et al. Aragonite saturation state in a monsoonal upwelling off Java, Indonesia. *J Marine syst*. 2015; 153: 10–17
20. Ma J, Liu H, Lin P, and Zhan H. Effects of the interannual variability in chlorophyll concentrations on sea surface temperatures in the east tropical Indian Ocean. *J Geophys Res-Oceans*. 2015; 120.10: 7015–7027
21. Kuswardani RTD, and Qiao F. Influence of the Indonesian Throughflow on the upwelling off the east coast of South Java. *Chinese Sci Bull*. 2014; 59: 4516–4523
22. Susanto RD, Gordon AL, and Zheng Q. Upwelling along the coasts of Java and Sumatra and its relation to ENSO. *Geophys Res Lett*. 2001; 28: 1599–1602
23. Qu T, Du Y, Strachan J, Meyers G, Slingo J. Sea surface temperature and its variability in the Indonesian region. *Oceanography*. 2005; 18: 50–61
24. Siswanto and Suratno. Seasonal pattern of wind induced upwelling over Java-Bali Sea. *Int J Remote Sens Earth Sci*. 2008; 5: 46–56
25. Saha S, Moorthi S, Pan HL, Wu X, Wang J, Nadiga S, et al. The NCEP Climate Forecast System Reanalysis. *B Am Meteorol Soc*. 2010; 91: 1015–1057
26. Nykjaer L, and Van Camp L. Seasonal and interannual variability of coastal upwelling along northwest Africa and Portugal from 1981 to 1991. *J Geophys Res*. 1994; 99: 14,197–14,207
27. Reynolds RW. What's new in Version 2. [Available at [http://www.ncdc.noaa.gov/oa/climate/research/sst/papers/whats\\_new\\_v2.pdf](http://www.ncdc.noaa.gov/oa/climate/research/sst/papers/whats_new_v2.pdf).] 2009
28. Reynolds RW, and Chelton DW. Comparisons of daily sea surface temperature analysis for 2007–08. *J Clim*. 2010; 23: 3545–3562
29. Carton JA, Chepurin GA, Cao X, Giese BS. A Simple Ocean Data Assimilation analysis of the global upper ocean 1950–1955, Part 1: Methodology, *J Geophys Res*. 2000a; 30: 294–309
30. Carton JA, Chepurin GA, Cao X. A Simple Ocean Data Assimilation analysis of the global upper ocean 1950–1955, Part 2: Methodology, *J Geophys Res*. 2000b; 30: 311–326
31. Gordon AL. Oceanography of the Indonesian seas and their throughflow. *Oceanography*. 2005; 18(4): 13–26
32. Gómez-Gesteira M, deCastro M, Álvarez I, Lorenzo MN, Gesteira JLG, and Crespo AJC. Spatio-temporal upwelling trends along the canary upwelling system (1967–2006). *Ann N Y Acad Sci*. 2008; 1146: 320–337 doi: [10.1196/annals.1446.004](https://doi.org/10.1196/annals.1446.004) PMID: [19076422](https://pubmed.ncbi.nlm.nih.gov/19076422/)
33. Barton ED, Aristegui J, Tett P, Cantón M, García-Braun J, Hernández-León S, et al. The transition zone of the Canary current upwelling region. *Prog Oceanogr*. 1998; 41: 455–504
34. Santos F, Gómez-Gesteira M, deCastro M. Coastal and Oceanic SST variability along the western Iberian Peninsula. *Cont shelf Res*. 2011; 31: 2012–2017
35. Barton ED, Field DB, Roy C. Canary current upwelling: more or less? *Prog Oceanogr*. 2013; 116: 167–178
36. Sydeman WJ, García-Reyes M, Schoeman DS, Rykaczewski RR, Thompson SA, Black BA, et al. Climate change and wind intensification in coastal upwelling ecosystems. *Science*. 2014; 345: 77–80 doi: [10.1126/science.1251635](https://doi.org/10.1126/science.1251635) PMID: [24994651](https://pubmed.ncbi.nlm.nih.gov/24994651/)
37. Patti B, Guisande C, Riveiro I, Thejil P, Cuttitta A, Bonanno A, et al. Effect of atmospheric CO2 and solar activity on wind regime and water column stability in the major global upwelling areas. *Est Coast Shelf Sci*. 2010; 88: 45–52
38. Narayan N, Paul A, Mulitza S, Schulz M. Trends in coastal upwelling intensity during the late 20th century. *Ocean Sci*. 2010; 6: 815–823
39. Pardo P, Padín X, Gilcoto M, Farina-Busto L, Pérez F. Evolution of upwelling systems coupled to the long term variability in sea Surface temperature and Ekman transport. *Clim Res*. 2011; 48: 231–246
40. Cropper TE, Hanna E, Bigg GR. Spatial and temporal seasonal trends in coastal upwelling off Northwest Africa, 1981–2012. *Deep-Sea Res*. 2014; 1(86): 94–111
41. Du Y, Qu T, Meyers G. Interannual variability of sea surface temperature off Java and Sumatra in a global GCM\*. *J Climate*. 2008; 21(11): 2451–2465.
42. Sprintall J, Wijffels S, Molcard R, Jaya I. Direct Evidence of the South Java Current System in Ombai Strait, *Dynam Atmos Oceans*. 2008; 50(2): 140–156.



# Differences in coastal and oceanic SST trends north of Yucatan Peninsula

\* R. Varela<sup>1</sup>, X. Costoya<sup>1,2</sup>, M. Gómez-Gesteira<sup>1</sup>, C. Enriquez<sup>3</sup>

*1 Ephyslab, Environmental Physics Laboratory, Facultad de Ciencias, Universidad de  
Vigo, 32004 Ourense, Spain, [ruvarela@uvigo.es](mailto:ruvarela@uvigo.es).*

*2 CESAM, Departamento de Física, Universidade de Aveiro, 3810-193 Aveiro,  
Portugal.*

*3 Facultad de Ciencias, Universidad Nacional Autónoma de México, Sisal Yucatán,  
México.*

## **Abstract**

The coastal area north of Yucatan has experienced a cooling SST trend from 1982 to 2015 during the upwelling season (May-September) that contrasts with the warming observed at the adjacent ocean area. Different drivers were analyzed to identify the possible causes of that unusual coastal cooling. Changes in coastal upwelling and in sea-atmosphere heat fluxes are not consistent with the observed coastal cooling. The eastward shift of the Yucatan Current observed over the last decades is hypothesized as the most probable cause of coastal cooling. This shift enhances the vertical transport of cold deeper water to the continental shelf from where it is pumped to the surface by upwelling favorable westerly winds.

**Keywords:** Upwelling, Yucatan, sea surface temperature, wind, current direction, shelf dynamics, warming, cooling

## **1. Introduction**

Over the last decades, the scientific community has focused its attention on the impact of climate change. Ocean plays a key role in regulating that impact since it has absorbed the vast majority of the heat gained by the Earth (Levitus et al., 2005, Mikaloff-Fletcher et al., 2006, Levitus et al., 2012).

Upwelling systems are productive oceanic areas with important socio-economic implications. In fact, upwelling systems only occupy 1% of the world's ocean but more than 20% of fish catches occurs there (Pauly and Christensen, 1995). These systems are especially vulnerable to climate change that can affect not only the physical component (water temperature and wind patterns) but also productivity of the area.

Regarding ocean temperature, several authors have observed different rates of warming depending on the location (Harrison and Carson, 2007; Lima and Wetthey, 2012, Cheung et al., 2013). This variability is even more marked at regional scale. In this way, a different warming rate has been observed for coastal and oceanic locations in some of the most important upwelling systems: Benguela, Canary, West Iberian Peninsula, Java or La Guajira (Lemos and Sansó, 2006, Santos et al., 2012a,b,c, Santos et al., 2016, Varela et al., 2016). Most of these studies have linked the different warming rates at coast and ocean with the strengthening of coastal upwelling, which can act as a moderator of climate change. A complete study about the evolution of upwelling in the main upwelling areas worldwide can be observed in Varela et al., (2015).

In the coastal zone of the Yucatan Peninsula two very different upwelling processes occur: a typical wind related upwelling in the northern coast of the Peninsula and a dynamic upwelling in the northeastern corner of the Peninsula. Yucatan is localized in the south-eastern area of the Gulf of Mexico around 21°N and between 269-274°E (Figure 1). The northern coast of the Yucatan Peninsula follows a marked zonal

orientation. In general, the area is characterized by a wide continental shelf that extends over 250 km (Ruiz-Castillo et al., 2016), being much narrower east of the Yucatan Peninsula. Easterly and northeasterly winds (trade winds) prevail throughout the year giving rise to conditions that favor upwelling over the northern coast of the Yucatan shelf (Merino, 1997, Pérez-Santos et al., 2010, Enríquez et al., 2013, Ruiz-Castillo et al., 2016). Ruiz-Castillo et al., (2016) examined coastal upwelling using Advanced Very High Resolution Radiometer (AVHRR) and Cross-Calibrated Multi-Platform (CCMP) from 1986 to 2009 and 1988 to 2011, respectively, to analyze SST and wind patterns. These authors obtained positive values of upwelling index (UI) throughout the year, with the highest values observed from March to July. Similar results were obtained by Pérez-Santos et al., (2010), who considered that Ekman Transport was the main process favoring permanent coastal upwelling at the northern coast of the Yucatan Peninsula. The prevalence of upwelling favorable winds confers this region distinguishable chlorophyll-a properties when compared with adjacent areas, highlighting the biological impact of upwelling (Salmerón-García et al., 2011, Pérez- Santos et al., 2014).

A different upwelling process occurs from April to September in the form of sharp and intense pulses of deeper water masses into the northeastern corner of Yucatan, attracting species of ecological and commercial interest as the whale shark (*Rhincodon typus*) (Cárdenas-Palomo et al., 2015). Actually, the upwelling region has been declared a biosphere reserve for this specie. It is crucial to analyze temperature variation in this area, especially within the context of climate change, since changes in warming patterns can induce changes in biodiversity at the ecosystem level (e.g: latitudinal shifts on the distribution of species).



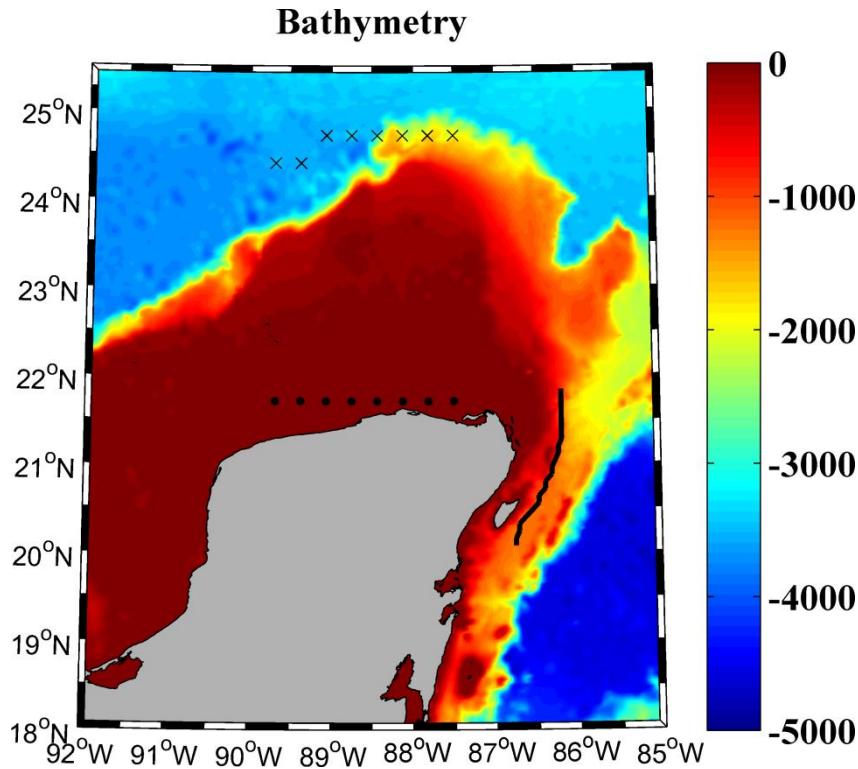


**Figure 1 | Bathymetry of the area under study.** Dots (crosses) mark the coastal (oceanic) location where wind and SST were obtained. The solid line represents the transect where temperature variability was analyzed.

Different authors have focused their research on SST patterns in this area. A cold band is observed during summer months along the coast associated with upwelling favorable winds (Zavala-Hidalgo et al., 2006, Ruiz-Castillo et al., 2016). A 7 year analysis of SST from AVHRR satellite carried out by Zavala-Hidalgo et al., (2006) showed cold coastal water in Yucatan from May to August with a peak in July, during these months the difference in temperature between coast and ocean can be up to 2°C. del Monte-Luna et al., (2015) related the recurrent upwelling in the area to the cold water found north of Yucatan Peninsula. Ruiz-Castillo et al., (2016) observed a cold water band in the inner shelf starting in April with differences up to 1°C with the warm waters off the Yucatan shelf. This effect continues at least until October. Regarding SST trends, Lima and Wethey, (2012) used data from AVHRR to analyze SST variations over the period

1982-2010. For the case of Yucatan, they obtained a slight cooling during most of the year. However, that cooling trend cannot be associated with positive trends of UI in the area, as observed in other regions (Santos et al., 2012a,b,c). In fact, Varela et al., (2015) obtained negative trends of wind stress for the area of Yucatan using wind stress data from the Climate Forecast System Reanalysis (CFSR) over the same period.

Other authors have pointed out that wind forcing is not enough to explain the appearance of colder water in the innermost area of the Yucatan shelf (Enríquez and Mariño-Tapia, 2014; Reyes-Mendoza et al., 2016; Souza et al., 2016; Carrillo et al., 2016). Enríquez and Mariño-Tapia, (2014) found that the characteristics of the Yucatan Current (YC) could influence the upwelling in the area, in such a way that, when YC separates from the continental slope, favors the enhancement of positive vertical velocities, which raise cold, nutrient rich water to the surface layer. Similar results were obtained by Carrillo et al., (2016) who observed an uplifting of the isotherms under the action of the YC, which evidence the existence of upwelling in the area. Thus, the enhancement of the YC can lead to the reinforcement of upwelling in the area (Enríquez and Mariño-Tapia, 2014; Carrillo et al., 2016, Souza et al., 2016).

The aim of this paper is to analyze SST variability along the Yucatan upwelling system over the last three decades. This variability will be related to different drivers like upwelling index, heat exchange with the atmosphere or changes in the Yucatan current.

## **2. Data and Methods**

### **2.1. Temperature data**

Daily SST values were retrieved from the Optimum Interpolation Sea Surface Temperature (OISST)  $\frac{1}{4}$  database (<http://www.ndc.noaa.gov/sst/>). This database was built by means of Advanced Very High Resolution radiometer (AVHRR) infrared

satellite SST data and data from ships and buoys (Reynolds, 2009 and Reynolds and Chelton, 2010). A special method of kriging (Optimum interpolation) was used to construct a regular grid ( $0.25^\circ \times 0.25^\circ$ ) containing data from 1982 to nowadays.

Sea Temperature data along the water column was obtained from the Hybrid Coordinate Ocean Model (HYCOM). HYCOM uses satellite altimeter observations, satellite and in-situ sea surface temperature. Also, in-situ vertical temperature and salinity profiles from XBTs, ARGO floats, and moored buoys, using the NRL-developed Navy Coupled Ocean Data Assimilation (NCODA) system (Cummings, 2005; Cummings and Smedstad, 2013). HYCOM has a horizontal resolution of  $1/12^\circ \times 1/12^\circ$  at 3-hour time steps and 40 standard depth levels covering the period from 1993 to present.

## 2.2. Wind data

Wind data were obtained from the NCEP CFSR database at <http://rda.ucar.edu/pub/cfsr.html> developed by the National Oceanic and Atmospheric Administration (NOAA). Data were acquired from the NOAA National Operational Model Archive and Distribution System, which is supported by the NOAA National Climatic Data Center (Saha et al., 2010). Wind was calculated at a reference height of 10 m with 6-hourly time resolution. The spatial resolution was  $0.3^\circ \times 0.3^\circ$  from January 1982 to April 2011 and  $0.2^\circ \times 0.2^\circ$  from then on. A common resolution over the whole period under study was used by interpolating data on a  $0.3^\circ \times 0.3^\circ$  grid. Daily wind data were averaged at monthly scale. Only coastal pixels with less than 25% of land were used to avoid problems with land contamination.

Ekman Transport components were calculated following:

$$Q_x = \frac{\rho_a C_d}{\rho_w f} (W_x^2 + W_y^2)^{\frac{1}{2}} W_y \quad (1)$$

$$Q_y = -\frac{\rho_a C_d}{\rho_w f} (W_x^2 + W_y^2)^{\frac{1}{2}} W_x \quad (2)$$

where  $W_x$  is the zonal wind component and  $W_y$  is the meridional wind component,  $\rho_w = 1025 \text{ Kg m}^{-3}$  is the sea water density,  $C_d = 1.4 \times 10^{-3}$  the drag coefficient,  $\rho_a = 1.22 \text{ Kg m}^{-3}$  the air density and  $f$  is the Coriolis parameter defined as  $f = 2\Omega \sin(\theta)$  where  $\Omega$  is the angular velocity and  $\theta$  the latitude.

UI is the Ekman transport component in the direction perpendicular to the shoreline (Nykjaer and Van Camp, 1994):

$$UI = -\sin\left(\Psi - \frac{\pi}{2}\right) Q_x + \cos\left(\Psi - \frac{\pi}{2}\right) Q_y \quad (3)$$

where  $\Psi$  is the angle of the unitary vector perpendicular to the coastline pointing oceanward. In this study the angle was set to  $90^\circ$  for the whole region. Positive (negative) upwelling indices correspond to upwelling-favorable (unfavorable) conditions.

### 2.3. Ocean currents

The velocity components (longitude and latitude) were also obtained from the HYCOM + NCODA Global  $1/12^\circ$  Reanalysis database (see description above). Each velocity component is characterized by three indices (i, j, k) that determine the grid point.

### 2.4. Heat flux data

Heat fluxes were also obtained from CFSR database (see description above). Shortwave, longwave, latent heat and sensible heat were retrieved at monthly scale from 1982 to 2015. Total net heat flux ( $Q_T$ ) through the ocean surface was calculated following equation (4):

$$Q_T = Q_{SW} + Q_{LW} + Q_S + Q_L \quad (4)$$

Where  $Q_{SW}$  is the shortwave flux,  $Q_{LW}$  is the longwave flux,  $Q_S$  is the sensible heat flux and  $Q_L$  is the latent heat flux. Negative (positive) heat fluxes imply that ocean is losing (gaining) heat.

### 2.5. Calculation of trends

Trends were calculated at each pixel as the slope of the linear regression of the anomaly of each variable versus time. Monthly anomalies were calculated by subtracting from the value of a certain month the mean value of that month over the period 1982–2015. All trends were calculated using raw data without any filter or running mean. The Spearman rank correlation coefficient was used to analyze the significance of trends due to its robustness to deviations from linearity and its resistance to the influence of outliers.

## 2.6. Control of thermohaline changes

Temperature variability along the water column will be interpreted using the model proposed by Bindoff and McDougall, (1994). According to their methodology it is possible to know if changes in a scalar property detected along isobars are due to changes on isopycnals or vertical displacements of isopycnals. Changes on isopycnals are related to heat flux variability (pure warming) and freshwater flux variability (pure freshening) in the water formation area (Jackett and McDougall, 1997; Arbic and Owens, 2001). On the other hand, vertical displacements of isopycnals are related to the process that Bindoff and McDougall, (1994) define as pure heaving. This process results in water masses sinking or rising without changing their intrinsic properties. These displacements are caused by wind stress variability or changes in the water formation rates. The model proposed by Bindoff and McDougall, (1994) is applied following

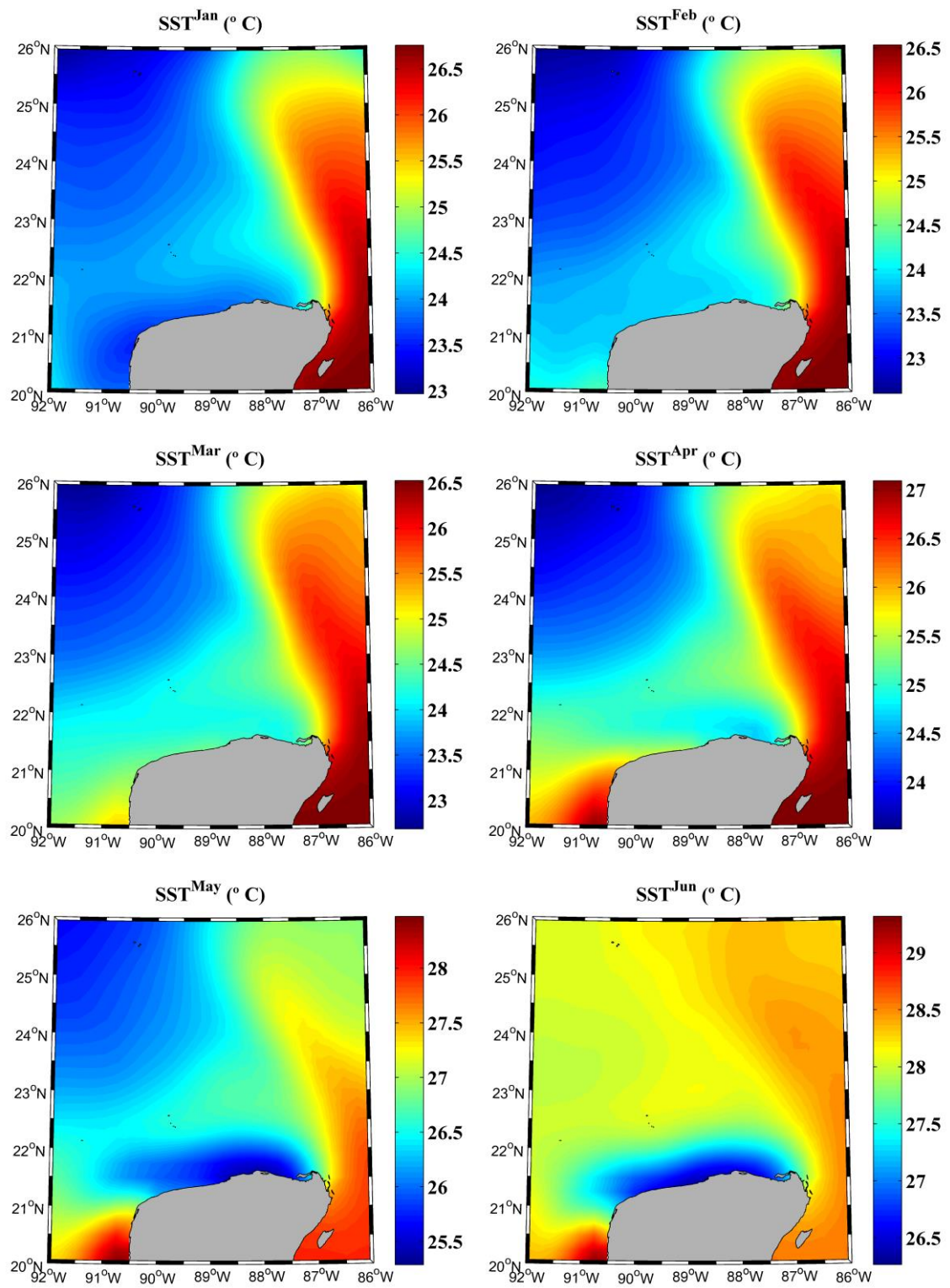
$$\left. \frac{d\varepsilon}{dt} \right|_p = \left. \frac{d\varepsilon}{dt} \right|_n - \left. \frac{dp}{dt} \right|_n \left( \frac{\partial \varepsilon}{\partial p} \right) \quad (5)$$

The left term accounts for time variation of a scalar property (potential temperature in the present study) along isobars. The first term on the right hand accounts for time variation of the scalar property along isopycnals. The last term takes into account the

rate of change of isopycnals displacements and the vertical gradient of the scalar property, which together refer to the vertical displacement of isopycnals. Vertical gradients are assumed to be constant in time.

### **3. Results and discussion**

Monthly SST mean fields are shown in Figure 2. Overall, two different patterns are observed in the area throughout the year. On the one hand, from November to April similar values are detected between coastal and oceanic locations on the Yucatan shelf (around 23.5-26°C depending on the month). Moreover, a tongue of warmer water (values around 26-27.5°C) spreads from the Caribbean Sea through the Yucatan Channel during these months. Colder water is observed from June to September near the northern coast of Yucatan in contrast with the warmer oceanic water. The difference between both water masses is close to 2.5°C. Finally, May and October can be considered as transition months since cold water is observed in the shelf of North Yucatan although the differences between coast and ocean are small. Seasonal SST differences between coast and ocean had been also observed in some of the most important upwelling systems in the world as Benguela, Canary, La Guajira or Java (Lemos and Sansó, 2006, Santos et al., 2012a,b,c, Santos et al., 2016, Varela et al., 2016). In the case of North Yucatan, SST differences between coast and ocean can be related to the existence of a relatively strong upwelling in the area (Pérez-Santos et al., 2010, Ruiz-Castillo et al., 2016). Mendoza et al., (2005) used a model based in the thermal energy equation to simulate SST in the Gulf of Mexico obtaining differences around 3°C in July between coast and the adjacent ocean zone. Similar results were obtained by Zavala-Hidalgo et al., (2006) who observed colder coastal water north of Yucatan Peninsula from May to August with a peak in July.





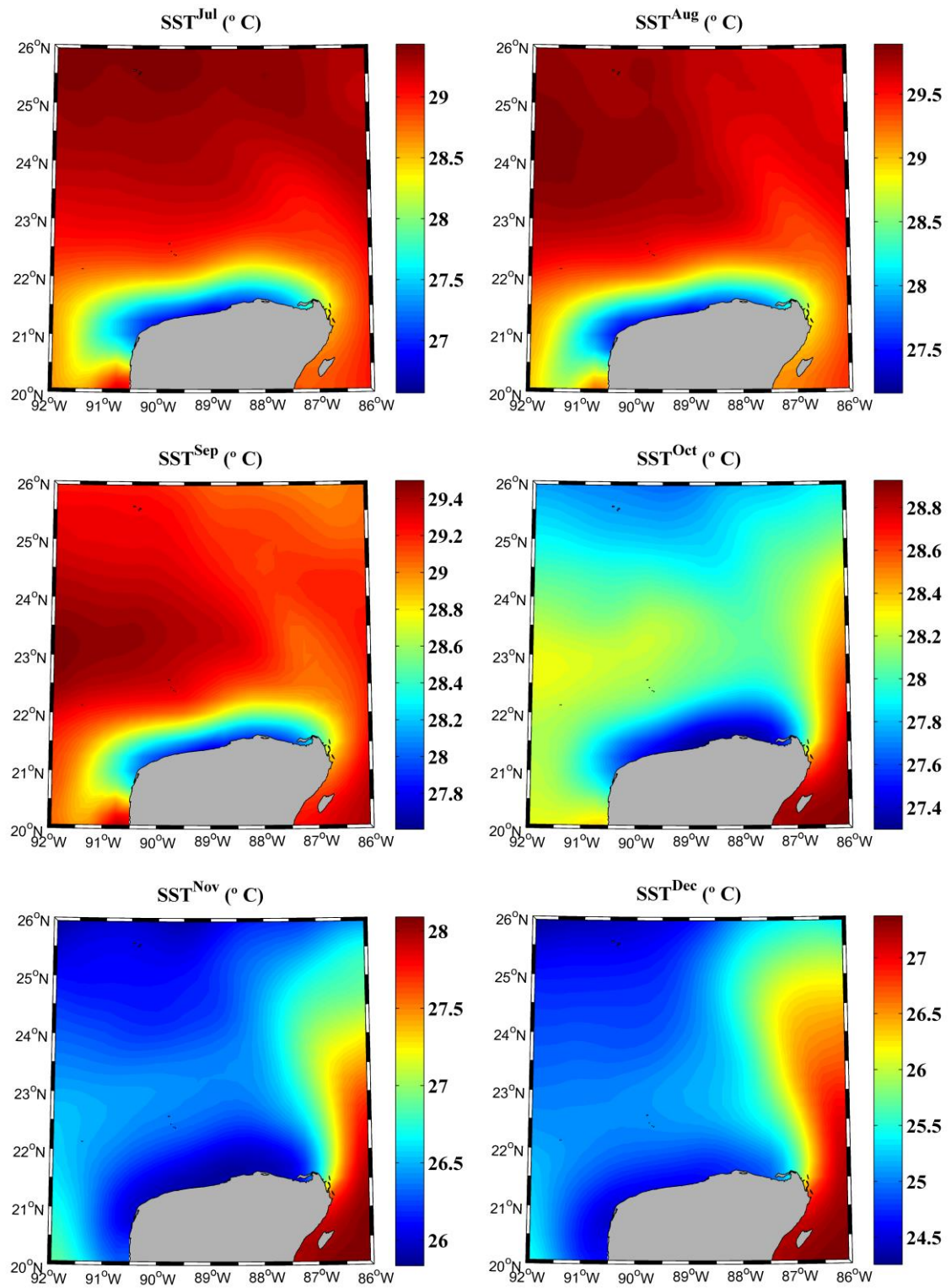


**Figure 2 | Monthly mean SST (°C) over the period 1982-2015 obtained from OISST<sup>1/4</sup> database.**

Differences between coastal and oceanic locations are represented in Figure 3. Points where SST was averaged to obtain coastal (black dots) and oceanic (black crosses) values are marked in Figure 1. Blue (red) line identifies the annual cycle of SST for coastal (oceanic) locations averaged meridionally. Oceanic SST shows higher values when compared with coastal locations. The lowest ocean temperatures are found from January to March (24°C) and the highest ones in August (up to 29.5°C). Similar results are observed near coast but the highest SST value was found in September (28°C). Although ocean SST is always higher than near coast, the greatest differences are found from May to September, ranging from around 1°C in May to near 2°C in August. Reyes-Mendoza et al., (2016), who analyzed the effects of wind on upwelling off Cabo Catoche, detected that upwelling was higher from March to September. These results are consistent with those obtained in Figure 2 and allow focusing the present study on May-September months, when the highest differences between coastal and oceanic SST were found.

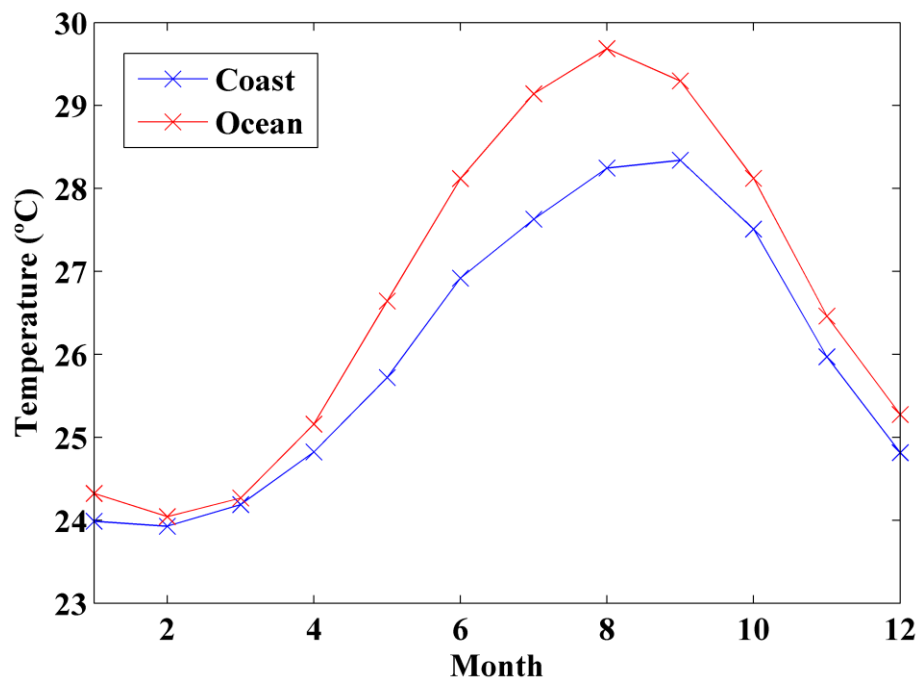


**Figure 3 | Annual cycle of SST (°C)** meridionally averaged at coastal (blue line) and ocean locations (red line) over the period 1982 to 2015 using OISST<sup>1/4</sup> database. Sampling points marked in Figure 1.

Figure 4 shows SST trends over the period May to September, when the difference between coast and ocean is more visible. An increasing pattern is obtained for ocean locations with values ranging from 0.1 to 0.2°C dec<sup>-1</sup>. A negative trend was observed at coastal locations (-0.1°C dec<sup>-1</sup>). Thus, the difference between coastal and oceanic rates is higher than 0.25°C dec<sup>-1</sup>. This behavior had also been observed in some of the major upwelling systems in the world. Santos et al., (2012b) found different rates between coast and ocean higher than 0.3°C dec<sup>-1</sup> in the Benguela Upwelling System from 1970 to 2009. In the case of Canary Upwelling System, Santos et al., (2012c) observed differences up to 0.1°C dec<sup>-1</sup> from 1982 to 2010. For the cases of Java or La Guajira, Varela et al., (2016) and Santos et al., (2016) found different rates between coast and ocean around 0.3°C dec<sup>-1</sup> respectively over the last three decades. A complete study of worldwide SST trends can be observed in Cheung et al., (2013).

Overall, the presence of cooling trends has been associated to the reinforcement of upwelling in some areas (Benguela, Canary, Peru) (Narayan et al., 2010, Patti et al., 2010, Rahn and Garreaud, 2013, Cropper et al., 2014). However, this behaviour has not been homogeneous among the worldwide upwelling systems showing, in some cases, a weakening in upwelling (Varela et al., 2015). To analyze the possible causes of these different warming rates, the upwelling index trend was calculated over the period 1982-2015 considering the spring-summer seasons (May-September) (Figure 5). Negative upwelling trends were obtained for the whole area with values between -0.055 m<sup>2</sup> s<sup>-1</sup> dec<sup>-1</sup> and -0.090 m<sup>2</sup> s<sup>-1</sup> dec<sup>-1</sup>. Thus, it is evident that the reinforcement of upwelling in

the area is not the main factor that drives cooling SST trends in the Northern coast of Yucatan.

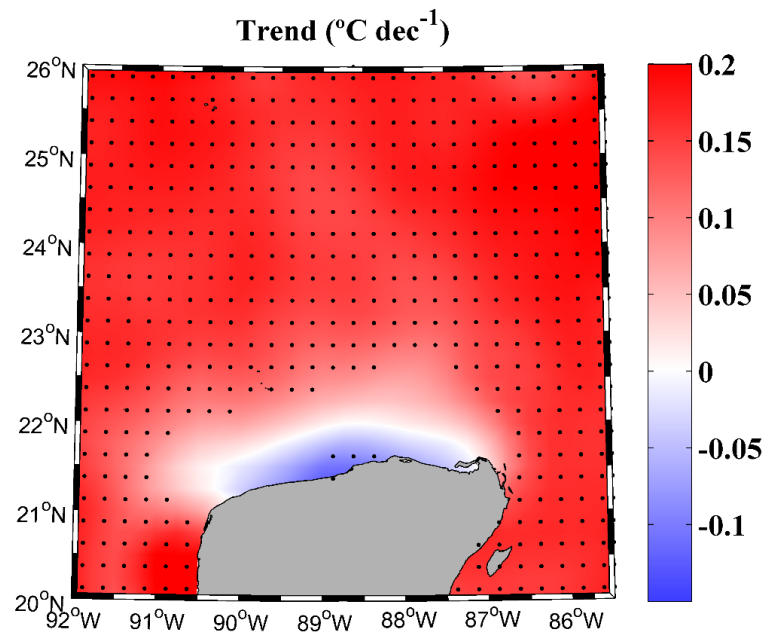


**Figure 4 | May-September SST trend ( $^{\circ}\text{C dec}^{-1}$ )** calculated over the period 1982-2015 using OISST<sup>1/4</sup> database.

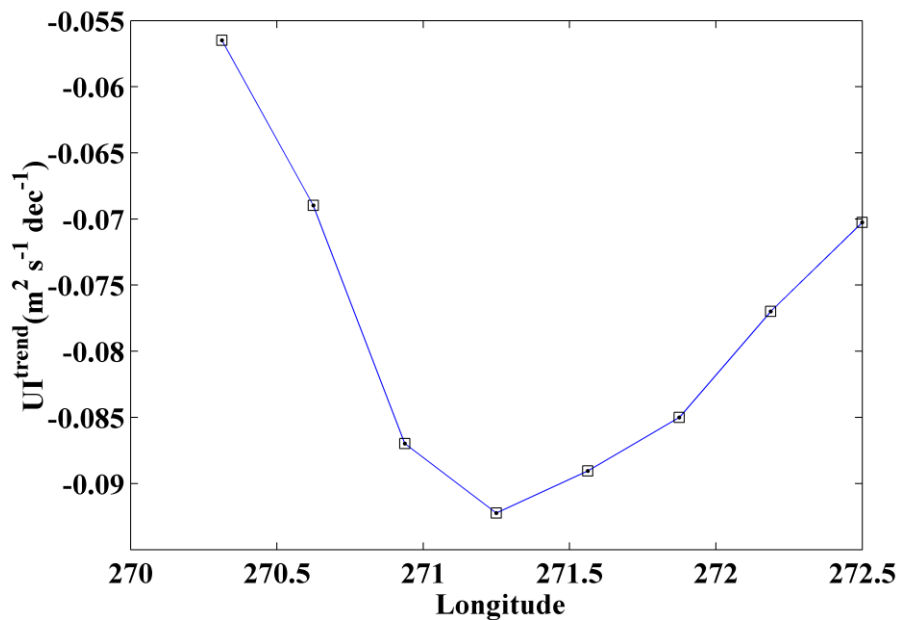


**Figure 5 | UI trend ( $\text{m}^2 \text{s}^{-1} \text{dec}^{-1}$ )** calculated over the period 1982 to 2015 averaged from May to September using CFSR database.

Once changes in upwelling have been dismissed as a driver in coastal cooling, variations in the total heat flux between atmosphere and sea were also calculated (Figure 6). Total heat flux trends show an increase for most of the area with values between 6–12  $\text{W m}^{-2} \text{dec}^{-1}$ , which means that ocean has gained heat during the last decades. Coastal and oceanic locations did not show any difference in heat exchange variability in the upwelling area so, heat exchange between atmosphere and ocean, should also be discarded as a key factor in the occurrence of near shore cooling.

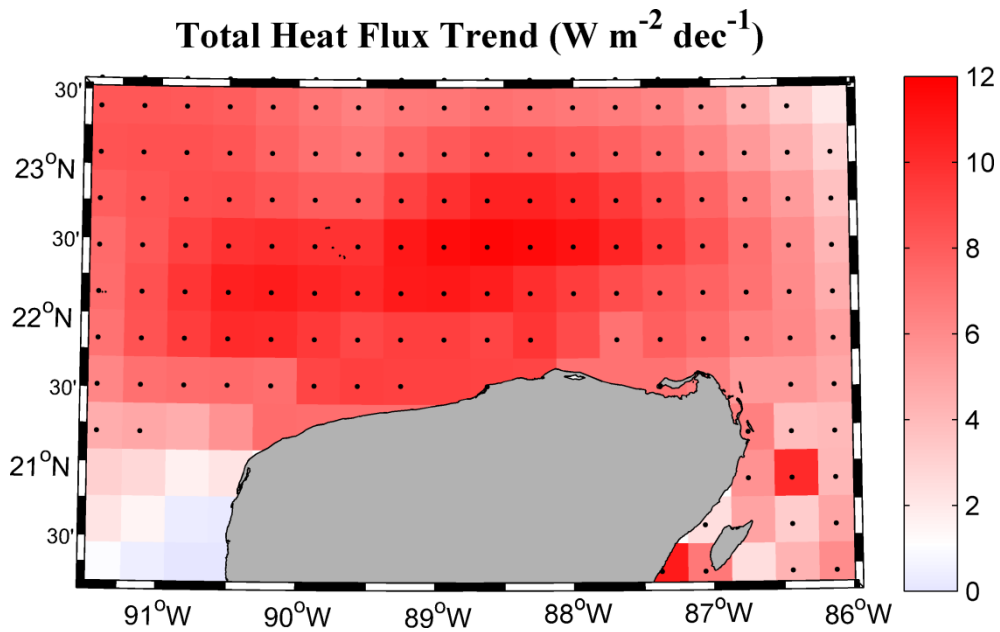


**Figure 6 | Heat flux trend ( $\text{W m}^{-2} \text{dec}^{-1}$ )** calculated over the period 1982–2015 (May–September). Black dots represent grid points with significance higher than 95%. A negative (positive) value implies that ocean is losing (gaining) heat.

As previously mentioned, the Yucatan Current can be one of the factors responsible of the SST variability detected along the North Yucatan coast because it conditions upwelling processes that bring water from the Caribbean Sea to the Yucatan Shelf (Merino, 1997; Zavala-Hidalgo et al., 2006; Carrillo et al., 2016; Souza et al., 2016). Different mechanisms have been suggested to explain the relation between the upwelled

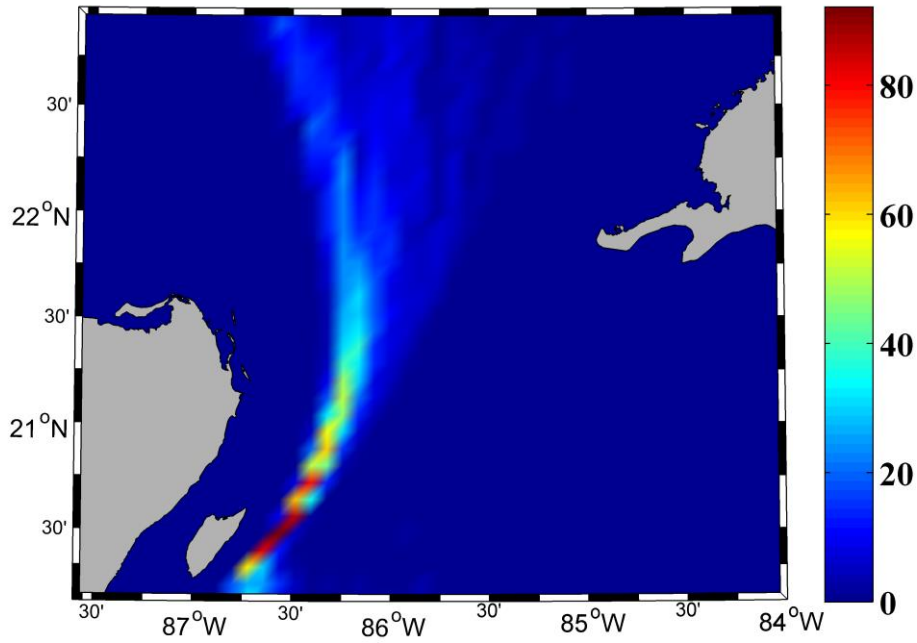
water and the YC. Cochrane, (1963, 1966) proposed that friction from the bottom layer with the YC generates a vertical Ekman transport, while Bulanienkov and García, (1973) suggested that the interaction between the YC and the undercurrent off Cuba originated the vertical transport. More recently, Enríquez and Mariño-Tapia, (2014) observed that the trajectory of the YC is important in the development of upwelling. Using a numerical model they proved that, when the YC is directed to the northeast, vertical velocities became positive along the continental slope favoring the appearance of colder water over the Yucatan Shelf. Thus, a northeast trajectory of the YC can lead to changes in the thermohaline properties of the sea water that extends towards the west along the Yucatan Shelf. In addition, Carrillo et al., (2016) observed through in-situ data collected in oceanographic cruises, that upwelling was stronger in the area north of 21°N when the YC separates from the coast. A similar phenomenon was previously described in the Agulhas Bank to explain upwelling (Lutjeharms et al., 2000). Souza et al., (2016) also hypothesized that the interaction between YC and topography could explain upwelling.

Therefore, it is crucial to analyze YC variability to know whether or not cooling along the north coast of Yucatan Peninsula can be related to changes in the YC trajectory. With this aim the following procedure was applied: a) The YC path along the eastern area of the Yucatan Peninsula was defined as the vein of maximum current velocity in the sub-surface (100m depth); b) the pixel with the maximum module velocity was selected for each latitude and for each month. Thus, for example, to detect where the core was at 20.25°N at a certain month all pixels corresponding to this latitude between 84-87°W were analyzed and the pixel with the maximum module velocity was considered as the location where the core of the YC flows at this particular month. A value of 1 was assigned to the selected pixel and 0 to the rest. This procedure was

repeated for each latitude (from 20.25°N to 23 °N) and for each month, considering only May-September months from 1993 to 2015. In this way, the summation of all images corresponding to each month show the most usual path (Figure 7a). Results are represented as the percentage of times that the maximum velocity was detected. Thus, a value of 70 means that the maximum current velocity at a particular latitude was found, at that pixel, 70% of the months. Figure 7a represents the most usual path where the YC core flows. This stream flows between 86°-87° W following the continental slope among 20-22° N (Figure 1). c) Once the path of the YC core was detected for each month, two periods (1993-2003 and 2005-2015) were compared to detect possible changes in the YC path. A composite of images was built for every period and the composite of the first period was subtracted from the one of the last period. Changes in the YC direction from 1993 to 2015 are shown in Figure 7b. Negative values (blue) denote the prevalent path during the first decade, while positive values (red) show the prevalent path during the last decade. Therefore, it was observed that YC has shifted to the east at 21-22° N. According to Enríquez and Mariño-Tapia, (2014), this shift should favor a greater vertical transport along the continental slope, which in turn, would cause thermohaline variations in the upwelled sea water. To confirm this fact, temperature variability was analyzed along the transect shown in Figure 1 (black solid line), which was selected following the procedure described above (see Figure 7a).



(a)



(b)

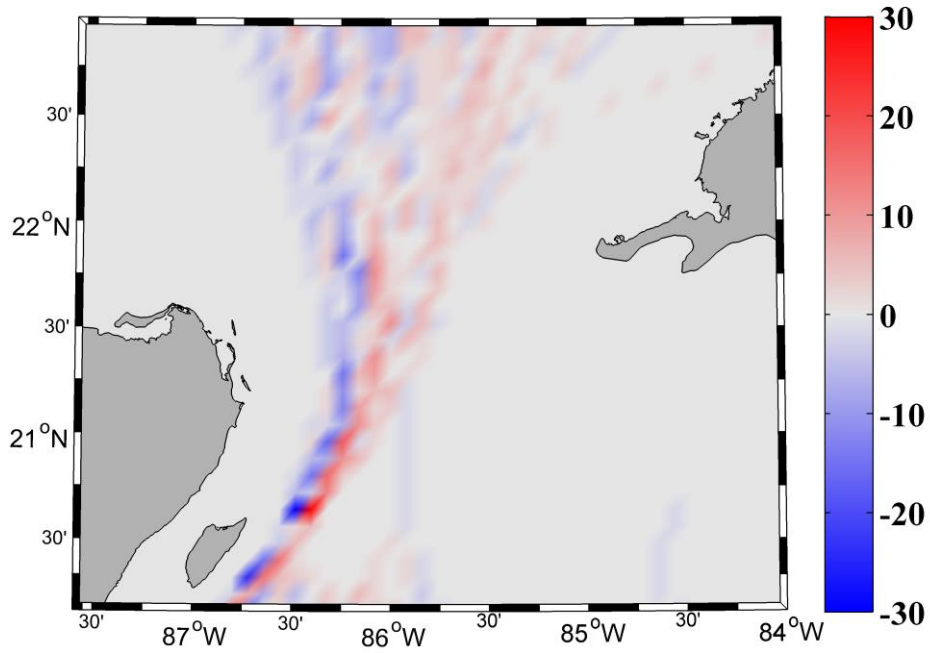


**Figure 7 | (a) Path followed by the Yucatan Current core averaged over the period 1993-2015 considering May-September months. (b) Evolution of the Yucatan Current path from 1993 to 2015 (May-September) using HYCOM database. Negative values (blue) denote the path of the YC in the first decade (1993-2003) and positive values (red) denote the path of the YC in the last decade (2005-2015).**

Thus, temperature trends for the upper 400m of the water column along that transect are represented in Figure 8 over the period 1993-2015 (May-September). The most remarkable feature is that cooling ( $\sim -0.3^{\circ}\text{C dec}^{-1}$ ) was observed between 50-200m only at the northern part of the studied transect. That area coincides with the location where the Caribbean Subtropical Underwater (CSUW) water mass upwells to the Yucatan shelf (Enríquez et al., 2013; Ramos-Musalem, 2013; Carrillo et al., 2016). This water mass has its core around 150m deep. Therefore it can be concluded that the sea water that upwells from Caribbean Sea and expands along the deepest layers of the Yucatan shelf has cooled over the period 1993-2015. This fact explains the contrast between cooling along the coast and warming in the oceanic area of the Yucatan shelf (Figure 4). The cold water that upwells at the Yucatan shelf occupies the bottom layers (Enríquez et al., 2013) and it only shows near surface at a narrow fringe near coast due to the upwelling caused by the prevalence of trade winds in the region.

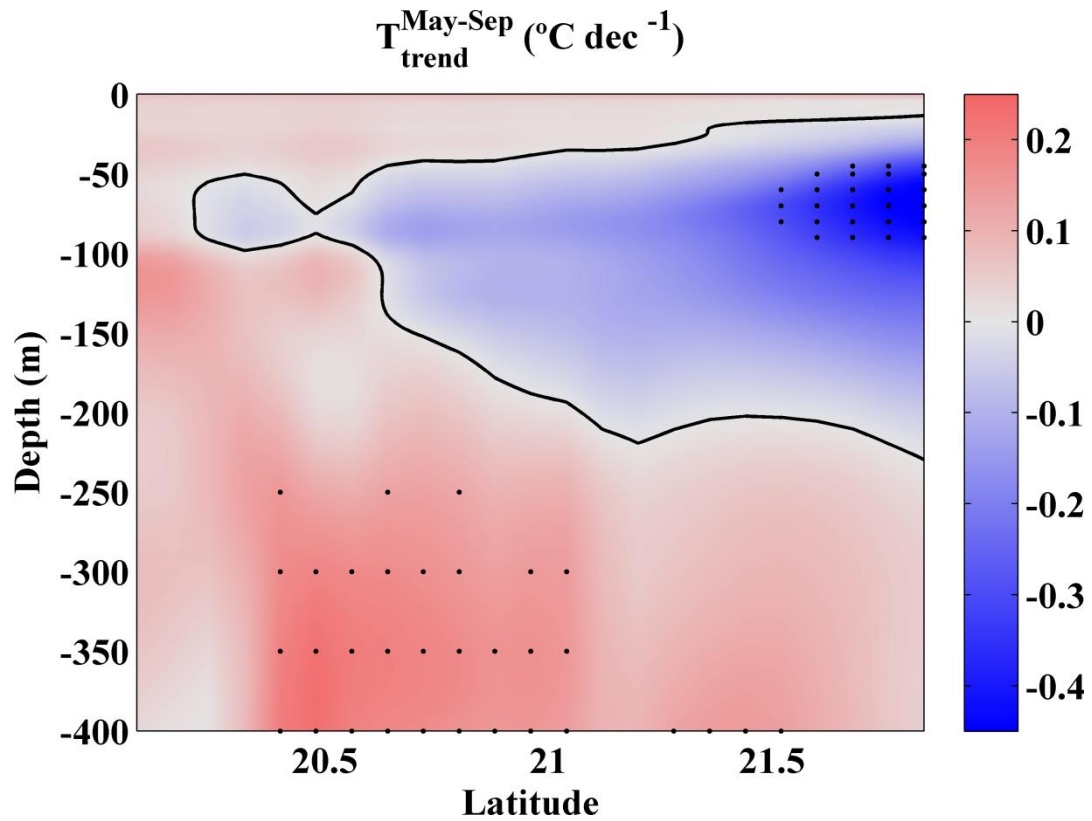


**Figure 8 | Temperature trend ( $^{\circ}\text{C dec}^{-1}$ )** calculated using HYCOM database over the period 1993-2015 for May-September months at the upper 400m of the water column (solid line in Figure 1). The contour line corresponds to the absence of trend.

Finally, the model proposed by Bindoff and McDougall, (1994) (see eq. (5)) was applied to analyze the cause of the changes detected in Figure 8. The model was applied to the northern half of the transect (north of  $21^{\circ}\text{N}$ ) since it is the area where significant cooling was observed. According to Figure 9, cooling was detected along isobars (red line) from 50m to 150m, in good agreement with Figure 8, with a maximum cooling rate ( $\sim -0.02^{\circ}\text{C y}^{-1}$ ) at  $\sim 75\text{m}$ . It can be observed that cooling is mainly due to vertical displacement of isopycnals (green line) in the upper part of the water column (50-100m), although a slight cooling was detected from 100m to 150m mainly due to changes in the intrinsic properties of the water (red line). Taking into account that temperature decreases with increasing depth, it can be concluded that the observed cooling was caused by the uplifting of isopycnals. This fact is consistent with previous research. Merino, (1997) observed the raise of isotherms and isohalines in the area. Ramos-Musalem, (2013) also found water uplift from 120m until less than 40m along the eastern part of the Yucatan Shelf.

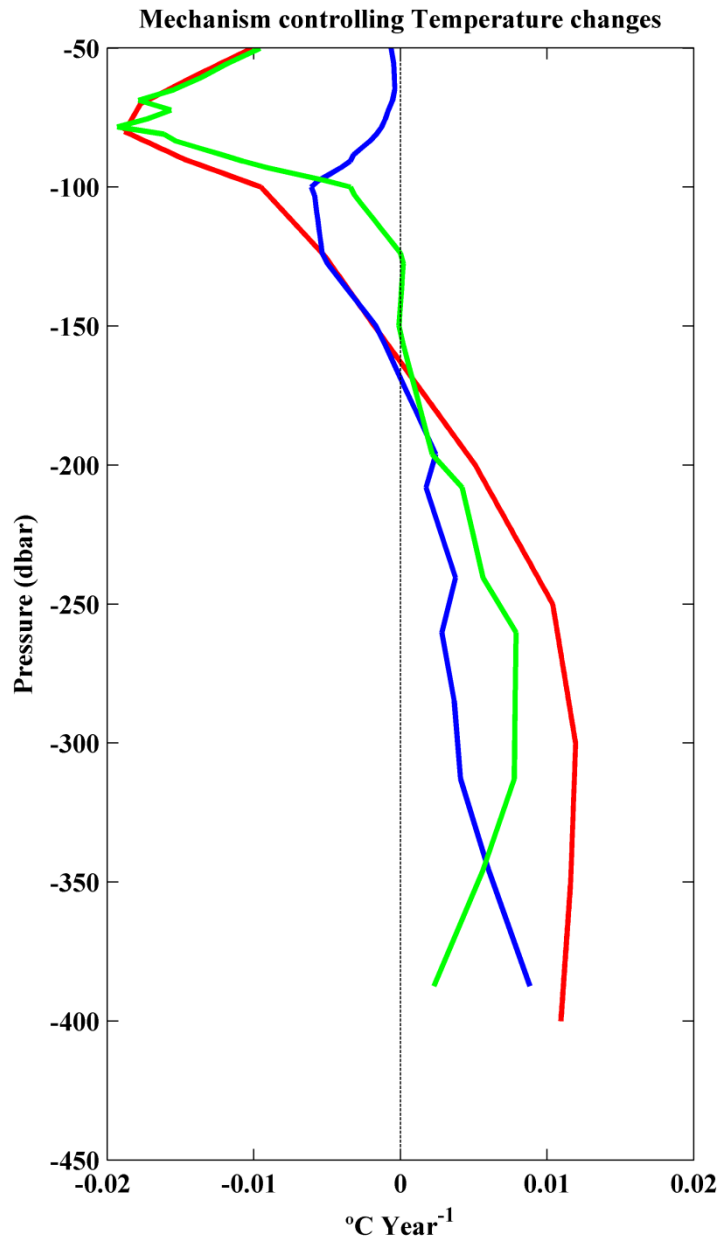


**Figure 9 | Decomposition of temperature changes** along isobars (red line) as the sum of changes along isopycnals (blue line) and changes due to vertical displacement of isopycnals (green line).

#### 4. Summary

Sea surface warming was detected at oceanic locations north of Yucatan Peninsula and cooling was observed at the coastal zone, especially over the period May-September.

Whilst the amplitude of ocean warming is similar to the amplitude found in most of the North Atlantic areas, coastal cooling constitutes a differential fact.

Analyzing near-shore thermal variability at the Yucatan shelf is a complex task since the area is under the influence of different drivers. Despite wind induced upwelling plays a key role in the area, the observed decrease in upwelling index is not consistent with coastal cooling. In a similar way, the sea-atmosphere heat exchange is homogeneous for the whole area, without differences between coast and ocean. Consequently, heat exchange should also be discarded as a possible reason for near-shore cooling.

On the other hand, the core of the Yucatan Current has experienced an eastward shift over the last decades. According to previous studies, this shift enhances vertical transport along the eastern part of the Yucatan shelf. Thus, a temperature decrease can be detected in the water mass that upwells at the Yucatan shelf. This cold water that occupies the deepest layers over the continental shelf is pumped by upwelling favorable westerly winds making the cold signal visible at sea surface near-shore.

### **Acknowledgment**

This research was partially supported by Xunta de Galicia under project GRC-2013-001 *Programa de Consolidación e Estructuración de Unidades de Investigación Competitivas (Grupos de Referencia Competitiva)* co-funded by European Regional Development Fund (FEDER). R. Varela is supported by the University of Vigo through the *Axudas predoutorais da convocatoria de axudas a investigación 2015*. X. Costoya is supported by the Portuguese Science Foundation (FCT) through a Post-doctoral grant (SFRH/BPD/118142/2016). CFSR data was obtained from Environmental Modeling Center/National Centers for Environmental Prediction/National Weather Service/NOAA/U.S. NCEP Climate Forecast System Reanalysis (CFSR) Monthly

Products. Research Data Archive at the National Center for Atmospheric Research, Computational and Information Systems Laboratory. <http://rda.ucar.edu/datasets/ds093.2/>. Funding for the development of HYCOM has been provided by the National Ocean Partnership Program and the Office of Naval Research. Data assimilative products using HYCOM are funded by the U.S. Navy. Computer time was made available by the DoD High Performance Computing Modernization Program. The output is publicly available at <http://hycom.org>.

## References

- 1- Levitus, S., Antonov, J. and Boyer, T. Warming of the world ocean, 1955–2003. *Geophysical Research Letters*, 2005, 32(2). DOI: 10.1126/science.287.5461.2225.
- 2- Mikaloff-Fletcher, S. E., Gruber, N., Jacobson, A. R., Doney, S. C., Dutkiewicz, S., Gerber, M., Follows, M., Joos, F., Lindsay, K., Menemenlis, D., Mouchet, A., Muller, S. A. and Sarmiento, J. L. Inverse estimates of anthropogenic CO<sub>2</sub> uptake, transport, and storage by the ocean. *Global Biogeochemical Cycles*, 2006, 20(2). DOI: 10.1029/2005GB002530.
- 3- Levitus, S., Antonov, J. I., Boyer, T. P., Baranova, O. K., Garcia, H. E., Locarnini, R. A., Mishonov, A. V., Reagan, J. R., Seidov, D., Yarosh, E. S. and Zweng, M. M. World ocean heat content and thermosteric sea level change (0–2000 m), 1955–2010. *Geophysical Research Letters*, 2012, 39(10). DOI: 10.1029/2012GL051106.
- 4- Pauly, D. and Christensen, V. Primary production required to sustain global fisheries. *Nature*, 1995, 374(6519), 255. DOI: 10.1038/376279b0.
- 5- Harrison, D. E. and Carson, M. Is the world ocean warming? Upper ocean trends, 1950–2000. *Journal of Physical Oceanography*; 2007, 37: 174–187. <https://doi.org/10.1175/JPO3005.1>

- 6-** Lima, F. P. and Wethey, D. S. Three decades of high-resolution coastal sea surface temperatures reveal more than warming. *Nature Communications*; 2012, 3: 704. DOI:10.1038/ncomms1713.
- 7-** Cheung, W. W. L., Watson, R. and Pauly, D. Signature of ocean warming in global fisheries catch, *Nature*, 2013, 497, 365- 369. DOI:10.1038/nature12156.
- 8-** Lemos, R. T. and Sansó, B. Spatio-temporal variability of ocean temperature in the Portugal Current System. *Journal of Geophysical Research*; 2006, 111: C04010. DOI: 10.1029/2005JC003051.
- 9-** Santos, F., Gómez-Gesteira, M., deCastro, M. and Álvarez, I. Variability of coastal and ocean water temperature in the upper 700 m along the Western Iberian Peninsula from 1975 to 2006. *PLoS One*; 2012a, 7(12): 1–7. <https://doi.org/10.1371/journal.pone.0050666>
- 10-** Santos, F., Gómez-Gesteira, M., deCastro, M. and Álvarez, I. Differences in coastal and oceanic SST trends due to the strengthening of coastal upwelling along the Benguela current system. *Continental Shelf Research*; 2012b, 34: 79–86. <https://doi.org/10.1016/j.csr.2011.12.004>
- 11-** Santos, F., Gómez-Gesteira, M., deCastro, M. and Álvarez, I. Differences in coastal and oceanic SST warming rates along the Canary Upwelling Ecosystem from 1982 to 2010. *Continental Shelf Research*; 2012c, 47: 1–6. <https://doi.org/10.1016/j.csr.2012.07.023>
- 12-** Santos, F., Gómez-Gesteira, M., Varela, R., Ruiz-Ochoa, M. and Días, J. M Influence of upwelling on SST trends in La Guajira system. *Journal of Geophysical Research: Oceans*, 2016, 121(4), 2469-2480. DOI: 10.1002/2015JC011420



- 13-** Varela, R., Santos, F., Gómez-Gesteira, M., Álvarez, I., Costoya, X. and Días, J. M. Influence of Coastal Upwelling on SST Trends along the South Coast of Java. *PloS one*, 2016, 11(9), e0162122. <https://doi.org/10.1371/journal.pone.0162122>
- 14-** Varela, R., Álvarez, I., Santos, F., deCastro, M. and Gómez-Gesteira, M. Has upwelling strengthened along worldwide coasts over 1982-2010? *Scientific reports*, 2015, 5. DOI:10.1038/srep10016
- 15-** Ruiz-Castillo, E., Gomez-Valdes, J., Sheinbaum, J. and Rioja-Nieto, R. Wind-driven coastal upwelling and westward circulation in the Yucatan shelf. *Continental Shelf Research*, 2016, 118, 63-76. <https://doi.org/10.1016/j.csr.2016.02.010>
- 16-** Merino, M. Upwelling on the Yucatan Shelf: hydrographic evidence. *Journal of Marine Systems*, 1997, 13(1-4), 101-121. [https://doi.org/10.1016/S0924-7963\(96\)00123-6](https://doi.org/10.1016/S0924-7963(96)00123-6)
- 17-** Pérez-Santos, I., Schneider, W., Sobarzo, M., Montoya-Sánchez, R., Valle-Levinson, A. and Garcés-Vargas, J. Surface wind variability and its implications for the Yucatan Basin-Caribbean Sea dynamics. *Journal of Geophysical Research*, 2010, 115. DOI: 10.1029/2010JC006292
- 18-** Enríquez, C., Marino-Tapia, I., Jerónimo, G. and Capurro-Filigrasso, L. Thermohaline processes in a tropical coastal zone. *Continental Shelf Research*, 2013, 69, 101-109. <https://doi.org/10.1016/j.csr.2013.08.018>
- 19-** Salmerón-García, O., Zavala-Hidalgo, J., Mateos-Jasso, A. and Romero-Centeno, R. Regionalization of the Gulf of Mexico from space-time chlorophyll-a concentration variability. *Ocean Dynamics*, 2011, 61(4), 439-448. <https://doi.org/10.1007/s10236-010-0368-1>
- 20-** Pérez-Santos, I., Schneider, W., Valle-Levinson, A., Garces-Vargas, J., Soto, I., Montoya-Sanchez, R. and Muller-Karger, F. Chlorophyll-a patterns and mixing

processes in the Yucatan Basin, Caribbean Sea. Patrones superficiales de la clorofila a y procesos de mezcla en la cuenca de Yucatán, mar Caribe. Ciencias Marinas, 2014, 40(1), 11-31. <http://dx.doi.org/10.7773/cm.v40i1.2320>

**21-** Cárdenas-Palomo, N., Herrera-Silveira, J., Velazquez-Abunader, I., Reyes-Mendoza, O. and Ordoñez, U. Distribution and feeding habitat characterization of whale sharks *Rhincodon typus* in a protected area in the north Caribbean Sea. Journal of Fish Biology, 2015, 86(2), 668-686. DOI: 10.1111/jfb.12589

**22-** Zavala-Hidalgo, J., Gallegos-García, A., Martínez-López, B., Morey, S. L and O'Brien, J. J. Seasonal upwelling on the western and southern shelves of the Gulf of Mexico. Ocean Dynamics, 2006, 56(3-4), 333-338. <https://doi.org/10.1007/s10236-006-0072-3>

**23-** del Monte-Luna, P., Villalobos, H. and Arreguín-Sánchez, F. Variability of sea surface temperature in the southwestern Gulf of Mexico. Continental Shelf Research, 2015, 102, 73-79. <https://doi.org/10.1016/j.csr.2015.04.017>

**24-** Enríquez, C. and Mariño-Tapia, I. Mechanisms driving a coastal dynamic upwelling. In Proceedings of the 17th Physics of Estuaries and Coastal Seas (PECS) Conference. 2014.

**25-** Reyes-Mendoza, O., Mariño-Tapia, I., Herrera-Silveira, J., Ruiz-Martínez, G., Enríquez, C. and Largier, J. L. The effects of wind on upwelling off Cabo Catoche. Journal of Coastal Research, 2016, 32(3), 638–650. <https://doi.org/10.2112/JCOASTRES-D-15-00043.1>

**26-** Souza, A. J., Mariño-Tapia, I. and J-M Hirschi, J. Mechanisms controlling upwelling on the Yucatan shelf; its interannual variability and predictability. In Abstract for the 18<sup>th</sup> Physics of Estuaries and Coastal Seas Conference. 2016.

- 27-** Carrillo, L., Johns, E. M., Smith, R. H., Lamkin, J. T. and Largier, J. L. Pathways and hydrography in the Mesoamerican Barrier Reef System Part 2: Water masses and thermohaline structure. *Continental Shelf Research*, 2016, 120, 41-58. <https://doi.org/10.1016/j.csr.2016.03.014>
- 28-** Reynolds, R. W. What's new in Version 2 [Available at [http://www.ncdc.noaa.gov/oa/climate/research/sst/papers/whats\\_new\\_v2.pdf](http://www.ncdc.noaa.gov/oa/climate/research/sst/papers/whats_new_v2.pdf).] 2009.
- 29-** Reynolds, R. W. and Chelton, D. W. Comparisons of daily sea surface temperature analysis for 2007–08. *Journal of Climate*; 2010, 23: 3545–3562. <https://doi.org/10.1175/2010JCLI3294.1>
- 30-** Cummings, J. A. Operational multivariate ocean data assimilation. *Quarterly Journal of the Royal Meteorological Society Part C.*, 2005, 131(613):3583-3604. DOI: 10.1256/qj.05.105
- 31-** Cummings, J. A. and Smedstad, O. M. Variational Data Assimilation for the Global Ocean. *Data Assimilation for Atmospheric, Oceanic and Hydrologic Applications vol. II*, chapter 13, 2013, 303-343. [https://doi.org/10.1007/978-3-642-35088-7\\_13](https://doi.org/10.1007/978-3-642-35088-7_13)
- 32-** Saha, S., Moorthi, S., Pan, H., Wu, X., Wang, J., Nadiga, S., Tripp, P., Kistler, R., Woollen, J., Behringer, D., Liu, H., Stokes, D., Grumbine, R., Gayno, G., Wang, J., Hou, Y., Chuang, H., Juang, H. H., Sela, J., Iredell, M., Treadon, R., Kleist, D., Van Delst, P., Keyser, D., Derber, J., Ek, M., Meng, J., Wei, H., Yang, R., Lord, S., Van Den Dool, H., Kumar, A., Wang, W., Long, C., Chelliah, M., Xue, Y., Huang, B., Schemm, J., Ebisuzaki, W., Lin, R., Xie, P., Chen, M., Zhou, S., Higgins, W., Zou, C., Liu, Q., Chen, Y., Han, Y., Cucurull, L., Reynolds, R. W., Rutledge, G. and Goldberg, M. The NCEP Climate Forecast System Reanalysis. *Bulletin of the American Meteorology Society*, 2010, 91: 1015–1057. <https://doi.org/10.1175/2010BAMS3001.1>

- 33-** Nykjaer, L. and Van Camp, L. Seasonal and interannual variability of coastal upwelling along northwest Africa and Portugal from 1981 to 1991. *Journal of Geophysical Research*; 1994, 99: 14,197–14,207. DOI: 10.1029/94JC00814
- 34-** Bindoff, N. L. and McDougall, T. J. Diagnosing climate change and ocean ventilation using hydrographic data. *Journal of Physical Oceanography*, 1994, 24, 1137–1152. [https://doi.org/10.1175/1520-0485\(1994\)024<1137:DCCAOV>2.0.CO;2](https://doi.org/10.1175/1520-0485(1994)024<1137:DCCAOV>2.0.CO;2)
- 35-** Jackett, D. R. and McDougall, T. J. A neutral density variable for the world's oceans. *Journal of Physical Oceanography*, 1997, 27, 237–263. [https://doi.org/10.1175/1520-0485\(1997\)027<0237:ANDVFT>2.0.CO;2](https://doi.org/10.1175/1520-0485(1997)027<0237:ANDVFT>2.0.CO;2)
- 36-** Arbic, B. K. and Owens, W. B. Climatic warming of the Atlantic intermediate waters. *Journal of Climate*, 2001, 14, 4091–4108. [https://doi.org/10.1175/1520-0442\(2001\)014<4091:CWOAIW>2.0.CO;2](https://doi.org/10.1175/1520-0442(2001)014<4091:CWOAIW>2.0.CO;2)
- 37-** Mendoza, V. M, Villanueva, E. E. and Adem, J. On the annual cycle of the sea surface temperature and the mixed layer depth in the Gulf of México. *Atmósfera*, 2005, 18(2), 127-148.
- 38-** Narayan, N., Paul, A., Mulitza, S. and Schulz, M. Trends in coastal upwelling intensity during the late 20th century. *Ocean Science*; 2010, 6: 815–823. DOI:10.5194/os-6-815-2010
- 39-** Patti, B., Guisande, C., Riveiro, I., Thejll, P., Cuttitta, A., Bonanno, A., Basilone, G., Buscaino, G. and Mazzola, S. Effect of atmospheric CO<sub>2</sub> and solar activity on wind regime and water column stability in the major global upwelling areas. *Estuarine, Coastal and Shelf Science*, 2010, 88(1), 45-52. <https://doi.org/10.1016/j.ecss.2010.03.004>

- 40-** Rahn, D. A. and Garreaud, R. D. A synoptic climatology of the near-surface wind along the west coast of South America. *International Journal of Climatology*, 2013, 34, 780-792. DOI: 10.1002/joc.3724
- 41-** Cropper, T. E, Hanna, E. and Bigg, G. R. Spatial and temporal seasonal trends in coastal upwelling off Northwest Africa, 1981–2012. *Deep-Sea Research*; 2014, 1(86): 94–111. <https://doi.org/10.1016/j.dsr.2014.01.007>
- 42-** Cochrane, J. D. Yucatan Current. Department of Oceanography and Meteorology, Texas A&M Univ. Ref., 1963, 63-18A, pp. 6-11
- 43-** Cochrane, J. D. The Yucatan Current, upwelling off northeastern Yucatan, and currents and waters of western equatorial Atlantic, *Oceanography of the Gulf of Mexico*. Progress Reports, 1966, TAMU Ref.\_66-23T, pp.14–32.
- 44-** Bulanienkov, S. K. and García, C. Influencia de los procesos atmosféricos en el afloramiento del banco de Campeche. *Revista de Investigación Pesquera*, 1973, 99-140.
- 45-** Lutjeharms, J. R. E., Cooper, J. and Roberts, M. Upwelling at the inshore edge of the Agulhas Current. *Continental Shelf Research*, 2000, 20(7), 737-761. [https://doi.org/10.1016/S0278-4343\(99\)00092-8](https://doi.org/10.1016/S0278-4343(99)00092-8)
- 46-** Ramos Musalem, A. K. Estudio numérico de los forzamientos que generan la surgencia de Yucatán (Bsc. Thesis). UNAM, Mexico, 2013, p. 77.



# Chapter 4

## *Discussion*

As it was previously mentioned in the introduction, the knowledge of upwelling evolution is a key factor in multiple sectors. This phenomenon has been extensively studied over the world with several papers published over the last decades analyzing the evolution of upwelling mainly in terms of wind-dependent variables (Patti et al., 2010; Narayan et al., 2010; García-Reyes and Largier, 2010; Pardo et al., 2011; Seo et al., 2012; Barton et al., 2013; Cropper et al., 2014; Sydeman et al., 2014). Thus, different variables as wind stress, wind speed, Ekman transport or Upwelling Index have been investigated mainly along the EBUS and several localized areas of strong upwelling events, providing valuable information about upwelling trends during the last period of strong climate change. Some of these published studies analysed upwelling evolution from annual averages, while others considered upwelling seasons (months under upwelling favourable winds). The analysis of different variables as well as the selection of different upwelling seasons, even over the same area, can make difficult to establish comparisons between the results from different works. In fact, Sydeman et al., (2014) compared several studies on upwelling-favorable winds along the major eastern boundary current systems published in the last decades based on time series ranging in duration from 17 to 61 years. They found a great heterogeneity in the results highlighting the dependence on the length of the time series and season and revealing contradictory results between observational data and model-data reanalysis. In addition, numerous available time series present a spatial resolution that is too coarse to accurately resolve conditions at the scale of coastal upwelling in intense and localized upwelling zones.

One of the main objectives of this thesis was to investigate temporal and spatial trends in the coastal upwelling regime worldwide using a single wind database (Climate Forecast System Reanalysis) with high spatial resolution ( $0.3^\circ$ ). The period under study was focused in the last three decades (1982-2010) to assess detailed estimation of upwelling trends over the recent period of strong global warming. Wind stress has been previously used in several papers as an indicator of upwelling. Bakun, (1990), analysed wind stress along the most important upwelling systems of the world from 1945 to 1985 finding a strengthening in upwelling and proposing the Bakun hypothesis. Since then, several studies have been conducted to investigate the Bakun hypothesis using wind stress from different databases over different upwelling regions (McGregor et al., 2007; Patti et al., 2010; Narayan et al., 2010; Cropper et al., 2014). The first part of this work



aims to go a step further in contributing to the knowledge of the upwelling evolution analysing wind stress over the worldwide coasts by a high spatial resolution database.

In this study, 3025 coastal points worldwide were analyzed to select the major upwelling regions and evaluate upwelling trends from 1982 to 2010. Ten upwelling systems were evaluated: Benguela, Canary, the southern Caribbean Sea, Chile, Peru, California (north and south), West Australia, Java, North Kenya, and Somalia–Oman. These systems were grouped together into several macroscopic zones, namely the eastern and western coasts of the Atlantic, Pacific, and Indian Oceans. No upwelling systems along the western Pacific Ocean were assessed. Alongshore wind stress was calculated over more than 600 points along this coast, and no region fulfilled the conditions required to be considered a coastal upwelling area.

Results obtained for different upwelling systems around the world illustrate that it is not possible to describe a homogenous behavior among them because trends change substantially, even in regions with similar oceanographic processes. Among the five major upwelling regions worldwide, increasing trends in upwelling were observed in the coastal areas of Benguela, Peru, Canary, and northern California, and the increases were statistically significant only for the two last systems. A general decrease in upwelling intensity was observed along the Chile, southern and central California, and central Somalia coasts, with significant values in all regions. Thus, no evidence for a general intensification of upwelling along these systems was observed.

The general trends found in this study were similar to those reported in studies in which wind stress data were used. It is important to note that controversial results were also obtained by different authors using the same variable and even the same period of time, which indicates a dependence of results on the database used. Different trends were also detected along the less studied upwelling regions. For example, significant decreasing trends were observed along the coast of Java and northern Kenya, whereas a tendency to an increase in upwelling-favorable winds was detected in western Australia.

This analysis covered the last three decades (1982–2010), which is the recent period of strongest global warming, thus it allowed detailed analysis of the influence of warming processes on upwelling trends. In fact, the general warming of ocean temperatures is also an important process to analyze coastal upwelling. In 2012, Lima and Wethey, (2012) reported that 71 % of the coast had been warming since the early 1980s, while 22% of the area had not been changing and 7% actually cooled significantly. The heterogeneity of warming has led to numerous regional studies (Mendelssohn and Schwing, 2002; Lemos and Pires, 2004; Qu et al., 2005; Gómez-Gesteira et al., 2008a,b; Demarcq, 2009; deCastro et al., 2009; Santos et al., 2011; Rao et al., 2011; Gutiérrez et al., 2011; Santos et al., 2012a,b; Chollett et al., 2012; Barton et al., 2013; IPCC, 2014; Santos et al., 2015; García-Reyes et al., 2015).

The second objective of this thesis intended to contribute to the study of SST trends over the worldwide coasts by determining warming rates in nearshore and offshore waters around the world, investigating whether differences between coastal and offshore locations were associated with upwelling regions. Thus, those areas under the effects of upwelling were compared with those unaffected to observe the influence of upwelling on the SST trends. SST data was obtained from the OISST  $\frac{1}{4}$  database for the last three decades of strong climate change (1982–2015).

Global analysis revealed that the great majority of coastal (87.1%) and offshore locations (92.0%) experienced warming over the last three decades, with temperatures rising more intensely at oceanic locations than at their coastal counterparts in 65.8% of the cases. Thus, although coastal temperatures are increasing, in 2/3 of the area the increase is slower than offshore. This difference is even more pronounced within upwelling regions, where more than 92% of the coastal locations have been warming slower than offshore locations. This contrasts with non-upwelling areas, where the percentage of coastal locations that have been warming less than their offshore equivalents is 58%. The fact that upwelling is highly variable in extension and intensity around the globe, may explain the heterogeneity in coastal warming rates previously reported in various studies (Belkin, 2009; Lima and Wetthey, 2012; Cheung et al., 2013) being probably a key factor buffering ocean warming.

To better analyze the influence of upwelling on the different rates of warming (or even cooling) between offshore and nearshore regions, localized studies are necessary to understand the particular conditions of each area. Thus, to complete the main objectives of this thesis three particular areas (La Guajira in Colombia, Java in the Eastern Indian Ocean and Yucatan in the South Gulf of Mexico) were considered to assess the influence of upwelling between warming rates at open ocean and coastal locations.

The evolution of the SST along La Guajira upwelling system showed that ocean trends were higher than  $0.2\text{ }^{\circ}\text{C dec}^{-1}$  during most of the year. A negative trend  $\sim -0.05\text{ }^{\circ}\text{C dec}^{-1}$  (no significant) was observed near coast for months under strong and well developed upwelling conditions (JFM). This contrasts with the significant positive trend observed at adjacent ocean locations. Despite their lack of significance, near shore trends prove that that region is affected by drivers different from the ones observed at open sea locations (e.g. coastal upwelling). In fact, this cooling was in good agreement with the upwelling increase observed in the region at a rate of  $0.04\text{ m}^2\text{ s}^{-1}\text{ dec}^{-1}$  during winter months.

Results obtained along the south coast of Java showed that ocean warming is significant and coastal warming negligible during the upwelling season (July to October). In addition, cooling is observed near shore and warming at the ocean during the central months of the upwelling season (August-September). Nevertheless, UI was observed to decrease in both cases. This behavior was different from the one observed at La Guajira upwelling system. To better understand this apparent contradiction, the role of heat exchange between ocean and atmosphere as well as the influence of advection processes were analyzed. Results suggested that heat exchange between ocean and atmosphere was not the forcing that drives the cooling pattern found in the upwelling area since no differences in heat exchange were detected between coastal and ocean locations. In this case, horizontal advection (cool water advected by the South Java Current (SJC)) and vertical entrainment due to upwelling, were the main forcings that drive cooling off Java. In spite of the moderate decrease in UI, the combination of both processes was still efficient to bring cooled water to the surface.

Finally, along the Yucatan upwelling system an increasing pattern in SST trends was obtained for ocean locations and a negative trend was observed at coastal locations. Negative upwelling trends were also obtained for the whole region suggesting that the reinforcement of upwelling in the area was not the main factor that drives cooling SST trends in the Northern coast of Yucatan. As along the south coast of Java, heat exchange between atmosphere and ocean was discarded as a key factor in the occurrence of near shore cooling due to coastal and oceanic locations did not show any difference in heat exchange variability in the upwelling area. The Yucatan Current was the main factor responsible of the SST variability detected along the North Yucatan coast because it conditions upwelling processes that bring water from the Caribbean Sea to the Yucatan Shelf.



# Chapter 5

## *Main conclusions*

In this chapter the main findings of all the research presented in this thesis are presented in an integrated approach. Thus, the main conclusions to be drawn from the previous work can be summarized as follows:

- Results obtained for different upwelling systems around the world illustrate that it is not possible to describe a homogenous behavior among them over the recent period of strongest global warming (1982-2010) because trends change substantially, even in regions with similar oceanographic processes. Among the five major upwelling regions worldwide, increasing trends in upwelling were observed in the coastal areas of Benguela, Peru, Canary, and northern California, and the increases were statistically significant only for the two last systems. A general decrease in upwelling intensity was observed along the Chile, southern and central California, and central Somalia coasts, with significant values in all regions. Thus, no evidence for a general intensification of upwelling along these systems was observed. Different trends were also detected along the less studied upwelling regions. For example, significant decreasing trends were observed along the coast of Java and northern Kenya, whereas a tendency to an increase in upwelling-favorable winds was detected in Western Australia. In the southern Caribbean upwelling region, a significant negative (positive) trend was found east (west) of  $71.25^{\circ}\text{W}$ .
- Positive SST trends (warming) were observed at most oceanic (92%) and coastal locations (~87%). These percentages were similar in all oceanic basins, except for the Eastern Pacific Ocean where they were considerably lower. This pattern is even more pronounced within upwelling regions, where more than 92% of the coastal locations have been warming less than their respective offshore locations. This contrasts with non-upwelling areas, where the percentage of coastal locations that have been warming less than their offshore equivalents is 58%. Although these results are already impressive, real differences are expected to be even more pronounced, given recent studies demonstrating that most remotely-sensed SST products largely overestimate coastal temperatures in areas dominated by upwelling.
- Within a context of climate change with a general upward trend in terms of SST, La Guajira upwelling system has shown a different behavior over the last three decades with a moderate cooling ( $-0.05^{\circ}\text{C dec}^{-1}$ ) for the months with strong upwelling (JFM). This cooling was in good agreement with the upwelling

increase observed in the region at a rate of  $0.04 \text{ m}^2 \text{ s}^{-1} \text{ dec}^{-1}$  during winter months, although the position of the peaks in upwelling and SST trends did not coincide exactly, which was probably due to the presence of the Caribbean Coastal Undercurrent.

- Along the south coast of Java a small coastal warming was detected over the upwelling season (July-October) with a moderate decrease in UI. The analysis of the heat exchange between ocean and atmosphere showed that this forcing was not the responsible of the cooling trend found in the upwelling area. The origin of coastal cooling was due to changes in the vertical structure of the water column showing that subsurface layers have experienced a cooling trend over the last three decades. A vein of subsurface water, which has cooled at a rate higher than  $-0.3^\circ\text{C}$  per decade, was observed to enter from the northwestern part of the study area following the South Java Current. This water only manifests at surface near coast, where it is pumped up by coastal upwelling. Thus, although UI presented a negative trend, it can still pump cooled water to the surface.
- Sea surface warming was detected at oceanic locations north of Yucatan Peninsula and cooling was observed at the coastal zone, especially over the period May-September. Analyzing near-shore thermal variability at the Yucatan shelf was a complex task since the area is under the influence of different drivers. Despite wind induced upwelling plays a key role in the area, the observed decrease in upwelling index was not consistent with coastal cooling. In a similar way, the sea-atmosphere heat exchange was homogeneous for the whole area, without differences between coast and ocean. On the other hand the core of the Yucatan Current has experienced an eastward shift over the last decades. According to previous studies, this shift enhances vertical transport along the eastern part of the Yucatan shelf. Thus, a temperature decrease can be detected in the water mass that upwells at the Yucatan shelf. This cold water, that occupies the deepest layers over the continental shelf, is pumped by upwelling favorable westerly winds making the cold signal visible at sea surface near-shore.
- Trends shown in this work confirm the interest of studying local areas where upwelling is an important forcing, taking advantage of the high spatial resolution of databases to resolve conditions at the scale of coastal upwelling. The obtained results also showed the interest of analyzing the properties of subsurface water masses, especially in areas where they can be brought to surface by upwelling.



## Acronym and abbreviation list

- **AVHRR:** Advanced Very High Resolution Radiometer
- **CaRD10:** California Reanalysis Downscaling
- **CCMP:** Cross-Calibrated Multi-Platform
- **CCU:** Caribbean Coastal Undercurrent
- **CFSR:** Climate Forecast System Reanalysis
- **CLLJ:** Caribbean Low-Level Jet
- **COADS:** Comprehensive Ocean-Atmosphere Data Set
- **CSUW:** Caribbean Subtropical Underwater
- **DOE:** Department Of Energy
- **EBCS:** Eastern Boundary Current Systems
- **EBUS:** Eastern Boundary Upwelling Systems
- **ERA:** European ReAnalysis
- **ECMWF:** European Center for Medium range Weather Forecasting
- **ENSO:** El Niño Southern Oscillation
- **ET:** Ekman Transport
- **HAdSST3:** Hadley Centre SST
- **HYCOM:** HYbrid Coordinate Ocean Model
- **ICES:** International Council for the Exploration of the Sea
- **IPCC:** Intergovernmental Panel on Climate Change
- **IPSL-CM4:** Institut Pierre Simon Laplace Climate Model
- **LC:** Leewin Current
- **MERRA:** Modern-Era Retrospective analysis for Research and Applications
- **NASA:** National Aeronautics and Space Administration



- **NCAR:** National Center for Atmospheric Research
- **NCEP:** National Center for Environmental Prediction
- **NCODA:** Navy Coupled Ocean Data Assimilation
- **NDBC:** National Data Buoy Center
- **NOAA:** National Oceanic and Atmospheric Administration
- **NRL:** U.S. Naval Research Laboratory
- **OISST  $\frac{1}{4}$ :** Optimum Interpolation Sea Surface Temperature
- **PFEL:** Pacific Fisheries Environmental Laboratory
- **PRECIS:** Providing Regional Climate for Impact Studies
- **QuikSCAT:** Quik SCATterometer
- **SJC:** South Java Current
- **SODA:** Simple Ocean Data Assimilation
- **SST:** Sea Surface Temperature
- **UI:** Upwelling Index
- **WASWind:** Wave and Anemometer-based Sea Surface Wind
- **WSp:** Wind Speed
- **WSt:** Wind Stress
- **XBTs:** EXpendable BaThythermograph
- **YC:** Yucatan Current



# List of figures

## Chapter 1: Introduction

<b>Figure 1:</b> Scheme of the interaction between wind and oceanic water that causes upwelling. Source: NC State University Education .....	1
<b>Figure 2:</b> Relation between fish catches and the area of the ocean during the period 1970-2006. Source: Adaptation of the Figure 30-1 from IPCC, (2014) .....	2
<b>Figure 3:</b> Situation of the Eastern Boundary Upwelling Systems (EBUS) .....	2
<b>Figure 4:</b> Warming rates for the period between 1982 and 2010, expressed in °C per decade. Red indicates warming and blue indicates cooling. Source: Lima and Wethey, (2012) .....	5
<b>Figure 5:</b> Potential impacts of changes in upwelling over the biodiversity. Source: Lluch-Cota et al., (2014).....	6
<b>Figure 6:</b> Taylor diagrams for wind speed for the comparison of buoy wind data and different wind products in four different locations. Source: Álvarez et al., (2014) .....	7

## Chapter 3.1: “Has upwelling strengthened along worldwide coasts over 1982-2010?”

<b>Figure 1:</b> Wind stress along the Eastern Atlantic Ocean. Annual cycle of alongshore wind stress ( $\text{Nm}^{-2}$ ) for the period 1982–2010. Red points on the map show the coastal points studied. Black lines indicate those regions considered to be coastal upwelling areas. This figure has been performed using Matlab.....	17
<b>Figure 2:</b> Upwelling trends in the selected areas along the Eastern Atlantic Ocean. (a) Alongshore wind stress trends along the southern Benguela coast calculated from September to March. (b) Alongshore wind stress trends along the northern Benguela coast calculated from July to November. (c) Alongshore wind stress trends along the Canary coast calculated from April to September. Those points with significance greater than 90% are marked with a circle, and those greater than 95% are marked with a square. A negative (positive) trend means a decrease (increase) in upwelling-favourable winds. This figure has been performed using Matlab .....	18
<b>Figure 3:</b> Wind stress along the Western Atlantic Ocean. Annual cycle of alongshore wind stress ( $\text{Nm}^{-2}$ ) for the period 1982–2010. Red points on the map show the coastal	

points analysed. Black lines indicate those regions considered to be coastal upwelling areas. This figure has been performed using Matlab ..... 18

**Figure 4:** Upwelling trends in the selected areas along the Western Atlantic Ocean. Alongshore wind stress trends in the southern Caribbean Sea calculated from December to April. Those points with significance greater than 90% are marked with a circle, and those greater than 95% are marked with a square. A negative (positive) trend means a decrease (increase) in upwelling-favourable winds. This figure has been performed using Matlab ..... 20

**Figure 5:** Wind stress along the Eastern Pacific Ocean. Annual cycle of alongshore wind stress ( $\text{Nm}^{-2}$ ) for the period 1982–2010. Red points on the map show the coastal points analysed. Black lines indicate those regions considered to be coastal upwelling areas. This figure has been performed using Matlab ..... 20

**Figure 6:** Upwelling trends in the selected areas along the Eastern Pacific Ocean. (a) Alongshore wind stress trends along the Chile coast calculated from October to April. (b) Alongshore wind stress trends along the Peru coast calculated from May to October. (c) Alongshore wind stress trends along the southern California coast calculated from April to September. (d) Alongshore wind stress trends along the northern California coast calculated from April to October. Those points with significance greater than 90% are marked with a circle, and those greater than 95% are marked with a square. A negative (positive) trend means a decrease (increase) in upwelling-favourable winds. This figure has been performed using Matlab ..... 21

**Figure 7:** Wind stress along the Eastern Indian Ocean. Annual cycle of alongshore wind stress ( $\text{Nm}^{-2}$ ) for the period 1982–2010. Red points on the map show the coastal points analysed. Black lines indicate those regions considered to be coastal upwelling areas. This figure has been performed using Matlab ..... 23

**Figure 8:** Upwelling trends in the selected areas along the Eastern Indian Ocean. (a) Alongshore wind stress trends along the Western Australia coast calculated from October to March. (b) Alongshore wind stress trends along the Java coast calculated from May to October. Those points with significance greater than 90% are marked with a circle, and those greater than 95% are marked with a square. A negative (positive) trend means a decrease (increase) in upwelling-favourable winds. This figure has been performed using Matlab ..... 23

**Figure 9:** Wind stress along the Western Indian Ocean. Annual cycle of alongshore wind stress ( $\text{Nm}^{-2}$ ) for the period 1982–2010. Red points on the map show the coastal points analysed. Black lines indicate those regions considered to be coastal upwelling areas. This figure has been performed using Matlab ..... 24

**Figure 10:** Upwelling trends in the selected areas along the Western Indian Ocean. (a) Alongshore wind stress trends along the Northern Kenya coast calculated from November to April. (b) Alongshore wind stress trends along the Somalia-Oman coast calculated from April to October. Those points with significance greater than 90% are

marked with a circle, and those greater than 95% are marked with a square. A negative (positive) trend means a decrease (increase) in upwelling-favourable winds. This figure has been performed using Matlab..... 24

## Chapter 3.2: “Coastal warming and wind-driven upwelling: a global analysis”

**Figure 1:** Worldwide coast-offshore differences in warming trends. Red (blue) indicates that nearshore waters SSTs are warmer (colder) than their respective offshore waters. Twenty upwelling areas were considered: SB (South Benguela), NB (North Benguela), CI (Canary Islands), IP (Iberian Peninsula), BR (Brazil), SC (South Caribbean), YU (Yucatan), CH (Chile), PE (Peru), CA (California), EA (East Australia), SA (South Australia), WA (West Australia), J-S (Java - Sumatra), EI (East India), AG (Agulhas), KE (Kenya), SO (Somalia), OM (Oman) and WI (West India) ..... 37

**Figure 2:** SST trends along the Eastern Atlantic Ocean. From left to right: (a) coast-offshore differences in warming trends. Red (blue) indicates that nearshore waters SSTs are warmer (colder) than their respective offshore waters; dashed rectangles circumscribe the upwelling areas of Iberian Peninsula (A), Canary Islands (B), North Benguela (C) and South Benguela (D). (b) Oceanic and (c) coastal SST trends ( $^{\circ}\text{C dec}^{-1}$ ) and (d) their differences. Dashed grey areas identify points in upwelling zones ..... 40

**Figure 3:** SST trends along the Western Atlantic Ocean. From left to right: (a) coast-offshore differences in warming trends. Red (blue) indicates that nearshore waters SSTs are warmer (colder) than their respective offshore waters; dashed rectangles circumscribe the upwelling areas of Yucatan (A), South Caribbean (B), and Brazil (C). (b) Oceanic and (c) coastal SST trends ( $^{\circ}\text{C dec}^{-1}$ ) and (d) their differences. Dashed grey areas identify points in upwelling zones ..... 42

**Figure 4:** SST trends along the Eastern Pacific Ocean. From left to right: (a) coast-offshore differences in warming trends. Red (blue) indicates that nearshore waters SSTs are warmer (colder) than their respective offshore waters; dashed rectangles circumscribe the upwelling areas of North (A) and South California (B) and the Chile-Peru system (C). (b) Oceanic and (c) coastal SST trends ( $^{\circ}\text{C dec}^{-1}$ ) and (d) their differences. Dashed grey areas identify points in upwelling zones ..... 44

**Figure 5:** SST trends along the Western Pacific Ocean (islands). From left to right: (a) coast-offshore differences in warming trends. Red (blue) indicates that nearshore waters SSTs are warmer (colder) than their respective offshore waters; dashed rectangles circumscribe the upwelling areas of East Australia (A). (b) Oceanic and (c) coastal SST trends ( $^{\circ}\text{C dec}^{-1}$ ) and (d) their differences. Dashed grey areas identify points in upwelling zones ..... 45

- Figure 6:** SST trends along the Western Pacific Ocean. From left to right: (a) coast-offshore differences in warming trends. Red (blue) indicates that nearshore waters SSTs are warmer (colder) than their respective offshore waters. (b) Oceanic and (c) coastal SST trends ( $^{\circ}\text{C dec}^{-1}$ ) and (d) their differences. Dashed grey areas identify points in upwelling zones ..... 47
- Figure 7:** SST trends along the Eastern Indian Ocean. From left to right: (a) coast-offshore differences in warming trends. Red (blue) indicates that nearshore waters SSTs are warmer (colder) than their respective offshore waters; dashed rectangles circumscribe the upwelling areas of East India (A), Java-Sumatra (B), West (C) and South Australia (D). (b) Oceanic and (c) coastal SST trends ( $^{\circ}\text{C dec}^{-1}$ ) and (d) their differences. Dashed grey areas identify points in upwelling zones..... 48
- Figure 8:** SST trends along the Western Indian Ocean. From left to right: (a) coast-offshore differences in warming trends. Red (blue) indicates that nearshore waters SSTs are warmer (colder) than their respective offshore waters; dashed rectangles circumscribe the upwelling areas of West India (A), Oman (B), Kenya and Somalia (C) and Agulhas (D). (b) Oceanic and (c) coastal SST trends ( $^{\circ}\text{C dec}^{-1}$ ) and (d) their differences. Dashed grey areas identify points in upwelling zones..... 50

### Chapter 3.3: “Influence of upwelling on SST Trends in La Guajira system”

- Figure 1:** Bathymetry of the area under study. Circles mark points where wind and SST data from CFSR and OI1/4 were sampled..... 63
- Figure 2:** Mean monthly SST ( $^{\circ}\text{C}$ ) calculated over the period 1982 to 2014 using OI1/4 database ..... 64-65
- Figure 3:** Mean monthly Ekman Transport ( $\text{m}^2 \text{s}^{-1}$ ) calculated over the period 1982-2014 using CFSR database ..... 66-67
- Figure 4:** Mean (a) SST ( $^{\circ}\text{C}$ ) and (b) UI ( $\text{m}^2 \text{s}^{-1}$ ) calculated along the coast, for the months of highest upwelling (JFM) ..... 68
- Figure 5:** Monthly SST trend ( $^{\circ}\text{C dec}^{-1}$ ) calculate over the period 1982-2014 using OI1/4 database. Black dots correspond to trends with significance  $p\text{-value} < 0.05$ .. 69-70
- Figure 6:** Trends in (a) SST ( $^{\circ}\text{C dec}^{-1}$ ) and in (b) UI ( $\text{m}^2 \text{s}^{-1} \text{dec}^{-1}$ ) along the coast of La Guajira upwelling system over the months JFM. Black squares (circles) mark trends with significance higher than 95% (90%) ..... 71

## Chapter 3.4: “Influence of Coastal Upwelling on SST Trends along the South Coast of Java”

**Figure 1:** Mean temperature ( $^{\circ}\text{C}$ ) calculated from 1982 to 2015 for the upwelling season (July to October) using OISST  $\frac{1}{4}$  database. Circles and crosses mark points where wind and SST data from CFSR and OISST  $\frac{1}{4}$  were considered ..... 77

**Figure 2:** (a) Annual cycle of SST ( $^{\circ}\text{C}$ ) along the coast of Java (Fig. 1 circles) calculated for the period 1982 to 2015 using OISST  $\frac{1}{4}$  database; (b) Annual cycle of UI ( $\text{m}^2 \text{s}^{-1}$ ) along the coast of Java (Fig. 1 circles) calculated for the period 1982 to 2015 using CFSR database ..... 79

**Figure 3:** (a) Annual cycle of SST ( $^{\circ}\text{C}$ ) meridionally averaged along the coastal (blue line) and ocean locations (red line) for the period 1982 to 2015 using OISST  $\frac{1}{4}$  database. (b-d) Monthly SST trends ( $^{\circ}\text{C} \text{dec}^{-1}$ ) calculated for the period 1982 to 2015 from July to October using OISST  $\frac{1}{4}$  database ..... 80

**Figure 4:** (a) SST mean ( $^{\circ}\text{C}$ ) along the coastal (blue line) and ocean locations (red line) from July to October for the period 1982 to 2015 using OISST  $\frac{1}{4}$  database. (b) SST trends ( $^{\circ}\text{C} \text{dec}^{-1}$ ) along the coastal (blue line) and ocean locations (red line) from July to October for the period 1982 to 2015 using OISST  $\frac{1}{4}$  database. (c) SST mean ( $^{\circ}\text{C}$ ) along the coastal (blue line) and ocean locations (red line) from August to September for the period 1982 to 2015 using OISST  $\frac{1}{4}$  database. (d) SST trends ( $^{\circ}\text{C} \text{dec}^{-1}$ ) along the coastal (blue line) and ocean locations (red line) from August to September for the period 1982 to 2015 using OISST  $\frac{1}{4}$  database. Those points with significance greater than 90% are marked with a circle and those with significance greater than 95% are marked with a square ..... 81

**Figure 5:** Rate of change of UI (%) along the coastal locations (Fig. 1 circles) calculated for the period 1982 to 2015 using CFSR database. Blue line corresponds to July-October and red line to August-September ..... 82

**Figure 6:** (a) Heat flux mean ( $\text{W m}^{-2}$ ) and (b) trend ( $\text{W m}^{-2} \text{dec}^{-1}$ ) calculated over the period 1982–2015 (July-October). Black dots represent grid points with significance higher than 95%. A negative (positive) value implies that ocean is losing (gaining) heat ..... 83

**Figure 7:** Temperature trend ( $^{\circ}\text{C} \text{dec}^{-1}$ ) calculated for the period 1982 to 2010 from July to October at different layers around the south coast of Java using SODA database .... 84

**Figure 8:** Temperature trend ( $^{\circ}\text{C} \text{dec}^{-1}$ ) calculated for the period 1982 to 2010 from July to October near coast (blue line) and at the ocean (red line) along the longitude  $110^{\circ}\text{E}$  using SODA database ..... 85

## Chapter 3.5: “Differences in coastal and oceanic SST trends north of Yucatan Peninsula”

<b>Figure 1:</b> Bathymetry of the area under study. Dots (crosses) mark the coastal (oceanic) location where wind and SST were obtained. The solid line represents the transect where temperature variability was analyzed .....	94
<b>Figure 2:</b> Monthly mean SST ( $^{\circ}\text{C}$ ) over the period 1982-2015 obtained from OISST <sup>1/4</sup> database .....	100-101
<b>Figure 3:</b> Annual cycle of SST ( $^{\circ}\text{C}$ ) meridionally averaged at coastal (blue line) and ocean locations (red line) over the period 1982 to 2015 using OISST <sup>1/4</sup> database. Sampling points marked in Figure 1 .....	102
<b>Figure 4:</b> May-September SST trend ( $^{\circ}\text{C dec}^{-1}$ ) calculated over the period 1982-2015 using OISST <sup>1/4</sup> database .....	104
<b>Figure 5:</b> UI trend ( $\text{m}^2 \text{s}^{-1} \text{dec}^{-1}$ ) calculated over the period 1982 to 2015 averaged from May to September using CFSR database .....	104
<b>Figure 6:</b> Heat flux trend ( $\text{W m}^{-2} \text{dec}^{-1}$ ) calculated over the period 1982–2015 (May-September). Black dots represent grid points with significance higher than 95%. A negative (positive) value implies that ocean is losing (gaining) heat.....	105
<b>Figure 7:</b> (a) Path followed by the Yucatan Current core averaged over the period 1993-2015 considering May-September months. (b) Evolution of the Yucatan Current path from 1993 to 2015 (May-September) using HYCOM database. Negative values (blue) denote the path of the YC in the first decade (1993-2003) and positive values (red) denote the path of the YC in the last decade (2005-2015) .....	108
<b>Figure 8:</b> Temperature trend ( $^{\circ}\text{C dec}^{-1}$ ) calculated using HYCOM database over the period 1993-2015 for May-September months at the upper 400m of the water column (solid line in Figure 1). The contour line corresponds to the absence of trend .....	109
<b>Figure 9:</b> Decomposition of temperature changes along isobars (red line) as the sum of changes along isopycnals (blue line) and changes due to vertical displacement of isopycnals (green line).....	111





# List of tables

## Chapter 1: Introduction

<b>Table 1:</b> Databases used in the present thesis. Temporal resolution is related to the periods used in the studies.....	8
--	---

## Chapter 3: Set of publications

<b>Table 1:</b> Resume of the particular characteristics of the journals where were published the papers of this thesis.....	14
--	----

## Chapter 3.1: “Has upwelling strengthened along worldwide coasts over 1982-2010?”

<b>Table 1:</b> Studies in which upwelling trends were analysed in terms of wind along the Benguela and Canary coasts. Variable abbreviations: WSt (Wind Stress), Ekman Transport (ET), WSp (Wind Speed).....	25
---	----

<b>Table 2:</b> Studies in which upwelling trends were analysed in terms of wind along the Chile, Peru, and California coasts. Variable abbreviations: WSt (Wind Stress), Ekman Transport (ET), WSp (Wind Speed).....	26
---	----

## Chapter 3.2: “Coastal warming and wind-driven upwelling: a global analysis”

<b>Table 1:</b> Geographical boundaries of the upwelling systems considered in this study. Upwelling systems were separated accordingly to the seasonality of upwelling: year-round (upper group) or monthly seasonality (lower group) .....	36
--	----

<b>Table 2:</b> Statistical analysis of the SST trends along the World’s coastlines. Oceanic warming indicates the percentage of oceanic points with positive (warming) SST trends. Coastal warming indicates the percentage of coastal points with positive (warming) SST	
--	--

trends. $\text{Trend}_{\text{ocean}} > \text{Trend}_{\text{coast}}$ shows the percentage of points with SST trends higher in the ocean than in the coast (colder waters nearshore) .....	38
--	----



# Bibliography

- [Ahumada, 1989] Ahumada, R., 1989. Producción y destino de la biomasa fitoplanctónica en un sistema de bahías en Chile Central: Una hipótesis, *Biología Pesquera*, 18, 53–66.
- [Álvarez et al., 2008] Álvarez, I., Gómez-Gesteira, M., deCastro, M. and Días, J. M., 2008. Spatiotemporal evolution of upwelling regime along the western coast of the Iberian Peninsula. *Journal of Geophysical Research: Oceans*, 113(C7).
- [Álvarez et al., 2014] Álvarez, I., Gómez-Gesteira, M., deCastro, M. and Carvalho, D., 2014. Comparison of different wind products and buoy wind data with seasonality and interannual climate variability in the southern Bay of Biscay (2000–2009). *Deep Sea Research Pt II*, 106, 38–48.
- [Andrade, 2000] Andrade, C. A., 2000. The circulation and variability of the Colombian basin in the Caribbean Sea, doctorate thesis 229 pp. University of Wales, Cardiff.
- [Andrade et al., 2003] Andrade, C.A., Barton E.D. and Mooers, C. N K., 2003. Evidence for an eastward flow along the Central and South American Caribbean coast, *Journal of Geophysical Research*, 108, C6, 3185.
- [Andrade and Barton, 2005] Andrade, C. A. and Barton, E. D., 2005. The Guajira upwelling system. *Continental Shelf Research*, 25(9), 1003-1022.
- [Andruleit, 2007] Andruleit, H., 2007. Status of the Java upwelling area (Indian Ocean) during the oligotrophic northern hemisphere winter monsoon season as revealed by coccolithophores. *Marine Micropaleontology*, 64, 36–51.
- [Aravena et al., 2014] Aravena, G., Broitman, B. and Stenseth, N. C., 2014. Twelve years of change in coastal upwelling along the central-northern coast of Chile: spatially heterogeneous responses to climatic variability. *PLoS One*, 9(2), e90276.
- [Arbic and Owens, 2001] Arbic, B. K. and Owens, W. B., 2001. Climatic warming of the Atlantic intermediate waters. *Journal of Climate*, 14, 4091–4108.
- [Arístegui et al., 2004] Arístegui, J., Barton, E. D., Tett, P., Montero, M. F., García-Muñoz, M., Basterretxea, G., Cussatlegras, A-S., Ojeda, A. and de Armas, D., 2004. Variability in plankton community structure, metabolism, and vertical carbon fluxes along an upwelling filament (Cape Juby, NW Africa). *Progress in Oceanography*, 62(2), 95-113.
- [Arístegui et al., 2009] Arístegui, J., Barton, E. D., Álvarez-Salgado, X. A., Santos, A. M. P., Figueiras, F. G., Kifani, S., Hernández-León, S., Mason, E., Machu, E. and Demarq, H., 2009. Subregional ecosystem variability in the Canary current upwelling. *Progress in Oceanography*, 83, 33–48.

- [Bakun, 1973] Bakun, A., 1973. Coastal upwelling indices, west coast of North America, 1946-71. NOAA-NMFS, Technical Memorandum, pp. 1–13.
- [Bakun, 1990] Bakun, A., 1990. Global climate change and intensification of coastal ocean upwelling. *Science*, 247(4939), 198-201.
- [Bakun et al., 2010] Bakun, A., Field, D., Redondo-Rodríguez, A. and Weeks, S., 2010. Greenhouse gas, upwelling-favorable winds, and the future of coastal ocean upwelling ecosystems. *Global Change Biology*, 16, 1213–28.
- [Barange et al., 1991a] Barange, M., Gibbons, M. J. and Carola, M., 1991. Diet and feeding of *Euphausia hansenii* and *Nematoscelis megalops* (Euphausiacea) in the northern Benguela Current: ecological significance of vertical space partitioning. *Marine Ecology Progress Series*, 173-181.
- [Barange et al., 1991b] Barange, M. and Stuart, V., 1991. Distribution patterns, abundance and population dynamics of the euphausiids *Nyctiphanes capensis* and *Euphausia hansenii* in the northern Benguela upwelling system. *Marine Biology*, 109(1), 93-101.
- [Barange et al., 2010] Barange, M., Field, J. G., Harris, R. P., Hofmann, E. E., Perry, R. I. and Werner, F., 2010. *Marine Ecosystems and Global Change*. Oxford University Press, Oxford, 412 pp.
- [Barton et al., 1998] Barton, E. D., Arístegui, J., Tett, P., Canton, M., García-Braun, J., Hernández-León, S., Nykjaer, L., Almeida, C., Ballesteros, S., Basterretxea, G., Escánez, J., García-Weill, L., Hernández-Guerra, A., López-Laatzén, F., Molina, R., Montero, M. F., Navarro-Pérez, E., Rodríguez, J. M., van Lenning, K., Vélez, H. and Wild, K., 1998. The transition zone of the Canary Current upwelling region. *Progress in Oceanography*, 41(4), 455-504.
- [Barton et al., 2013] Barton, E. D., Field, D. B. and Roy, C., 2013. Canary current upwelling: More or less? *Progress in Oceanography*, 116, 167-178.
- [Baumgart et al., 2010] Baumgart, A., Jennerjahn, T., Mohtadi, M. and Hebbeln, D., 2010. Distribution and burial of organic carbon in sediments from the Indian Ocean upwelling region off Java and Sumatra, Indonesia. *Deep Sea Research*, 57, 458–467.
- [Belkin, 2009] Belkin, I. M., 2009. Rapid warming of large marine ecosystems. *Progress in Oceanography*, 81(1), 207-213.
- [Belveze and Erzini, 1983] Belveze, H. and Erzini, K., 1983. The influence of hydroclimatic factors on the availability of the sardine (*Sardina pilchardus* Walbaum) in the Moroccan Atlantic fishery. *FAO Fisheries Report (FAO)*. no. 291.
- [Bernal et al., 2010] Bernal, G., Ruíz-Ochoa, M. and Beier, E., 2010. Variabilidad estacional e interanual océano-atmósfera en la cuenca Colombia in *Cuadernos del*

- Caribe. La investigación en ciencias del mar de la Universidad Nacional de Colombia: 30 años de la biología marina.
- [Bindoff and McDougall, 1994] Bindoff, N. L. and McDougall, T. J., 1994. Diagnosing climate change and ocean ventilation using hydrographic data. *Journal of Physical Oceanography*, 24, 1137–1152,
- [Black et al., 1999] Black, D. E., Peterson, L. C., Overpeck, J. T., Kaplan, A., Evans, M. N. and Kashgarian, M., 1999. Eight centuries of North Atlantic Ocean atmosphere variability. *Science*, 286(5445), 1709-1713.
- [Borges et al., 2003] Borges, M. F., Santos, A. M. P., Crato, N., Mendes, H. and Mota, B., 2003. Sardine regime shifts off Portugal: a time series analysis of catches and wind conditions. *Scientia Marina*, 67, 235–244.
- [Brandhorst, 1971] Brandhorst, W., 1971. Condiciones oceanograficas estivales frente a la costa de Chile, *Revista de Biología Marina, Valparaíso*, 14(3), 45– 84.
- [Bulanienkov and García, 1973] Bulanienkov, S. K. and García, C., 1973. Influencia de los procesos atmosféricos en el afloramiento del banco de Campeche. *Revista de Investigación Pesquera*, 99-140.
- [Cáceres and Arcos, 1991] Cáceres, M. and Arcos, D., 1991. Variabilidad en la estructura espaciotemporal de un área de surgencia frente a la costa de Concepción, Chile, *Investigaciones Pesqueras*, 36, 27– 38.
- [Cahuin et al., 2013] Cahuin, S. M., Cubillos, L. A., Escribano, R., Blanco, J. L., Ñiquen, M. and Serra, R., 2013. Sensitivity of recruitment rates anchovy (*Engraulis ringens*) to environmental changes in Southern Peru—Northern Chile. *Environmental Development*, 7, 88-101.
- [Cane et al., 1997] Cane, M. A., Clement, A. C., Kaplan, A., Kushnir, Y., Pozdnyakov, D., Seager, R., Zebiak, S. E. and Murtugudde, R., 1997. Twentieth-century sea surface temperature trends. *Science*, 275(5302), 957-960.
- [Cárdenas-Palomo et al., 2015] Cárdenas-Palomo, N., Herrera-Silveira, J., Velázquez-Abunader, I., Reyes-Mendoza, O. and Ordoñez, U., 2015. Distribution and feeding habitat characterization of whale sharks *Rhincodon typus* in a protected area in the north Caribbean Sea. *Journal of Fish Biology*, 86(2), 668-686.
- [Carr and Kearns, 2003] Carr, M. E. and Kearns, E. J., 2003. Production regimes in four Eastern Boundary Current systems. *Deep Sea Research Part II: Topical Studies in Oceanography*, 50(22), 3199-3221.
- [Carrillo et al., 2016] Carrillo, L., Johns, E. M., Smith, R. H., Lamkin, J. T. and Largier, J. L., 2016. Pathways and hydrography in the Mesoamerican Barrier Reef System Part 2: Water masses and thermohaline structure. *Continental Shelf Research*, 120, 41-58.

- [Carton et al., 2000a] Carton, J. A., Chepurin, G. A., Cao, X. and Giese, B. S., 2000a. A Simple Ocean Data Assimilation analysis of the global upper ocean 1950–1955, Part 1: Methodology. *Journal of Geophysical Research*, 30: 294–309.
- [Carton et al., 2000b] Carton, J. A., Chepurin, G. A. and Cao, X., 2000b. A Simple Ocean Data Assimilation analysis of the global upper ocean 1950–1955, Part 2: Methodology. *Journal of Geophysical Research*, 30: 311–326.
- [Carvalho et al., 2014a] Carvalho, D., Rocha, A., Gómez-Gesteira, M. and Silva Santos, C., 2014a. Comparison of reanalyzed, analyzed, satellite-retrieved and NWP modelled winds with buoy data along the Iberian Peninsula coast. *Remote Sensing Environment*, 152, 480–492.
- [Carvalho et al., 2014b] Carvalho, D., Rocha, A. and Gómez-Gesteira, M., 2014b. Offshore wind energy resource simulation forced by different reanalysis: comparison with observed data in the Iberian Peninsula. *Applied Energy*, 134, 57–64.
- [Castelao and Barth, 2006] Castelao, R. M. and Barth, J. A., 2006. Upwelling around Cabo Frio, Brazil: The importance of wind stress curl. *Geophysical Research Letters*, 33(3).
- [Cheung et al., 2013] Cheung, W. W., Watson, R. and Pauly, D., 2013. Signature of ocean warming in global fisheries catch. *Nature*, 497(7449), 365–368.
- [Chollett et al., 2012] Chollett, I., Müller-Karger, F. E., Heron, S. F., Skirving, W. and Mumby, P. J., 2012. Seasonal and spatial heterogeneity of recent sea surface temperature trends in the Caribbean Sea and southeast Gulf of Mexico. *Marine Pollution Bulletin*, 64(5), 956–965.
- [Church et al., 1989] Church, J. A., Cresswell, G. and Godfrey, J. S., 1989. The Leeuwin Current. In: Neshyba S.J., Mooers Ch. N. K., Smith R.L., Barber R.T., editors. Poleward flow along eastern ocean boundaries. *Coastal and Estuarine Studies*, 34. New York: Springer-Verlag, p 230–54.
- [Cochrane, 1963] Cochrane, J. D., 1963. Yucatan Current. Department of Oceanography Meteorology, Texas A&M Univ. Ref. 63-18A, pp. 6-11. @htpubl. Rep.).
- [Cochrane, 1966] Cochrane, J. D., 1966. The Yucatan Current, upwelling off northeastern Yucatan, and currents and waters of western equatorial Atlantic, Oceanography of the Gulf of Mexico. Progress Reports, TAMU Ref.\_66-23T, pp.14–32.
- [Conan and Brummer, 2000] Conan, S. H. and Brummer, G. J. A., 2000. Fluxes of planktic foraminifera in response to monsoonal upwelling on the Somalia Basin margin. *Deep Sea Research Part II: Topical Studies in Oceanography*, 47(9), 2207–2227.



- [Costanza et al., 1997] Costanza, R., d'Arge, R., De Groot, R., Farber, S., Grasso, M., Hannon, B., Limburg, K., Naeem, S., O'Neill, R. V., Paruelo, J., Raskin, R. G., Sutton, P. and van den Belt, M., 1997. The value of the world's ecosystem services and natural capital. *Nature*, 387(6630), 253-260.
- [Corredor, 1979] Corredor, J. E., 1979. Phytoplankton response to low level nutrient enrichment through upwelling in the Colombian Caribbean Basin. *Deep Sea Research*, 26A, 731-741.
- [Criales-Hernández et al., 2006] Criales-Hernández, M. I., García, C. B. and Wolff, M., 2006. Flujos de biomasa y estructura de un ecosistema de surgencia tropical en La Guajira, Caribe colombiano. *Revista de Biología Tropical*, 54 (4), 1257-1282.
- [Cropper et al., 2014] Cropper, T. E., Hanna, E. and Bigg, G. R., 2014. Spatial and temporal seasonal trends in coastal upwelling off Northwest Africa, 1981–2012. *Deep Sea Research Part I: Oceanographic Research Papers*, 86, 94-111.
- [Cummings, 2005] Cummings, J. A., 2005. Operational multivariate ocean data assimilation. *Quarterly Journal of the Royal Meteorological Society, Part C.*, 131(613):3583-3604.
- [Cummings and Smedstad, 2013] Cummings, J. A. and Smedstad, O. M., 2013. Variational Data Assimilation for the Global Ocean. *Data Assimilation for Atmospheric, Oceanic and Hydrologic Applications vol. II*, chapter 13, 303-343.
- [Currie et al., 2013] Currie, J. C., Lengaigne, M., Vialard, J., Kaplan, D. M., Aumont, O., Naqvi, S. W. A. and Maury, O., 2013. Indian Ocean Dipole and El Niño/Southern Oscillation impacts on regional chlorophyll anomalies in the Indian Ocean. *Biogeosciences*, 10: 5841–5888.
- [Cury and Roy, 1989] Cury, P. and Roy, C., 1989. Optimal environmental window and pelagic fish recruitment success in upwelling areas. *Canadian Journal of Fisheries and Aquatic Sciences*, 46, 670–680.
- [Cushing, 1969] Cushing, D. H., 1969. Upwelling and fish production. *FAO Fisheries Technical Papers*, 84:40.
- [de Boyer Montegut, 2007] Montegut, C. B., Vialard, J., Shenoi, S. S., Shankar, D., Durand, F., Ethe, C. and Madec, G., 2007. Simulated seasonal and interannual variability of the mixed layer heat budget in the northern Indian Ocean. *Journal of Climate*, 20(13), 3249-3268.
- [deCastro et al., 2009] deCastro, M., Gómez-Gesteira, M., Álvarez, I. and Gesteira, J. L. G., 2009. Present warming within the context of cooling–warming cycles observed since 1854 in the Bay of Biscay. *Continental Shelf Research* 29, 1053–1059.
- [deCastro et al., 2014] deCastro, M., Gómez-Gesteira, M., Costoya, X. and Santos, F., 2014. Upwelling influence on the number of extreme hot SST days along the

- Canary Upwelling ecosystem, *Journal Geophysical Research Oceans*, 119, 3029–3040.
- [del Monte-Luna et al., 2015] del Monte-Luna, P., Villalobos, H. and Arreguín-Sánchez, F., 2015. Variability of sea surface temperature in the southwestern Gulf of Mexico. *Continental Shelf Research*, 102, 73-79.
- [Demarcq, 2009] Demarcq, H., 2009. Trends in primary production, sea surface temperature and wind in upwelling systems (1998–2007). *Progress in Oceanography*, 83(1), 376-385.
- [Di Lorenzo et al., 2005] Di Lorenzo, E., Miller, A. J., Schneider, N. and McWilliams, J. C., 2005. The warming of the California Current System: Dynamics and ecosystem implications. *Journal of Physical Oceanography*, 35(3), 336-362.
- [Dorman et al., 2005] Dorman, J. G., Bollens, S. M. and Slaughter, A. M., 2005. Population biology of euphausiids off northern California and effects of short time-scale wind events on *Euphausia pacifica*. *Marine Ecology Progress Series*, 288, 183-198.
- [Du et al., 2007] Du, Y., Qu, T. and Meyers, G., 2007. Interannual variability of the sea surface temperature off Java and Sumatra in a global GCM. *Journal of Climate*, 21: 2451–2465.
- [Duineveld et al., 1997] Duineveld, G. C. A., De Wilde, P. A. W. J., Berghuis, E. M., Kok, A., Tahey, T. and Kromkamp, J., 1997. Benthic respiration and standing stock on two contrasting continental margins in the western Indian Ocean: the Yemen-Somali upwelling region and the margin off Kenya. *Deep Sea Research Part II: Topical Studies in Oceanography*, 44(6), 1293-1317.
- [Ekman, 1905] Ekman, V. W., 1905. On the influence of the earth's rotation on ocean-currents.
- [Enríquez et al., 2013] Enríquez, C., Mariño-Tapia, I. J., Jerónimo, G. and Capurro-Filigrasso, L., 2013. Thermohaline processes in a tropical coastal zone. *Continental Shelf Research*. 69, 101-109.
- [Enríquez and Mariño-Tapia, 2014] Enríquez, C. and Mariño-Tapia, I. J., 2014. Mechanisms driving a coastal dynamic upwelling. In *Proceedings of the 17th Physics of Estuaries and Coastal Seas (PECS) Conference*.
- [Falvey and Garreaud, 2009] Falvey, M. and Garreaud, R. D., 2009. Regional cooling in a warming world: Recent temperature trends in the southeast Pacific and along the west coast of subtropical South America (1979–2006). *Journal of Geophysical Research: Atmospheres*, 114(D4).
- [Fennel, 1999] Fennel, W., 1999. Theory of the Benguela upwelling system. *Journal of Physical Oceanography*, 29(2), 177-190.
- [Furnas, 2007] Furnas, M., 2007. Intra-seasonal and inter-annual variations in phytoplankton biomass, primary production and bacterial production at North

- West Cape, Western Australia: Links to the 1997–1998 El Niño event. *Continental Shelf Research*, 27, 958–980.
- [García et al., 2007] García, C. B., Duarte, L. O., Altamar, J. and Manjarres, L. M., 2007. Demersal fish density in the upwelling ecosystem off Colombia, Caribbean Sea: Historic outlook. *Fisheries Research*, 85, 68–73.
- [García-Reyes and Largier, 2010] García-Reyes, M. and Largier, J., 2010. Observations of increased wind-driven coastal upwelling off central California. *Journal of Geophysical Research*, C, 115, C04010.
- [García-Reyes et al., 2014] García-Reyes, M., Largier, J. L. and Sydeman, W. J., 2014. Synoptic-scale upwelling indices and prediction of phyto- and zooplankton populations. *Progress in Oceanography*, 120, 177–188.
- [García-Reyes et al., 2015] García-Reyes, M., Sydeman, W. J., Schoeman, D. S., Rykaczewski, R. R., Black, B. A., Smit, A. J. and Bograd, S. J., 2015. Under pressure: climate change, upwelling, and eastern boundary upwelling ecosystems. *Frontiers in Marine Science*, 2, 109.
- [Garreaud and Falvey, 2009] Garreaud, R. D. and Falvey, M., 2009. The coastal winds off western subtropical South America in future climate scenarios. *International Journal of Climatology*, 29, 543–554 (2009).
- [Gersbach et al., 1999] Gersbach, G. H., Pattiaratchi, C. B., Ivey, G. N. and Cresswell, G. R., 1999. Upwelling on the south-west coast of Australia — source of the Capes Current? *Continental Shelf Research*, 19, 363–400.
- [Gill and Schumann, 1979] Gill, A.E. and Schumann, E.H., 1979. Topographically induced changes in the structure of an inertial coastal jet: application to the Agulhas Current. *Journal of Physical Oceanography* 9, 975–991.
- [Gill et al., 2011] Gill, P. C., Morrice, M. G., Page, B., Pirzl, R., Levings, A. H. and Coyne, M., 2011. Blue whale habitat selection and within-season distribution in a regional upwelling system off southern Australia. *Marine Ecology Progress Series*, 421, 243–263.
- [Goes et al., 2005] Goes, J. I., Thoppil, P. G., Gomes, H. do R. and Fasullo, J. T., 2005. Warming of the Eurasian landmass is making the Arabian Sea more productive. *Science*, 308, 545–547.
- [Gómez-Gesteira et al., 2008a] Gómez-Gesteira, M., deCastro, M., Álvarez, I., Lorenzo, M. N., Gómez-Gesteira, J. L. and Crespo, A. J. C., 2008a. Spatio-temporal Upwelling Trends along the Canary Upwelling System (1967–2006). *Annals of the New York Academy of Sciences*, 1146(1), 320–337.
- [Gómez-Gesteira et al., 2008b] Gómez-Gesteira, M., deCastro, M., Álvarez, I. and Gómez-Gesteira, J. L., 2008b. Coastal sea surface temperature warming trend along the continental part of the Atlantic Arc (1985–2005). *Journal of Geophysical Research: Oceans*, 113(C4).

- [Gómez-Gesteira et al., 2011] Gómez-Gesteira, M., Gimeno, L., deCastro, M., Lorenzo, M. N., Álvarez, I., Nieto, R., Taboada, J. J., Crespo, A. J. C., Ramos, A. M., Iglesias, I., Gómez-Gesteira, J. L., Santo, F. E., Barriopedro, D. and Trigo, I. F., 2011. The state of climate in NW Iberia. *Climate Research*, 48(2/3), 109-144.
- [Gordon, 2005] Gordon, A. L., 2005. Oceanography of the Indonesian seas and their throughflow. *Oceanography*, 18(4): 13–26.
- [Goubanova et al., 2011] Goubanova, K., Echevin, V., Dewitte, B., Codron, F., Takahashi, K., Terray, P. and Vrac, M., 2011. Statistical downscaling of sea-surface wind over the Peru–Chile upwelling region: diagnosing the impact of climate change from the IPSL-CM4 model. *Climate Dynamics*, 36(7-8), 1365-1378.
- [Gray, 1997] Gray, J. S., 1997. Marine biodiversity: patterns, threats and conservation needs. *Biodiversity & Conservation*, 6(1), 153-175.
- [Gutiérrez et al., 2011] Gutiérrez, D., Bouloubassi, I., Sifeddine, A., Purca, S., Goubanova, K., Graco, M., Field, D., Mejanelle, L., Velazco, F., Lorre, A., Salvatelli, R., Quispe, D., Vargas, G., Dewitte, B. and Ortlieb, L., 2011. Coastal cooling and increased productivity in the main upwelling zone off Peru since the mid-twentieth century. *Geophysical Research Letters*, 38(7).
- [Halpern et al., 2008] Halpern, B. S., Walbridge, S., Selkoe, K. A., Kappel, C. V., Micheli, F., D'agrosa, C., Bruno, J. F., Casey, K. S., Ebert, C., Fox, H. E., Fujita, R., Heinemann, D., Lenihan, H. S., Madin, E. M. P., Perry, M. T., Selig, E. R., Spalding, M., Steneck, R. and Watson, R., 2008. A global map of human impact on marine ecosystems. *Science*, 319(5865), 948-952.
- [Hansen et al., 2006] Hansen, J., Sato, M., Ruedy, R., Lo, K., Lea, D. W. and Medina-Elizade M., 2006. Global temperature change, *Proceedings of the National Academy of Sciences*, U. S. A., 103, 14,288–14,293.
- [Hansen et al., 2010] Hansen, J., Ruedy, R., Sato, M. and Lo, K., 2010. Global surface temperature change. *Reviews of Geophysics*, 48, RG4004.
- [Hanson et al., 2005] Hanson, C. E., Pattiaratchi, C. B. and Waite, A. M., 2005. Sporadic upwelling on a downwelling coast: phytoplankton responses to spatially variable nutrient dynamics off the Gascoyne region of Western Australia. *Continental Shelf Research*, 25, 1561–1582.
- [Harley et al., 2006] Harley, C. D., Randall Hughes, A., Hultgren, K. M., Miner, B. G., Sorte, C. J., Thornber, C. S., Rodríguez, L. F., Tomanek, L. and Williams, S. L., 2006. The impacts of climate change in coastal marine systems. *Ecology letters*, 9(2), 228-241.
- [Harrison and Carson, 2007] Harrison, D. E. and Carson, M., 2007. Is the world ocean warming? Upper-ocean temperature trends: 1950–2000. *Journal of Physical Oceanography*, 37(2), 174-187.

- [Hartman et al., 2013] Hartmann, D. L., Klein Tank, A. M. G., Rusticucci, M., Alexander, L. V., Brönnimann, S., Charabi, Y., Dentener, F. J., Dlugokencky, E. J., Easterling, D. R., Kaplan, A., Soden, B. J., Thorne, P. W., Wild, M. and Zhai, P. M., 2013. Observations: Atmosphere and Surface. In: Stocker, T. F., Qin, D., Plattner, G.-K., Tignor, M., Allen, S. K., Boschung, J., Nauels, A., Xia, Y., Bex, V. and Midgley, P. M. (eds.) *Climate Change 2013: The Physical Science Basis. Contribution of Working Group I to the Fifth Assessment Report of the Intergovernmental Panel on Climate Change* (pp. 159-254). Cambridge; New York: Cambridge University Press
- [Hewitson and Cruickshank, 1993] Hewitson, J. D. and Cruickshank, R. A., 1993. Production and consumption by planktivorous fish in the northern Benguela ecosystem in the 1980s. *South African Journal of Marine Science*, 13(1), 15-24.
- [Hoegh-Guldberg and Bruno, 2010] Hoegh-Guldberg, O. and Bruno, J. F., 2010. The impact of climate change on the world's marine ecosystems. *Science*, 328(5985), 1523-1528.
- [Hooff and Peterson, 2006] Hooff, R. C. and Peterson, W. T., 2006. Copepod biodiversity as an indicator of changes in ocean and climate conditions of the northern California current ecosystem. *Limnology and Oceanography*, 51(6), 2607-2620.
- [ICES, 2002] Headquarters, I. C. E. S. Working Group on the Assessment of Mackerel, Horse Mackerel, Sardine, and Anchovy, 2002.
- [Iles et al., 2012] Iles, A. C., Gouhier, T. C., Menge, B. A., Stewart, J. S., Haupt, A. J. and Lynch, M. C., 2012. Climate-driven trends and ecological implications of event-scale upwelling in the California Current System. *Global Change Biology*, 18(2), 783-796.
- [IPCC, 2014] Intergovernmental Panel on Climate Change, 2014. *Climate Change 2014—Impacts, Adaptation and Vulnerability: Regional Aspects*. Cambridge University Press.
- [Iskandar et al., 2009] Iskandar, I., Sasaki, H., Sasai, Y., Masumoto, Y. and Mizuno, K. A., 2009. Numerical investigation of eddy-induced chlorophyll bloom in the southeastern tropical Indian Ocean during Indian Ocean Dipole—2006. *Ocean Dynamics*, 60: 731–742.
- [Izumo et al., 2008] Izumo, T., Montegut, C. B., Luo, J. J., Behera, S. K., Masson, S. and Yamagata, T., 2008. The role of the western Arabian Sea upwelling in Indian monsoon rainfall variability. *Journal of Climate*, 21(21), 5603-5623.
- [Jackett and McDougall, 1997] Jackett, D. R. and McDougall, T. J., 1997. A neutral density variable for the world's oceans. *Journal of Physical Oceanography*, 27, 237–263.

- [Jouanno et al., 2008] Jouanno, J., Sheinbauma, J., Barnierb, B., Molinesb, J. M., Debreuc, L. and Lemariec, F., 2008. The mesoscale variability in the Caribbean Sea. Part I: Simulations and characteristics with and embedded model, *Ocean Modelling*, 23, 82-101.
- [Kämpf et al., 2004] Kämpf, J., Doubell, M., Griffin, D., Matthews, R. L. and Ward, T. M., 2004. Evidence of a large seasonal coastal upwelling system along the southern shelf of Australia. *Geophysical Research Letters*, 31(9).
- [Kämpf, 2010] Kämpf, J., 2010. On preconditioning of coastal upwelling in the eastern Great Australian Bight. *Journal of Geophysical Research: Oceans*, 115(C12).
- [Kämpf and Chapman, 2016] Kämpf, J. and Chapman, P., 2016. The Benguela Current Upwelling System. In *Upwelling Systems of the World* (pp. 251-314). Springer International Publishing.
- [Kifani, 1998] Kifani, S., 1998. Climate dependant fluctuations of the Moroccan sardine and their impact on fisheries. In: Durand, M. H., Cury, P., Mendelssohn, R., Roy, C., Bakun, A. and Pauly, D. (Eds.), *Global Versus Local Changes in Upwelling Systems* ORSTOM Editions, Paris, pp. 235–248.
- [Koning et al., 2001] Koning, E., Van Iperen, J. M., Van Raaphorst, W., Helder, W., Brummer, G. J. and Van Weering, T. C. E., 2001. Selective preservation of upwelling-indicating diatoms in sediments off Somalia, NW Indian Ocean. *Deep Sea Research Part I: Oceanographic Research Papers*, 48(11), 2473-2495.
- [Krishna, 2008] Krishna, K. M., 2008. Coastal upwelling along the southwest coast of India? ENSO modulation. *Ocean Science Discussions*, 5(1), 123-134.
- [Kromkamp et al., 1997] Kromkamp, J., De Bie, M., Goosen, N., Peene, J., Van Rijswijk, P., Sinke, J. and Duinevel, G. C., 1997. Primary production by phytoplankton along the Kenyan coast during the SE monsoon and November intermonsoon 1992, and the occurrence of *Trichodesmium*. *Deep Sea Research Part II: Topical Studies in Oceanography*, 44(6-7), 1195-1212.
- [Kuswardani and Qiao, 2014] Kuswardani, R. T. D. and Qiao, F., 2014. Influence of the Indonesian Throughflow on the upwelling off the east coast of South Java. *Chinese Science Bulletin*, 59: 4516-4523.
- [Leet, 2001] Leet, W. S., (2001). *California's living marine resources: A Status Report*. UCANR Publications.
- [Lemos and Pires, 2004] Lemos, R.T. and Pires, H.O., 2004. The upwelling regime off the west Portuguese coast, 1941–2000. *International Journal of Climatology* 24, 511-524.
- [Lemos and Sansó 2006] Lemos, R. T. and Sansó, B., 2006. Spatio-temporal variability of ocean temperature in the Portugal Current System. *Journal of Geophysical Research*, 111: C04010.



- [Levitus et al., 2000] Levitus, S., Antonov, J. I., Boyer, T. P. and Stephens, C., 2000. Warming of the world ocean. *Science*, 287(5461), 2225-2229.
- [Levitus et al., 2005] Levitus, S., Antonov, J. and Boyer, T., 2005. Warming of the world ocean, 1955–2003. *Geophysical Research Letters*, 32(2).
- [Levitus et al., 2012] Levitus, S., Antonov, J. I., Boyer, T. P., Baranova, O. K., Garcia, H. E., Locarnini, R. A., Mishonov, A. V., Reagan, J. R., Seidov, D., Yarosh, E. S. and Zweng, M. M., 2012. World ocean heat content and thermosteric sea level change (0–2000 m), 1955–2010. *Geophysical Research Letters*, 39(10).
- [Lima and Wetthey, 2012] Lima, F. P. and Wetthey, D. S., 2012. Three decades of high-resolution coastal sea surface temperatures reveal more than warming. *Nature Communications*, 3: 704
- [Lluch-Cota et al., 2014] Lluch-Cota, S. E., Hoegh-Guldberg, O., Karl, D. M., Pörtner, H. O., Sundby, S. and Gattuso, J. P., 2014. Cross-chapter box on uncertain trends in major upwelling ecosystems. In *Climate Change 2014: Impacts, Adaptation, and Vulnerability. Part A: Global and Sectoral Aspects. Contribution of Working Group II to the Fifth Assessment Report of the Intergovernmental Panel of Climate Change* (pp. 149-151). Cambridge University Press.
- [Lonin et al., 2010] Lonin, S. A., Hernández, J. L. and Palacios, D. M., 2010. Atmospheric events disrupting coastal upwelling in the southwestern Caribbean. *Journal of Geophysical Research*, 115, C06030.
- [Lorenzetti and Gaeta, 1996] Lorenzetti, J. A. and Gaeta, S. A., 1996. The Cape Frio upwelling effect over the South Brazil Bight northern sector shelf waters: a study using AVHRR images. *International Archives of Photogrammetry and Remote Sensing*, 21(part B7).
- [Lutjeharms et al., 2000] Lutjeharms, J. R. E., Cooper, J. and Roberts, M., 2000. Upwelling at the inshore edge of the Agulhas Current. *Continental Shelf Research*, 20(7), 737-761.
- [Ma et al., 2015] Ma, J., Liu, H., Lin, P. and Zhan, H., 2015. Effects of the interannual variability in chlorophyll concentrations on sea surface temperatures in the east tropical Indian Ocean. *Journal of Geophysical Research-Oceans*, 120.10: 7015-7027.
- [Macías et al., 2012] Macías, D., Landry, M. R., Gershunov, A., Miller, A. J. and Franks, P. J., 2012. Climatic control of upwelling variability along the western North-American coast. *Plos One*, 7(1), e30436.
- [Mason and Bakun, 1986] Mason, J. E. and Bakun, A., 1986. Upwelling index update, U.S. west coast 33N-48N latitude. NOAA-NMFS, Southwest Fisheries Center, Tech. Memo 67, (8), 1 pp.
- [McClanahan, 1988] McClanahan, T. R., 1988. Seasonality in East Africa's coastal waters. *Marine Ecology Progress Series*, 44, 191–199.

- [McGregor et al., 2007] McGregor, H. V., Dima, M., Fischer, H. W. and Mulitza, S., 2007. Rapid 20th-Century Increase in Coastal Upwelling off Northwest Africa. *Science*; 315, 637–639.
- [Mendelssohn and Schwing, 2002] Mendelssohn, R. and Schwing, F. B., 2002. Common and uncommon trends in SST and wind stress in the California and Peru–Chile current systems. *Progress in Oceanography*, 53(2), 141–162.
- [Mendoza et al., 2005] Mendoza, V. M, Villanueva, E. E. and Adem, J., 2005. On the annual cycle of the sea surface temperature and the mixed layer depth in the Gulf of México. *Atmósfera*, 18(2), 127–148.
- [Mengesha et al., 1999] Mengesha, S., Dehairs, F., Elskens, M. and Goeyens, L., 1999. Phytoplankton nitrogen nutrition in the western Indian Ocean: Ecophysiological adaptations of neritic and oceanic assemblages to ammonium suppl. *Estuarine, Coastal and Shelf Science*, 48, 589–598.
- [Merino, 1997] Merino, M., (1997). Upwelling on the Yucatan Shelf: hydrographic evidence. *Journal of Marine Systems*, 13(1-4), 101–121.
- [Messie et al., 2009] Messie, M., Ledesma, J., Kolber, D. D., Michisaki, R. P., Foley, D. G. and Chavez, F. P., 2009. Potential new production estimates in four eastern boundary upwelling ecosystems. *Progress in Oceanography*, 53(1), 151–158.
- [Mikaloff-Fletcher et al., 2006] Mikaloff-Fletcher, S. E., Gruber, N., Jacobson, A. R., Doney, S. C., Dutkiewicz, S., Gerber, M., Follows, M., Joos, F., Lindsay, K., Menemenlis, D., Mouchet, A., Muller, S. A. and Sarmiento, J. L., 2006. Inverse estimates of anthropogenic CO<sub>2</sub> uptake, transport, and storage by the ocean. *Global Biogeochemical Cycles*, 20(2).
- [Miller and Sydeman, 2004] Miller, A. K. and Sydeman, W. J., 2004. Rockfish response to low-frequency ocean climate change as revealed by the diet of a marine bird over multiple time scales. *Marine Ecology Progress Series*, 281, 207–216.
- [Müller-Karger et al., 2004] Müller-Karger, F., Varela, R., Thunell, R., Astor, Y., Zhang, H., Luerksen, R. and Hu, C., 2004. Processes of coastal upwelling and carbon flux in the Cariaco Basin. *Deep Sea Research Part II: Topical Studies in Oceanography*, 51(10), 927–943.
- [Muthumbi et al., 2004] Muthumbi, A. W., Vanreusel, A., Duineveld, G., Soetaert, K. and Vincx, M., 2004. Nematode community structure along the continental slope off the Kenyan Coast, Western Indian Ocean. *International Review der Gesamten Hydrobiologie*, 89, 188–205.
- [Mwaluma et al., 2003] Mwaluma, J., Osore, M., Kamau, J. and Wawiye, P., 2003. Composition, abundance and seasonality of zooplankton in Mida Creek, Kenya. Western Indian Ocean. *Journal of Marine Science*, 2, 147–155.



- [Narayan et al., 2010] Narayan, N., Paul, A., Mulitza, S. and Schulz, M., 2010. Trends in coastal upwelling intensity during the late 20th century. *Ocean Science*, 6, 815–823.
- [Nelson and Hutchings, 1983] Nelson, G. and Hutchings, L., 1983. The Benguela upwelling area. *Progress in Oceanography*, 12(3), 333–356.
- [Nykjaer and Van Camp, 1994] Nykjaer, L. and Van Camp, L., 1994. Seasonal and Interannual variability of coastal upwelling along northwest Africa and Portugal from 1981 to 1991, *Journal of Geophysical Research*, 99, 14197–14207.
- [Oke and Middleton, 2000] Oke, P. R. and Middleton, J. H., 2000. Topographically induced upwelling off eastern Australia. *Journal of Physical Oceanography*, 30(3), 512–531.
- [Páramo et al., 2011] Páramo, J., Correa, M. and Núñez, S., 2011. Evidencias de desacople físico-biológico en el sistema de surgencia en La Guajira, Caribe colombiano. *Revista de biología marina y oceanografía*, 46(3), 421–430. ISO 690.
- [Pardo et al., 2011] Pardo, P., Padín, X., Gilcoto, M., Farina-Busto, L. and Pérez, F., 2011. Evolution of upwelling systems coupled to the long term variability in sea Surface temperature and Ekman transport. *Climate Research*, 48, 231–246.
- [Patti et al., 2008] Patti, B., Guisande, C., Vergara, A. R., Riveiro, I., Maneiro, I., Barreiro, A., Bonanno, A., Buscaino, G., Cuttitta, A., Basilone, G. and Mazzola, S., 2008. Factors responsible for the differences in satellite-based chlorophyll a concentration between the major global upwelling areas. *Estuarine, Coastal and Shelf Science*, 76, 775–786.
- [Patti et al., 2010] Patti, B., Guisande, C., Riveiro, I., Thejll, P., Cuttitta, A., Bonanno, A., Basilone, G., Buscaino, G. and Mazzola, S., 2010. Effect of atmospheric CO<sub>2</sub> and solar activity on wind regime and water column stability in the major global upwelling areas. *Estuarine, Coastal and Shelf Science*, 88(1), 45–52.
- [Pauly and Christensen, 1995] Pauly, D. and Christensen, V., 1995. Primary production required to sustain global fisheries. *Nature*, 374(6519), 255.
- [Pearce, 1991] Pearce, A. F., 1991. Eastern boundary currents of the southern hemisphere. *Journal of the Royal Society of Western Australia*, 74, 35–45.
- [Pérez-Santos et al., 2010] Pérez-Santos, I., Schneider, W., Sobarzo, M., Montoya-Sánchez, R., Valle-Levinson, A. and Garcés-Vargas, J., 2010. Surface wind variability and its implications for the Yucatan Basin-Caribbean Sea dynamics. *Journal of Geophysical Research*, 115.
- [Pérez-Santos et al., 2014] Pérez-Santos, I., Schneider, W., Valle-Levinson, A., Garcés-Vargas, J., Soto, I., Montoya-Sánchez, R. and Müller-Karger, F., 2014. Chlorophyll-a patterns and mixing processes in the Yucatan Basin, Caribbean Sea. *Patrones superficiales de la clorofila a y procesos de mezcla en la cuenca de Yucatán, mar Caribe. Ciencias Marinas*, 40(1), 11–31.

- [Peterson et al., 1988] Peterson, W., Arcos, D., McManus, G., Dam, H., Bellantoni, D., Johnson, T. and Tiselius, P., 1988. The nearshore zone during coastal upwelling: Daily variability and coupling between primary and secondary production off central Chile, *Progress in Oceanography*, 20, 1–40.
- [Piontkovski et al., 2012] Piontkovski, S. A., AL-Gheilani, H. M. H., Jupp, B. P., Al-Azri, A. R. and Al-Hashmi, K. A., 2012. Interannual changes in the Sea of Oman ecosystem. *Open Marine Biology Journal*, 6, 38–52.
- [Prell, 1984] Prell, W. L., 1984. Variation of monsoonal upwelling: a response to changing solar radiation. In: Hansen, J., T. Takahashi, T. (Eds.), *Climate processes and climate sensitivity*, AGU, pp. 48–57.
- [Purba, 2007] Purba, M., 2007. Dynamics of south off Java—Sumbawa Island in Southeast Monsoon. *Torani Jurnal Ilmu Kelautan dan Perikanan*, 2: 140–150 (in Indonesian)
- [Qu et al., 2005] Qu, T., Du, Y., Strachan, J., Meyers, G. and Slingo, J., 2005. Sea surface temperature and its variability in the Indonesian region. *Oceanography*, 18: 50–61.
- [Rahn, 2012] Rahn, D. A., 2012. Influence of large scale oscillations on upwelling-favorable coastal wind off central Chile. *Journal of Geophysical Research: Atmospheres*, 117(D19).
- [Rahn and Garreaud, 2013] Rahn, D. A. and Garreaud, R. D., 2013. A synoptic climatology of the near-surface wind along the west coast of South America. *International Journal of Climatology*, 34(3), 780–792.
- [Ramos-Musalem, 2013] Ramos Musalem, A. K., 2013. Estudio numérico de los forzamientos que generan la surgencia de Yucatán (Bsc. Thesis). UNAM, Mexico, p. 77.
- [Rao, 2002] Rao, T. N., 2002. Spatial distribution of upwelling off the central east coast of India. *Estuarine, Coastal and Shelf Science*, 54(2), 141–156.
- [Rao et al., 2002] Rao, S. A., Behera, S. K., Masumoto, Y. and Yamagata, T., 2002. Interannual variability in the subsurface tropical Indian Ocean. *Deep-Sea Research II*, 2002; 49: 1549–1572.
- [Rao et al., 2011] Rao, S. A., Dhakate, A. R., Saha, S. K., Mahapatra, S., Chaudhari, H. S., Pokhrel, S. and Sahu, S. K., 2011. Why is Indian Ocean warming consistently? *Climatic change*, 110(3), 709–719.
- [Relvas et al., 2009] Relvas, P., Luis, J. and Santos, A. M. P., 2009. Importance of the mesoscale in the decadal changes observed in the northern Canary upwelling system, *Geophysical Research Letters*., 36, L22601.
- [Renault et al., 2009] Renault, L., Dewitte, B., Falvey, M., Garreaud, R., Echevin, V. and Bonjean, F., 2009. Impact of atmospheric coastal jet off central Chile on sea

- surface temperature from satellite observations (2000–2007). *Journal of Geophysical Research: Oceans*, 114(C8).
- [Reyes-Mendoza et al., 2016] Reyes-Mendoza, O.; Mariño-Tapia, I.; Herrera-Silveira, J.; Ruiz-Martínez, G.; Enríquez, C. and Largier, J.L., 2016. The effects of wind on upwelling off Cabo Catoche. *Journal of Coastal Research*, 32(3), 638–650. Coconut Creek (Florida), ISSN 0749-0208.
- [Reynolds, 2009] Reynolds, R. W., 2009. What's new in Version 2? [Available at [http://www.ncdc.noaa.gov/oa/climate/research/sst/papers/whats\\_new\\_v2.pdf](http://www.ncdc.noaa.gov/oa/climate/research/sst/papers/whats_new_v2.pdf).]
- [Reynolds and Chelton, 2010] Reynolds, R. W. and Chelton, D. W., 2010. Comparisons of daily sea surface temperature analysis for 2007–08. *Journal of Climate*, 23: 3545–3562.
- [Ridgway, 2007] Ridgway, K.R., 2007. Long-term trend and decadal variability of the southward penetration of the East Australian Current. *Geophysical Research Letters*, 34.
- [Roemmich and McGowan, 1995] Roemmich, D. and McGowan, J., 1995. Climatic warming and the decline of zooplankton in the California Current. *Science*, 267(5202), 1324.
- [Rousseaux et al., 2012] Rousseaux, C. S. G., Lowe, R. J., Feng, M., Waite, A. M. and Thompson, P. A., 2012. The role of the Leeuwin Current and mixed layer depth on the autumn phytoplankton bloom off Ningaloo Reef, Western Australia. *Continental Shelf Research*, 32, 22–35.
- [Rueda-Roa and Müller-Karger, 2013] Rueda-Roa, D. T. and Müller-Karger, F., 2013. The southern Caribbean upwelling system: sea surface temperature, wind forcing and chlorophyll concentration patterns. *Deep Sea Research Part I: Oceanographic Research Papers*, 78, 102–114.
- [Ruiz-Castillo et al., 2016] Ruiz-Castillo, E., Gómez-Valdes, J., Sheinbaum, J. and Rioja-Nieto, R., 2016. Wind-driven coastal upwelling and westward circulation in the Yucatan shelf. *Continental Shelf Research*, 118, 63–76.
- [Ruiz-Ochoa, 2011] Ruiz-Ochoa, M., 2011. Variabilidad de la Cuenca Colombia (mar Caribe) asociada con El Niño-Oscilación del Sur, vientos Alisios y procesos locales. Thesis.
- [Ruiz-Ochoa et al., 2012] Ruiz-Ochoa, M., Beier, E., Bernal, G. and Barton, E. D., 2012. Sea surface temperature variability in the Colombian Basin, Caribbean Sea. *Deep Sea Research Part I: Oceanographic Research Papers*, 64, 43–53.
- [Rykaczewski and Checkley, 2008] Rykaczewski, R. R. and Checkley, D. M., 2008. Influence of ocean winds on the pelagic ecosystem in upwelling regions, *Proceedings of the National Academy of Sciences*, 105, 1965–1970.
- [Ryther, 1969] Ryther, J. H., 1969. Photosynthesis and fish production in the sea. *Science*, 166: 72–6.

- [Saha et al., 2010] Saha, S., Moorthi, S., Pan, H., Wu, X., Wang, J., Nadiga, S., Tripp, P., Kistler, R., Woollen, J., Behringer, D., Liu, H., Stokes, D., Grumbine, R., Gayno, G., Wang, J., Hou, Y., Chuang, H., Juang, H. H., Sela, J., Iredell, M., Treadon, R., Kleist, D., Van Delst, P., Keyser, D., Derber, J., Ek, M., Meng, J., Wei, H., Yang, R., Lord, S., Van Den Dool, H., Kumar, A., Wang, W., Long, C., Chelliah, M., Xue, Y., Huang, B., Schemm, J., Ebisuzaki, W., Lin, R., Xie, P., Chen, M., Zhou, S., Higgins, W., Zou, C., Liu, Q., Chen, Y., Han, Y., Cucurull, L., Reynolds, R. W., Rutledge, G. and Goldberg, M., 2010. The NCEP Climate Forecast System Reanalysis. *Bulletin of the American Meteorology Society*, 91: 1015–1057.
- [Saji et al., 1999] Saji, N. H., Goswami, B. N., Vinayachandran, P. N. and Yamagata, T., 1999. A dipole mode in the tropical Indian Ocean. *Nature*, 401: 360-363.
- [Salmerón-García et al., 2011] Salmerón-García, O., Zavala-Hidalgo, J., Mateos-Jasso, A. and Romero-Centeno, R., 2011. Regionalization of the Gulf of Mexico from space-time chlorophyll-a concentration variability. *Ocean Dynamics*, 61(4), 439-448.
- [Santos et al., 2011] Santos, F., Gómez-Gesteira, M. and deCastro, M., 2011. Coastal and oceanic variability along the western Iberian peninsula. *Continental Shelf Research* 31, 2012–2017.
- [Santos et al., 2012a] Santos, F., Gómez-Gesteira, M., deCastro, M. and Álvarez, I., 2012a. Variability of coastal and ocean water temperature in the upper 700 m along the Western Iberian Peninsula from 1975 to 2006. *PLoS One*, 7(12): 1–7.
- [Santos et al., 2012b] Santos, F., Gómez-Gesteira, M., deCastro, M. and Álvarez, I., 2012b. Differences in coastal and oceanic SST warming rates along the Canary Upwelling Ecosystem from 1982 to 2010. *Continental Shelf Research*, 47:1–6.
- [Santos et al., 2012c] Santos, F., Gómez-Gesteira, M., deCastro, M. and Álvarez, I., 2012c. Differences in coastal and oceanic SST trends due to the strengthening of coastal upwelling along the Benguela current system. *Continental Shelf Research*, 34: 79–86.
- [Santos et al., 2015] Santos, F., Gómez-Gesteira, M., deCastro, M. and Días, J. M., 2015. A dipole-like SST trend in the Somalia region during the monsoon season. *Journal of Geophysical Research: Oceans*, 120(2), 597-607.
- [Santos et al., 2016] Santos, F., Gómez-Gesteira, M., Varela, R., Ruiz-Ochoa, M. and Días, J. M., 2016. Influence of upwelling on SST trends in La Guajira system. *Journal of Geophysical Research: Oceans*, 121(4), 2469-2480.
- [Schirripa and Colbert, 2006] Schirripa, M. J. and Colbert, J. J., 2006. Interannual changes in sablefish (*Anoplopoma fimbria*) recruitment in relation to oceanographic conditions within the California Current System. *Fisheries Oceanography*, 15(1), 25-36.

- [Schroeder and Love, 2002] Schroeder, D. M. and Love, M. S., 2002. Recreational fishing and marine fish populations in California. California Cooperative Oceanic Fisheries Investigations Report, 182-190.
- [Schroeder et al., 2009] Schroeder, I. D., Sydeman, W. J., Sarkar, N., Thompson, S. A., Bograd, S. J. and Schwing, F. B., 2009. Winter pre-conditioning of seabird phenology in the California Current. Marine Ecology Progress Series, 393, 211-223.
- [Schwartzlose et al., 1999] Schwartzlose, R. A., Alheit, J., Bakun, A., Baumgartner, T. R., Cloete, R., Crawford, R. J. M. and Lluch-Belda, D., 1999. Worldwide large-scale fluctuations of sardine and anchovy populations. South African Journal of Marine Science, 21(1), 289-347.
- [Seabra et al., 2015] Seabra, R., Wethey, D. S., Santos, A. M. and Lima, F. P., 2015. Understanding complex biogeographic responses to climate change. Scientific reports, 5.
- [Semeneh et al., 1995] Semeneh, M. F., Dehairs, F. and Goeyens, L., 1995. Uptake of nitrogenous nutrients by phytoplankton in the tropical Western Indian Ocean (Kenyan Coast): monsoonal and spatial variability. In: Heip C. M. A., Hemminga M. J. M. (Eds), Monsoons and Ecosystems in Kenya. Kenya Marine Fisheries Research Institute, Mombasa, Kenya, 101–104.
- [Seo et al., 2012] Seo, H., Brink, K. H., Dorman, C. E., Koracin, D. and Edwards, C. A., 2012. What determines the spatial pattern in summer upwelling trends on the U.S. West Coast? Journal of Geophysical Research, 117, C08012.
- [Serra et al., 2012] Serra, R., Akester, M., Bouchon, M. and Gutiérrez, M., 2012. Sustainability of the Humboldt Current large marine ecosystem. In: Sherman, Kenneth, McGovern, Galen (Eds.), Frontline Observations on Climate Change and Sustainability of Large Marine Ecosystems (Eds.) United Nations Development Programme, pp. 112–134. Chapter 7.
- [Sherman and Hempel, 2009] Sherman, K. and Hempel, G., 2009. The UNEP large marine ecosystem report: a perspective on changing conditions in LMEs of the world's regional seas. UNEP Regional Seas Reports and Studies, Vol 182. United Nations Environment Programme, Nairobi.
- [Shi et al., 2000] Shi, W., Morrison, J. M., Bohm, E. and Manghnani, V., 2000. The Oman upwelling zone during 1993, 1994 and 1995. Deep Sea Research Part II: Topical Studies in Oceanography, 47(7), 1227-1247.
- [Shiu et al., 2009] Shiu, C. J., Liu, S. C. and Chen, J. P., 2009. Diurnally asymmetric trends of temperature, humidity, and precipitation in Taiwan. Journal of climate, 22(21), 5635-5649.

- [Siswanto and Suratno, 2008] Siswanto and Suratno, 2008. Seasonal pattern of wind induced upwelling over Java-Bali Sea. *International Journal of Remote Sensing Earth Science*, 5: 46–56
- [Smith et al., 1991] Smith, R. L., Huyer, A., Godfrey, J. S. and Church, J. A., 1991. The Leeuwin current off Western Australia, 1986–1987, *Journal of Physical Oceanography*, 21, 323–345.
- [Smitha et al., 2008] Smitha, B. R., Sanjeevan, V. N., Vimalkumar, K. G. and Revichandran, C., 2008. On the upwelling off the southern tip and along the west coast of India. *Journal of Coastal Research*, 24(sp3), 95-102.
- [Snyder et al., 2003] Snyder, M. A., Sloan, L. C., Diffenbaugh, N. S. and Bell, J. L., 2003. Future climate change and upwelling in the California Current. *Geophysical Research Letters*, 30(15).
- [Sprintall et al., 2008] Sprintall, J., Wijffels, S., Molcard, R. and Jaya, I., 2008. Direct Evidence of the South Java Current System in Ombai Strait, *Dynamic of Atmospheres and Oceans*, 50(2): 140-156.
- [Sobarzo et al., 2007] Sobarzo, M., Shearman, R. K. and Lentz, S., 2007. Near-inertial motions over the continental shelf off Concepción, central Chile. *Progress in Oceanography*, 75(3), 348-362.
- [Souza et al., 2016] Souza, A. J., Mariño-Tapia, I. and J-M Hirschi, J., 2016. Mechanisms controlling upwelling on the Yucatan shelf; its interannual variability and predictability. In *Abstract for the 18th Physics of Estuaries and Coastal Seas Conference*.
- [Strub et al., 1998] Strub, T., Mesias, J., Montecino, V., Rutlant, J. and Salinas, S., 1998, Coastal ocean circulation off western South America, Coastal Segment (6,E), in *The Sea*, vol. 11, edited by A. Robinson and K. Brink, pp. 273– 313, John Wiley, Hoboken, N. J.
- [Susanto et al., 2001] Susanto, R. D., Gordon, A. L. and Zheng, Q., 2001. Upwelling along the coasts of Java and Sumatra and its relation to ENSO. *Geophysical Research Letters*, 28: 1599–1602.
- [Susanto and Marra, 2005] Susanto, R. D. and Marra, J., 2005. Effect of the 1997/98 El Niño on chlorophyll a variability along the coasts of Java and Sumatra. *Progress in Oceanography*, 18, 124–127.
- [Susanto et al., 2006] Susanto, R. D., Moore, T. S. and Marra, J., 2006. Ocean color variability in the Indonesian Seas during the SeaWiFS era. *Geochemistry, Geophysics, Geosystem*, 7: Q05021.
- [Sydeman et al., 2014] Sydeman, W. J., Thompson, S. A., Garcia-Reyes, M., Kahru, M., Peterson, W. T. and Largier, J. L., 2014. Multivariate ocean-climate indicators (MOCI) for the central California Current: Environmental change, 1990–2010. *Progress in Oceanography*, 120, 352-369.



- [Thompson et al., 2011] Thompson, P. A., Bonham, P., Waite, A. M., Clementson, L. A., Cherukuru, N., Hassler, C. and Doblin, M. A., 2011. Contrasting oceanographic conditions and phytoplankton communities on the east and west coasts of Australia. *Deep Sea Research Part II: Topical Studies in Oceanography*, 58(5), 645-663.
- [Timonin et al., 1992] Timonin, A. G., Arashkevich, E. G., Drits, A. V. and Semenova, T. N., 1992. Zooplankton dynamics in the northern Benguela ecosystem, with special reference to the copepod *Calanoides carinatus*. *South African Journal of Marine Science*, 12(1), 545-560.
- [Valsala, 2009] Valsala, K. V., 2009. Different spreading of Somali and Arabian coastal upwelled waters in the northern Indian Ocean: A case study, *Journal of Oceanography*, 65, 803–816.
- [Varela et al., 2015] Varela, R., Álvarez, I., Santos, F., deCastro, M. and Gómez-Gesteira, M., 2015. Has upwelling strengthened along worldwide coasts over 1982-2010? *Scientific Reports*, 5:10016.
- [Varela et al., 2016] Varela, R., Santos, F., Gómez-Gesteira, M., Álvarez, I., Costoya, X. and Días, J. M., 2016. Influence of Coastal Upwelling on SST Trends along the South Coast of Java. *PloS one*, 11(9), e0162122.
- [Villanueva and Sánchez, 1993] Villanueva, R. and Sánchez, P., 1993. Cephalopods of the Benguela Current off Namibia: new additions and considerations on the genus *Lycoteuthis*. *Journal of Natural History*, 27(1), 15-46.
- [Wang et al., 2015] Wang, Y., Castelao, R. M. and Yuan, Y., 2015. Seasonal variability of alongshore winds and sea surface temperature fronts in Eastern Boundary Current Systems. *Journal of Geophysical Research: Oceans*, 120(3), 2385-2400.
- [Webster et al., 1999] Webster, P. J., Moore, A. M., Loschnigg, J. P. and Leben, R. R., 1999. Coupled ocean temperature dynamics in the Indian Ocean during 1997-98. *Nature*, 401: 356-360
- [Wilson et al., 2003] Wilson, S. G., Carleton, J. H. and Meekan, M. G., 2003. Spatial and temporal patterns in the distribution and abundance of macrozooplankton on the southern North West Shelf, Western Australia. *Estuarine Coastal Shelf Science*, 56, 897–908.
- [Woo et al., 2006] Woo, M., Pattiaratchi, C. B. and Schroeder, W., 2006. Summer surface circulation along the Gascoyne continental shelf, Western Australia. *Continental Shelf Research*, 26, 132–152.
- [Wooster and Reid, 1963] Wooster, W. S. and Reid, J., 1963. Eastern boundary currents. *The sea*, 2, 253-280.
- [Wyrtki, 1973] Wyrtki, K., 1973. Physical oceanography of the Indian Ocean. Pp. 18–36 in B. Zeitzschel, ed. *The biology of the Indian Ocean*. Springer-Verlag, New York.

- [Xu et al., 2013] Xu, J., Lowe, R. J., Ivey, G. N., Pattiaratchi, C., Jones, N. L. and Brinkman, R., 2013. Dynamics of the summer shelf circulation and transient upwelling off Ningaloo Reef, Western Australia. *Journal of Geophysical Research: Oceans*, 118(3), 1099-1125.
- [Xue et al., 2015] Xue, L., Wang, H., Jiang, L. Q., Cai, W. J., Wei, Q., Song, H., Kuswardani, R. T. D., Pranowo, W. S., Beck, B., Liu, L. and Yu, W., 2016. Aragonite saturation state in a monsoonal upwelling system off Java, Indonesia. *Journal of Marine Systems*, 153, 10-17.
- [Yeh et al., 2010] Yeh, S. W., Park, Y. G., Min, H., Kim, C. H. and Lee, J. H., 2010. Analysis of characteristics in the sea surface temperature variability in the East/Japan Sea. *Progress in Oceanography*, 85(3), 213-223.
- [Yuras et al., 2005] Yuras, G., Ulloa, O. and Hormazábal, S., 2005. On the annual cycle of coastal and open ocean satellite chlorophyll off Chile (18–40 S). *Geophysical Research Letters*, 32(23).
- [Zavala-Hidalgo et al., 2006] Zavala-Hidalgo, J., Gallegos-García, A., Martínez-López, B., Morey, S. L. and O'Brien, J. J., 2006. Seasonal upwelling on the western and southern shelves of the Gulf of Mexico. *Ocean Dynamics*, 56(3-4), 333-338.



## List of publications

Picado, A., Álvarez, I., Vaz, N., **Varela, R.**, Gómez-Gesteira, M. and Días, J. M., 2014. Assessment of chlorophyll variability along the northwestern coast of Iberian Peninsula. *Journal of sea research*, 93, 2-11.

**Varela, R.**, Álvarez, I., Santos, F., deCastro, M. and Gómez-Gesteira, M., 2015. Has upwelling strengthened along worldwide coasts over 1982-2010? *Scientific Reports*, 5:10016.

Santos, F., Gómez-Gesteira, M., **Varela, R.**, Ruiz-Ochoa, M. and Días, J. M., 2016. Influence of upwelling on SST trends in La Guajira system. *Journal of Geophysical Research: Oceans*, 121(4), 2469-2480.

**Varela, R.**, Santos, F., Gómez-Gesteira, M., Álvarez, I., Costoya, X. and Días, J. M., 2016. Influence of Coastal Upwelling on SST Trends along the South Coast of Java. *PloS one*, 11(9), e0162122.

**Varela, R.**, Costoya, X., Gómez-Gesteira, M. and Enríquez, C., 2018. Differences in coastal and oceanic SST trends north of Yucatan Peninsula. *Journal of marine systems*. Under review.

**Varela, R.**, Lima, F. P., Seabra, R., Meneghesso, C. and Gómez-Gesteira, M., 2018. Coastal warming and wind-driven upwelling: a global analysis. *Science of the total environment*. Under review.